Reliability-oriented sensitivity analysis under probabilistic model uncertainty – Application to aerospace systems

Vincent Chabridon

Université Clermont Auvergne
École Doctorale
Sciences pour l'Ingénieur de Clermont-Ferrand

THÈSE

présentée par

Vincent CHABRIDON

Ingénieur IFMA

en vue d'obtenir le grade de

Docteur d'Université

Spécialité doctorale : Génie Mécanique

Analyse de sensibilité fiabiliste avec prise en compte d'incertitudes sur le modèle probabiliste – Application aux systèmes aérospatiaux

soutenue publiquement le **lundi 26 novembre 2018**, à l'Office National d'Études et de Recherches Aérospatiales de Palaiseau, devant un jury composé de :

Dr. Mathieu BALESDENT	ONERA, Palaiseau	Co-encadrant
Dr. Jean-Marc BOURINET	SIGMA, Clermont-Ferrand	Co-encadrant
Pr. Nicolas GAYTON	SIGMA, Clermont-Ferrand	Co-directeur
Dr. Christian GOGU	Université Toulouse III	Examinateur
Dr. Bertrand IOOSS	EDF R&D, Chatou	Rapporteur
Pr. Béatrice LAURENT-BONNEAU	INSA, Toulouse	Examinatrice
Pr. Jérôme MORIO	ONERA & ISAE, Toulouse	Co-directeur
Pr. Carsten PROPPE	KIT, Karlsruhe	Rapporteur
Pr. Bruno SUDRET	ETH, Zürich	Président du jury

ONERA/DTIS, Université Paris Saclay,
F-91123 Palaiseau Cedex, France

• • •

Université Clermont Auvergne, CNRS, SIGMA Clermont, Institut Pascal,
F-63000 Clermont-Ferrand, France

Reliability-oriented sensitivity analysis under probabilistic model uncertainty – Application to aerospace systems

A dissertation submitted by

Vincent CHABRIDON

in partial fulfillment of the requirements for the degree of

Doctor of Philosophy
(Mechanical Engineering)

UNIVERSITY CLERMONT AUVERGNE
Clermont-Ferrand, France

&

ONERA – THE FRENCH AEROSPACE LAB
Palaiseau, France

defended publicly on November 26, 2018 in front of a defense committee made up of:

Dr. Mathieu BALESDENT	ONERA, Palaiseau	Co-advisor
Dr. Jean-Marc BOURINET	SIGMA, Clermont-Ferrand	Co-advisor
Pr. Nicolas GAYTON	SIGMA, Clermont-Ferrand	Thesis co-director
Dr. Christian GOGU	Université Toulouse III	Examiner
Dr. Bertrand IOOSS	EDF R&D, Chatou	Reviewer
Pr. Béatrice LAURENT-BONNEAU	INSA, Toulouse	Examiner
Pr. Jérôme MORIO	ONERA & ISAE, Toulouse	Thesis co-director
Pr. Carsten PROPPE	KIT, Karlsruhe	Reviewer
Pr. Bruno SUDRET	ETH, Zürich	President

This manuscript was typeset with LaTeX 2ε (MacTeX-2017 distribution containing TeXLive 2017). It is based on the *Masters / Doctoral Thesis* template (version 2.5). The source files were edited using TeXstudio 2.12.6. The body font used is *Mathpazo*. Graphical illustrations were produced with Matlab®, Ti*k*Z, Inkscape and Matplotlib (running Python 3.6). The bibliography was compiled using BibLaTeX with BibTeX backend.

BibTeX entry:

```
@PHDTHESIS{Chabridon_PhD_2018,
author = {Chabridon, V.},
year = 2018,
title = {{Reliability-oriented sensitivity analysis under probabilistic
model uncertainty -- Application to aerospace systems}},
school = {Universit\'e Clermont Auvergne}
}
```

À mes parents,
À mon frère et ma sœur,
À Odette et Athina,
À ma chérie . . .

Remerciements / Acknowledgements

L'écriture des remerciements constitue l'étape clé censée clôturer le travail de thèse. Je présente par avance mes excuses à celles et/ou ceux que j'aurais éventuellement oubliés dans ces remerciements.

Avant toute chose, je me dois de remercier les personnes qui, de par leur décision propre, m'ont permis d'écrire ces remerciements et de publier cette thèse. À Messieurs Carsten PROPPE et Bertrand IOOSS, j'adresse mes plus profonds remerciements pour avoir accepté la lourde tâche d'être rapporteurs de ces travaux. Je vous remercie pour vos rapports détaillés, bienveillants et enthousiastes ainsi que pour l'ensemble de vos remarques et suggestions ! Ces éléments ainsi que vos questions lors de la soutenance sont autant de sources de réflexions personnelles scientifiques sur le sens à donner à mes travaux et forment de nombreuses pistes de travaux pour la suite : merci à vous deux. À Monsieur Bruno SUDRET, qui a accepté de présider mon jury de soutenance, j'adresse mes plus chaleureux remerciements. Vous avoir eu comme président de mon jury a été un grand honneur et un véritable plaisir. Enfin, j'aimerais remercier les deux derniers membres extérieurs du jury qui ont accepté d'examiner ces travaux de thèse. À Madame Béatrice LAURENT-BONNEAU et Monsieur Christian GOGU, j'adresse mes plus sincères remerciements ainsi que toute ma gratitude pour leur bienveillance à l'égard de mes travaux et pour leurs multiples questions lors de ma soutenance.

Après avoir remercié les membres externes de mon jury, il ne faudrait pas que j'oublie les quatre autres membres, les « *Fabulous Four* » comme je me suis longtemps plu à les appeler avec affection :

- À Nicolas GAYTON, j'adresse mes plus profonds remerciements pour avoir accepté d'être mon co-directeur de thèse clermontois. Nicolas, outre nos liens depuis l'IFMA, tu as toujours été présent pour me donner confiance en moi et me réconforter dans l'idée que j'étais sur le droit chemin en choisissant la recherche. Tu m'as ouvert les yeux sur mes capacités à aller toujours plus loin dans mes idées, tout en me donnant des gardes-fou qui m'ont permis de trouver le bon chemin. Je te remercie pour tout ce que tu m'as apporté durant ces trois années et durant ma scolarité à l'IFMA.
- À Jérôme MORIO, mon deuxième co-directeur de thèse, toulousain quant à lui, j'adresse mes plus profonds remerciements pour avoir été le véritable initiateur de cette thèse. Jérôme, tu es celui qui m'a donné la possibilité de travailler pendant ces trois ans (et six mois, avec le stage de fin d'études) à l'ONERA. Je suis heureux d'avoir pu faire tout ce chemin grâce à toi. Tu m'as poussé à faire ce qui était le mieux pour moi et en vue de mes aspirations futures. Sur le plan scientifique, tu as su isoler et identifier de nombreuses pistes déterminantes pour cette thèse, et tu as même mis « la main à la pâte » dans les calculs et les simulations pour m'aider et me faire avancer. Merci à toi pour ta confiance et pour tout ce que tu m'as apporté, dans les bons moments comme dans les moments difficiles.
- À Jean-Marc BOURINET, mon co-encadrant clermontois, j'adresse mes plus profonds remerciements pour tout ce qu'il m'a apporté pendant et avant la thèse. Jean-Marc, après avoir été successivement mon « Tuteur IFMA » dès ma première année, mon professeur de nombreux cours déterminants pour moi, tu as été le grand organisateur de toute ma « carrière » à l'IFMA : de mon stage de deuxième année à mon stage de fin d'études à l'ONERA, en passant par une année internationale... Tu as été un mentor hors pair. Je te dois énormément pour tout ce que tu m'as apporté.
- À Mathieu BALESDENT, mon co-encadrant palaisien, je me dois d'être plus direct : MERCI POUR TOUT ! L'utilisation des majuscules ici ne veut pas dire que ce sont des variables aléatoires, mais bien que ta contribution à cette thèse en tant qu'encadrant au quotidien fut déterminante. Tu m'as suivi au quotidien. Tu as réussi à me pousser à vaincre les difficultés

et combler mes points faibles. À tes côtés, j'ai compris ce que représente un investissement personnel total. Tes capacités de travail et de concentration sont impressionnantes. Merci de m'avoir appris tant de choses, sur la recherche et sur moi-même.

Encore une fois, merci à tous les quatre d'avoir été très présents pour moi et de m'avoir poussé à donner le meilleur de moi-même. J'espère sincèrement que nous pourrons retravailler ensemble dans le futur.

Toujours du point de vue de l'influence scientifique, je tiens ici aussi à transmettre mes remerciements à des personnes qui ont contribué, de façon ponctuelle ou sur le plus long terme, à influencer ma vision de la recherche et des pistes à suivre. Je tiens donc à remercier Sébastien DA VEIGA pour l'ensemble des conseils qu'il m'a prodigués ainsi que Guillaume PERRIN pour son aide déterminante concernant les travaux présentés au Chapitre 7. Sa bienveillance et sa réactivité m'ont permis de finir cette thèse dans de bonnes conditions. Je tiens à vivement remercier Merlin KELLER et Gilles DEFAUX pour m'avoir, par des discussions ponctuelles, redonné confiance (peut-être sans le savoir) et conforté dans l'idée que mes travaux de thèse n'étaient peut-être pas inutiles pour tout le monde. Je tiens aussi à remercier deux anciens collègues et amis, Paul B. et Tarik B., pour leur soutien à chacune de nos rencontres, à Clermont, Moissy, Lille ou Compiègne. *Moreover, I would like to thank successively Frank* GROOTEMAN *(NLR) and Prof. Wei* CHEN *(Northwestern University) for having accepted me in their lab. My internships there undoubtedly comforted me to pursue research by doing a PhD. Finally, I would like to thank Dr. Sergei* KUCHERENKO *who accepted to kindly examine my work and provided me some advice during his stay in Clermont-Ferrand.*

Après avoir remercié les personnes qui ont directement contribué sur le plan scientifique à cette thèse, je me dois d'avoir une pensée pour toutes les personnes qui, sans le savoir, ont véritablement aidé au bon déroulement de ces trois années. Ce travail de thèse a été rendu possible par l'établissement d'un co-financement entre l'ONERA et l'école d'ingénieur.e.s SIGMA Clermont. La thèse a donc été réalisée pour partie à Palaiseau et à Clermont-Ferrand. Je remercie mes amis doctorants clermontois pour les bons moments lors de mes différents passages. Parmi eux, un grand merci à Mathieu S. et Nicolas L. pour leur gentillesse et leurs coups de pouce technico-informatiques à chacun de mes passages. Merci à Cécile M. et Pierre B., mes deux anciens (jeunes) professeurs à l'IFMA, de m'avoir toujours fait bénéficier de leurs précieux conseils. Merci aussi à Jacqueline M. et Marion L. pour leur aide administrative et leur bienveillance envers les doctorants. Concernant la vie parisienne, je remercie la troupe de choc, {PYB, Rémi, Théo}, avec qui j'ai passé quelques soirées arrosées dont Paris se souvient encore... Merci aussi à Pierre G. pour nos petits cafés lors de tes passages à Paris. Merci à mon ami ifmalien Julien F. d'avoir toujours été présent pour moi et d'être venu pour m'aider en préparation de la thèse. Merci à Thomas B. d'avoir continué à m'inviter à venir voir des matchs de l'ASM chez lui, et ce, malgré mes refus du type « j'peux pas, j'ai thèse ce week-end ». Je tiens aussi à remercier Maxime F. pour tous les bons moments passés à Paris lors de nos soirées, sur les quais ou pour les délicieux repas dégustés chez toi. Pour finir, je me dois de remercier mes amis membres du collectif des *Thésards Anonymes + d Docteurs*, un groupe de soutien ésotérique qui propose une thérapie par « l'humour fin et subtil » : merci à Quentin, Mathieu S., Mathieu C., Cédric, Rudy et Adrien pour m'avoir permis de gâcher plusieurs vies à mourir de rire ! En particulier, je remercie Rudy pour avoir été un ami et un guide hors pair durant tout mon parcours à l'IFMA. Il a su me prodiguer une foultitude de conseils et m'embarquer dans ses pas en Année Internationale. Enfin, merci aussi à mon cher ami historien Géraud qui n'a cessé durant ces trois années de m'inviter à divers dîners/apéros/pique-nique dont les saveurs m'ont toujours rempli de joie et de souvenirs de notre Auvergne natale...

Concernant mon aventure palaisienne, je tiens à remercier l'ensemble des personnes du *Département Traitement de l'Information et Systèmes* (DTIS) de l'ONERA qui ont œuvré à la mise en place et au bon fonctionnement (tant sur les plans scientifiques qu'humains et administratifs)

de cette thèse. Toutes ces personnes ont contribué à forger un petit cocon scientifique et humain où il a fait bon-vivre chaque jour. En particulier, je tiens à remercie Florence M., secrétaire au DTIS, pour son aide sans faille et son extrême gentillesse sur l'ensemble de ces trois années. J'ai une pensée émue pour mes ami.e.s thésard.e.s et stagiaires de l'ONERA et de SIGMA Clermont. Ils/Elles ont réussi à transformer un quotidien, parfois morne et terne, en de véritables journées passionnantes. Qu'il s'agisse de nos discussions du matin (bienveillantes), du midi (clivantes) ou du soir (marrantes), ou de nos soirées (alcoolisées ou non, à bases de jeux dont je ne connais ni ne comprends jamais les règles...), chacun de ces moments privilégiés m'a aidé à voir autrement et à apprécier chaque moment passé. Ainsi, je tiens à dire un grand merci en particulier à : Gaétan (et Maude, encore merci à vous pour le super mariage de veille-d'envoi-du-manuscrit), Carlos (et ses cours très particuliers d'espagnol pas très recommandable), Christophe (et les découvertes gustatives), le duo {Raphaël L., Romain G.} (et les soirées Versaillaises *&* Parisiennes), Claire (et son super encadrant de TP, paraît-il !), Monsieur Michel (pour l'anniversaire de son frère), Léon (et ses jolis origamis et cactus), Camille S. (et son goût prononcé pour les tagliatelles au bleu vegan et pour le mojito à la rose), Sergio (et sa recette mondialement reconnue de la Paëlla), Rodolphe (et ses délicieuses crêpes du Val-de-Grâce), ainsi que les petits nouveaux, Baptiste, Jean-Lynce, Denis, Thomas, Sofiane, Enzo, Camille P. et Guillaume, à qui je souhaite de très belles aventures, à l'ONERA ou ailleurs ! De plus, je souhaiterais remercier Riccardo B. pour m'avoir entrainé dans ses multiples voyages à travers des espaces mathématiques insoupçonnables. Merci à Émilien F. pour son incroyable capacité à comprendre des problèmes incompréhensibles et pour m'avoir aidé à lire des papiers illisibles. Je remercie aussi mes deux amis du Bureau-d'à-côté : Julien P. (mon demi-frère de thèse, qui fait de l'optimisation que je ne comprends pas) pour nos nombreuses soirées et nos discussions infinies au sujet de la vie et de nos névroses, et Ali H. (mon autre demi-frère de thèse, qui fait de l'optimisation que personne ne comprend) pour les parties de foot et pour sa gentillesse non bornée. Enfin, j'adresse un grand merci à Ioannis S. pour tout ce qu'il m'a apporté en tant qu'ami, tant par sa culture scientifique que par son humanisme sans limite qui transparaît directement derrière un sourire quotidien. Merci à vous tous pour ces différents moments passés durant ces trois années. Il me reste à dire merci à un duo de choc à qui je dois énormément : Romain et Elinirina. Ces deux énergumènes ont réussi, chacun à leur manière, à m'apprivoiser et à m'accepter tel que je suis. Nous avons débuté le même jour, nous avons fini (presque) en même temps. Nous avons combattu et pourfendu les incertitudes, chacun dans nos domaines, en restant unis : des méchants réseaux bayésiens et vilaines chroniques, à l'horrible *remaining useful life* accompagnée de ses impitoyables observateurs à entrées inconnues par intervalles, en passant par les indignes estimateurs à noyaux gaussiens et les monstrueux indices de Sobol sur la fonction indicatrice, nous avons réussi à les dompter et à leur faire entendre raison ! Nos trois thèses racontent des histoires complémentaires dans lesquelles les incertitudes occupent le premier rôle. J'espère que nos chemins ne divergeront pas de sitôt !

Pour finir avec les amis, je tiens à remercier mes amis d'enfance, Timothée, Xavier, Guillaume et Benoit. Merci d'avoir toujours été là pour moi pendant toutes ces belles années.

Pour conclure ces remerciements, je tiens à m'adresser à mes proches. Cette thèse n'aurait pas été possible sans un soutien indéfectible de la part de mes parents, de mon frère et de ma sœur et de ma famille au sens large. Je remercie ainsi ma (belle-)famille pour tout ce qu'elle m'a apporté durant ces trois années. Merci à mon frère et ma sœur d'avoir montré l'exemple en faisant de brillantes études. Merci à mes parents d'avoir veillé à ce que nous ne manquions de rien, matériellement et culturellement parlant. Merci à eux de m'avoir donné tant d'amour. Je leur dédie cette thèse...

Le dernier mot ira, je l'espère, droit au cœur de la personne qui a vécu cette thèse de l'intérieur et qui connaît, elle aussi, le sacrifice que cela représente... Je ne la remercierai jamais assez pour tout ce qu'elle m'a apporté. Je l'aime et je suis fier de tout ce qu'elle a achevé !

Paris, le 21 décembre 2018

"The very essence of romance is uncertainty."
Oscar WILDE, *The Importance of Being Earnest*, 1895.

❧

« J'ai heurté, savez-vous, d'incroyables Florides
Mêlant aux fleurs des yeux de panthères à peaux
D'hommes ! Des arcs-en-ciel tendus comme des brides
Sous l'horizon des mers, à de glauques troupeaux !
...
Or moi, bateau perdu sous les cheveux des anses,
Jeté par l'ouragan dans l'éther sans oiseau,
Moi dont les Monitors et les voiliers des Hanses
N'auraient pas repêché la carcasse ivre d'eau ;
...
J'ai vu des archipels sidéraux ! et des îles
Dont les cieux délirants sont ouverts au vogueur :
– Est-ce en ces nuits sans fonds que tu dors et t'exiles,
Million d'oiseaux d'or, ô future Vigueur ? »
Arthur RIMBAUD, *Le Bateau ivre*, 1871.

❧

« Il vaut mieux mobiliser son intelligence sur des bêtises
que mobiliser sa bêtise sur des choses intelligentes. »
Devise Shadok

Contents

List of Figures

List of Tables

CHAPTER 1

Introduction

Context

Aerospace systems can be classified among *complex engineering systems*, mainly due to their multidisciplinary nature while gathering a large panel of heterogeneous components, a relatively moderate number of production units compared to other industrial mass production branches and, finally, subject to high-performance requirements while facing greater reliability and safety concerns. The term "aerospace systems" encompasses a wide family of systems, from civil and military aircrafts to space launchers, tactical ballistic missiles and satellites. As one may see, the previous complexity sources have to be balanced between, for instance, a civil aircraft (mass-manufactured system, highly reliable regarding passengers' safety) and a satellite (custom-manufactured system, highly reliable regarding the induced costs). Thus, the similarity between all of these systems is their *highly-safe* property while operating in extreme environments.

Complex aerospace systems analysis and design rely intensely on the use of high-fidelity computer models to efficiently simulate their behavior, especially when physical phenomena cannot be directly observed nor measured on test specimens (e.g., extreme phenomena such as a collision between a space debris and a satellite). The computer models that are used often rely on solving sets of ordinary or partial differential equations such as in finite element simulations in structural analysis, or finite volume differences for computational fluid dynamics.

A large amount of computer models used to design and simulate complex aerospace systems are *deterministic models*, that is, for two identical sets of inputs (e.g., applied structural loads on a structural part of an aircraft wing), the same output will be obtained (e.g., the tip deflection or Von Mises equivalent stress). However, it may happen that some models may be *chaotic* (i.e., deterministic but presenting an extreme sensitivity to initial conditions), such as those used for the numerical simulation of large deformation such as appearing in vehicle crash or buckling, or even *stochastic* (e.g., such as the natural variability appearing in material properties over a specimen).

Assessing reliability and system safety implies to take into account the various sources of uncertainties which might affect the behavior of the system. Uncertainties may occur in the initial conditions, in the physical properties of the system (i.e., variability of mechanical properties of materials due the manufacturing process), in the environmental variables affecting the system (i.e., wind speed and induced loadings) or finally, in the modeling itself (e.g., due to the use of an imperfect mathematical model and its numerical resolution using algorithms, with a limited accuracy). Nonetheless, these uncertainties have to be incorporated as soon as possible in the design process to ensure to get an optimized, reliable and safe design regarding standards

and customers' requirements. This can be achieved following a general *uncertainty quantification methodology* such as presented in the next section.

General methodology for uncertainty quantification

Uncertainty quantification (UQ) regroups a wide panel of both theoretical and applied tools arising from numerous fields such as probability theory, statistics, computational sciences and several other fields from both mathematics, physics and computer science. More importantly, the UQ tools are now pouring into almost all of the engineering branches such as demonstrated by several recent textbooks on this subject (see, e.g., Sullivan, 2015; Ghanem et al., 2017; Soize, 2017). However, the interdisciplinary nature of UQ can be summarized in a few fundamental steps gathered in the so-called "*UQ methodology*" (De Rocquigny, 2006a; De Rocquigny, 2006b; Sudret, 2007; Iooss, 2009) as illustrated in Figure 1.1.

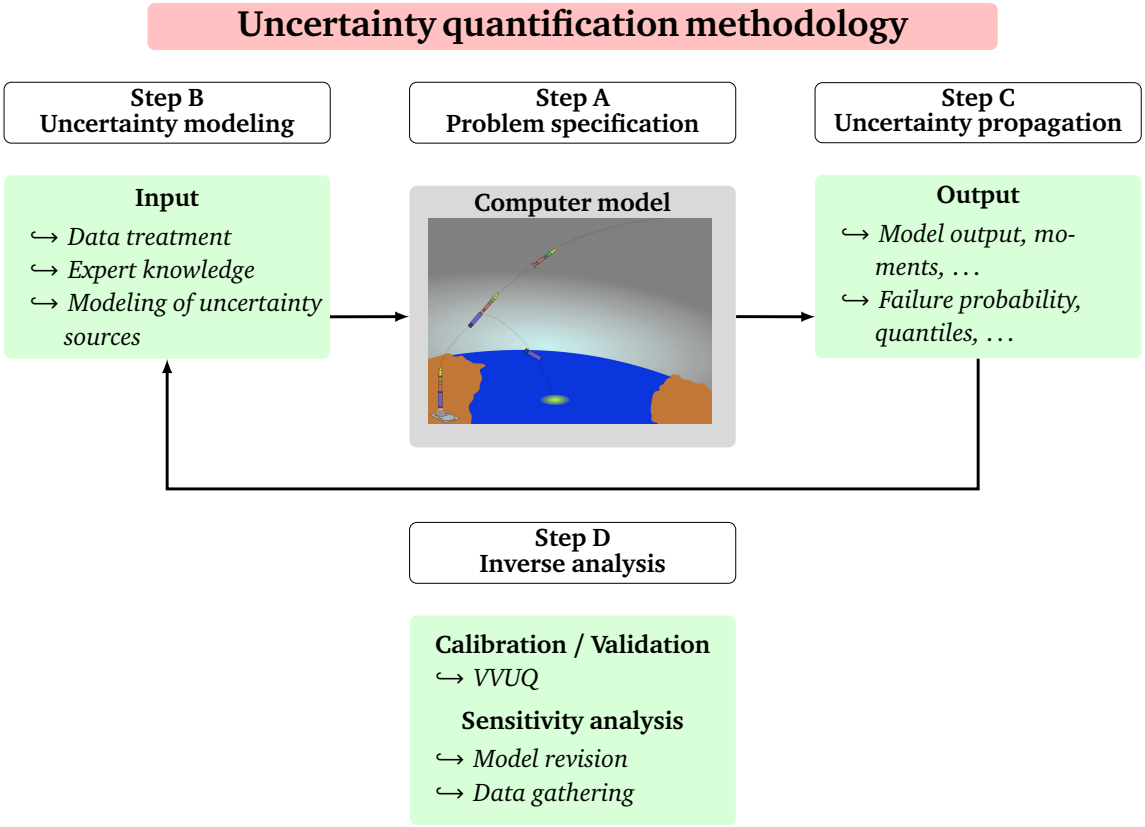

FIGURE 1.1: Illustration scheme of the uncertainty quantification methodology.

The UQ methodology presented in Figure 1.1 can be divided into four basic steps [1] which are detailed herebelow:

- **Step A → Problem specification**: the first step consists in defining the real system under study and to build a computer model that is able to accurately predict and mimick the

[1] Note that, going from Steps B to Step C is often denoted as *forward UQ*, while Step D is called *backward / inverse UQ* (see, e.g., Sullivan, 2015).

behavior of the system. Thus, depending on the case, it can be either an analytical formula to a full multidisciplinary computational workflow (e.g., in the aerospace context, mixing structural analysis, propulsion, trajectory and aerodynamics). Specifying the problem includes to define all the set of parameters intrinsic to the computer model, i.e., from the input variables to which output quantity will be returned by the code. Finally, all the tuning parameters (e.g., algorithmic parameters such as tolerances) should be chosen;

- **Step B $\rightarrow$ Uncertainty modeling**: the second step aims at identifying all the sources of uncertainties affecting the input variables. Several tools are available to model uncertain input variables: one can choose either the probabilistic framework, the interval framework or imprecise probabilities. The choice of one of these frameworks may vary depending on the nature (e.g., datasets or expert opinions) and quality of the available information about input variables. The aim of the analysis may also drive the choice of a type of uncertainty modeling;

- **Step C $\rightarrow$ Uncertainty propagation**: the third step generally consists in transfering the input uncertainties through the computer model. As a result, the output quantity is thus affected by uncertainties too. Depending on the mathematical framework used to model the input uncertainties, the form of the output has to be consistent with it (e.g., a probability distribution, an interval, a probability-box, ...). Finally, a statistical treatment of the output can be performed in order to achieve various tasks such as, e.g., reliability or risk assessment;

- **Step D $\rightarrow$ Inverse analysis**: the fourth step mainly involves two types of analyses. The first one, which is beyond the scope of this manuscript, mainly gathers the *validation*, *verification* and *calibration* phases of the computer model w.r.t. available data [2]. All these analyses are often gathered under the acronym "*VVUQ*". The second one, which is of major interest in this thesis, is called *sensitivity analysis* (SA) and gathers a set of methods whose aim is to study how the variability in output can be apportioned to the input one.

As a remark, as mentioned in Saltelli et al. (2004), SA and VVUQ may be strongly linked to each other. However, in the present manuscript, the computer models under study are assumed to be verified, validated and calibrated following a global VVUQ methodology. Thus, in the inverse analysis (i.e., Step D), one only focuses on SA.

Problem statement

From a general point of view, this thesis deals with the problem of reliability assessment (more specifically, the problem of rare event probability estimation) and sensitivity analysis for highly safe systems, i.e., systems characterized by a rare occurence of the failure events. In a probabilistic framework, the phenomenological uncertainties can be modeled by assuming that input variables are a set of random variables following some parametric probability distributions. However, the distribution parameters which are usually set by the analyst may be affected by uncertainty arising from a lack of data (i.e., statistical uncertainty due to a limited amount of data) or resting on expert recommendations. Consequently, given a failure scenario, reliability measures (e.g., failure probability, reliability index) which are estimated regarding the distribution of the output should take this second uncertainty level into account. As a result, one has to consider a *bi-level input uncertainty* composed of:

- the *phenomenological uncertainties* (a.k.a. *natural variability*) affecting the inputs, thus represented by random variables;

[2] Despite the fact that this type of analysis is not discussed in this manuscript, the interested reader may refer, e.g., to Oberkampf and Roy (2010) and Damblin (2015) for a deeper presentation about the VVUQ topic.

- the *probabilistic model uncertainty* which characterizes the lack-of-knowledge about the distribution parameters.

Such a problem is of major interest in the UQ community. If pioneering works such as those from Ditlevsen (1979a), Ditlevsen (1979b), Der Kiureghian and Liu (1986), and Der Kiureghian (1988) have already clearly stressed the need for taking both natural variability and probabilistic model uncertainty into account in the reliability models and methods, it appears that such an issue is still at stake nowadays. This is mainly due to the various developments in terms of advanced sampling-based techniques for rare event probability estimation (e.g., adaptive importance sampling, subset sampling), the increasing complexity and fidelity of computer models (e.g., multidisciplinary computational workflows) and the advances in surrogate modeling. Moreover, various complementary mathematical frameworks to the traditional probabilistic one have emerged (e.g., Bayesian techniques, imprecise probabilities) to handle various sources of uncertainties and to propose alternative numerical treatments adapted to the other UQ challenges (see, e.g., Nagel, 2017; Schöbi, 2017).

In this thesis, the focus is put on accounting the bi-level input uncertainty all along the UQ methodology, in the context of rare event probability estimation of complex aerospace computer models. Consequently, the core problem under study in this thesis can be stated as follows:

How to deal with this bi-level input uncertainty all along the UQ methodology?

More specifically, one can decompose this issue into three questions which are themselves related to the steps mentioned above:

Q1 – How to model this second level of uncertainty? ($\hookrightarrow$ **Step B**)

Q2 – How does this bi-level input uncertainty impact the reliability measure? ($\hookrightarrow$ **Step C**)

Q3 – How to link the variability of the reliability measure to this bi-level input uncertainty? ($\hookrightarrow$ **Step D**)

Thus, in the present work, it is proposed to develop, at each step, starting from the uncertainty modeling phase (i.e., Step B), to the inverse analysis phase (i.e., Step D), several tools to handle this bi-level input uncertainty. To do so, several scientific objectives are stated in the next section.

Objectives and outline of the thesis

Based on the previous problem statement, this thesis aims at developing a consistent strategy for satisfying the following objectives:

O1 Draw up a state-of-the-art review about the available techniques and methods for both uncertainty modeling, uncertainty propagation and sensitivity analysis which could be used/adapted regarding the present problem statement;

O2 Develop an efficient strategy to combine both probabilistic model uncertainty and rare event probability estimation;

O3 Propose new tools to achieve reliability-oriented sensitivity analysis under probabilistic model uncertainty;

O4 Demonstrate the consistency of the proposed tools regarding realistic complex aerospace computer codes.

All along the chapters, these objectives are recalled, justified and expanded. If one lets the introduction and conclusion chapters aside, this manuscript is composed of seven chapters whose contents are detailed below.

Chapter 2 aims at introducing a few fundamental concepts appearing in UQ, with a focus on the probabilistic framework. Core notions of sources and types of uncertainties are described. The class of models under study is introduced and an inventory of the possible output quantities of interests is provided.

Chapter 3 presents an overview of a variety of uncertainty propagation techniques adapted to rare event probability estimation. For each technique, a brief presentation is proposed together with a summary of the formulation and its main advantages/drawbacks. Finally, a synthesis gathers the most important guidelines about the use of rare event probability estimation techniques.

Chapter 4 presents an overview of several methods for sensitivity analysis. In a first part, the methods related to *sensitivity analysis of model output* (SAMO) are presented. Then, in a second part, one introduces the paradigm of *reliability-oriented sensitivity analysis* (ROSA) and describes a wide panel of methods, while exhibiting several links and differences between all of these methods. This second part aims at providing a thorough literature review about the current trends and challenges in the ROSA context.

Chapter 5 addresses the problem of rare event probability estimation under probabilistic model uncertainty. To do so, the uncertainty affecting the probabilistic model is treated using a Bayesian framework by assuming a prior distribution over the stochastic distribution parameters. Then, the reliability measure under consideration is no longer the traditional failure probability, but the *predictive failure probability* which incorporates the effects of both levels of uncertainties. Finally, two different numerical approaches are presented to estimate such a quantity, namely the *nested reliability approach* (NRA) and the *augmented reliability approach* (ARA). A numerical comparison is led so as to determine which one is more suitable to the current objectives of the thesis.

Chapter 6 aims at extending the results obtained in Chapter 5. Starting from the estimation of the predictive failure probability by the augmented reliability approach, the idea is to propose reliability-oriented sensitivity estimators so as to evaluate the robustness of the estimated probability w.r.t. the bi-level input uncertainty. More specifically, one assumes that, due to the Bayesian hierarchical structure in input, one would like to test the robustness of the reliability measure regarding the hyper-parameters of the prior distribution characterizing the epistemic uncertainty on the probabilistic model. Due to the local nature of the problem, local derivative-based sensitivity measures are derived using the concept of *score functions*. Then, a sampling-based technique is proposed so as to efficiently estimate both the predictive failure probability and the sensitivities at the same time, without extra call to the computer model. Finally, this methodology is applied on two test-cases to demonstrate the efficiency, especially when the occurrence of the failure event becomes very rare.

Chapter 7 aims at completing the work achieved in Chapter 6 by investigating the use of global indices adapted to ROSA in the context of bi-level input uncertainty. These indices are called *Sobol indices on the indicator function*. Their formulation and their extension to bi-level input uncertainty is studied using a disaggregated vision of the input variables affected by epistemic uncertainty. Then, a methodology to efficiently estimate these indices in the context of rare event probability estimation is proposed. This methodology relies on the combination between approximation-based estimators recently derived for these indices and a new approach for *kernel density estimation*. If these recent contributions are extracted from recent literature, the originality of the present work consists in their coupling and their adaptation to the context of bi-level input

uncertainty. Finally, this methodology is applied to two benchmark applications to demonstrate its efficiency, especially when the occurrence of the failure event becomes very rare. Moreover, the numerical applications highlight the possible additional insights the analyst can get from such a methodological tool.

Chapter 8 presents a representative aerospace test-case issued from a launch vehicle trajectory simulation model. This case is based on the dynamical modeling of the balistic fallout phase of the first stage of an expendable space launcher. In this chapter, all the methodological tools developed in the three previous chapters are tested on this case so as to validate them and to analyze both their advantages and limits.

As a remark, if all the chapters are, for most of them, written so as to be "self-contained" (some of them being directly linked to supplementary material provided in the appendices), the reading of the whole manuscript should be conducted in chronological order so as to be consistent with the UQ methodology viewpoint. Finally, Table 1.1 provides a summary for each chapter of the content of the manuscript and specifies their links to the global objectives of the thesis. For each chapter, a mention "SOA" versus (vs.) "NEW" specifies whether the content is more related to a "state-of-the-art" review or to a contribution proposed by the author.

TABLE 1.1: Summary of the content of the thesis.

Keywords	**Chapter**	**Content**	**Objectives**
Uncertainty modeling / Probability theory / Black-box	Chapter 2	SOA	O1
Rare event estimation techniques / Failure probability	Chapter 3	SOA	O1
SA on model output / Reliability-oriented SA (ROSA)	Chapter 4	SOA/NEW	O1
Predictive failure probability / Epistemic / NRA / ARA	Chapter 5	NEW	O2
Local ROSA / Score functions / Bounded distributions	Chapter 6	NEW	O3
Global ROSA / Sobol indices / Indicator function	Chapter 7	NEW	O3
Aerospace systems / Launcher stage fallout	Chapter 8	NEW	O4

Publications and communications

The research contribution presented in this manuscript is based on the published works listed herebelow.

Book Chap. Derennes P., V. Chabridon, J. Morio, M. Balesdent, F. Simatos, J.-M. Bourinet and N. Gayton (2018). "Nonparametric importance sampling techniques for sensitivity analysis and reliability assessment of a launcher stage fallout". In: *Optimization in Space Engineering*. Ed. by G. Fasano and J. Pintér. Springer International Publishing. (To Appear).

Jour. Pap. Chabridon V., M. Balesdent, J.-M. Bourinet, J. Morio and N. Gayton (2017). "Evaluation of failure probability under parameter epistemic uncertainty: application to aerospace system reliability assessment". In: *Aerospace Science and Technology* 69, pp. 526–537.

Chabridon V., M. Balesdent, J.-M. Bourinet, J. Morio and N. Gayton (2018). "Reliability-based sensitivity estimators of rare event probability in the presence of distribution parameter uncertainty". In: *Reliability Engineering and System Safety* 178, pp. 164–178.

Int. Conf. Chabridon V., M. Balesdent, J.-M. Bourinet, J. Morio and N. Gayton (2017). "Reliability-based sensitivity analysis of aerospace systems under distribution parameter uncertainty using an augmented approach". In: *Proc. of the 12th International Conference on Structural Safety & Reliability (ICOSSAR 2017)*, Vienna, Austria. (+Talk)

Nat. Conf. Chabridon V., N. Gayton, J.-M. Bourinet, M. Balesdent and J. Morio (2017). "Some Bayesian insights for statistical tolerance analysis". In: *Actes du 23ème Congrès Français de Mécanique (CFM 2017)*, Lille, France. (+Talk)

Chabridon V., M. Balesdent, J.-M. Bourinet, J. Morio and N. Gayton (2018). "Reliability-based sensitivity analysis under distribution parameter uncertainty – Application to aerospace systems". In: *Proc. of the 13th Mascot-Num Annual Conference (MASCOT-NUM 2018)*, Nantes, France. (+Poster)

Chabridon V., M. Balesdent, J.-M. Bourinet, J. Morio and N. Gayton (2018). "Nonparametric adaptive importance sampling strategy for reliability assessment and sensitivity analysis under distribution parameter uncertainty – Application to launch vehicle fallback zone estimation". In: *Actes des 10èmes Journées Fiabilité des Matériaux et des Structures (JFMS 2018)*, Bordeaux, France. (+Talk)

CHAPTER 2

Uncertainty modeling for input-output computer models

Contents

2.1 Introduction and motivations

Numerical modeling and simulation are two cornerstones of modern engineering and scientific computing. When dealing with complex aerospace systems, computer models are required to design, simulate and predict the behavior of such systems in their environment since real experiments are, most of the time, nearly impossible to carry out. Reliability assessment of these systems is a mandatory phase as their failure may have dramatic consequences in terms of human safety, environmental impact and money losses.

As an illustrative example of what is at stake in aerospace engineering, one can focus on the problem of *space debris* (i.e., *orbital debris* and *reentering debris*). Space debris is defined, according to the formal definition given by the Inter-Agency Space Debris Coordination Committee (IADC), as "all man made objects including fragments and elements thereof, in Earth orbit or re-entering the atmosphere, that are non functional" (Klinkrad, 2006). Historically, these debris mainly originate from accidental and intentional breakups (e.g., created after explosions or collisions) and from intentionally released ones during space launches' operations (e.g., inactive satellites, rocket upper stages and other fragments). With the increasing number of space launches combined to the increasing number of collisions, the number of space debris dramatically increased in the last decades, despite the widespread adoption of mitigation measures advocated by the IADC. Several famous collisions between satellites and catalogued debris have been studied and a dedicated literature is available on this subject (see, e.g., Klinkrad, 2006; Chan, 2008).

Determining the *collision probability* between orbiting debris and a satellite is of utmost importance to plan the future possible needs in terms of collision avoidance maneuvers. In such a case, the study is driven by the modeling of the space objects, of their relative trajectories and of the uncertainties that may affect several variables and parameters. Due to the singularity of the underlying phenomenon, and because of the impossibility to produce dedicated experimental data, this study requires the intensive use of complex computer models to simulate and predict the behavior of such a scenario. Assessing reliability of satellites thus imposes to take uncertainties into account in this preliminary study to ensure the ability for the simulation to predict future hazardous situations that may cause collision.

For reentering debris, determining their fallout safety zone and the associated *impact probability* is another crucial problem. Indeed, a misestimation may have dramatic consequences in terms of human security and environmental pollution.

The previous motivating examples are given here for the sake of illustration. In this thesis, the specific scenario under study issued from aerospace engineering concerns a launch vehicle fallout zone estimation. Moreover, general problems arising in structural reliability will also be used to illustrate and validate the proposed approaches.

This chapter aims at introducing various core ingredients appearing further in the thesis. It is organized as follows. Section 2.2 introduces the class of models under study. Section 2.3 draws up an inventory of the input uncertainties affecting the phenomenon and model of interests defined previously. Section 2.4 provides mathematical tools for the modeling of these uncertainties regarding the available information in input. Finally, Section 2.5 focuses on describing the different output quantities of interest.

2.2 Input-output black-box computer model

A computer code simulating the behavior of a complex aerospace (or other) system can be formally seen as an *input-output computer model*. A mathematical formulation of such a model

can be given by the following scalar-valued function:

$$\mathcal{M} : \left| \begin{array}{rcl} \mathcal{D}_{\mathbf{x}} \subseteq \mathbb{R}^d & \longrightarrow & \mathcal{D}_y \subseteq \mathbb{R} \\ \mathbf{x} & \longmapsto & y \end{array} \right. \tag{2.1}$$

where $\mathbf{x} = (x_1, \ldots, x_d)^\top$ is a set of d input variables (e.g., environmental or physical variables) and y a scalar ouput [1]. In general, the mapping $\mathcal{M}(\cdot)$ can be either defined using an analytical formula (or a system of formulas) or a high-fidelity computational model. Various examples can be found in the fields of structural design, propulsion, computational fluid dynamics or trajectory estimation. It is assumed here that $\mathcal{M}(\cdot)$ is *deterministic* (i.e., no intrinsic stochasticity) and *static* (i.e., time is not an explicit variable). It can be either linear or highly nonlinear and potentially expensive-to-evaluate, i.e., that a single run of the model can take several days (e.g., for codes involving finite element or finite volume analyses). Finally, this model may intricate a chain of multi-physics simulation codes (see, e.g., Balesdent, 2011; Brevault, 2015 in the context of multidisciplinary design optimization of launch vehicles). Regarding these multiple sources of complexity, this computer model will be considered as a *black-box* model only known pointwise. In the rest of the thesis, the different strategies under consideration are *non-intrusive* with respect to (w.r.t.) this black-box model. An illustration of the "black-box viewpoint" adapted to the simulation of satellite-debris collision is proposed in Figure 2.1.

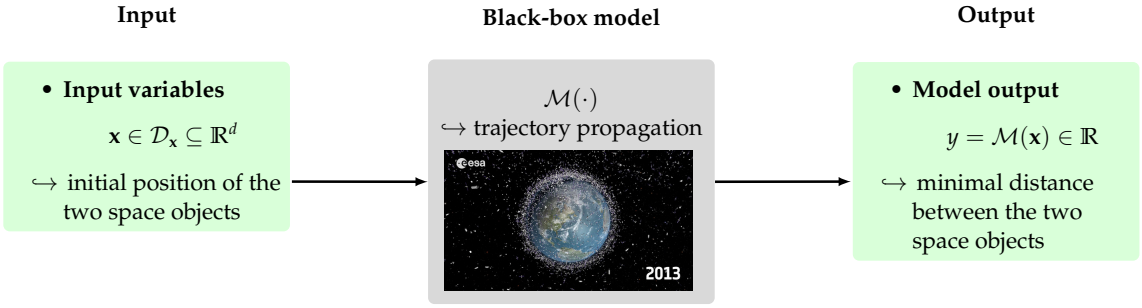

FIGURE 2.1: Example of the "black-box computer model" viewpoint (picture extracted from the video "*The story of space debris*" by ESA©, see http://www.esa.int).

As a remark, one should notice that considering a black-box computer model should not prevent the analyst from any possible comprehension of the phenomena that are at stake inside the computer model. Indeed, any information (e.g., about the inputs or regarding the code characteristics) that could provide the analyst a better understanding about the model should be taken into account. This remark is of utmost importance, especially when the black-box model is used in a context of reliability assessment.

Using simulation models in engineering does not prevent from the existence of several uncertainties and errors which may affect either the simulation or the real system. Depending at which conceptual step the analyst is working on (i.e., preliminary design phase, advanced design phase, certification phase or risk analysis), the potential impact of these uncertainties and errors ranges from soft to dramatic consequences (e.g., in terms of human safety, environmental impact and financial aspects). Thus, a key step in the UQ methodology (see Figure 1.1) is to draw up an inventory of the sources of uncertainties and to provide a dedicated mathematical framework to characterize and model them.

[1] In this thesis, it is assumed that the output of such a model can be reduced to a single scalar. Computer codes with vectorial or functional outputs are beyond the scope of the present manuscript.

2.3 Sources of uncertainties

For a successful use of a computer model, one needs to quantify its ability to predict the response of the real system. It is thus of paramount importance to quantify the uncertainties affecting the real system together with the various uncertainties and errors induced by the modeling phase.

Identifying the sources of uncertainties and errors is not an easy task as they affect all the different steps of the modeling and simulation processes. Moreover, the semantics used to characterize these uncertainties and errors varies from a scientific field to another one (see, e.g., the inventory proposed by Thunissen, 2005). Following Der Kiureghian and Ditlevsen (2009), one can state that engineering problems are studied within the confine of a model universe, i.e., within a certain given domain of validity, carrying its own set of models, equations, data. Thus, the model and its associated sources of uncertainties are defined by the analyst' choices, in order to make further decisions (e.g., for design, certification or risk analysis purposes).

In this thesis, the following classification of sources is adopted:

- *variability*: relates to the natural variability observed in the real system (e.g., inherent variability appearing in a manufacturing process of mechanical parts, or in the wind loads impacting an aircraft);
- *modeling errors*: relate either to the model form inadequacy (i.e., affecting $\mathcal{M}(\cdot)$) and model parameters' calibration, or to the numerical approximation errors;
- *input modeling uncertainties*: relate to the modeling of the inputs $\mathbf{x}$ based on available information (i.e., possible sparse and/or imprecise or qualitative data, measurement errors, expert opinions, standards). These uncertainties are often related to *statistical uncertainty* and *measurement uncertainty* arising in experimental procedures for data collection.

Once the sources of uncertainties have been clearly identified, one needs to characterize them following whether the analyst can, in near-term and regarding a reasonable budget, reduce them or not so as to improve the accuracy of the predictions. From an engineering point of view, one can distinguish between two types of uncertainties:

- *aleatory uncertainty* refers to natural randomness affecting physical phenomena (e.g., the pressure field in turbulent boundary layer or the geometrical distribution of inclusions in a biphasic microstructure). In a given context of maximum allowable budget, this type of uncertainty is considered as *irreducible*. Basically, referring to Eq. (2.1), aleatory uncertainty affects the input vector $\mathbf{x}$ of the environmental/physical variables;
- *epistemic uncertainty* refers to the lack of knowledge of the analyst and is potentially *reducible* by acquiring more information (i.e., data, measurements, expert judgements). Basically, referring to Eq. (2.1), epistemic uncertainty affects either the modeling of input vector $\mathbf{x}$ based on the available information (due to statistical uncertainty, measure uncertainty) or the model $\mathcal{M}(\cdot)$ by the specification of its parameters;

Again, following Der Kiureghian and Ditlevsen (2009), such a distinction between aleatory and epistemic uncertainty should not be considered as a classification of phenomena, but only a pragmatic way of distinguishing between the uncertainties on which the analyst can allocate some budget for gaining knowledge and those for which it is impossible. Based on this classification, the analyst can take information-based choices.

2.4 Probabilistic modeling of input uncertainties

Uncertainties in environmental or physical variables can be modelled using various frameworks and different mathematical concepts (see, e.g., Apostolakis, 1990; Paté-Cornell, 1996; Ferson and Ginzburg, 1996; Qiu et al., 2008; Ferson and Oberkampf, 2009). Usually, the choice for such a framework depends on the nature and amount of information available in input. Among various frameworks, one can distinguishes between the common *probabilistic framework* vs. the *imprecise probabilities* (see, e.g., Schöbi, 2017, Chap. 2). If the former requires to be able to construct a full input probabilistic model (e.g., by characterizing the joint probability distribution), the latter gathers various different (but connected techniques) which go beyond the probabilistic framework by using different tools such as, for instance, intervals, random sets, fuzzy probabilities and probability-bounds (among others). These two frameworks have demonstrated their respective usefulness in a large panel of engineering applications. As discussed in Beer et al. (2014), they should be seen more as complementary tools for the analyst than competing frameworks.

In this thesis, one assumes that sufficient information is available to construct an operational probabilistic model for the inputs. Imprecise probabilities are not presented hereafter for the sake of conciseness but a detailed description of the methods can be found in Beer et al. (2013) and Schöbi (2017). Thus, the following subsections aim at introducing the notations and to select the core probabilistic concepts that will be used throughout the thesis. It is important to highlight that, in the hereby manuscript, measure theory is not required to understand and use the concepts discussed further in this thesis (as exposed, e.g., in Jacod and Protter (2004) and Gut (2009)). For a broader view of probability theory and stochastic modeling for uncertainty quantification, the reader can refer, e.g., to the monographs by Sullivan (2015) and Soize (2017).

2.4.1 Elements of probability theory and stochastic modeling

Let the stochastic modeling of the natural variability affecting some inputs [2] of a computer model be represented by a d-dimensional continuous input vector $\mathbf{X} = (X_1, \ldots, X_d)^\top$. To define it formally, it implies to consider, first, a *probability space* $(\Omega, \mathcal{A}, \mathbb{P})$. This triplet contains, in order of appearance, the sample space Ω (each element $\omega \in \Omega$ can be seen as a combination of causes affecting the realization $\mathbf{x}$ of $\mathbf{X}$), a sigma-algebra $\mathcal{A}$ (whose elements are called *events*) and a probability measure $\mathbb{P} : \mathcal{A} \to [0,1]$. A *random vector* $\mathbf{X}$ (a.k.a. *multivariate random variable*) is a (measurable) function such that $\mathbf{X} : \Omega \to \mathcal{D}_{\mathbf{X}} \subseteq \mathbb{R}^d$, $\omega \mapsto \mathbf{X}(\omega) = \mathbf{x}$.

The distribution of a random vector $\mathbf{X}$ can be described, mostly, using two tools [3]:

- either by its joint *cumulative distribution function* (CDF) $F_{\mathbf{X}} : \mathbb{R}^d \to [0,1]$ which assigns a probability to the event $\{\mathbf{X} \leq \mathbf{x}\}$,
  i.e., $F_{\mathbf{X}}(\mathbf{x}) = F_{X_1,\ldots,X_d}(x_1, \ldots, x_d) = \mathbb{P}(\mathbf{X} \leq \mathbf{x}) = \mathbb{P}(X_1 \leq x_1, \ldots, X_d \leq x_d)$;
- or (assuming it exists, in the absolutely continuous case) by its joint *probability density function* (PDF) $f_{\mathbf{X}} : \mathbb{R}^d \to \mathbb{R}_+$ defined such that
  $f_{\mathbf{X}}(\mathbf{x}) = f_{X_1,\ldots,X_d}(x_1, \ldots, x_d) = \frac{\partial^d F_{\mathbf{X}}(\mathbf{x})}{\partial x_1 \ldots \partial x_d}$.

In addition, one can define several characteristics for the random vectors, e.g., its first two moments which are its mean vector $\mathbf{m}_{\mathbf{X}} = \mathbb{E}[\mathbf{X}]$ and its covariance matrix $\mathbf{\Sigma}_{\mathbf{X}} = \mathrm{Cov}[\mathbf{X}]$. They

[2] In this thesis, it is assumed that only continuous input variables are considered. When dealing with input/output variables, uppercase letters stands for quantities that are supposed to be random (i.e., considering mostly X, U, Θ and Y, but not other mathematical objects such as, e.g., N and T, which respectively refers to a number of samples and a transformation).

[3] Note that other probabilistic tools such as the *probability distribution* or the *characteristic function* could be considered (Soize, 2017).

respectively read:

$$\mathbf{m}_{\mathbf{X}} = \mathbb{E}[\mathbf{X}] = \int_{\mathcal{D}_{\mathbf{X}}} \mathbf{x} f_{\mathbf{X}}(\mathbf{x}) \mathrm{d}\mathbf{x} = (\mathbb{E}[X_1], \ldots, \mathbb{E}[X_d])^\top = (\mu_{X_1}, \ldots, \mu_{X_d})^\top \tag{2.2}$$

$$\begin{aligned} \mathbf{\Sigma}_{\mathbf{X}} &= \mathbb{E}\left[(\mathbf{X} - \mathbf{m}_{\mathbf{X}})(\mathbf{X} - \mathbf{m}_{\mathbf{X}})^\top\right] = \int_{\mathcal{D}_{\mathbf{X}}} (\mathbf{x} - \mathbf{m}_{\mathbf{X}})(\mathbf{x} - \mathbf{m}_{\mathbf{X}})^\top f_{\mathbf{X}}(\mathbf{x}) \mathrm{d}\mathbf{x} \\ &= \begin{bmatrix} \mathrm{Var}[X_1] & \mathrm{Cov}[X_1, X_2] & \ldots & \mathrm{Cov}[X_1, X_d] \\ \mathrm{Cov}[X_2, X_1] & \mathrm{Var}[X_2] & \ddots & \vdots \\ \vdots & \ddots & \ddots & \vdots \\ \mathrm{Cov}[X_d, X_1] & \ldots & \ldots & \mathrm{Var}[X_d] \end{bmatrix}. \end{aligned} \tag{2.3}$$

where:

- $\mathbb{E}[X_i] = \mu_{X_i} = \int x_i f_{X_i}(x_i) \mathrm{d}x_i$ is the expected value of X_i;
- $\mathrm{Var}[X_i] = \mathbb{E}[(X_i - \mathbb{E}[X_i])^2]$ is the variance of X_i;
- $\mathrm{Cov}[X_i, X_j] = \mathbb{E}\left[(X_i - \mathbb{E}[X_i])(X_j - \mathbb{E}[X_j])\right]$, for $i \neq j$, denotes the covariance between X_i and X_j (note that, if $i = j$, then $\mathrm{Cov}[X_i, X_i] = \mathrm{Var}[X_i]$).

Finally, one can introduce the *standard deviation* (s.d.) $\sigma_{X_i} = \sqrt{\mathrm{Var}[X_i]}$ and the *coefficient of variation* (c.v.) $\delta_{X_i} = \sigma_{X_i} / |\mu_{X_i}|$ (provided $\mu_{X_i} \neq 0$).

In this thesis, it is assumed that, for any random vector $\mathbf{X}$ under consideration, $\mathbf{X}$ is a second order random vector, i.e., that it belongs to $L^2(\Omega, \mathbb{R}^d)$, which ensures that $\mathbb{E}\left[\|\mathbf{X}\|_2^2\right] < +\infty$ [4]. Thus, the previous moments and quantities are assumed to be well-defined and finite.

Associated to these first two moments, the linear correlation matrix $\mathbf{R} = [\rho_{ij}]_{d \times d}$ is often encountered in probabilistic modeling. In this matrix, the coefficients ρ_{ij} are the *linear correlations* (a.k.a. *Pearson's correlations*) and are defined as follows:

$$\rho_{ij} = \frac{\mathrm{Cov}[X_i, X_j]}{\sqrt{\mathrm{Var}[X_i]\,\mathrm{Var}[X_j]}} = \frac{\mathrm{Cov}[X_i, X_j]}{\sigma_{X_i}\,\sigma_{X_j}}. \tag{2.4}$$

At this point, one needs to mention a fundamental theorem which allows one to define the probabilities of interest appearing in uncertainty quantification of industrial systems (e.g., probability of failure). This theorem is known as the *transport theorem* (see, e.g., Barbe and Ledoux, 2007).

Theorem 1 (Transport theorem). *Let $\mathbf{X}$ be a d-dimensional random vector with $f_{\mathbf{X}}$ as joint PDF. Assume that $\phi : \mathbb{R}^d \to \mathbb{R}$ a measurable function. Then $\mathbb{E}[\phi(\mathbf{X})]$ is given by:*

$$\begin{aligned} \mathbb{E}[\phi(\mathbf{X})] &= \int_{\mathbb{R}^d} \phi(\mathbf{x}) f_{\mathbf{X}}(\mathbf{x}) \mathrm{d}\mathbf{x} \\ &= \int_{\mathbb{R}^d} \phi(x_1, \ldots, x_d) f_{X_1, \ldots, X_d}(x_1, \ldots, x_d) \mathrm{d}x_1 \ldots \mathrm{d}x_d \end{aligned} \tag{2.5}$$

if the integral is absolutely convergent.

In the following, several results rely on the use of two fundamental convergence theorems in probability: namely, the *law of large numbers* (LLN) and the *central limit theorem* (CLT). These two

[4] $L^2(\Omega, \mathbb{R}^d)$ denotes the vector space (Hilbert space) of all the square integrable functions defined on Ω with values in $\mathbb{R}^d$ and $\|\cdot\|_2$ denotes the canonical Euclidean norm on $\mathbb{R}^d$.

theorems are not recalled here for the sake of conciseness, however, the interested reader may refer to Jacod and Protter (2004), Gut (2009) or Durrett (2010) concerning any further information.

As a remark, in the following of the thesis, as soon as it will be necessary, the sampling density w.r.t. to which the expected value is computed will be explicitly mentioned to avoid any confusion. As an example, Eq. (2.5) may be rewritten as $\mathbb{E}_{f_{\mathbf{X}}}[\phi(\mathbf{X})]$.

When independence is assumed (or verified) between input variables, one can write that the joint CDF or PDF consists of the product of the marginal distributions, i.e., that $F_{\mathbf{X}}(\mathbf{x}) = \prod_{i=1}^{d} F_{X_i}(x_i)$ and $f_{\mathbf{X}}(\mathbf{x}) = \prod_{i=1}^{d} f_{X_i}(x_i)$. When the assumption of independence is not verified, a full specification of the joint distribution of $\mathbf{X}$ (i.e., either the CDF $F_{\mathbf{X}}$ or the PDF $f_{\mathbf{X}}$) is supposed to be composed of:

- *d marginal distributions* (assumed to be known through their PDFs f_{X_i} or CDFs F_{X_i}, for $i = 1, \ldots, d$);
- a stochastic dependence structure modeled by a *copula* C (see Appendix A).

Basically, estimating marginal distributions is a traditional task performed using common statistical tools described in the next subsection. As for the copula, it represents a *measure of dependence* which is required to properly define the stochastic dependence within a random vector. In common engineering practice, people only estimate linear correlation coefficients defined in Eq. (2.4). These scalar measures are not sufficient to completely describe the stochastic dependence. A brief overview about basic elements of copula theory is provided in Appendix A. For more details about it, the interested reder should refer to Nelsen (2006) and Lebrun (2013). From a pragmatic point of view, if copulas may be difficult to identify and to estimate in real applications, classical linear correlation coefficients could be replaced by more advanced measures, easier to estimate than the copula, to summarize the dependence structure (Dutfoy and Lebrun, 2009). In this thesis, for the sake of simplicity, it will be assumed that the dependence structures considered can be either modeled by the *independent copula* or by the *normal copula* (see Appendix A).

Finally, in the following, $\mathbf{X}$ is called the vector of "*basic variables*" (instead of "environmental" or "physical" variables) since they are assumed to be observable and that possible empirical data could be available to characterize them (Der Kiureghian and Ditlevsen, 2009). These variables express the natural variability, as exposed in Section 2.3, that may occur in the system itself (e.g., variability of material properties) or arising in its environment (e.g., wind loads on a structure).

2.4.2 Estimating the joint input probability distribution

Engineering practice often relies on various heterogeneous sources of information to construct the joint distribution. For instance, one can dispose of experimental data and measurements (e.g., wind tunnel experiments, flight tests), high-fidelity numerical data (e.g., data issued from an expensive-to-evaluate computer model), expert judgments, literature-based recommendations or standards. Depending on the information type, one can use dedicated methods to construct an underlying probabilistic model.

From the data analysis point of view (i.e., the experimental or numerical data), one would like to find the underlying probabilistic model that produced these data. To do so, one can assume that an empirical dataset of *n data points* (a.k.a. *observations*) about an input variable X (instead of the vector $\mathbf{X}$ for the sake of clarity) of the computer model is available. This dataset is denoted by $\mathcal{X} = \{x^{(1)}, \ldots, x^{(n)}\}$. Moreover, it is assumed that these observations are *independent and identically distributed* (i.i.d.). Thus, two different statistical points of view can be adopted concerning the underlying probabilistic model that led to these observations:

- either one makes the prior assumption that the underlying probability distribution belongs to an algebraic class of distributions (i.e., a parametric family) and that a full specification of the distribution requires to estimate its parameters. This point of view refers to the *parametric statistics* (see, e.g., Rhode, 2014).;
- or, no prior assumption is required on the underlying probability distribution. This point of view refers to the *nonparametric statistics*. These methods directly approximate the unknown distribution without any parameter estimation (e.g., by means of *kernel density estimation*, see, e.g., Silverman, 1986; Wand and Jones, 1995; Scott, 2015).

In this thesis, it is assumed that the type of the joint distribution (i.e., either the CDF or the PDF) of the random vector of the basic variables $\mathbf{X}$ is known. The joint distribution (here the PDF) is supposed to belong to a parametric family $\mathcal{P}$ such that:

$$\mathcal{P} = \{f_{\mathbf{X}}(\cdot;\boldsymbol{\theta}) \mid \boldsymbol{\theta} \in \mathcal{D}_{\boldsymbol{\theta}} \subseteq \mathbb{R}^{n_\theta}\} \tag{2.6}$$

where $\boldsymbol{\theta}$ stands for the distribution/law parameters. Throughout the thesis, the following notation will be used to denote that "$\mathbf{X}$ *is distributed according to* $f_{\mathbf{X}}$": "$\mathbf{X} \sim f_{\mathbf{X}}$". Sometimes, one will express that "$\mathbf{X}$ *follows a given probability distribution*" by "$\mathbf{X} \sim \mathcal{D}\text{istrib}(\boldsymbol{\theta})$" (e.g., in the multivariate Gaussian case, $\mathbf{X} \sim \mathcal{N}_d(\mathbf{m}_{\mathbf{X}}, \boldsymbol{\Sigma}_{\mathbf{X}})$).

The first assumption (i.e., the parametric assumption) relies on the prior fact that sufficient data is available to estimate the marginal distributions and the dependence structure. Then, estimating the distribution parameters can be achieved by several methods which are not detailed here for the sake of conciseness. For the interested reader, a brief summary about this topic is provided in Appendix B.

As for the choice of the parametric family $\mathcal{P}$, it is assumed that it can be achieved by using some *goodness-of-fit* tests to get an objective measure of the best distribution type that would fit the given data (Ditlevsen, 1993). For instance, one can cite, among others, the *Kolmogorov-Smirnov* test, the *Cramer-von Mises* test or the *Anderson-Darling* test (see, e.g., Nikolaidis et al., 2004, Chap. 26). Another common approach to rationally find an input distribution is to use the *Maximum Entropy Principle* (see, e.g., Soize, 2017, Chap. 5).

2.4.3 Mapping to the standard normal space

An interesting feature allowed by considering an input probabilistic modeling is that, when necessary, one can apply a *transformation* (a.k.a. *mapping*) from the *original space* (a.k.a. *physical space* or just "$\mathbf{x}$-space") to the so-called *standard normal space* (denoted as "$\mathbf{u}$-space") in which all the random components of $\mathbf{X} \sim f_{\mathbf{X}}$ become independent standard Gaussian variates gathered in the vector $\mathbf{U} \sim \varphi_d$, with $\varphi_d : \mathbb{R}^d \to \mathbb{R}_+$ is the d-dimensional standard Gaussian PDF recalled here for the sake of clarity:

$$\varphi_d(\mathbf{u}) = \frac{1}{(2\pi)^{d/2}} \exp\left[-\frac{\|\mathbf{u}\|_2^2}{2}\right]. \tag{2.7}$$

Various reasons can be invoked for applying such a mapping on the input variables. As a first reason, one can argue that, due to the mixing between several different input variables, which may represent heterogeneous physical quantities (different units, different ranges of magnitude), the $\mathbf{x}$-space can be potentially unscaled and asymmetric (and the joint probability distribution may have a very distorted shape). Dealing with a centered and scaled input space potentially provides an easier way to analyze the input space. Another interesting feature is that, after having applied the transformation, the input variables become independent. Several mathematical and numerical tools used in the various steps of the UQ methodology (e.g., with

some specific sensitivity analysis methods) require the inputs to be independent. A last argument, which is more a combination of the two others, is related to some historical methodological developments, appeared in the early 1970s among the structural reliability community, which stressed the need for the introduction of the following transformations detailed below. A few details about these connections are recalled in Section 2.5 and in Chapter 3, since they are prerequisite for the development of several methods and safety measures.

More rigorously, one needs first to construct a $\mathcal{C}^1$-diffeomorphism [5] such that $T : \mathcal{D}_{\mathbf{X}} \to \mathbb{R}^d$ and allowing (in terms of probability distributions) to get:

$$\mathbf{U} = T(\mathbf{X}) \Leftrightarrow \mathbf{X} = T^{-1}(\mathbf{U}) \tag{2.8}$$

where $\mathbf{U} = (U_1, \ldots, U_d)^\top$ is a d-dimensional standard Gaussian vector of independent normal variates U_i with zero means and unit standard deviations.

Depending on the available information about $\mathbf{X}$ (i.e., characteristics of its distribution), one can choose between different types of transformations (e.g., Nataf transformation, Rosenblatt transformation). These transformations potentially involve technical steps which are not recalled here for the sake of conciseness. Some details about these transformations are gathered in Appendix C.

2.5 Output quantities of interest

2.5.1 The goal-oriented viewpoint

Once the input probabilistic model for $\mathbf{X}$ has been set up, it is crucial, from the black-box point of view, to define what is/are the possible *quantity(ies) of interest* (QoI/QoIs). The in-between step of propagating the uncertainties through the black-box computer model can be achieved using several techniques which are *non-intrusive* w.r.t. the code, meaning that the inner part of the code is not modified by the propagation of uncertainties. Some of these techniques are reviewed in Chapter 3. Thus, prior to this step, one needs to define what the "*goal*" of the study is (Rachdi, 2011).

Due to the uncertainties in input, by propagating them through the code (which is assumed to be deterministic), the model output thus becomes a random variable denoted Y (assumed to be scalar in this thesis). The description of the computer model thus reads:

$$\mathcal{M} : \left| \begin{array}{ccc} \mathcal{D}_{\mathbf{X}} \subseteq \mathbb{R}^d & \longrightarrow & \mathcal{D}_Y \subseteq \mathbb{R} \\ \mathbf{X}(\omega) & \longmapsto & Y = \mathcal{M}(\mathbf{X}(\omega)) \end{array} \right. . \tag{2.9}$$

In the following, the dependence w.r.t. ω will be dropped for the sake of conciseness. At this point, for a set of N i.i.d. simulated inputs $\{\mathbf{X}^{(j)}\}_{j=1}^N$, one gets N simulated outputs $\{Y^{(j)}\}_{j=1}^N$. As a consequence, depending on the goal of the study, several different QoIs can be derived:

- one can reconstruct, respectively, the entire CDF $F_Y(\cdot)$ or PDF $f_Y(\cdot)$, to characterize the variability of the output;
- one can estimate some moments (e.g., $\mathbb{E}[Y]$ or $\mathrm{Var}[Y]$) to analyze the statistical behavior of Y;
- one can estimate a conservative measure, such as a quantile, for risk analysis:

$$q_\alpha = \inf_{y \in \mathbb{R}} \{F_Y(y) \geq \alpha\} \tag{2.10}$$

[5] A $\mathcal{C}^1$-diffeomorphism is a bijective mapping which is $\mathcal{C}^1$ (i.e., continuously-differentiable and whose inverse is $\mathcal{C}^1$ too.)

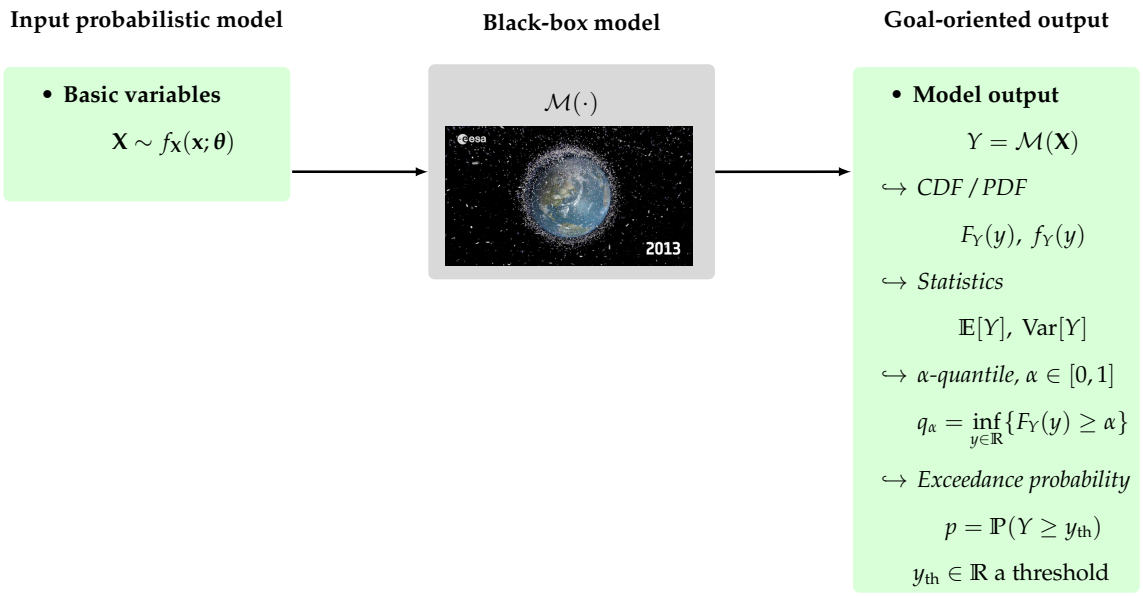

FIGURE 2.2: Goal-oriented viewpoint.

where q_α is the *α-quantile* of Y, with $\alpha \in [0,1]$ the *order*;

- one can estimate an exceedance probability w.r.t. a safety threshold for reliability analysis purpose:
$$p = \mathbb{P}(Y \geq y_{\mathrm{th}}) \tag{2.11}$$
where $y_{\mathrm{th}} \in \mathbb{R}$ is a scalar threshold level characterizing the system safety.

Such a "goal-oriented viewpoint" is illustrated in Figure 2.2 in the context of collision probability estimation. In such a case, the goal is to estimate a probability defined such that in Eq. (2.11). More generally, this thesis will focus on the specific goal of estimating rare event probabilities as the one defined hereinabove. As one may notice, the different goals listed above refer to different quantities which can imply to set up dedicated approaches. For instance, on the one hand, focusing on either the CDF, the PDF or the first moments of the model output Y requires to focus more on the central tendency and spread of the distribution of this random variable. On the other hand, focusing either on a quantile or an exceedance probability, thus requires to be very efficient in the characterization of the tails of the distribution of the model output.

2.5.2 A specific goal: estimating a rare event probability

It is assumed that the performance of the system of interest, modeled by $\mathcal{M}(\cdot)$, is measured by a deterministic scalar function $g : \mathbb{R}^d \to \mathbb{R}$ called the *limit-state function* (LSF) (a.k.a. *performance function*). A classical formulation for the LSF in the context of reliability assessment can be that the exceedance of a characteristic threshold output value, $y_{\mathrm{th}} \in \mathbb{R}$, beyond that the system is considered as in a failure state (see Eq. (2.11)). The LSF thus takes the form:

$$g(\mathbf{X}) = y_{\mathrm{th}} - \mathcal{M}(\mathbf{X}). \tag{2.12}$$

Based on the definition of $g(\cdot)$, one can remark that the zero values of this function represent an hypersurface in $\mathbb{R}^d$ called the *limit-state surface* (LSS) and defined by $\mathcal{F}_{\mathbf{x}}^0 = \{\mathbf{x} \in \mathcal{D}_{\mathbf{X}} \mid g(\mathbf{x}) = 0\}$. This LSS splits the input space of realizations into two canonical domains:

- the *failure domain* given by $\mathcal{F}_{\mathbf{x}} = \{\mathbf{x} \in \mathcal{D}_{\mathbf{X}} \mid g(\mathbf{x}) \leq 0\}$, which in fact does include the LSS $\mathcal{F}_{\mathbf{x}}^0$;
- the *safe domain* given by $\mathcal{S}_{\mathbf{x}} = \{\mathbf{x} \in \mathcal{D}_{\mathbf{X}} \mid g(\mathbf{x}) > 0\}$.

As an illustration of how all these domains are connected, one can consider a two-dimensional example as depicted in Figure 2.3.

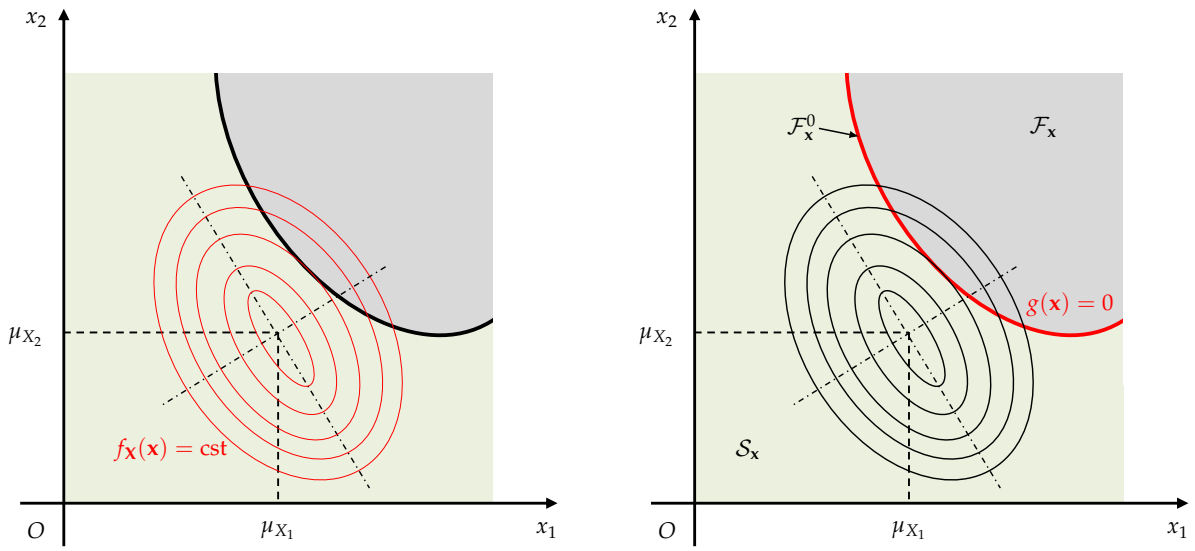

(a) Joint PDF isovalues.

(b) Safe $\mathcal{S}_{\mathbf{x}}$ vs. failure $\mathcal{F}_{\mathbf{x}}$ domains and LSS $\mathcal{F}_{\mathbf{x}}^0$.

FIGURE 2.3: Illustration on a two-dimensional example of the way the joint PDF $f_{\mathbf{X}}$ may intersect with the failure domain $\mathcal{F}_{\mathbf{x}}$.

Again, as a consequence of the black-box nature of the model $\mathcal{M}(\cdot)$, the LSF $g(\cdot)$ can only be evaluated pointwise and may possibly be defined only implicitly. The LSF is characterized by the same constraints as $\mathcal{M}(\cdot)$ (e.g., possibly expensive-to-evaluate, highly nonlinear). However, in more general settings, $g(\cdot)$ can involve a nonlinear equation of the model output, or may be defined through a combination of multiple failure criteria (e.g., as a union or intersection of failure events, often described as *system reliability*). For more information about this point, see, e.g., Lemaire et al. (2009).

A widely used *safety measure* in reliability assessment is the *failure probability*, denoted p_{f}, which is the probability that the system under consideration would fail w.r.t. the LSF defined in Eq. (2.12) and the input probabilistic model of $\mathbf{X}$. This probability is given by the following d-fold integral:

$$\begin{aligned} p_{\mathrm{f}} = \mathbb{P}(Y \geq y_{\mathrm{th}}) &= \mathbb{P}\left(g(\mathbf{X}) \leq 0\right) \\ &= \int_{\mathcal{F}_{\mathbf{x}}} f_{\mathbf{X}}(\mathbf{x}) \mathrm{d}\mathbf{x} = \int_{\mathcal{D}_{\mathbf{X}}} \mathbb{1}_{\mathcal{F}_{\mathbf{x}}}(\mathbf{x}) f_{\mathbf{X}}(\mathbf{x}) \mathrm{d}\mathbf{x} = \mathbb{E}_{f_{\mathbf{X}}}\left[\mathbb{1}_{\mathcal{F}_{\mathbf{x}}}(\mathbf{X})\right] \end{aligned} \tag{2.13}$$

where $\mathrm{d}\mathbf{x} = \mathrm{d}x_1 \ldots \mathrm{d}x_d$ and $\mathbb{1}_{\mathcal{F}_{\mathbf{x}}}(\cdot)$ is the *indicator function* of the failure domain defined such that $\mathbb{1}_{\mathcal{F}_{\mathbf{x}}}(\mathbf{x}) = 1$ if $\mathbf{x} \in \mathcal{F}_{\mathbf{x}}$ and $\mathbb{1}_{\mathcal{F}_{\mathbf{x}}}(\mathbf{x}) = 0$ otherwise. As a remark, one can notice that, properly writing, reliability assessment could refer to the estimation of another safety measure: the *reliability* R of a system. It is simply defined as the complementary of the failure probability p_{f}, i.e., $R = 1 - p_{\mathrm{f}}$.

In the rest of this thesis, it will be assumed that the failure event is rare, i.e., that the failure probability p_f is small (i.e., $p_f \ll \frac{1}{N}$ with N the available simulation budget). In daily engineering practice, rare event failure probabilities often vary from 10^{-2} to 10^{-8} (Lemaire et al., 2009). The latter order of magnitude may often characterize highly-safe complex engineering systems for which the safety requirements are drastic (e.g., aerospace systems, nuclear power plants or civil engineering structures).

An interesting feature about rare event probability estimation is related to the standard normal space mapping $T(\cdot)$ presented in Subsection 2.4.3. As a matter of fact, one can show that applying such a transformation should preserve the failure probability estimate.

To do so, one should first redefine the LSF in the standard normal space. It leads to consider the mapping $\mathring{g} : \mathbb{R}^d \to \mathbb{R}$ defined such that:

$$\mathbf{u} \mapsto \mathring{g}(\mathbf{u}) = \left(g \circ T^{-1}\right)(\mathbf{u}). \tag{2.14}$$

As a consequence, based on the proper construction of $T(\cdot)$ and due to its properties (see Appendix C), one can rewrite the problem in Eq. (2.13) as follows:

$$p_f = \mathbb{P}\left(\mathring{g}(\mathbf{U}) \leq 0\right) = \int_{\mathcal{F}_\mathbf{u}} \varphi_d(\mathbf{u}) \mathrm{d}\mathbf{u} = \int_{\mathbb{R}^d} \mathbb{1}_{\mathcal{F}_\mathbf{u}}(\mathbf{u}) \varphi_d(\mathbf{u}) \mathrm{d}\mathbf{u} = \mathbb{E}_{\varphi_d}\left[\mathbb{1}_{\mathcal{F}_\mathbf{u}}(\mathbf{U})\right] \tag{2.15}$$

where $\mathcal{F}_\mathbf{u} = \{\mathbf{u} \in \mathbb{R}^d \mid \mathring{g}(\mathbf{u}) \leq 0\}$ stands for the failure domain in the standard space, $\mathrm{d}\mathbf{u} = \mathrm{d}u_1 \ldots \mathrm{d}u_d$ and φ_d is the d-dimensional standard Gaussian PDF given in Eq. (2.7).

To conclude, this "duality of working spaces" offers a lot of possibilities for rare event estimation. Due to the powerful transformations recalled in Appendix C, the analyst may use several algorithms whose implementation requires to work in the **x**-space or in the **u**-space. Due to the properties of the transformation, p_f remains an invariant which makes reliability assessment relevant in any of those spaces. As a counterpart, the relative interpretations one can postulate about specific numerical results (e.g., sensitivities, behavior of $g(\cdot)$ vs. $\mathring{g}(\cdot)$, independent vs. dependent inputs) may be tricky and switching between both spaces is not simple. A deeper discussion about this last point will be provided in Chapter 3 and Chapter 4.

2.6 Conclusion

This chapter has set the general framework of uncertainty modeling for black-box input-output computer models. Starting from the formal definition of the type of model under study (i.e., black-box, deterministic, static models), an inventory of the sources of uncertainty arising in input of the model has been provided. The probabilistic characterization of these uncertainties has been presented before describing the possible output QoIs one can investigate. Thus, choosing a particular QoI (e.g., an exceedance probability) may imply to consider dedicated strategies for uncertainty propagation and for sensitivity analysis. The goal-oriented viewpoint imposed by the choice of this QoI will impact the possible interpretation of the results of these two other types of analyses.

In the next chapter, a brief review of the main uncertainty propagation techniques for rare event probability estimation is provided. These techniques are core ingredients for estimating probabilities such as those written in Eqs. (2.13) and (2.15). Similarly, it will be shown how the duality between **x**-space and **u**-space leads to different techniques and can be utilized in practical implementations.

CHAPTER 3

Rare event probability estimation

Contents

3.1 Introduction and motivations

Reliability assessment of complex systems is a problem whose final aim remains a *decision-making process* (Benjamin and Cornell, 1970). Indeed, reliability analysis cannot itself prevent real failure from happening. It is just a scientific (rational) way for providing relevant information, consistent with the underlying or explicit assumptions adopted w.r.t. the set of models under study (i.e., the model of the system itself and the associated uncertainties affecting its behavior), to the decision-maker (Au and Wang, 2014). Among several possible indicators (e.g., some are more qualitative, others are more quantitative), a set of *safety measures* is available. In this thesis, a particular focus is given on the *failure probability* p_f which is a widely used measure. For the sake of clarity, one recalls the two core definitions of p_f, respectively in the $\mathbf{x}$-space :

$$p_\mathrm{f} = \mathbb{P}\left(g(\mathbf{X}) \leq 0\right) = \int_{\mathcal{F}_\mathbf{x}} f_\mathbf{X}(\mathbf{x})\mathrm{d}\mathbf{x} = \int_{\mathcal{D}_\mathbf{X}} \mathbb{1}_{\mathcal{F}_\mathbf{x}}(\mathbf{x}) f_\mathbf{X}(\mathbf{x})\mathrm{d}\mathbf{x} = \mathbb{E}_{f_\mathbf{X}}\left[\mathbb{1}_{\mathcal{F}_\mathbf{x}}(\mathbf{X})\right] \tag{3.1}$$

and in the $\mathbf{u}$-space :

$$p_\mathrm{f} = \mathbb{P}\left(\mathring{g}(\mathbf{U}) \leq 0\right) = \int_{\mathcal{F}_\mathbf{u}} \varphi_d(\mathbf{u})\mathrm{d}\mathbf{u} = \int_{\mathbb{R}^d} \mathbb{1}_{\mathcal{F}_\mathbf{u}}(\mathbf{u})\varphi_d(\mathbf{u})\mathrm{d}\mathbf{u} = \mathbb{E}_{\varphi_d}\left[\mathbb{1}_{\mathcal{F}_\mathbf{u}}(\mathbf{U})\right]. \tag{3.2}$$

The key topic raised in this chapter concerns the efficient evaluation (i.e., numerical approximation) of these d-fold integrals by diverse techniques. Generally speaking, these techniques are known as *uncertainty propagation* techniques since their aim is to propagate the uncertainties from the input to the output of the computer model. However, as presented in the previous chapter, different goals (e.g., focusing on the central tendency and spread of the output distribution of Y vs. the tail of the distribution to get p_f) may require different techniques to propagate the uncertainties. Here, the QoI is a rare failure probability (i.e., $p_\mathrm{f} \ll \frac{1}{N}$ with N the available simulation budget) and thus, only the relevant estimation techniques regarding such a type of QoI are reviewed.

This chapter does not aim at presenting an exhaustive review about uncertainty propagation techniques, but only providing a compendium about a few of them which are widely used in the context of rare event estimation. These mathematical techniques arise from different periods (from the last 1950s to the early 2000s for those presented hereinafter) and spread through various scientific communities (neutronics, civil engineering, aerospace engineering and finance). Presenting them imposes to find an underlying rationale. To find it, one can analyze the two previous formulas in Eqs. (3.1) and (3.2). As suggested by these equations, the estimation of these two expected values (both equal to p_f) finally rely on two fundamental components (**Cpnt. #1** and **Cpnt. #2**) which appear in the integrands:

- **Cpnt. #1**: the *failure region*, embodied by the indicator function $\mathbb{1}_{\mathcal{F}_\bullet}(\cdot)$ or, similarly, by the integration domain $\mathcal{F}_\bullet$ (where $\bullet$ stands for $\mathbf{x}$ or $\mathbf{u}$). These elements are directly related to the behavior of the model $\mathcal{M}(\cdot)$ w.r.t. to a specific failure scenario given by the LSF $g(\cdot)$ (or $\mathring{g}(\cdot)$);
- **Cpnt. #2**: the *distribution of samples* given by the sampling densities $f_\mathbf{X}$ (or φ_d), which is related to the input probabilistic model (either directly in the $\mathbf{x}$-space or indirectly, via the transformation $T(\cdot)$, in the $\mathbf{u}$-space).

As one should notice, these two components do work together. If the **Cpnt. #1** refers to the location of the unknown failure region in the input space, **Cpnt. #2** refers to the way the samples are "likely to go" towards this failure region or not. By keeping this in mind (i.e., *Where does the failure region is likely to be located?* and *How does the algorithm go there?*), one may better understand the underlying rationale between all the following rare event estimation techniques.

This chapter is organized as follows. Section 3.2 reviews the crude Monte Carlo sampling. Then, three families of more advanced estimation techniques are presented. First, approximation-based reliability techniques are reviewed in Section 3.3. Then, importance sampling techniques (gathering multiple variants) are reviewed in Section 3.4. Finally, subset sampling is reviewed in Section 3.5. A synthesis and further discussions are proposed in Section 3.6.

3.2 Crude Monte Carlo sampling

Presentation. Historically, the *crude Monte Carlo* (CMC) sampling technique has been the first one used for uncertainty propagation in some pioneering works related to nuclear and particle physics in the early 1950s (Metropolis and Ulam, 1949; Kahn and Harris, 1951). The underlying principle of CMC sampling is the ability to generate random or pseudo-random samples from a given probability distribution (Gentle, 2003). The application of CMC sampling through various rare event estimation problems can be illustrated by a large amount of scientific production. Among others, the interested reader may refer to the books by Rubinstein and Kroese (2008), Rubino and Tuffin (2009), and Zio (2013).

Formulation. Considering a sample $\{\mathbf{X}^{(j)}\}_{j=1}^{N} \overset{\text{i.i.d.}}{\sim} f_{\mathbf{X}}$ of N i.i.d. copies of the input random vector $\mathbf{X}$ drawn according to $f_{\mathbf{X}}$. One recalls from Eq. (3.1) that:

$$p_{\mathrm{f}} = \int_{\mathcal{D}_{\mathbf{X}}} \mathbb{1}_{\mathcal{F}_{\mathbf{x}}}(\mathbf{x}) f_{\mathbf{X}}(\mathbf{x}) \mathrm{d}\mathbf{x} = \mathbb{E}_{f_{\mathbf{X}}}\left[\mathbb{1}_{\mathcal{F}_{\mathbf{x}}}(\mathbf{X})\right]. \tag{3.3}$$

The CMC estimator of p_{f} is given by:

$$\widehat{p}_{\mathrm{f}}^{\,\mathrm{CMC}} = \frac{1}{N} \sum_{j=1}^{N} \mathbb{1}_{\mathcal{F}_{\mathbf{x}}}(\mathbf{X}^{(j)}). \tag{3.4}$$

This estimator is a random variable as it is a sum of N i.i.d. Bernoulli random variables given by the indicator functions $\{\mathbb{1}_{\mathcal{F}_{\mathbf{x}}}(\mathbf{X}^{(j)})\}_{j=1}^{N}$. It converges almost surely to the target probability p_{f} as a consequence of the *law of large numbers* (LLN) [1]. No regularity condition is required on the performance function $g(\cdot)$ in order to apply LLN. Only finite expectation, such that $\mathbb{E}[|\mathbb{1}_{\mathcal{F}_{\mathbf{x}}}(\mathbf{X}^{(j)})|] < +\infty$, is required. The variance of this estimator is given by:

$$\mathrm{Var}\left[\widehat{p}_{\mathrm{f}}^{\,\mathrm{CMC}}\right] = \frac{1}{N} p_{\mathrm{f}}(1 - p_{\mathrm{f}}), \tag{3.5}$$

and its estimator is:

$$\widehat{\mathrm{Var}}\left[\widehat{p}_{\mathrm{f}}^{\,\mathrm{CMC}}\right] = \frac{1}{N} \widehat{p}_{\mathrm{f}}^{\,\mathrm{CMC}}(1 - \widehat{p}_{\mathrm{f}}^{\,\mathrm{CMC}}). \tag{3.6}$$

Using the *central limit theorem* (CLT), confidence intervals associated to the probability estimator can be calculated. Another widely used statistic to assess the sampling accuracy is the coefficient of variation (c.v.) of the estimator which writes as follows:

$$\delta_{\widehat{p}_{\mathrm{f}}^{\,\mathrm{CMC}}} = \frac{\sqrt{\mathrm{Var}\left[\widehat{p}_{\mathrm{f}}^{\,\mathrm{CMC}}\right]}}{\mathbb{E}[\widehat{p}_{\mathrm{f}}^{\,\mathrm{CMC}}]} = \sqrt{\frac{1 - p_{\mathrm{f}}}{N p_{\mathrm{f}}}}. \tag{3.7}$$

Advantages and drawbacks. As one may notice, whatever the dimension d of the input vector, the CMC convergence speed depends only on N and p_{f}. It means that CMC does not suffer from

[1] Consequently, this estimator is unbiased (i.e., $\mathbb{E}_{f_{\mathbf{X}}}\left[\widehat{p}_{\mathrm{f}}^{\,\mathrm{CMC}}\right] = p_{\mathrm{f}}$).

the so-called "*curse of dimensionality*" and is thus able to handle high-dimensional problems. Moreover, as mentioned before, this technique converges regardless the regularity of the LSF. Finally, another interesting aspect is its highly-distributable aspect which allows the respective calls to the LSF to be run in parallel. These three aspects are the main advantages of CMC sampling.

However, following Eq. (3.7), if p_f corresponds to a rare event probability, one can see that:

$$\lim_{p_\mathrm{f}\to 0} \delta_{\widehat{p}_\mathrm{f}^{\mathrm{CMC}}} = \lim_{p_\mathrm{f}\to 0} \frac{1}{\sqrt{N p_\mathrm{f}}} = +\infty. \tag{3.8}$$

Thus, the c.v. is unbounded. As a consequence, a practical rule of thumb to estimate a probability p_f of the order of $10^{-\alpha}$ with a 10% c.v. indicates that $N = 10^{\alpha+2}$ samples are required. Consequently, in a rare event context, the CMC technique requires a huge number of samples in order to achieve convergence on the estimation. Such a computational burden is often unaffordable in many industrial contexts due to the cost of a single run of a complex computer code (e.g., finite element or finite volume analyses).

Finally, assuming a substantial computational effort to achieve convergence, CMC is often considered as the "*reference method*" for failure probability estimation due to its strong statistical properties and its main advantages recalled hereabove.

Remarks. As a first remark, one should notice that, in the CMC sampling case, no transformation $T(\cdot)$ to the **u**-space is required. All the sampling phase is performed in the **x**-space. A second remark consists in noticing that CMC sampling can be used to estimate various quantities different from p_f. For instance, it can be used to get the empirical CDFs of the model output and the LSF (Dubourg, 2011, Chap. 3). It can also be used to estimate an α-quantile on the model output such as presented in Section 2.5 (Morio and Balesdent, 2015, Chap. 5). A third remark concerns the so-called *quasi Monte Carlo* (QMC) techniques (Lemieux, 2009): these techniques rely on the generation of quasi-random samples (i.e., samples drawn from low-discrepancy sequences). However, if they allow to reduce the computational cost for general uncertainty propagation over a general space, they are not adapted to rare event estimation since they provide a better global covering of the input space (i.e., they are said to be "space-filling"), but they poorly cover the tails of the input distribution (Morio and Balesdent, 2015, Chap. 5). In a sense, they are quite similar to the so-called *sparse grids* (a.k.a. *Smolyak's quadrature rules*, see, e.g., Bungartz and Griebel, 2004) which are deterministic quadrature rules adapted to high-dimensional problems. As a final remark, one should notice that, in the context of costly-to-evaluate computer models, hybrid strategies combining surrogate models and CMC have been proposed in Vazquez and Bect (2009), Echard et al. (2011), Bect et al. (2012), and Schöbi et al. (2017).

As a conclusion, following the goal-oriented viewpoint which is defined by the QoI one desires to estimate, i.e., a rare event probability p_f, CMC sampling seems to be unadapted to this task since it relies on sampling over the entire input space, no matter where the failure domain is. Consequently, the computational cost may become cumbersome for highly-safe industrial systems as getting samples in the failure domain may be difficult due to the rareness of the failure event. In addition, if the computer model is expensive to evaluate, CMC may become impractical. In the following, alternative techniques are reviewed, either based on taking better advantage of possible information about the failure domain, or based on more advanced sampling strategies.

3.3 Most-probable-failure-point-based techniques

Presentation. A first class of techniques regroups the so-called *most-probable-failure-point*-based (MPFP) techniques. Under this generic name, one more precisely refers mainly to the *first-order reliability method* (FORM) and the *second-order reliability method* (SORM). Historically developed among the structural reliability community, respectively in the mid 1970s and 1980s, these methods derived from earlier pioneering works such as, for instance, those of Rjanitzyne (late 1950s) and Cornell (1969) [2]. For the sake of conciseness, in the following, only FORM/SORM are presented and the interested reader is invited to refer to general textbooks on this subject (Madsen et al., 1986; Melchers, 1999; Ditlevsen and Madsen, 2007; Lemaire et al., 2009) for more information about the historical and technical developments of these methods.

Formulation. Contrary to CMC, whose strategy is to draw samples covering the entire $\mathbf{x}$-space so that some of these points may fall into the failure domain, the basic idea of MPFP-based techniques is to replace sampling by finding the point over the failure border, in the $\mathbf{u}$-space, corresponding to the maximum probability of occurrence of the failure event. This point is known as the *most probable failure point* (MPFP) (a.k.a. *design point*) and is denoted by P^*. As a consequence, the initial sampling problem set in Eq. (3.2) is replaced by an optimization problem whose aim is to find the coordinate vector $\mathbf{u}^*$ associated to P^*, such that:

$$\mathbf{u}^* = \underset{\mathbf{u}\in\mathbb{R}^d}{\arg\max}\ \mathbb{1}_{\mathcal{F}_\mathbf{u}}(\mathbf{u})\varphi_d(\mathbf{u}). \tag{3.9}$$

By definition of the $\mathbf{u}$-space, the previous problem can be rewritten as:

$$\begin{aligned}\mathbf{u}^* &= \underset{\mathbf{u}\in\mathbb{R}^d}{\arg\max}\ \frac{1}{(2\pi)^{d/2}}\exp\left[-\frac{1}{2}\mathbf{u}^\top\mathbf{u}\right] \quad \text{s.t.} \quad \mathbf{u}\in\mathcal{F}_\mathbf{u} \\ &= \underset{\mathbf{u}\in\mathbb{R}^d}{\arg\min}\ \mathbf{u}^\top\mathbf{u} \quad \text{s.t.} \quad \mathring{g}(\mathbf{u}) \leq 0.\end{aligned} \tag{3.10}$$

The quadratic optimization problem under nonlinear constraint, defined hereabove, can be solved by using dedicated algorithms (Rackwitz and Fiessler, 1978; Zhang and Der Kiureghian, 1994). Finally, the MPFP P^* appears to be the closest failure point w.r.t. the origin O of the standard normal space. As an illustration, one can refer to Figure 3.1 which allows a visualization in a two-dimensional space of the previous quantities. One can notice that, due to the exponential decay of the density in both radial and tangential directions, the MPFP P^* is thus the point providing the highest contribution to the integral in Eq. (3.2).

Assuming that the MPFP is unique, solving the optimization problem set in Eq. (3.10) allows one to compute the vector of coordinates $\mathbf{u}^*$. Thus, one can define a new safety measure, called the *Hasofer-Lind reliability index* (Hasofer and Lind, 1974), denoted by β_{HL} and defined such that:

$$\begin{aligned}\beta_{\text{HL}} = \beta &= \min_{\mathring{g}(\mathbf{u})=0}\ (\mathbf{u}^\top\mathbf{u})^{1/2} \\ &\equiv \boldsymbol{\alpha}^\top\mathbf{u}^*\end{aligned} \tag{3.11}$$

[2] The first safety measure defined in reliability is the *Rjanitzyne-Cornell reliability index* (Ditlevsen and Madsen, 2007; Lemaire et al., 2009). This index is based on the definition of the problem set in the $\mathbf{x}$-space, and thus, is not invariant w.r.t. linear transformations of the LSF. This problem led researchers to take advantage of the $\mathbf{u}$-space and the associated transformations to define invariant safety measures.

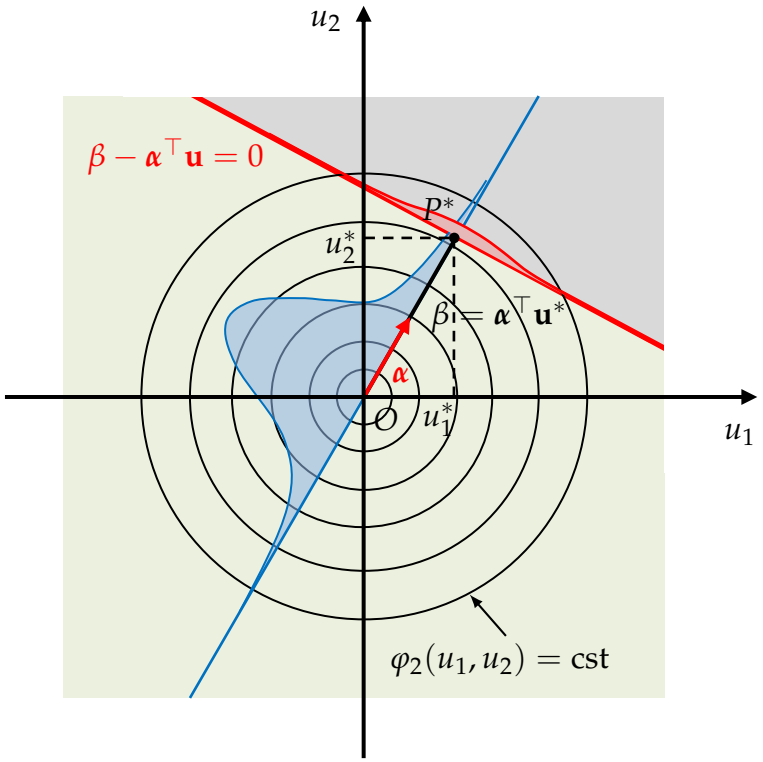

FIGURE 3.1: Illustration on a two-dimensional example of the standard normal space properties.

where $\boldsymbol{\alpha}$ is unit vector built as the opposite normalized gradient of the LSF [3], in the standard normal space, evaluated at the MPFP (see Figure 3.1):

$$\boldsymbol{\alpha} = -\frac{\nabla_{\mathbf{u}} \mathring{g}(\mathbf{u}^*)}{\left\| \nabla_{\mathbf{u}} \mathring{g}(\mathbf{u}^*) \right\|_2}. \tag{3.12}$$

In most cases, the origin O of the standard normal space lies in the safe domain. Consequently, β is positive and represents the shortest Euclidean distance between the origin O and the hyperplane that approximates the LSF (see Figure 3.1). As for $\boldsymbol{\alpha}$, it represents the unit vector pointing at the MPFP, thus providing a *most probable failure direction* on the (O, P^*) axis (see Figure 3.1). Assuming that the LSF is continuous, smooth and differentiable around the MPFP, one can apply the first-order Taylor series expansion such that:

$$\mathring{g}(\mathbf{u}) = \mathring{g}_1(\mathbf{u}) + o\left(\|\mathbf{u} - \mathbf{u}^*\|_2^2 \right) \tag{3.13}$$

with:

$$\mathring{g}_1(\mathbf{u}) = \mathring{g}(\mathbf{u}^*) + \nabla_{\mathbf{u}} \mathring{g}(\mathbf{u}^*)^\top (\mathbf{u} - \mathbf{u}^*). \tag{3.14}$$

[3] In some cases, it may appear that the gradient of the LSF approaches zero in a large area. It may happen when "saturation phenomena" occur which prevents traditional gradient-based optimization algorithms from convergence as noticed in Walz and Riesch-Oppermann (2006). Thus, using other strategies such as surrogate-based optimization algorithms can be relevant in this case (see, e.g., Chocat et al., 2016).

Since $\mathring{g}(\mathbf{u}^*) = 0$ by definition (recall that $P^* \in \mathcal{F}_{\mathbf{u}}^0$), and combining with Eq. (3.12), one gets:

$$\mathring{g}_1(\mathbf{u}) = \left\| \nabla_{\mathbf{u}} \mathring{g}(\mathbf{u}^*) \right\|_2 \left(\boldsymbol{\alpha}^\top \mathbf{u}^* - \boldsymbol{\alpha}^\top \mathbf{u} \right). \tag{3.15}$$

Thus, the *first-order reliability method* (FORM) consists in approximating the unknown probability p_{f} given in Eq. (2.13) by the following integral:

$$p_{\mathrm{f}}^{\mathrm{FORM}} = \mathbb{P}(\mathring{g}_1(\mathbf{U}) \leq 0) = \int_{\mathbb{R}^d} \mathbb{1}_{\mathcal{F}_{\mathbf{u},1}}(\mathbf{u}) \varphi_d(\mathbf{u}) \mathrm{d}\mathbf{u} \tag{3.16}$$

where $\mathcal{F}_{\mathbf{u},1} = \{\mathbf{u} \in \mathbb{R}^d \mid \mathring{g}_1(\mathbf{u}) \leq 0\} = \{\mathbf{u} \in \mathbb{R}^d \mid \beta - \boldsymbol{\alpha}^\top \mathbf{u} \leq 0\}$ (see Figure 3.1 for the visualization of this hyperplane). Eventually, this integral takes the form:

$$p_{\mathrm{f}}^{\mathrm{FORM}} = \mathbb{P}\left(-\boldsymbol{\alpha}^\top \mathbf{u} \leq -\beta \right) = \Phi(-\beta) = 1 - \Phi(\beta) \tag{3.17}$$

where $\Phi(\cdot)$ denotes the standard Gaussian CDF [4]. To summarize, the FORM approximation, illustrated on a two-dimensional example, is sketched in Figure 3.2a.

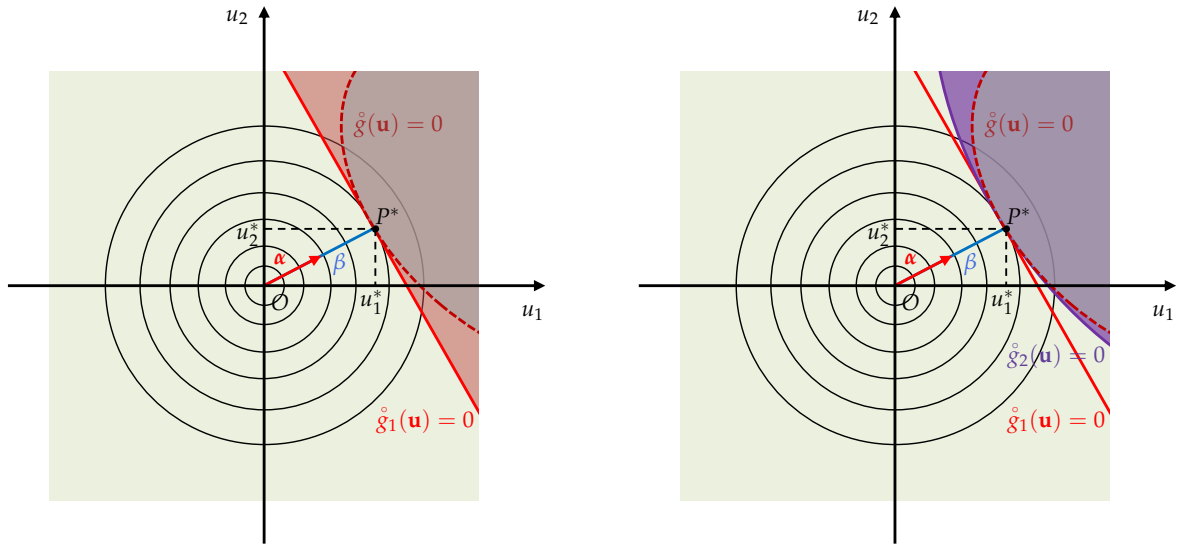

(a) FORM approximation.

(b) SORM approximation.

FIGURE 3.2: Illustration on a two-dimensional example of the FORM and SORM approximations.

When facing nonlinear LSS (e.g., a curvature at the MPFP), the FORM approximation may become too inaccurate. A second-order approximation can then be considered. Indeed, the *second-order reliability method* (SORM) consists in looking at the previous Taylor series expansion cut at the quadratic term such that:

$$\mathring{g}_2(\mathbf{u}) = \nabla_{\mathbf{u}} \mathring{g}(\mathbf{u}^*)^\top (\mathbf{u} - \mathbf{u}^*) + \frac{1}{2} (\mathbf{u} - \mathbf{u}^*)^\top \nabla^2_{\mathbf{u},\mathbf{u}} \mathring{g}(\mathbf{u}^*) (\mathbf{u} - \mathbf{u}^*) \tag{3.18}$$

where $\nabla^2_{\mathbf{u},\mathbf{u}}$ is the Hessian operator. Then, one can distinguish between two different SORM methods (Bourinet, 2018):

[4] By definition, $\Phi : \mathbb{R} \to \mathbb{R}_+$, $u \mapsto \frac{1}{\sqrt{2\pi}} \int_{-\infty}^{u} \exp\left[-\frac{\|t\|_2^2}{2} \right] \mathrm{d}t$.

- the *curvature-fitting* SORM (SORM-cf);
- the *point-fitting* SORM (SORM-pf).

These two methods provide approximate formulas for estimating p_f. For the sake of illustration, one can cite the asymptotic approximation (i.e., for $\beta \to +\infty$) proposed by Breitung (1984) in the SORM-cf context:

$$p_f^{\text{SORM-cf}} \approx \Phi(-\beta) \prod_{i=1}^{d-1} \frac{1}{\sqrt{1+\beta\kappa_i}} \tag{3.19}$$

where the κ_i, for $i = 1, \ldots, d-1$ being the principal curvatures of the LSS. As a remark, one should notice that the SORM-cf method requires to compute the Hessian matrix $\nabla^2_{\mathbf{u},\mathbf{u}} \mathring{g}(\mathbf{u}^*)$ which can be numerically cumbersome. For the sake of conciseness, the interested reader may refer to the textbook by Lemaire et al. (2009) and the monograph from Bourinet (2018) for a complete review of these formulations. To summarize, the SORM approximation, illustrated on the same two-dimensional example, is sketched in Figure 3.2b.

As one may notice, Eqs. (3.17) and (3.19) are built under the assumption of the uniqueness of the design point. Yet, in practice, nonlinear LSFs may present several failure regions of almost equal importance, which implies that several points may be candidate to be MPFPs. As an illustration, Figure 3.3 displays a two-dimensional example presenting two MPFPs of equal importance (denoted by $P^{*(1)}$ and $P^{*(2)}$) and the two FORM approximations of the LSS (denoted by $\mathring{g}_1^{(1)}(\mathbf{u}) = 0$ and $\mathring{g}_1^{(2)}(\mathbf{u}) = 0$) [5]. The analyst is often not aware of the existence of these regions before performing FORM/SORM analyses (i.e., that in Figure 3.3, the true LSS $\mathring{g}(\mathbf{u}) = 0$ is unknown for black-box computer models). To solve this problem, a technique (called "*multi*-FORM" in this thesis, by abuse of notation) proposed by Der Kiureghian and Dakessian (1998) aims at finding successively the various MPFPs. To do so, the first MPFP is found by applying a FORM analysis, and then, repeating another FORM analysis while modifying the LSF in order to evict the previous MPFP. The modification of the LSF consists in replacing the LSF area by a bulge centered at the current MPFP (see Der Kiureghian and Dakessian, 1998). Finally, the procedure is repeated until a spurious MPFP is obtained. Such a point arises due in the foot of the bulge and is just an artifical MPFP. For any further detail about this multi-FORM algorithm, the interested reader should refer, e.g., to Der Kiureghian and Dakessian (1998), Dubourg (2011), and Bourinet (2018).

Advantages and drawbacks. MPFP-based approximation techniques are intensively used in daily industrial practice. This can be explained by some undeniable advantages: provided that the LSF is linear and the input dimension is moderate, FORM may approximate very low failure probabilities at a negligible simulation cost. This makes FORM be one of the less expensive rare event estimation technique. For checking about the presence of multiple MPFPs, the multi-FORM algorithm is available. Finally, if the LSF is nonlinear, SORM may potentially overcome this difficulty and provide an estimate of p_f at a reduced cost compared to sampling techniques. On this point, one should remark that SORM thus requires, in addition to finding the MPFP by a preliminary FORM analysis, the evaluation of the Hessian matrix $\nabla^2_{\mathbf{u},\mathbf{u}} \mathring{g}(\mathbf{u}^*)$ at P^* which can be cumbersome (e.g., estimated by finite differences, see Bourinet (2018, Chap. 1)).

Among the limitations attributed to FORM/SORM, one can mention the fact that they rely on prior approximations of the LSF which may be not validated a posteriori. Another key drawback remains that no control of the estimation error is available contrary to sampling-based techniques. Finally, a last drawback which does affect both FORM/SORM efficiencies is the input dimension d. As d gets larger, if the LSF is highly nonlinear, the estimation error of p_f may

[5] Note that real application cases of reliability assessment under multiple failure regions of almost equal weights, issued from the field of structural mechanics, can be found in Bourinet (2018, Chap. 3).

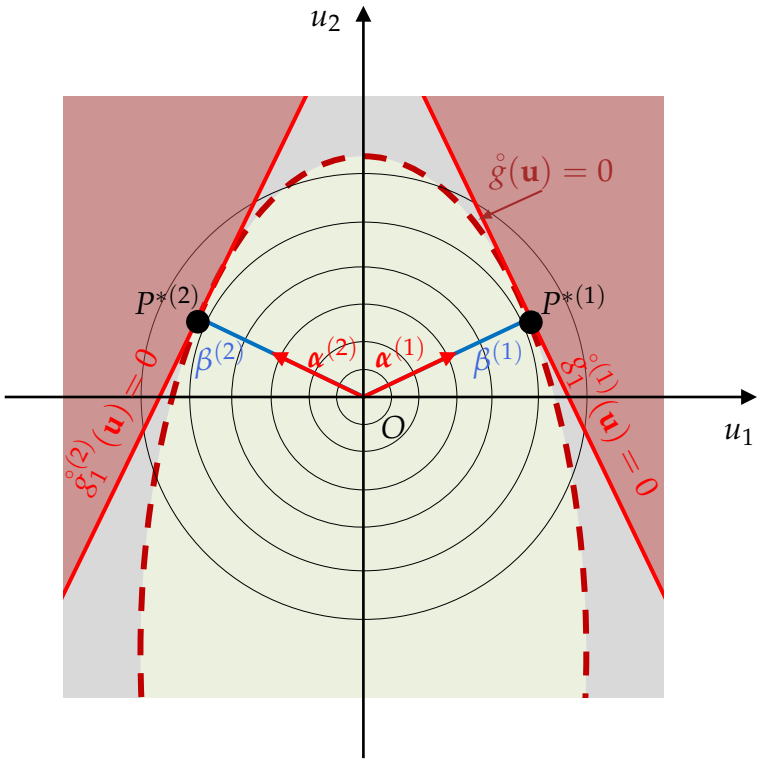

FIGURE 3.3: Illustration of a two-dimensional example presenting two MPFPs.

dramatically increase. Such a feature has been first pointed out by Schuëller and Stix (1987). In addition, a deeper geometric analysis proposed by Katafygiotis and Zuev (2008) and Valdebenito et al. (2010) shows that the notion of MPFP P^* loses its relevance for large d. Indeed, based on the geometric study of high-dimensional standard normal space, it can be shown that most of the probability mass of d-dimensional standard Gaussian PDF belongs to a spherical ring called the *important ring* (IR) (Katafygiotis and Zuev, 2008) which is approximately located at a distance of $\sqrt{d}$ from the origin of the $\mathbf{u}$-space. Thus, for large d, it can be proved, first, that the MPFP does not belong to the IR, and second, that its vicinity has a negligible contribution to the failure probability calculation. Thus, for high-dimensional problems, FORM/SORM approximations may induce significant errors for regions far from the MPFP (point where the Taylor series expansion is achieved), but which mostly contribute to the estimation of p_f (Valdebenito et al., 2010). Finally, as noticed by Hurtado (2012), if high-dimensional problems make the MPFP and its vicinity lacking of physical meaning, some relevant information about the failure region can still be used by looking at the vector $\boldsymbol{\alpha}$ as defined in Eq. (3.12) (being careful about the adopted sign convention).

Remarks. As a remark, an interesting feature about MPFP-based techniques consists of the various *by-products* (e.g., various different sensitivities) one can get from a reliability analysis using these techniques. This topic will be further discussed in Chapter 4.

As a conclusion, MPFP-based techniques may be very efficient in terms of cost reduction regarding the rareness of the failure event. However, they are often based on very restrictive assumptions w.r.t. the unknown LSF. In a context of black-box complex computer code, their efficiency is thus compromised. Another problem of these techniques may be their lack of ability

to efficiently find possible multiple failure regions due to the nonlinearities of the LSF. In the next section, the idea is to review some advanced sampling methods which are more efficient than CMC and which enable to concentrate the sampling effort in the regions of interest.

3.4 Importance sampling

General presentation. When facing the tremendous simulation cost imposed by CMC, one can use either approximation techniques such as those presented hereinabove, or to derive more efficient sampling techniques. One possible way to reduce the simulation cost associated to a rare event probability estimation is to use *variance reduction techniques* [6].

The underlying idea of this family of techniques is to derive estimators (e.g., of p_f) allowing a variance reduction of the estimation compared to the CMC estimator (Bucklew, 2004; Rubinstein and Kroese, 2008). Among them, *importance sampling* (IS) plays a major role for rare event probability estimation. The underlying idea of IS is to replace the initial sampling distribution $f_{\mathbf{X}}$ by an *auxiliary* (a.k.a. *instrumental*) distribution denoted by $h_{\mathbf{X}}$ in order to increase the number of samples drawn into the failure domain.

General formulation. Starting from Eq. (3.1) [7], one can notice that the representation of p_f as an expectation is not unique. Indeed, one can introduce a simple change in the sampling distribution (known as the "*importance sampling trick*") such that:

$$\begin{aligned} p_f &= \mathbb{E}_{f_{\mathbf{X}}}\left[\mathbb{1}_{\mathcal{F}_x}(\mathbf{X})\right] = \int_{\mathcal{D}_{\mathbf{X}}} \mathbb{1}_{\mathcal{F}_x}(\mathbf{x}) f_{\mathbf{X}}(\mathbf{x}) \mathrm{d}\mathbf{x} = \int_{\mathcal{D}_{\mathbf{X}}} \mathbb{1}_{\mathcal{F}_x}(\mathbf{x}) \frac{f_{\mathbf{X}}(\mathbf{x})}{h_{\mathbf{X}}(\mathbf{x})} h_{\mathbf{X}}(\mathbf{x}) \mathrm{d}\mathbf{x} \\ &= \mathbb{E}_{h_{\mathbf{X}}}\left[\mathbb{1}_{\mathcal{F}_x}(\mathbf{X}) \frac{f_{\mathbf{X}}(\mathbf{X})}{h_{\mathbf{X}}(\mathbf{X})}\right] \qquad (3.20) \\ &= \mathbb{E}_{h_{\mathbf{X}}}\left[\mathbb{1}_{\mathcal{F}_x}(\mathbf{X}) w_{\mathbf{X}}(\mathbf{X})\right] \qquad (3.21) \end{aligned}$$

where $w_{\mathbf{X}}(\mathbf{x}) \overset{\text{def}}{=} f_{\mathbf{X}}(\mathbf{x}) / h_{\mathbf{X}}(\mathbf{x})$ is called the *likelihood ratio*. Formally, the auxiliary PDF $h_{\mathbf{X}}$ should be such that it dominates the product $\mathbb{1}_{\mathcal{F}_x}(\mathbf{x}) f_{\mathbf{X}}(\mathbf{x})$ in the absolutely continuous sense:

$$h_{\mathbf{X}}(\mathbf{x}) = 0 \Rightarrow \mathbb{1}_{\mathcal{F}_x}(\mathbf{x}) f_{\mathbf{X}}(\mathbf{x}) = 0 \Longleftrightarrow \mathbb{1}_{\mathcal{F}_x}(\mathbf{x}) f_{\mathbf{X}}(\mathbf{x}) \neq 0 \Rightarrow h_{\mathbf{X}}(\mathbf{x}) \neq 0. \qquad (3.22)$$

This condition simply means that $\mathrm{supp}(\mathbb{1}_{\mathcal{F}_x} f_{\mathbf{X}}) \subseteq \mathrm{supp}(h_{\mathbf{X}})$. Hence, acknowledging that $\mathbb{1}_{\mathcal{F}_x}$ is more sensitivite to specific realizations $\mathbf{x}$ (i.e., those drawn in the failure region), the new "biased" density $h_{\mathbf{X}}$ should be chosen such that it favors the sampling within the important region.

The IS estimator of p_f, for $\{\mathbf{X}^{(j)}\}_{j=1}^{N} \overset{\text{i.i.d.}}{\sim} h_{\mathbf{X}}$, is given by:

$$\widehat{p}_f^{\,\mathrm{IS}} = \frac{1}{N} \sum_{j=1}^{N} \mathbb{1}_{\mathcal{F}_x}(\mathbf{X}^{(j)}) \frac{f_{\mathbf{X}}(\mathbf{X}^{(j)})}{h_{\mathbf{X}}(\mathbf{X}^{(j)})}. \qquad (3.23)$$

[6] This name gathers under the same heading various techniques such as: QMC, conditional MC, control variates, antithetic variates, stratified sampling, subset sampling and importance sampling. Giving a precise definition of each one is beyond the scope of this thesis. For a precise comparison and a focus on the links between all of these techniques, the interested reader should refer to Cannaméla (2007) and Munoz Zuniga (2011)

[7] Note that, here, derivations are performed in the $\mathbf{x}$-space to make the link with CMC. However, based on the same principle, similar derivations can be achieved in the $\mathbf{u}$-space.

This estimator is unbiased (i.e., $\mathbb{E}_{h_{\mathbf{X}}}\left[\widehat{p}_{\mathrm{f}}^{\mathrm{IS}}\right] = p_{\mathrm{f}}$) due to the previous dominating property of $h_{\mathbf{X}}$ and convergent by applying CLT. Its variance is given by:

$$\begin{aligned}\mathrm{Var}\left[\widehat{p}_{\mathrm{f}}^{\mathrm{IS}}\right] &= \frac{1}{N}\left(\mathrm{Var}_{h_{\mathbf{X}}}\left[\mathbb{1}_{\mathcal{F}_{\mathbf{x}}}(\mathbf{X})\frac{f_{\mathbf{X}}(\mathbf{X})}{h_{\mathbf{X}}(\mathbf{X})}\right]\right) \\ &= \frac{1}{N}\left(\mathbb{E}_{h_{\mathbf{X}}}\left[\left(\mathbb{1}_{\mathcal{F}_{\mathbf{x}}}(\mathbf{X})\frac{f_{\mathbf{X}}(\mathbf{X})}{h_{\mathbf{X}}(\mathbf{X})}\right)^2\right] - p_{\mathrm{f}}^2\right). \end{aligned} \tag{3.24}$$

and can be estimated using:

$$\widehat{\mathrm{Var}}\left[\widehat{p}_{\mathrm{f}}^{\mathrm{IS}}\right] = \frac{1}{N-1}\left(\frac{1}{N}\sum_{j=1}^{N}\mathbb{1}_{\mathcal{F}_{\mathbf{x}}}(\mathbf{X}^{(j)})w_{\mathbf{X}}^2(\mathbf{X}^{(j)}) - (\widehat{p}_{\mathrm{f}}^{\mathrm{IS}})^2\right). \tag{3.25}$$

To make IS efficient as a variance reduction technique, the auxiliary PDF needs to ensure that:

$$\mathrm{Var}_{h_{\mathbf{X}}}\left[\mathbb{1}_{\mathcal{F}_{\mathbf{x}}}(\mathbf{X})\frac{f_{\mathbf{X}}(\mathbf{X})}{h_{\mathbf{X}}(\mathbf{X})}\right] < \mathrm{Var}_{f_{\mathbf{X}}}\left[\mathbb{1}_{\mathcal{F}_{\mathbf{x}}}(\mathbf{X})\right]. \tag{3.26}$$

Theoretically, the optimal IS auxiliary PDF leading to the best variance reduction (i.e., the variance reducing to zero in Eq. (3.24)) is given by (Bucklew, 2004, Chap. 4):

$$h_{\mathbf{X}}^{*}(\mathbf{x}) = \frac{\mathbb{1}_{\mathcal{F}_{\mathbf{x}}}(\mathbf{x})f_{\mathbf{X}}(\mathbf{x})}{p_{\mathrm{f}}}. \tag{3.27}$$

Similar derivations in the $\mathbf{u}$-space would have led to a similar result, thus given by:

$$h_{\mathbf{U}}^{*}(\mathbf{u}) = \frac{\mathbb{1}_{\mathcal{F}_{\mathbf{u}}}(\mathbf{u})\varphi_d(\mathbf{u})}{p_{\mathrm{f}}}. \tag{3.28}$$

The practical use of these optimal densities is impossible due to their explicit dependence w.r.t. the unknown QoI one wants to estimate, which is p_{f}. Usually, the common strategy adopted is to find a so-called "sub-optimal" auxiliary density which approaches the theoretical one defined in Eqs. (3.27) and (3.28). Such an approximation procedure for finding a sub-optimal IS density can be achieved by several manners. In the following, three different IS techniques are reviewed:

- the nonadaptive IS techniques based on the design point;
- the *(parametric) adaptive importance sampling by cross-entropy* (AIS-CE);
- the *nonparametric adaptive importance sampling* (NAIS).

Figure 3.4 illustrates the problem of reliability estimation in the presence of multiple MPFPs on a real test-case proposed by Der Kiureghian and Dakessian (1998). The parabolic LSF is given by $\mathring{g}(\mathbf{u}) = b - u_2 - \kappa(u_1 - e)^2$, with u_1 and u_2 two standard normal variables, and b, κ and e three deterministic parameters. In this case, the optimal auxiliary density is multimodal and the approximation of the two modes is illustrated by the iso-contour lines.

3.4.1 Nonadaptive importance sampling techniques based on the design point

Presentation. The introduction of IS in the reliability community dates back from the 1980s (see, e.g., Shinozuka, 1983; Harbitz, 1986; Schuëller and Stix, 1987; Melchers, 1989) and is, thus, was spread through contemporary MPFP-based techniques. However, the idea of IS is already present in former rare event literature such as in Kahn and Harris (1951).

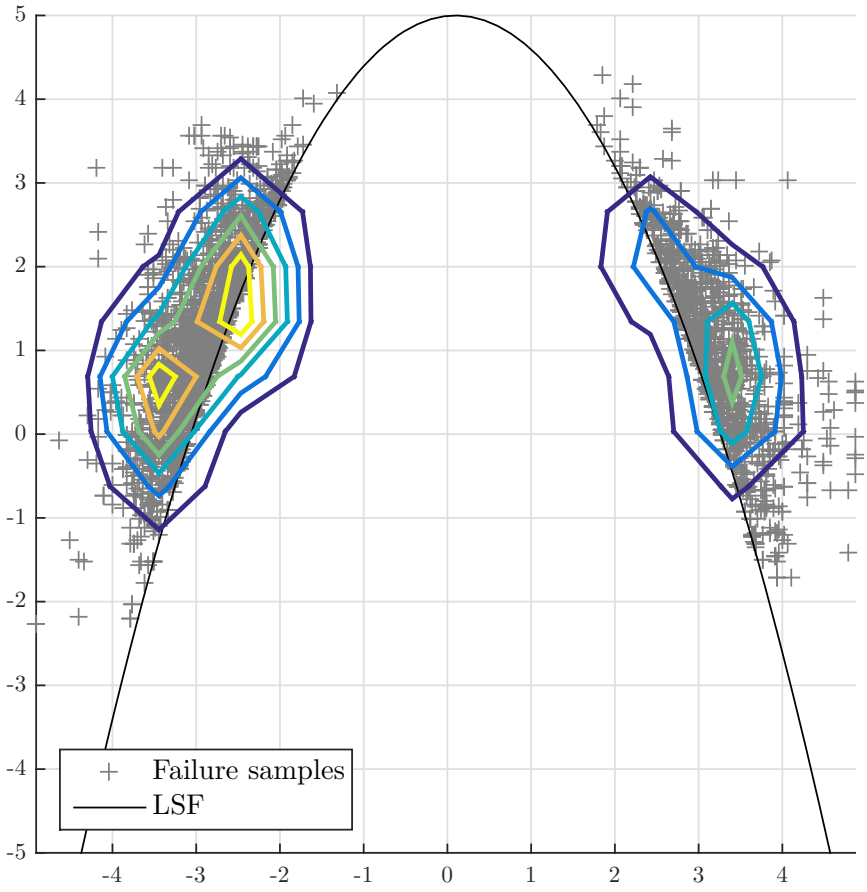

FIGURE 3.4: Illustration of the iso-contour lines of the approximation of the optimal auxiliary density for the parabolic LSF proposed by Der Kiureghian and Dakessian (1998) with the following parametrization: $b = 5$, $\kappa = 0.5$ and $e = 0.1$.

Formulation. Basically, the idea is to use the information brought by the MFPF to efficiently sample in its vicinity. Thus, assuming that the MPFP has been previously identified (e.g., using FORM or multi-FORM), Schuëller and Stix (1987) and Melchers (1989) propose to use the following sub-optimal auxiliary density in the $\mathbf{u}$-space:

$$h_{\mathbf{U}}^{\text{FORM}-\text{IS}}(\mathbf{u}) = \varphi_d(\mathbf{u} - \mathbf{u}^*) \tag{3.29}$$

which is, in fact, a d-dimensional standard normal PDF centered at the MPFP. The failure probability, assuming $\{\mathbf{U}^{(j)}\}_{j=1}^{N} \overset{\text{i.i.d.}}{\sim} h_{\mathbf{U}}^{\text{FORM}-\text{IS}}$, is then computed by:

$$\widehat{p}_{\text{f}}^{\text{FORM-IS}} = \frac{1}{N} \sum_{j=1}^{N} \mathbb{1}_{\mathcal{F}_{\mathbf{u}}}(\mathbf{U}^{(j)}) \frac{\varphi_d(\mathbf{U}^{(j)})}{h_{\mathbf{U}}^{\text{FORM}-\text{IS}}(\mathbf{U}^{(j)})}. \tag{3.30}$$

Another kind of MPFP-based IS, proposed independently by Harbitz (1986) and Bernard and Fogli (1986), differs from the previous one in the sense that, instead of centering the sampling density on the MPFP, it tries to exclude a β-sphere so as to prevent from drawing samples within the safe domain. This method is known in literature as *truncated importance sampling*

(TIS) or *radial-based importance sampling* (RBIS). The failure probability is then estimated, assuming $\{\mathbf{U}^{(j)}\}_{j=1}^{N} \overset{\text{i.i.d.}}{\sim} \varphi_d$, by the following formula:

$$\widehat{p}_{\text{f}}^{\text{TIS}} = (1 - F_{\chi_d^2}(\beta^2)) \frac{1}{N} \sum_{j=1}^{N} \mathbb{1}_{\{\|\mathbf{u}\|_2 > \beta\}}(\mathbf{U}^{(j)}) \tag{3.31}$$

where β is the β_{HL} presented in Section 3.3, $F_{\chi_d^2}(\cdot)$ the CDF of the chi-square distribution with d degrees of freedom (i.e., the number of input variables), and $\mathbb{1}_{\{\|\mathbf{u}\|_2 > \beta\}}$ the indicator function of the *outer* β-sphere domain.

Advantages and drawbacks. These nonadaptive techniques do require, at least, the knowledge of the MPFP (either its coordinates $\mathbf{u}^*$, or the associated reliability index β). However, in several cases, multiple unknown MPFPs have to be considered. Thus, by their nonadaptive character, these techniques can be restrictive and may focus on a certain failure region while ignoring others. A more complete review about these techniques is provided by Engelund and Rackwitz (1993).

Remarks. As a remark, and just to motivate the next subsection, it is worth to mention that the TIS/RBIS technique presented above has been extended by Grooteman (2008) and Grooteman (2011) with an adaptive sampling scheme using directional simulations [8]. Finally, one should notice that, in the context of expensive-to-evaluate computer models, a hybrid strategy combining a surrogate model and FORM-IS has been proposed by Echard et al. (2013).

In the following, one will focus more on adaptive techniques whose aim is to learn the optimal auxiliary sampling density with an iterative procedure.

3.4.2 Parametric adaptive importance sampling using cross-entropy optimization

Presentation. A first way to find a sub-optimal auxiliary density which approaches the optimal one, either defined in Eq. (3.27) or in Eq. (3.28), is to consider that such a PDF belongs to a *parametric family* of distributions. Then, the idea is to optimize the distribution parameters such that it may lead to the best variance reduction (Rubinstein, 1997), or similarly, such that the obtained density is the closest to the optimal one (Rubinstein, 1999). The optimization algorithm used here is called the *cross-entropy* (CE) method (see, e.g., Rubinstein and Kroese (2004) or Rubinstein and Kroese (2008, Chap. 8) for a review). Originally proposed by Rubinstein (1997), this method has been widely used for rare event estimation, such as in Homem-de-Mello and Rubinstein (2002), Kurtz and Song (2013), Mattrand and Bourinet (2014), Wang and Song (2016), and Geyer et al. (2019). Finally, as one will see below, the AIS-CE technique combines the IS point of view (i.e., optimal sampling), and a parametric adaptive fashion to modify the auxiliary density so as to evoluate towards the region of interest.

Formulation. Assume that $h_{\mathbf{X}}$ [9] belongs to a parametric family $\mathcal{H}$ such that:

$$\mathcal{H} = \{h_{\mathbf{X}}(\cdot; \boldsymbol{\lambda}) \mid \boldsymbol{\lambda} \in \mathcal{D}_{\boldsymbol{\lambda}} \subseteq \mathbb{R}^{n_{\boldsymbol{\lambda}}}\} \tag{3.32}$$

[8] Note that *directional simulations* (a.k.a. *directional sampling*) is another sampling technique which is not reviewed in this thesis, by sake of conciseness. Nonetheless, the interested reader may refer to Bjerager (1988) or Morio and Balesdent (2015, Chap. 7) for any further information.

[9] Note that, here, derivations are performed in the **x**-space. However, based on the same principle, similar derivations can be achieved in the **u**-space. For a full presentation of the CE method in the **u**-space, the interested reader may refer to Bourinet (2018).

with $\boldsymbol{\lambda} = (\lambda_1, \ldots, \lambda_{n_\lambda})$ a n_λ-(finite)-dimensional vector of distribution parameters. Then, the idea is to find $\boldsymbol{\lambda}$ such that $h_{\mathbf{X}}$ is the "closest" to the optimal density $h^*_{\mathbf{X}}$. Such a closeness between two densities can be measured by the so-called *Kullback-Leibler* (KL) *divergence* (a.k.a. *Kullback-Leibler distance* [10]) (Kullback and Leibler, 1951)

Definition 1 (Kullback-Leibler divergence)**.** *Let F_1 and F_2 be two probability distributions defined by their PDFs f_1 and f_2 with support $\mathbb{R}^d$. The Kullback-Leibler divergence between the two PDFs f_1 and f_2 is defined by:*

$$\mathcal{D}_{\mathrm{KL}}(f_1, f_2) = \int_{\mathbb{R}^d} f_1(\mathbf{x}) \ln\left(\frac{f_1(\mathbf{x})}{f_2(\mathbf{x})}\right) \mathrm{d}\mathbf{x}. \tag{3.33}$$

Thus, in the IS setting, the KL divergence between $h^*_{\mathbf{X}}$ and $h_{\mathbf{X}}$ is given by:

$$\begin{aligned}\mathcal{D}_{\mathrm{KL}}(h^*_{\mathbf{X}}, h_{\mathbf{X}}) &= \int_{\mathcal{D}_{\mathbf{X}}} h^*_{\mathbf{X}}(\mathbf{x}) \ln\left(\frac{h^*_{\mathbf{X}}(\mathbf{x})}{h_{\mathbf{X}}(\mathbf{x};\boldsymbol{\lambda})}\right) \mathrm{d}\mathbf{x} \\ &= \int_{\mathcal{D}_{\mathbf{X}}} h^*_{\mathbf{X}}(\mathbf{x}) \ln\left(h^*_{\mathbf{X}}(\mathbf{x})\right) \mathrm{d}\mathbf{x} - \int_{\mathcal{D}_{\mathbf{X}}} h^*_{\mathbf{X}}(\mathbf{x}) \ln(h_{\mathbf{X}}(\mathbf{x};\boldsymbol{\lambda}))\mathrm{d}\mathbf{x}. \end{aligned} \tag{3.34}$$

The value $\boldsymbol{\lambda}^*$ is thus obtained with:

$$\boldsymbol{\lambda}^* = \arg\min_{\boldsymbol{\lambda}\in\mathcal{D}_\lambda} \ \mathcal{D}_{\mathrm{KL}}(h^*_{\mathbf{X}}, h_{\mathbf{X}}) \tag{3.35}$$

$$= \arg\max_{\boldsymbol{\lambda}\in\mathcal{D}_\lambda} \ \int_{\mathcal{D}_{\mathbf{X}}} h^*_{\mathbf{X}}(\mathbf{x}) \ln(h_{\mathbf{X}}(\mathbf{x};\boldsymbol{\lambda}))\mathrm{d}\mathbf{x}. \tag{3.36}$$

Solving the above optimization problem is not straightforward since it explicitly depends on the unknown optimal density $h^*_{\mathbf{X}}$. However, it can be proved, following Rubinstein and Kroese (2004) and noticing that $h^*_{\mathbf{X}}(\mathbf{x}) \propto \mathbb{1}_{\mathcal{F}_x}(\mathbf{x}) f_{\mathbf{X}}(\mathbf{x})$ in Eq. (3.27), that it is equivalent to solve:

$$\boldsymbol{\lambda}^* = \arg\max_{\boldsymbol{\lambda}\in\mathcal{D}_\lambda} \ \int_{\mathcal{D}_{\mathbf{X}}} \mathbb{1}_{\mathcal{F}_x}(\mathbf{x}) \ln(h_{\mathbf{X}}(\mathbf{x};\boldsymbol{\lambda})) f_{\mathbf{X}}(\mathbf{x})\mathrm{d}\mathbf{x} \tag{3.37}$$

$$= \arg\max_{\boldsymbol{\lambda}\in\mathcal{D}_\lambda} \ \mathbb{E}_{f_{\mathbf{X}}}\left[\mathbb{1}_{\mathcal{F}_x}(\mathbf{X}) \ln(h_{\mathbf{X}}(\mathbf{X};\boldsymbol{\lambda}))\right]. \tag{3.38}$$

Again, to solve the above problem more efficiently, one can use the IS trick (i.e., by considering that one would prefer to sample according to a suitable density $h_{\mathbf{X}}(\cdot;\mathbf{q})$ rather than according to the initial density $f_{\mathbf{X}}(\cdot;\boldsymbol{\theta})$), one can get:

$$\boldsymbol{\lambda}^* = \arg\max_{\boldsymbol{\lambda}\in\mathcal{D}_\lambda} \ \int_{\mathcal{D}_{\mathbf{X}}} \mathbb{1}_{\mathcal{F}_x}(\mathbf{x}) \ln(h_{\mathbf{X}}(\mathbf{x};\boldsymbol{\lambda})) \frac{f_{\mathbf{X}}(\mathbf{x};\boldsymbol{\theta})}{h_{\mathbf{X}}(\mathbf{x};\mathbf{q})} h_{\mathbf{X}}(\mathbf{x};\mathbf{q})\mathrm{d}\mathbf{x} \tag{3.39}$$

$$= \arg\max_{\boldsymbol{\lambda}\in\mathcal{D}_\lambda} \ \mathbb{E}_{h_{\mathbf{X}}(\cdot;\mathbf{q})}\left[\mathbb{1}_{\mathcal{F}_x}(\mathbf{X})\ w_{\mathbf{X}}(\mathbf{X};\boldsymbol{\theta},\mathbf{q}) \ln(h_{\mathbf{X}}(\mathbf{X};\boldsymbol{\lambda}))\right]. \tag{3.40}$$

From a practical point of view, one can estimate $\boldsymbol{\lambda}^*$ by using the *stochastic counterpart* (see, e.g., Rubinstein, 1997; Dussault et al., 1997; Rubinstein and Kroese, 2004) of Eq. (3.40), that is, for

[10] Note that $\mathcal{D}_{\mathrm{KL}}(f_1, f_2)$ is a positive quantity and is equal to zero if and only if $f_1 = f_2$ almost everywhere. However, $\mathcal{D}_{\mathrm{KL}}(f_1, f_2)$ is not a distance since it is not symmetric (i.e., $\mathcal{D}_{\mathrm{KL}}(f_1, f_2) \neq \mathcal{D}_{\mathrm{KL}}(f_2, f_1)$).

$\{\mathbf{X}^{(j)}\}_{j=1}^{N} \overset{\text{i.i.d.}}{\sim} h_{\mathbf{X}}(\cdot;\mathbf{q})$:

$$\boldsymbol{\lambda}^* = \underset{\boldsymbol{\lambda}\in\mathcal{D}_{\boldsymbol{\lambda}}}{\arg\max}\ \frac{1}{N}\sum_{j=1}^{N} \mathbb{1}_{\mathcal{F}_{\mathbf{x}}}(\mathbf{X}^{(j)})\, w_{\mathbf{X}}(\mathbf{X}^{(j)};\boldsymbol{\theta},\mathbf{q}) \ln(h_{\mathbf{X}}(\mathbf{X}^{(j)};\boldsymbol{\lambda})). \tag{3.41}$$

The IS density $h_{\mathbf{X}}(\cdot;\mathbf{q})$ introduced in Eq. (3.41) gets different distribution parameters denoted as $\mathbf{q}$ to distinguish between the parameters at stake in the optimization process, i.e., $\boldsymbol{\lambda}$, and those uses for sampling (here $\mathbf{q}$). By denoting $\mathcal{E}_{\mathbf{x}} = \{\mathbf{X}^{(j)} \mid \mathbb{1}_{\mathcal{F}_{\mathbf{x}}}(\mathbf{X}^{(j)}) = 1\}$ as the *elite* set, i.e., the samples that lead to failure regarding the indicator function (or, in other words, the samples which belong to $\mathcal{F}_{\mathbf{x}}$), one can rewrite the previous equation as:

$$\boldsymbol{\lambda}^* = \underset{\boldsymbol{\lambda}\in\mathcal{D}_{\boldsymbol{\lambda}}}{\arg\max}\ \frac{1}{N}\sum_{\mathbf{X}^{(j)}\in\mathcal{E}_{\mathbf{x}}} w_{\mathbf{X}}(\mathbf{X}^{(j)};\boldsymbol{\theta},\mathbf{q}) \ln(h_{\mathbf{X}}(\mathbf{X}^{(j)};\boldsymbol{\lambda})). \tag{3.42}$$

The right-hand side term defined in Eq. (3.42) is reasonably assumed to be convex and differentiable w.r.t. $\boldsymbol{\lambda}$ (see, e.g., Rubinstein and Kroese, 2004; De Boer et al., 2005). Thus, a solution can be obtained by cancelling the gradient of Eq. (3.42), which leads to solve the following system of equations:

$$\frac{1}{N}\sum_{\mathbf{X}^{(j)}\in\mathcal{E}_{\mathbf{x}}} w_{\mathbf{X}}(\mathbf{X}^{(j)};\boldsymbol{\theta},\mathbf{q}) \nabla_{\boldsymbol{\lambda}} \ln(h_{\mathbf{X}}(\mathbf{X}^{(j)};\boldsymbol{\lambda})) = \mathbf{0}. \tag{3.43}$$

However, in the context of rare event probability estimation, the above equations are affected by the fact that the elite set $\mathcal{E}_{\mathbf{x}}$ may not contain enough failure points. As a remark, one can notice that Eq. (3.43) makes appear the gradient term $\nabla_{\boldsymbol{\lambda}} \ln(h_{\mathbf{X}})$ which is a *score function* (i.e., the partial derivative of the log-density). Such a quantity will be further used in the context of sensitivity analysis in Chapter 4 (see Section 4.4.1.2). This problem can be adaptively solved by the so-called *multilevel cross-entropy* (m-CE) technique as proposed by Rubinstein and Kroese (2004). This m-CE algorithm provides the adaptiveness of the AIS-CE technique. The idea is to introduce, jointly, a set of decreasing intermediate thresholds $\{y_s, s \in \mathbb{N}_+\}$ and a set of parameters $\{\boldsymbol{\lambda}_s, s \in \mathbb{N}\}$ (with $\boldsymbol{\lambda}_0 = \boldsymbol{\theta}$ for instance [11]) and iterate on both y_s and $\boldsymbol{\lambda}_s$. It is important to notice that the thresholds $\{y_s, s \in \mathbb{N}_+\}$ are iteratively estimated as α_{CE}-quantiles (with $\alpha_{\text{CE}} \in]0,1[$ a *rarity parameter*) from the set of N samples of LSF outputs $\mathcal{G}_{\mathbf{x}} = \{g(\mathbf{X}^{(j)})\}_{j=1}^{N}$. Finally, the quasi-optimal parameters $\{\boldsymbol{\lambda}_s, s \in \mathbb{N}\}$ are estimated as follows (assuming that $[k]$ is the current step):

$$\boldsymbol{\lambda}_{[k]} = \underset{\boldsymbol{\lambda}\in\mathcal{D}_{\boldsymbol{\lambda}}}{\arg\max}\ \frac{1}{N}\sum_{\mathbf{X}^{(j)}\in\mathcal{E}_{\mathbf{x},[k]}} \frac{f_{\mathbf{X}}(\mathbf{X}^{(j)})}{h_{\mathbf{X}}(\mathbf{X}^{(j)};\boldsymbol{\lambda}_{[k-1]})} \ln(h_{\mathbf{X}}(\mathbf{X}^{(j)};\boldsymbol{\lambda})) \tag{3.44}$$

where $\mathcal{E}_{\mathbf{x},[k]}$ is the elite set gathering the failure points regarding the current threshold $y_{[k]}$. As soon as the stopping criterion is satisfied, i.e., $y_{[k_\#]} \leq 0$ where $[k_\#]$ denotes the last step, the failure probability can be estimated by:

$$\begin{aligned}\widehat{p}_{\text{f}}^{\text{AIS-CE}} &= \frac{1}{N}\sum_{j=1}^{N} \mathbb{1}_{\{g(\mathbf{X}^{(j)})\leq y_{[k_\#]}\}}(\mathbf{X}^{(j)}) \frac{f_{\mathbf{X}}(\mathbf{X}^{(j)})}{h_{\mathbf{X}}(\mathbf{X}^{(j)};\boldsymbol{\lambda}_{[k_\#-1]})} \\ &= \frac{1}{N}\sum_{\mathbf{X}^{(j)}\in\mathcal{E}_{\mathbf{x},[k_\#]}} \frac{f_{\mathbf{X}}(\mathbf{X}^{(j)})}{h_{\mathbf{X}}(\mathbf{X}^{(j)};\boldsymbol{\lambda}_{[k_\#-1]})}\end{aligned} \tag{3.45}$$

[11] Note that, it is not compulsory to choose $h_{\mathbf{X}}$ in the same family of densities as $f_{\mathbf{X}}$.

where one sets $y_{[k_\#]} = 0$ according to the definition adopted in this thesis regarding the threshold [12]. In practice, AIS-CE algorithm requires to set several tuning parameters which are detailed in a dedicated part in Appendix D.

Advantages and drawbacks. The most noteworthy advantage of the AIS-CE technique is related to the fact that, when dealing with probability distributions belonging to the *natural exponential family* (NEF) (Rubinstein and Kroese, 2008, Appendix A.3), the CE problem set in Eq. (3.43) has an analytical solution. Thus, in the case of the m-CE algorithm, analytical updating formulas (e.g., in the Gaussian case) can be derived for distribution parameters (see, e.g., Morio and Balesdent, 2015, Chap. 5). Another advantage concerns its ability to be performed in both $\mathbf{x}$-space and $\mathbf{u}$-space which can be useful for some complex input probabilistic models (see, e.g., Bourinet, 2018). Finally, a last advantage concerns the fact that, similarly to CMC, one can directly control the estimation error using the estimator of the variance given in Eq. (3.25).

The main drawbacks pointed out for the AIS-CE technique concern the assumption that the auxiliary density belongs to a family of parametric *unimodal* distributions and often assumes statistical independence between random variables so that the parameters of the marginals can be updated separately. Thus, AIS-CE may become less efficient than other sampling techniques to approximate optimal densities when multiple failure regions present similar weights. To tackle this issue, several recent works try to combine AIS-CE and Gaussian mixtures (Kurtz and Song, 2013). However, in the case of Gaussian mixtures, closed-form expressions for the update of parameters cannot be derived (Geyer et al., 2019). Another problem concerns the potential high-dimensionality in input. As explained in Section 3.3 concerning the inefficiency of MPFP-based techniques for high-dimensional problems, AIS-CE suffers from a generic problem affecting IS techniques in general, i.e., the incapacity to sample within the important ring (Au and Beck, 2003; Katafygiotis and Zuev, 2008). Recent papers address this issue by considering other kind of mixtures than Gaussian ones (e.g., von Mises-Fisher mixture in Wang and Song (2016)) or demonstrate the poor performance of AIS-CE with Gaussian mixtures for high-dimensional problems (Geyer et al., 2019). Recently, a numerical comparison between AIS-CE and subset sampling (presented in Section 3.5) has been proposed in Bourinet (2018, Chap. 1). The numerical efficiency of these two sampling strategies are compared over three test-cases, included a high-dimensional problem and a series system reliability problem presenting multiple failure regions of equal weights. It appears that, provided the dimension is not too large and the LSF is smooth enough (and not presenting multiple failure regions of similar importance), the AIS-CE technique may be more efficient than subset sampling for very low failure probability and may be more accurate than subset sampling.

Remarks. As a first remark, one can mention a few works related to the CE method adapted to IS, aiming at bypassing the parametric assumption and thus proposing nonparametric-CE-based extensions of the traditional AIS-CE technique (see, e.g., Homem-de-Mello, 2007; Botev et al., 2007). As a second remark, one should notice that, in the context of costly-to-evaluate computer models, a hybrid strategy combining a surrogate model and AIS-CE has been proposed by Balesdent et al. (2013).

3.4.3 Nonparametric adaptive importance sampling by kernel density estimation

Presentation. Contrary to the parametric assumption made in AIS-CE, the *nonparametric adaptive importance sampling* (NAIS) relies on approximating the optimal auxiliary density by means

[12] Note that, for the interested reader who would be more familiar with "threshold exceeding" probability, similar algorithm is detailed following this notation in Morio and Balesdent (2015).

of *kernel density estimation* (KDE) (see Appendix B). The nonparametric view of IS dates back from the late 1990s, with pioneering works from Zhang (1996), Givens and Raftery (1996), and Au and Beck (1999). Then, several works explored the possibilities of NAIS for rare event estimation, in several different contexts for applications, such queueing systems and option pricing in Kim et al. (2000), Neddermeyer (2009), and Neddermeyer (2010) or reliability and risk assessment with Swiler and West (2010), Morio (2010), Morio (2011c), Morio (2012), Balesdent et al. (2014), and Morio and Balesdent (2016).

Formulation. The mathematical formulation of NAIS relies on KDE (see, for instance, Appendix B for a brief presentation of KDE) but is relatively similar to the m-CE algorithm presented previously. Considering a set of decreasing intermediate thresholds $\{y_s, s \in \mathbb{N}_+\}$ estimated as α_{NAIS}-quantiles from the set of N samples of LSF outputs $\mathcal{G}_{\mathbf{x}} = \{g(\mathbf{X}^{(j)})\}_{j=1}^{N}$ with $\alpha_{\text{NAIS}} \in]0,1[$ the *rarity parameter*, the NAIS algorithmic mechanism provides an iterative scheme for adaptively updating the kernel-based sampling auxiliary density. Thus, as an example, denoting by $[k]$ the current step (and omitting the subscripts "$\mathbf{X}$" for h and w for the sake of clarity), the updated auxiliary density therefore reads:

$$\widehat{h}_{[k+1]}(\mathbf{x}) = \frac{\det(\mathbf{H}_{[k]})^{-1/2}}{k\,N\,\widehat{I}_{[k]}} \sum_{[i]=1}^{[k]} \sum_{j=1}^{N} w_{[i]}(\mathbf{X}_{[i]}^{(j)})\; K_d\left(\mathbf{H}_{[k]}^{-1/2}(\mathbf{x} - \mathbf{X}_{[i]}^{(j)})\right) \tag{3.46}$$

where the likelihood ratio $w_{[i]}(\mathbf{X}_{[i]}^{(j)})$ is given by:

$$w_{[i]}(\mathbf{X}_{[i]}^{(j)}) = \mathbb{1}_{\{g(\mathbf{X}_{[i]}^{(j)}) \leq y_{[k]}\}}(\mathbf{X}^{(j)}) \frac{f_{\mathbf{X}}(\mathbf{X}_{[i]}^{(j)})}{\widehat{h}_{[i-1]}(\mathbf{X}_{[i]}^{(j)})} \tag{3.47}$$

and $\widehat{I}_{[k]}$ is estimated by:

$$\widehat{I}_{[k]} = \frac{1}{k\,N} \sum_{[i]=1}^{[k]} \sum_{j=1}^{N} w_{[i]}(\mathbf{X}_{[i]}^{(j)}). \tag{3.48}$$

To sum up and clarify the previous equations, one needs to recall that Eq. (3.46) expresses the fact that, if one considers all the samples drawn from the beginning till iteration $[k]$ which led to failure realizations regarding the current threshold $y_{[k]}$, and taking their weights into account (see Eq. (3.47)), these samples follow the optimal density for estimating the failure probability corresponding to the threshold $y_{[k]}$. As a result, one will use these samples to approach, by means of a weighted KDE, this optimal density. As a final remark, one can notice that, in Eq. (3.47), the optimal density is hidden but can be found again by replacing the denominator by the corresponding intermediate failure probability at iteration $[i-1]$. Similarly to AIS-CE, as soon as the stopping criterion is satisfied (i.e., $y_{[k_\#]} \leq 0$, with $[k_\#]$ denoting the last step), the failure probability can be estimated by:

$$\widehat{p}_{\text{f}}^{\text{NAIS}} = \frac{1}{N} \sum_{j=1}^{N} \mathbb{1}_{\{g(\mathbf{X}_{[k_\#]}^{(j)}) \leq y_{[k_\#]}\}}(\mathbf{X}_{[k_\#]}^{(j)}) \frac{f_{\mathbf{X}}(\mathbf{X}_{[k_\#]}^{(j)})}{\widehat{h}_{[k_\#]}(\mathbf{X}_{[k_\#]}^{(j)})} \tag{3.49}$$

where one sets $y_{[k_\#]} = 0$ according to the definition adopted in this thesis regarding the threshold. For more details [13] about the NAIS algorithm, one can refer to the dedicated generic algorithm provided in Appendix D.

[13] Again, for the interested reader who would be more familiar with "threshold exceeding" probability, similar algorithm is detailed following this notation in Morio and Balesdent (2015).

Advantages and drawbacks. The main advantage of NAIS is its flexibility to handle complex shapes for optimal auxiliary densities (e.g., in the case of multimodal densities corresponding to multiple failure regions having almost equal importance). On this point, it is considered to be more efficient than the use of parametric AIS-CE. As another advantage, one can mention that, similarly to AIS-CE and CMC, the estimation error can be controled using Eq. (3.25).

However, the efficiency of kernel density estimators is getting worse as the input dimension increases. As the curse of dimensionality affects the KDE, NAIS consequently suffers from it in terms of probability estimation. Moreover, NAIS bandwidth (either scalar or matrix) estimation and optimization can be complex and is often considered as the key problem in kernel-based estimation. A wide literature is devoted to this specific technical point (see Appendix B).

Remarks. As a first remark, one should mention the work of Proppe (2008) which proposes a slightly different strategy based on a local approximation of the LSS at the most important failure regions, using moving least-squares. This LSS approximation is proposed together with an adaptive strategy which can be combined with existing IS techniques (e.g., with a FORM-based IS or with a KDE-based IS as proposed in Au and Beck (1999)). As a second remark, one should notice that, in the context of expensive-to-evaluate computer models, hybrid strategies combining surrogate models and nonparametric sampling have been proposed. For instance, Balesdent et al. (2013) directly combines a Kriging surrogate model and NAIS. However, in Dubourg et al. (2013), the Kriging surrogate itself is used to approximate a sub-optimal auxiliary density for IS in order to estimate a low failure probability.

As a conclusion, IS techniques may be very efficient in terms of cost reduction compared to CMC. The major difficulty is to construct an efficient quasi-optimal auxiliary density. Parametric and nonparametric techniques, despite their own advantages and drawbacks, remain powerful adaptive strategies to get a suitable auxiliary density compared to nonadaptive IS techniques relying on the MPFP. In the following, one will see that constructing, in an adaptive manner, such a quasi-optimal density may be achieved by adopting another strategy than the parametric or nonparametric ones.

3.5 Subset sampling

Presentation. *Subset sampling* (SS) belongs to the family of variance reduction techniques. However, due to its mathematical formulation, several variants have been proposed in different scientific communities. For example, one can cite, among others, the pioneering work of Kahn and Harris (1951) (called *splitting*) in the field of neutronics physics, the study of Glasserman et al. (1999) (called *multilevel splitting*) from the branching processes point of view, the development by Au and Beck (2001) (called *subset simulation*) for reliability assessment purpose or finally, the theoretical studies from the Markov processes point of view by Cérou and Guyader (2007) (called *adaptive multilevel splitting*) and Cérou et al. (2012) from the sequential Monte Carlo point of view.

All in all, these splitting techniques rely on the same idea: a rare event should be "split" into several less rare events, these events corresponding to some "subsets" containing the true failure set. Thus, the probability associated to each subset should be stronger, and consequently, easier to estimate. As an example, on can illustrate this by considering that a failure probability p_f of the order of 10^{-m} can be split into a product of m terms of probability $1/10$. In the following, for the sake of conciseness, only the formulation proposed by Au and Beck (2001) is discussed. For any further information about subset/splitting techniques for rare event simulation, the interested reader could refer to the following references (Lagnoux, 2006; Caron et al., 2014; Morio et al., 2014).

Formulation. The formulation of SS proposed by Au and Beck (2001) is derived in the **u**-space [14] and is the one presented hereafter. Let $E = \{\mathring{g}(\mathbf{u}) \leq 0\}$ denote a failure event sufficiently rare, one can consider a set of *intermediate nested events* E_s with $s = 1, \ldots, m$ such that $E = E_m \subset E_{m-1} \subset \cdots \subset E_2 \subset E_1$. Applying chain rule for conditional probabilities, one gets:

$$\begin{aligned} p_{\mathrm{f}} = \mathbb{P}(E) &= \mathbb{P}(E_m) \\ &= \mathbb{P}(E_m|E_{m-1})\,\mathbb{P}(E_{m-1}) \\ &= \mathbb{P}(E_m|E_{m-1})\,\mathbb{P}(E_{m-1})\,\mathbb{P}(E_{m-1}|E_{m-2})\ldots\mathbb{P}(E_2|E_1)\,\mathbb{P}(E_1) \\ &= \prod_{s=1}^{m} p_s \end{aligned} \tag{3.50}$$

where $p_1 = \mathbb{P}(E_1)$ and $p_s = \mathbb{P}(E_s|E_{s-1})$ for $s = 2, \ldots, m$. To this collection of nested failure events, one can define a set of *intermediate nested failure domains* (which are the so-called "subsets") such that:

$$\mathcal{F}_{\mathbf{u},s} = \{\mathbf{u} \in \mathbb{R}^d \mid \mathring{g}(\mathbf{u}) \leq y_s\}, \quad s = 1, \ldots, m \tag{3.51}$$

where y_s belongs to a set of decreasing intermediate thresholds such that $y_m = 0$ (i.e., corresponding to the true LSF) and $y_1 > y_2 > \cdots > y_{m-1} > y_m$. Similarly to AIS-CE and NAIS, these thresholds are estimated as α_{SS}-quantiles from the set of N samples of LSF outputs $\mathcal{G}_{\mathbf{u}} = \{\mathring{g}(\mathbf{U}^{(j)})\}_{j=1}^{N}$ with $\alpha_{\mathrm{SS}} \in]0,1[$ the *rarity parameter* [15]. Consequently, one can notice that $\mathcal{F}_{\mathbf{u}} = \mathcal{F}_{\mathbf{u},m} \subset \mathcal{F}_{\mathbf{u},m-1} \subset \cdots \subset \mathcal{F}_{\mathbf{u},2} \subset \mathcal{F}_{\mathbf{u},1}$. As an illustration, the underlying mechanism of the SS is illustrated on a two-dimensional example in Figure 3.5. In Figure 3.5a, the true, but unknown, LSS is sketched. Then, one considers successive intermediate nested failure domains which adaptively evolve towards the true failure LSS (see Figures 3.5b, 3.5c and 3.5d).

Thus, the rare event estimation problem set in Eq. (3.2) can be split into a sequence of m subproblems with larger probabilities to estimate. For the first level $s = 1$, the probability reads:

$$p_1 = \mathbb{P}(E_1) = \mathbb{E}_{\varphi_d}\left[\mathbb{1}_{\mathcal{F}_{\mathbf{u},1}}(\mathbf{U})\right] \tag{3.52}$$

and for $s = 2, \ldots, m$:

$$p_s = \mathbb{P}(E_s|E_{s-1}) = \mathbb{E}_{\varphi_d(\cdot|E_{s-1})}\left[\mathbb{1}_{\mathcal{F}_{\mathbf{u},s}}(\mathbf{U})\right]. \tag{3.53}$$

The associated estimators are given, respectively for $\{\mathbf{U}_1^{(j)}\}_{j=1}^{N} \overset{\text{i.i.d.}}{\sim} \varphi_d$, by:

$$\widehat{p}_1 = \frac{1}{N}\sum_{j=1}^{N} \mathbb{1}_{\mathcal{F}_{\mathbf{u},1}}(\mathbf{U}_1^{(j)}) \tag{3.54}$$

and, for $\{\mathbf{U}_s^{(j)}\}_{j=1}^{N} \overset{\text{i.i.d.}}{\sim} \varphi_d(\cdot|E_{s-1})$, by:

$$\widehat{p}_s = \frac{1}{N}\sum_{j=1}^{N} \mathbb{1}_{\mathcal{F}_{\mathbf{u},s}}(\mathbf{U}_s^{(j)}) \tag{3.55}$$

where N denotes the number of samples, supposed to be a constant for each level y_s, and the indicator function satisfies $\mathbb{1}_{\mathcal{F}_{\mathbf{u},s-1}}(\mathbf{u}) = 1$ if $\mathring{g}(\mathbf{u}) \leq y_{s-1}$ and $\mathbb{1}_{\mathcal{F}_{\mathbf{u},s-1}}(\mathbf{u}) = 0$ otherwise. Basically,

[14] Note that, here, similar derivations could be achieved in the **x**-space. This last formulation is the one proposed, for instance, by Cérou and Guyader (2007). For a full presentation of the *adaptive multilevel splitting*, one can refer to Rubino and Tuffin (2009) or Morio and Balesdent (2015, Chap. 5).

[15] For more information, the reader is invited to refer to the dedicated generic algorithm provided in Appendix D.

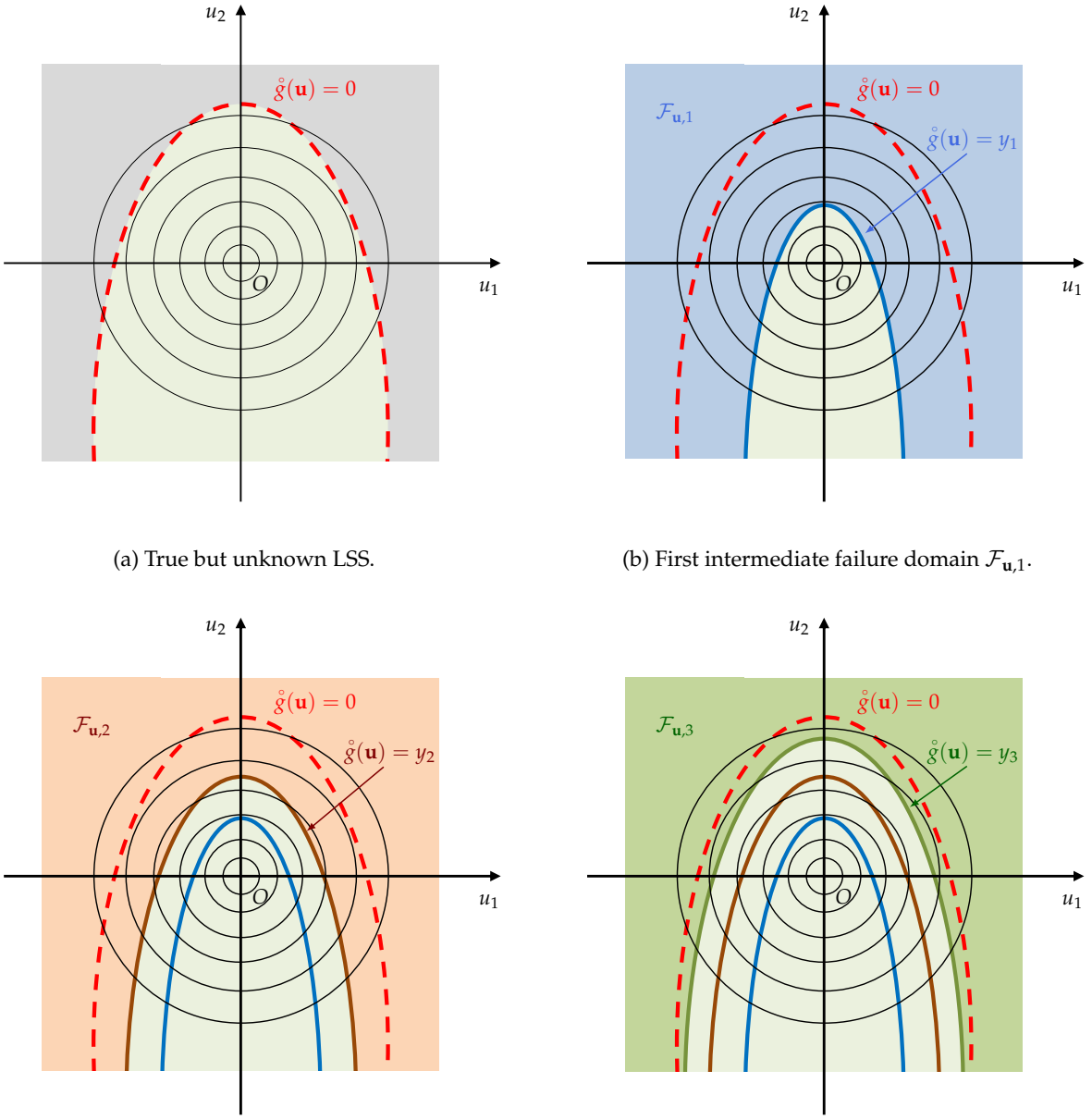

(a) True but unknown LSS.

(b) First intermediate failure domain $\mathcal{F}_{\mathbf{u},1}$.

(c) Second intermediate failure domain $\mathcal{F}_{\mathbf{u},2}$.

(d) Third intermediate failure domain $\mathcal{F}_{\mathbf{u},3}$.

FIGURE 3.5: Illustration on a two-dimensional example of the SS mechanism.

the SS estimator for p_f is given by:

$$\widehat{p}_\mathrm{f}^{\,\mathrm{SS}} = \widehat{p}_1 \prod_{s=2}^{m} \widehat{p}_s. \tag{3.56}$$

Moreover, it appears that the conditional sampling PDF $\varphi_d(\cdot|E_{s-1})$ takes the form:

$$\varphi_d(\mathbf{u}|E_{s-1}) = \frac{\varphi_d(\mathbf{u})\mathbb{1}_{\mathcal{F}_{\mathbf{u},s-1}}(\mathbf{u})}{\mathbb{P}\left(E_{s-1}\right)} = \frac{\varphi_d(\mathbf{u})\mathbb{1}_{\mathcal{F}_{\mathbf{u},s-1}}(\mathbf{u})}{p_{s-1}}, \quad s = 2, \ldots, m \tag{3.57}$$

This formula evokes the equation encountered when dealing with the optimal auxiliary density in the **u**-space (see Eq. (3.28)). For the sake of clarity, this equation is recalled below:

$$h^*_{\mathbf{U}}(\mathbf{u}) = \frac{\varphi_d(\mathbf{u})\mathbb{1}_{\mathcal{F}_\mathbf{u}}(\mathbf{u})}{p_\mathrm{f}}. \tag{3.58}$$

As a consequence, if one does want to achieve variance reduction with SS compared to CMC (and thus, to decrease the computational cost in context of very low failure probability), one should be able to sample sequentially from a quasi-optimal auxiliary PDF as expressed in Eq. (3.57). Such a problem can be adressed by using dedicated algorithms based on the *Markov chain Monte Carlo* (MCMC) sampling technique (see, e.g., Robert and Casella, 2004; Asmussen and Glynn, 2007). For instance, dedicated algorithms such as the standard *Metropolis-Hastings* (MH) sampler (Metropolis et al., 1953; Hastings, 1970) can be used. In the specific context of SS, the *modified Metropolis-Hastings* (m-MH) sampler originally proposed by Au and Beck (2001) has been proposed to deal with possible higher-dimensional reliability problems than the ones standard MH algorithm traditionally used. Some details about these algorithms are gathered in Appendix D.

Concerning the statistical properties of the estimator of $\widehat{p}_\mathrm{f}^{\mathrm{SS}}$ in Eq. (3.56), Au and Beck (2001) point out the fact that this estimator is biased due to the correlation between the intermediate probability estimators $\widehat{p}_s$ for $s = 1, \ldots, m$. Such a correlation comes from the way the m-MH sampler is seeded at each step (see, e.g., Bourinet (2018) or Dubourg (2011) for more details). It is also proved that the estimator $\widehat{p}_\mathrm{f}^{\mathrm{SS}}$ is asymptotically unbiased (Au and Beck, 2001). As for the c.v. $\delta_{\widehat{p}_\mathrm{f}^{\mathrm{SS}}}$, Au and Beck (2001) show that it is bounded such that:

$$\sum_{s=1}^{m} \delta_s \leq \delta^2_{\widehat{p}_\mathrm{f}^{\mathrm{SS}}} \leq \sum_{s_1=1}^{m}\sum_{s_2=1}^{m} \delta_{s_1}\delta_{s_2}. \tag{3.59}$$

where $\delta^2_{\widehat{p}_\mathrm{f}^{\mathrm{SS}}} = \mathbb{E}\left[\left(\frac{\widehat{p}_\mathrm{f}^{\mathrm{SS}} - p_\mathrm{f}}{p_\mathrm{f}}\right)^2\right]$ and δ_s are the c.v. of $\widehat{p}_s$, for $s = 1, \ldots, m$. For the sake of conciseness, formulas for computing these quantities can be found in Au and Beck (2001) or Bourinet (2018). The upper bound is established under the assumption of fully-correlated intermediate probability estimators $\widehat{p}_s$. Instead of using this upper bound, one can use the lower bound, established under the assumption of independent probability estimators $\widehat{p}_s$. Indeed, although it underestimates the true c.v. , it appears that, in practice (see, e.g., Au et al., 2007), it may give a reasonable approximation and approaches the empirical c.v. obtained by repetitions of the SS algorithm.

Advantages and drawbacks. On the one hand, the main advantages of SS in rare event probability estimation are its ability to handle complex LSFs (e.g., highly nonlinear, with possibly multiple failure regions) and to behave better than other techniques regarding the input dimension. Moreover, SS may present some interesting features concerning possible parallelization as exposed in Bourinet (2018). However, in its traditional formulation, SS is not a fully parallel multilevel splitting (Walter, 2015).

On the other hand, SS also presents some potential drawbacks. Firstly, even if SS provides a variance reduction compared to CMC, the number of samples required to achieve convergence may be, in some cases, larger than that required with other IS techniques. Secondly, the estimation error is not directly given by an analytical formula (e.g., variance estimators for CMC and IS) but has to be estimated using the bounds provided in Eq. (3.59) or by repetition. Thirdly, another intrinsic difficulty of SS is the tuning of parameters (e.g., the fixed vs. adaptive levels $\{y_s\}_{s=1}^m$, the number of samples N per step and other related parameters in the MCMC algorithm) which can be, in some cases, very influential on the efficiency of the algorithm. Fourthly, as proved in Au and Beck (2001) and recalled by Walter (2016, Chap. 1), the SS formulation leads to a biased estimator of p_f. Other algorithms such as the *Last Particle Algorithm* by Guyader et al.

(2011) or the *Moving Particles* algorithm by Walter (2015) can be used. A numerical investigation about relative efficiencies of both SS and LPA/MP through the tuning of MCMC parameters has been recently proposed by Proppe (2017). Fourthly, when input dimension d is large, SS may be indirectly affected if the traditional MH sampler is used as it becomes inefficient in high dimension. Using the m-MH sampler introduced by Au and Beck (2001) allows to overcome this difficulty. As a an alternative, one could also use another variant of m-MH as proposed in Zuev and Katafygiotis (2011). Finally, as mentioned in Au and Wang (2014) and Breitung (2019), counterexamples (e.g., specific shapes of LSS) can be found to invalidate SS convergence towards the true failure probability. This remark highlights the fact that any insight regarding the physical behavior of the system or about the LSF can be useful for the analyst to avoid dramatic errors in terms of rare event probability estimation.

Remarks. As a remark, one can notice that SS can be efficiently coupled with surrogate models (Bourinet et al., 2011; Bourinet, 2016; Bect et al., 2017) to assess reliability regarding expensive-to-evaluate computer models. In such a case, possible limiting properties of the surrogate model (e.g., limits concerning the input dimensionality and the smoothness of the LSF) may impact the usual properties of SS evoked just before.

3.6 Synthesis and discussion

Several uncertainty propagation techniques for rare event probability estimation have been reviewed in this section. They rely on various underlying strategies (e.g., random sampling for CMC, advanced sampling for IS and SS, optimization for FORM/SORM) to efficiently estimate p_f and present both advantages and drawbacks. However, as a synthesis, one can discuss a few generic challenges (which can be seen as strong constraints) in rare event probability estimation which may reduce either the efficiency or the robustness of the techniques reviewed above and thus the analyst should be aware of.

Other rare event probability estimation techniques. As a first preliminary remark, one needs to mention that the previous section is a non-exhaustive list and only focuses, for the sake of conciseness and without loss of generality, on the most used rare event estimation techniques in the context defined in Chapter 2. However, throughout this section, multiple references to other techniques (e.g., *line sampling*, *directional sampling*, *stratified sampling*, *last particle algorithm*, *moving particles*) has been provided in several remarks, and the interested reader is invited to refer to the related references mentioned all along the section.

Switching from x-space to u-space, and vice versa. As mentioned throughout this section, various techniques (e.g., CMC, AIS-CE, NAIS and SS) presented here may be set either in the $\mathbf{x}$-space or in the $\mathbf{u}$-space. However, others (e.g., FORM/SORM, FORM-IS and TIS) are only relevant in the $\mathbf{u}$-space. Switching between these two spaces (see Section 2.4.3 and Appendix C) may be not difficult when considering the sole problem of probability estimation as formulated in Eqs. (3.1) and (3.2). However, one should mention that, if working in the $\mathbf{u}$-space often facilitates calculations, the interpretation of results may have to be done carefully as a lot of input information is hidden w.r.t. the $\mathbf{x}$-space.

Tuning parameters of rare event algorithms. Another key remark is related to the fact that almost all the techniques presented hereabove (except CMC) come along with their own set of tuning parameters (see, e.g., the tuning parameters for IS and SS techniques in Appendix D) and several variants (e.g., considering fixed or variable intermediate threshold values in SS). Thus,

the proper tuning of these parameters have consequences on the efficiency of the technique such as discussed in Au et al. (2007), Dubourg (2011), and Balesdent et al. (2015).

Rareness of the failure event. When the rareness of the failure event increases (i.e., that the failure probability p_f gets smaller), CMC clearly becomes intractable. Thus, other available techniques are suitable to deal with this challenge, provided the technique under consideration meets some requirements about the validity of the following points. Notice that, in general, the true failure probability is unknown. One may just want to make sure that the estimated one is below a target failure probability.

High-nonlinearity of the LSF and multiple failure regions. A first driving point concerns the computer code under study. Since it is black-box, it is often difficult to get any information about the nonlinearity of the code. If, after transformation, the LSF $\mathring{g}(\cdot)$ is linear or almost linear, then approximation techniques such as FORM/SORM may be sufficient to get an accurate estimate of p_f at a reduced computational cost. In the case of a nonlinear LSF (or without any further information), getting a prior information about the main characteristics of the code by studying the output characteristics may provide a better insight about its behavior (see, e.g., the work by Moutoussamy (2015) about rare event probability estimation under monotonicity constraint). Such a prior code exploration study is conceivable provided the computer code has a short unitary runtime.

Constrained simulation budget. If the computer code presents a long unitary runtime, or if the simulation budget is drastically constrained, then, one can use a *surrogate model* (a.k.a. *metamodel*), whose aim is to mimick the code, to fasten the computations. However, one needs to ensure that the surrogate model is sufficiently refined in the regions of interest and that the modeling error is controled. Several references based on coupling rare event estimation techniques and surrogate models have been mentioned throughout this section.

Controling the estimation error. Controling the estimation error may be a key requirement for some applications. In this case, FORM/SORM does not provide any indicator about this estimation error. For other techniques, as mentioned previously, this error may be estimated, either directly by using analytical formulas (e.g., for CMC or IS), or using error bounds on the c.v. of the failure probability (e.g., for SS).

High-dimensional input vector. For large input dimension d [16], almost all of the techniques reviewed hereabove (except CMC) get their efficiency affected by this constraint. As mentioned for MPFP-based techniques (i.e., FORM/SORM, FORM-IS and TIS), the notion of MPFP loses its meaning due to geometric considerations. Similarly, IS techniques may become inefficient due to the difficulty to sample within the so-called "important ring". Another limit may arise in the use of kernel-based estimators (e.g., for NAIS) whose efficiency in high dimension is limited. As for SS, standard MH sampler used to get conditional samples becomes inefficient regarding the large input dimension. The m-MH sampler proposed by Au and Beck (2001) is far less affected by the input dimension, but may also attain its limits for very high dimensional problems. Finally, none of these methods manages to easily handle very high-dimensional problems. However, being aware of that, the analyst should perform prior code exploration (e.g., using *sensitivity analysis*) so as to, if possible and regarding the goal of the study, reduce the input dimension (e.g., by identifying the *effective input dimension*). However, this type of analysis may

[16] Note that "large input dimension" is a generic but vague vocabulary. Indeed, large dimension may start from $d \approx 10$ to $d \approx 10^3$ in some scientific communities. In this thesis, input dimension will not exceed $d = 10$.

also present its own limits (e.g., possibly high simulation costs induced by sensitivity analysis methods, restricted hypotheses about the independence of the inputs).

Robustness of the probability estimate. As a final remark, one should mention that all the techniques presented in this section rely on the assumption that the input probabilistic model is perfectly known and thus, the probability estimate is sufficiently representative of what could be the true (but unknown) p_f. However, such an estimate is directly conditional on the input probabilistic modeling and may be affected if some changes occur in this latter. This remark directly motivates the next chapter whose aim is to review some of the available techniques to test and potentially justify the robustness of the estimated rare event probability regarding the input probabilistic model.

3.7 Conclusion

This chapter provided a review of several rare event probability estimation techniques that can be used for black-box input-output computer models. For all these techniques, a common description framework has been adopted through a four-step summary: i.e., *Presentation - Formulation - Advantages and drawbacks - Remarks*. As a consequence, the role of the analyst is of utmost importance in terms of correctly specifying the problem under study and choosing an adequate technique to estimate p_f. When dealing with a black-box computer model, with no prior information about the code (i.e., just minimal input probabilistic information), testing several techniques (when possible) and comparing their results remain the simplest way to ensure robustness of the reliability assessment.

In the next chapter, a brief review of the main sensitivity analysis methods is provided. Following the "goal-oriented viewpoint" adopted in this thesis (see Section 2.5), these methods are distinguished between two categories regarding the QoI they focus on:

- *sensitivity analysis of model output* (a.k.a. SAMO) methods when the QoI is the model output Y;
- *reliability-oriented sensitivity analysis* (a.k.a. ROSA) methods when the QoI is, either related to the failure domain (e.g., value taken by the LSF or by the indicator function of the failure domain) or a safety measure (e.g., a failure probability or a reliability index).

CHAPTER 4

Sensitivity analysis of model output and reliability measure

Contents

4.1 Introduction and motivations

When performing *forward* UQ (i.e., modeling and propagation of uncertainties, as presented in Figure 1.1), one may be interested in some *backward* UQ, i.e., by investigating "how the uncertainty in the output of a model (numerical or otherwise) can be apportioned to different sources of uncertainty in the model input" (Saltelli et al., 2004). Thus, *sensitivity analysis* (SA) can be seen as a backward study whose aim is to bridge the gap from the output to the input [1].

Traditionally, SA has been widely studied as the analysis of the model output of black-box computer models. For this reason, the denomination "*sensitivity analysis of model output*" (SAMO) is often encountered in SA literature (Saltelli et al., 1993; Chan et al., 1997). One recalls here that, in this manuscript, the model output is supposed to be scalar. As stressed by several authors, SAMO should be performed according to a range of general conceptual objectives, called *SA settings*, properly defined in various references (see, e.g., Saltelli et al., 2004; Borgonovo, 2017). These objectives can be listed such as below (Saltelli et al., 2004):

- **factor prioritization** (FP-setting): the aim is to identify the key inputs driving the model behavior. Thus, a possible reduction of the uncertainty affecting these inputs may lead to the largest reduction of the output uncertainty;
- **factor fixing** (FF-setting): the aim is to identify the noninfluential inputs which could be fixed at some given values without any loss of information about the output;
- **variance cutting** (VC-setting): the aim is to identify which inputs should be fixed so as to reach a target value on the output variance;
- **factor mapping** (FM-setting): the aim is to identify the key inputs responsible for producing values of the output in a given region of interest;

to which Borgonovo (2017) suggests adding:

- **model structure** (MS-setting): the aim is to analyze the possible interactions between inputs;
- **sign of change** (SC-setting): the aim is to identify whether an increase in the inputs gives rise to an increase or a decrease in the model output;
- **stability** (S-setting): the aim is to analyze whether perturbations in the inputs may cause the preferred alternative to change.

Consequently, SA should be performed in light of one (or several) of the previous SA settings. Thus, similarly to the previous chapter, a "goal-oriented view" can be apply to SA. However, it is of paramount importance to notice that all the previous SA settings aim at providing qualitative or quantitative indicators which, finally, should lead to a pragmatic counterpart in terms of decision (e.g., fixing some inputs and reducing the input dimension).

In the context of rare failure probability estimation, as explained in Chapter 3, one can consider that the goal is different than a direct study of the model output. Moreover, the simulation cost may be expensive and the uncertainty propagation methods used to estimate p_f may vary from the traditional ones used to study the variability in Y. As a consequence, the restriction to a specific critical domain of the model output distribution (e.g., in a tail) and the definition of a failure scenario implies to focus on a specific "*reliability objective*". If some of the previous SA settings may be adapted to reliability measures such as p_f, one needs to ensure that the pragmatic counterparts listed hereabove do not lead to dramatic consequences in terms of safety. Thus, in

[1] Note that, in SA literature, the name "input" is traditionally replaced by "factor". In this thesis, one will use both of them indistinctly.

the present chapter, a special focus on "*reliability-oriented sensitivity analysis*" (a.k.a. ROSA) methods is provided. The aim is, for the reader, to be presented the strong links (i.e., similarities and borrowed methods from SAMO to ROSA) and the key differences between these two types of analyses. As an illustration, Figure 4.1 conceptually presents the different goals of, respectively, SAMO and ROSA.

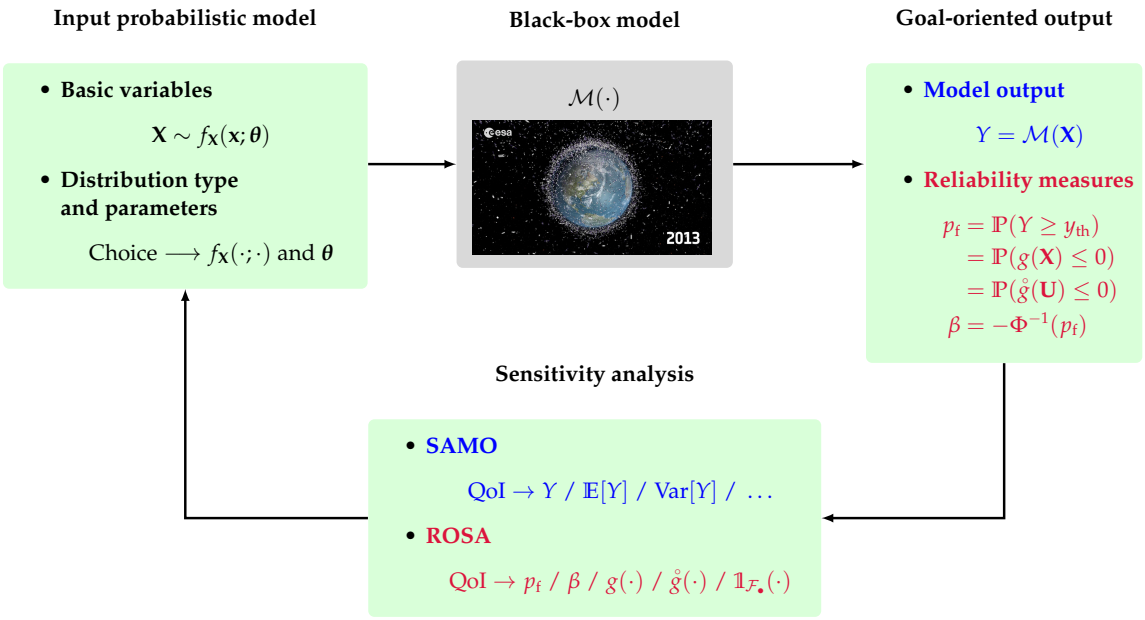

FIGURE 4.1: Illustration of the SAMO vs. ROSA points of view within the UQ methodology.

This chapter is organized as follows. Section 4.2 aims at introducing the basic principles of SAMO and presenting a few SAMO methods which exhibit some theoretical and/or computational links or similarities with the ROSA methods presented further. Section 4.3 proposes a synthesis of SAMO methods and highlights the motivations for considering ROSA methods. Section 4.4 first draws up an inventory of the main ROSA methods when the distribution parameters are of interest. Section 4.5 provides an inventory when the input variables are of interest. Section 4.6 proposes a synthesis about ROSA and recapitulates the most important features about ROSA. Finally, a conclusion summarizing the most important results of this chapter is given in Section 4.7.

4.2 Sensitivity analysis of model output (SAMO)

As a preliminary remark, one should notice that, a common distinction is first made between two different families of SAMO methods (Shekhar et al., 2017):

- the *local* SAMO methods which imply to study the local impact of inputs' variations on model output by concentrating on the sensitivity in the vicinity of a set of input values. Such sensitivities are often evaluated through gradients or partial derivatives of the model output at these input values. Finally, the values of other inputs are kept constant when studying the local sensitivity of a specific input;
- the *global* SAMO methods which imply to study the effects of various simultaneous inputs' variation over their entire domain on the model output. Thus, one can look closer at both output variations induced by individual inputs and/or interactions between several of them (i.e., groups of input variables).

This section does not aim at presenting an exhaustive review about SAMO methods, but only providing a compendium about a few of them which are widely used and thus will be adapted in the ROSA context. For the sake of brevity, only the basic principles and core equations are reviewed in this section. The interested reader can refer to more comprehensive reviews such as in Helton et al. (2006), Morio (2011a), Iooss and Lemaître (2015), Wei et al. (2015b), and Borgonovo and Plischke (2016).

4.2.1 Local SAMO methods

Historically, local SAMO methods are the first ones which have been applied to determine the impact of small input perturbations on the model output. Among local SAMO methods, one can distinguish between *differential* and *adjoint* methods.

Differential methods rely on calculating or estimating the partial derivatives of the model output at some specific values (e.g., around a nominal value such as the mean of an input random variable). That is, assuming a particular realization $\mathbf{x}^0$ of the input vector, the aim is to estimate the following quantity:

$$\Delta_i(\mathbf{x}^0) = \frac{\partial \mathcal{M}}{\partial x_i}(\mathbf{x}^0) = \frac{\partial \mathcal{M}}{\partial x_i}(x_1^0, \ldots, x_d^0) \tag{4.1}$$

This quantity characterizes the effect of a perturbation of the input X_i near a given value x_i^0 on the model output Y. In practice, assuming that the above equation cannot be solved by analytical differentiation, such a quantity can be estimated by several manners. For instance, one can use a *finite difference* (FD) [2] scheme such that (here, a *forward* scheme):

$$\Delta_i^{\mathrm{FD}}(\mathbf{x}) = \frac{\mathcal{M}(x_1, \ldots, x_{i-1}, x_i + \delta_{\mathrm{FD}}, x_{i+1}, \ldots, x_d) - \mathcal{M}(\mathbf{x})}{\delta_{\mathrm{FD}}} \tag{4.2}$$

where δ_{FD} is a perturbation step such that $\Delta_i(\mathbf{x}) = \lim_{\delta_{\mathrm{FD}} \to 0} \Delta_i^{\mathrm{FD}}(\mathbf{x})$. The choice of such a perturbation step is of major importance for ensuring accuracy of the FD scheme which and remains tricky in practice (see, e.g., Iott et al., 1985). Similarly, such a local index can be approximated using the *one-variable-at-a-time* (OAT) design (Ekström and Broed, 2006). The idea is to consider a range for each input variable (e.g., an interval of $\pm 10\%$, or a regular grid if the inputs have been preliminary scaled, or mapped to a scaled space such as the d-dimensional unit hypercube) and varying only one variable while the others are kept fixed at a baseline value. These methods have been applied in various fields (see, e.g., Ekström and Broed (2006), Castillo et al. (2008), and Martins (2012) for some applications).

Adjoint methods (Cacuci, 1981; Cacuci, 2003; Cacuci et al., 2005) are also widely used in numerous fields when an explicit formulation of the adjoint is available, which can be the case for some problems (Allaire, 2015). However, in the context of black-box computer code, deriving an adjoint problem and using these dedicated methods are often impossible.

As a conclusion, one can recall that local SAMO methods have been the first methods developed for SA. The estimation of local indices is easy as soon as an analytical formula for the model (and its adjoint) is available. Automatic differentiation methods can also be considered (see, e.g., Walter, 2014, Chap. 6). However, for complex black-box computer code, the use of FD schemes can be prohibitive, while automatic differentiation can be even impossible. Finally, the interpretation of these local indices regarding the SA settings, presented in Section 4.1, can be difficult if the variables are very heterogeneous in terms of probability laws and supports. However, they still play a key role regarding robustness of a result w.r.t. a local perturbation and can be directly used for optimization purposes.

[2] Note that here, a *forward* scheme is given as an example, but both *backward* and *central* FD schemes could be considered too.

4.2.2 From local to global: the screening methods

When multiple inputs are varied in the same time over a wider region of interest (i.e., no longer around a specific value, but over the full definition domain of an input), local SAMO methods are no longer suitable to catch the overall impact on the QoI. However, the local index they provide can be generalized if the local perturbations are repeated a sufficient number of times over the entire region of interest. This is the basic idea of the following two methods. *Screening methods* are based on a discretization of the input space in fixed levels (i.e., grid) and the evaluation of indices at well-chosen points of this grid (Iooss and Lemaître, 2015). In this sense, they can be seen as a generalization of the previous local methods over the entire input space and are directly linked to the theory of *design of experiments* (DOE) (see, e.g., Morris, 2017).

4.2.2.1 Elementary effects and the Morris method

The *Morris method* (Morris, 1991) is based on the repetition of a set of randomized OAT schemes. A preliminary normalizing phase is required by mapping the input space to the d-dimensional unit hypercube $H^d = [0,1]^d = \bigtimes_{i=1}^{d}[0,1]$ (Cartesian product of d sets).

The method consists in discretizing the input space in n_{level} levels by input (i.e., creating a grid in the over $[0,1]^d$) and performing a number n_{OAT} of OAT designs following randomly chosen sample paths along the grid. To estimate the sensitivity, one needs to define the *elementary effect* (EE) computed while perturbating the i-th input X_i at the j-th repetition step, such that:

$$\Delta_i^{\text{EE}}(\mathbf{x}^{(j)}) = \frac{\mathcal{M}(\mathbf{x}^{(j)} + \delta_{\text{EE}}\, \mathbf{e}_i) - \mathcal{M}(\mathbf{x}^{(j)})}{\delta_{\text{EE}}} \overset{\text{def}}{=} \Delta_i^{\text{EE},(j)} \tag{4.3}$$

where δ_{EE} is the perturbation step (set as a multiple of $1/(n_{\text{level}}-1)$) and $\mathbf{e}_i$ is a vector of the standard Euclidean basis. Note that the grid-point where the OAT design is performed and the direction of the perturbation (i.e., $\mathbf{e}_i$) are randomly chosen. Thus, for each input variable, one defines a set of two indices as follows (Morris, 1991): $\mu_{\Delta_i^{\text{EE}}} = \mathbb{E}[\Delta_i^{\text{EE}}]$ and $\sigma_{\Delta_i^{\text{EE}}} = \sqrt{\text{Var}\left[\Delta_i^{\text{EE}}\right]}$. However, to avoid "vanishing" effects due to opposite signs (e.g., in the case of non-monotonic models) in the expected value above, Campolongo et al. (2007) propose to use the absolute value of the elementary effect $|\Delta_i^{\text{EE},(j)}|$ in the mean index (while the standard deviation index is not modified) leading to the definition of the following indices:

$$\mu^*_{|\Delta_i^{\text{EE}}|} = \mathbb{E}[|\Delta_i^{\text{EE}}|], \quad \sigma_{\Delta_i^{\text{EE}}} = \sqrt{\text{Var}\left[\Delta_i^{\text{EE}}\right]}. \tag{4.4}$$

and their empirical estimators:

$$\widehat{\mu}^*_{|\Delta_i^{\text{EE}}|} = \frac{1}{n_{\text{OAT}}} \sum_{j=1}^{n_{\text{OAT}}} |\Delta_i^{\text{EE},(j)}|, \quad \widehat{\sigma}_{\Delta_i^{\text{EE}}} = \sqrt{\frac{1}{n_{\text{OAT}}} \sum_{j=1}^{n_{\text{OAT}}} \left(\Delta_i^{\text{EE},(j)} - \frac{1}{n_{\text{OAT}}} \sum_{j=1}^{n_{\text{OAT}}} \Delta_i^{\text{EE},(j)}\right)^2}. \tag{4.5}$$

As for the interpretation of these indices, $\widehat{\mu}^*_{|\Delta_i^{\text{EE}}|}$ measures the influence of the i-th input on the dispersion of the model output (the larger this index, the more influential the input) and $\widehat{\sigma}_{\Delta_i^{\text{EE}}}$ measures the nonlinear effects and/or the possible interactions between multiple inputs. If $\widehat{\sigma}_{\Delta_i^{\text{EE}}}$ is small, it suggests a linear relationship between X_i and Y, while a large $\widehat{\sigma}_{\Delta_i^{\text{EE}}}$ implies either a nonlinear effect between X_i and Y or a combined effect between X_i and other inputs. Finally, another feature of the method is that these two indices can be plotted on a same graph (i.e., $\widehat{\sigma}_{\Delta_i^{\text{EE}}}$ as a function of $\widehat{\mu}^*_{|\Delta_i^{\text{EE}}|}$) which provides a qualitative tool to distinguish the various effects of the input variables on the output.

The advantages of such a method is to provide a qualitative manner to fastly explore the behavior of a black-box computer code, at a low computational cost. The practical implementation relies on the definition of a set of matrices (e.g., orientation and permutation matrices) and setting the two parameters n_{level} and n_{OAT} (see Saltelli et al. (2004)). If the method is fully described in Morris (1991), more details about practical implementation can be found in Ekström and Broed (2006) and Bolado-Lavin and Costescu Badea (2008). This method is said to be global in the sense that it averages local measures over the input space. Finally, the Morris method is tractable when facing problems with large d. However, its main drawback is that it is not possible to distinguish between nonlinear effects and interaction effects which can be a critical information in terms of decision making. Moreoever, due to the normalized grid, it does not really take into account the input distributions.

As a remark, one can notice that the Morris method provides relevant indices regarding both the FF- and MS-settings described in Section 4.1.

4.2.2.2 Derivative-based global sensitivity measures

Derivative-based global sensitivity measures (DGSM) can be seen, either as a direct generalization of the local differential methods provided in Subsection 4.2.1 (by getting a global measure from local derivatives) or as a generalization of the Morris method (by adopting a global strategy but using strict local derivatives and not variations on a fixed grid, which enables to take the input distributions into account). DGSM have been first introduced by Sobol and Gershman (1995) and then further investigated, e.g., in Kucherenko et al. (2009) and Patelli et al. (2010). Thereafter, some theoretical links between the DGSM and the *Sobol indices* [3] (these indices are presented further in Subsection 4.2.3.1) have been proved and investigated in Lamboni et al. (2013) and Roustant et al. (2014). For the interested reader, details and references about the DGSM can be found in Kucherenko and Iooss (2017).

Assuming $\mathbf{X} = (X_1, \ldots, X_d)^\top$ a d-dimensional vector of d independent Gaussian random variables, with joint PDF $f_{\mathbf{X}}$ defined on $\mathbb{R}^d$, the DGSM index ν_i associated with the i-th input X_i, introduced by Sobol and Kucherenko (2009), is given by:

$$\nu_i = \int_{\mathbb{R}^d} \left(\frac{\partial \mathcal{M}(\mathbf{x})}{\partial x_i} \right)^2 f_{\mathbf{X}}(\mathbf{x}) \mathrm{d}\mathbf{x} = \mathbb{E}\left[\left(\frac{\partial \mathcal{M}(\mathbf{X})}{\partial X_i} \right)^2 \right]. \tag{4.6}$$

Other DGSM indices can be defined depending on the types of probability distributions (e.g., for uniformly distributed random variables over the unit hypercube H^d, see Kucherenko and Iooss, 2017).

The main advantage of DGSM relies on their reduced cost compared to other global sensivity methods and the bounding properties which enable a qualitative analysis regarding the FP-, FF-settings defined in Section 4.1. However, it should be noted that the ranking of the most influential variables may be different between DGSM and Sobol indices, especially when dealing with nonlinear models (Kucherenko and Iooss, 2017).

As a remark, one should notice that, in the context of costly-to-evaluate computer models, hybrid strategies combining surrogate models and DGSM have been proposed in Mai and Sudret (2015) and De Lozzo and Marrel (2016a).

As a conclusion of this subsection, screening methods are known to be efficient for a rough but fast exploration of the input space and the code behavior. However, the information they

[3] Note that the theoretical links rely on bounding Sobol indices using DGSM. These bounds can be derived using Poincaré inequalities and their associated Poincaré constants (which some of them can be optimal), derived for multiple probability distributions. See Lamboni et al. (2013), Kucherenko and Iooss (2017), and Roustant et al. (2017) for further information about these bounds.

provide is more qualitative than quantitative. In the next subsection, quantitative global methods providing *importance measures* (i.e., proper measure allowing a ranking between input variables w.r.t. their relative influence) are investigated.

4.2.3 A few importance measures for global SAMO

Contrary to screening methods which allow a qualitative and fast exploration of computer codes, global SAMO methods aim at providing *importance measures* which are of major interest for FP-, FF- and VC-settings.

4.2.3.1 Functional decomposition of variance and Sobol indices

One needs first to consider that the model $\mathcal{M}(\cdot)$ under study can be possibly nonlinear and non-monotonic. Then, assuming $\mathcal{M}(\cdot)$ is square-integrable and defined on the unit hypercube $[0,1]^d$ [4], with $\mathbf{X}$ gathering d independent [5] variables, the model output Y can be decomposed such that (Hoeffding, 1948):

$$Y = \mathcal{M}(\mathbf{X}) = \mathcal{M}_0 + \sum_{i=1}^{d} \mathcal{M}_i(X_i) + \sum_{i<j}^{d} \mathcal{M}_{ij}(X_i, X_j) + \cdots + \mathcal{M}_{1\ldots d}(\mathbf{X}) \tag{4.7}$$

where $\mathcal{M}_0 = \mathbb{E}[\mathcal{M}(\mathbf{X})] = \int_{[0,1]^d} \mathcal{M}(\mathbf{x}) f_{\mathbf{X}}(\mathbf{x}) \mathrm{d}\mathbf{x}$, and where $f_{\mathbf{X}}$ is supposed to be a product of d uniform marginals over $[0,1]$. The other terms are given by:

$$\mathcal{M}_i(X_i) = \mathbb{E}[\mathcal{M}(\mathbf{X})|X_i] - \mathcal{M}_0 \tag{4.8}$$

$$\mathcal{M}_{ij}(X_i, X_j) = \mathbb{E}[\mathcal{M}(\mathbf{X})|X_i, X_j] - \mathbb{E}[\mathcal{M}(\mathbf{X})|X_i] - \mathbb{E}[\mathcal{M}(\mathbf{X})|X_j] - \mathcal{M}_0 \tag{4.9}$$

and $\mathcal{M}_{1\ldots d}(\mathbf{X})$ is given by the difference between $\mathcal{M}(\mathbf{X})$ and the sum of all other terms of increasing dimension such that Eq. (4.7) is verified. The uniqueness of this functional decomposition is ensured if the following orthogonality property is verified (Sobol, 1993):

$$\int_0^1 \mathcal{M}_{j_1\ldots j_s}(x_{j_1}, \ldots, x_{j_s}) \mathrm{d}x_{j_k} = 0, \quad \forall k \in \{1, \ldots, s\}, \quad \forall \{j_1, \ldots, j_s\} \subseteq \{1, \ldots, d\}. \tag{4.10}$$

This unique functional decomposition of the model output leads to consider the following *functional decomposition of variance* (a.k.a. functional *analysis of variance* or F-ANOVA):

$$\mathrm{Var}\,[Y] = \sum_{i=1}^{d} D_i(Y) + \sum_{i<j}^{d} D_{ij}(Y) + \cdots + D_{1\ldots d}(Y) \tag{4.11}$$

[4] Note that this assumption is taken by Sobol (1993) but can be generalized to any other type of input distribution by transformation as mentioned in Chastaing (2013, Chap. 1) and Baudin and Martinez (2014).

[5] Note that, in this manuscript, only the Sobol indices in the case of independent inputs. For dependent inputs, a generalized Hoeffding-Sobol decomposition has been proposed in Chastaing (2013). Moreover, it can be shown that, in the dependent case, four types of Sobol indices are necessary. More details and related references can be found in Iooss and Prieur (2017).

with $D_i(Y) = \text{Var}\left[\mathbb{E}[Y|X_i]\right]$, $D_{ij}(Y) = \text{Var}\left[\mathbb{E}[Y|X_i, X_j]\right] - D_i(Y) - D_j(Y)$ and so on for higher order interaction terms. The *Sobol indices* (Sobol, 1993; Sobol, 2001) are thus defined as follows:

$$S_i = \frac{D_i(Y)}{\text{Var}\left[Y\right]} = \frac{\text{Var}\left[\mathbb{E}[Y|X_i]\right]}{\text{Var}\left[Y\right]} \tag{4.12}$$

$$S_{ij} = \frac{D_{ij}(Y)}{\text{Var}\left[Y\right]} = \frac{\text{Var}\left[\mathbb{E}[Y|X_i, X_j]\right] - D_i(Y) - D_j(Y)}{\text{Var}\left[Y\right]} \tag{4.13}$$

$$\dots$$

Eq. (4.12) is known as the *first-order Sobol index* and quantifies the part of variance of Y due to the variability in X_i (a.k.a. the *main effect*) while Eq. (4.13) is the *second-order Sobol index* and measures the effect of the interaction between X_i and X_j. Higher order Sobol indices can be derived following the same principle [6]. However, in practice, deriving all of the indices can be tedious, especially when d is large, and one thus prefers to compute the *total Sobol index* introduced by Homma and Saltelli (1996) and defined such that:

$$S_{T_i} = \sum_{j \in \{\#i\}} S_j \tag{4.14}$$

where $\{\#i\}$ represents all the subsets of $\{1, \dots, d\}$ containing i. The total Sobol index measures the part of output variance which can be explained by all the combined effects (a.k.a. the *total effect*) in which X_i is part of. Finally, this total Sobol index can be rewritten as follows:

$$S_{T_i} = 1 - \frac{\text{Var}\left[\mathbb{E}[Y|\mathbf{X}^{-i}]\right]}{\text{Var}\left[Y\right]} \tag{4.15}$$

where $\mathbf{X}^{-i}$ stands for $\mathbf{X}$ without the i-th component X_i. In practice, the total index is often considered under the following equivalent form (see, e.g., Saltelli et al., 2008):

$$S_{T_i} = \frac{\mathbb{E}\left[\text{Var}\left[Y|\mathbf{X}^{-i}\right]\right]}{\text{Var}\left[Y\right]}. \tag{4.16}$$

Numerical estimation of Sobol indices can be achieved by CMC sampling using *pick-freeze* [7] estimators as proposed by Homma and Saltelli (1996), Sobol (2001), and Saltelli (2002). However, the computational cost to get converged estimates is often demanding. Other sampling techniques such as QMC sampling or *Fourier amplitude sensitivity test* (FAST) have been proposed and various formulas have been proposed to enhance the numerical estimation (see, e.g., Lemaître (2014) and Iooss and Lemaître (2015) for further details).

The main advantage of Sobol indices is that they provide a clear quantitative interpretation of the respective contributions of each input to the variance of the output. However, as a drawback, one needs to ensure that the variance is the real moment of interest characterizing the model output. For instance, in a context of multimodal or highly-skewed output distribution, the variance is no longer representative. Another common drawback pointed out is the cost associated with the estimation of Sobol indices in the CMC setting.

As a remark, one should notice that, in the context of costly-to-evaluate computer models, the use of surrogate models can serve as an efficient basis for SAMO. For instance, on the one hand, Sobol indices can be efficiently derived and estimated using *polynomial chaos expansion* (PCE) as shown in Sudret (2008). One can get the Sobol indices by a simple post-processing of

[6] Note that, when d is the input dimension, the total number of indices is $2^d - 1$.

[7] For a deeper theoretical study of statistical properties of pick-freeze estimators for Sobol indices, one can refer to Gamboa et al. (2015).

the PCE coefficients. On the other hand, using *Gaussian processes* (GP), as proposed in Marrel et al. (2009), allows one to efficiently derive confidence intervals for the indices. For the interested reader, a thorough review of these methods can be found in Le Gratiet et al. (2017). Note that other surrogate models can be used (e.g., *law-rank approximation* (LRA) as presented in Konakli and Sudret (2016)).

4.2.3.2 Sensitivity indices based on dissimilarity measures

To overcome the restrictions due to focusing only on the variance of the model output as stated in the formulation of Sobol indices, several sensitivity indices have been proposed to enhance these limitations. Even if the following indices presented herebelow have been, for most of them, proposed under various assumptions and remain different in terms of technical details (e.g., formulas, estimation, interpretation of the results), they can be considered as members of a wider family containing sensitivity indices based on *dissimilarity measures* (Da Veiga, 2015; Rahman, 2016). Indeed, the basic idea is to consider that the impact of an input X_i on the model output Y can be measured by the differences between the output probability distribution, denoted P_Y and the conditional probability distribution $P_{Y|X_i}$ (Borgonovo, 2007). However, this distributional changes have to be measured through the use of a *dissimilarity measure* (Da Veiga, 2015; Rahman, 2016).

Under the assumption of a continuous model $\mathcal{M}(\cdot)$ and an input vector $\mathbf{X}$ gathering d independent random variables, one can define the following sensitivity index:

$$S_i^{\mathcal{D}} = \mathbb{E}_{f_{X_i}}[\mathcal{D}(P_Y, P_{Y|X_i})] \tag{4.17}$$

where $\mathcal{D}(\cdot,\cdot)$ is a *dissimilarity measure* between two probability distributions. Thus, one can notice that the choice of $\mathcal{D}(\cdot,\cdot)$ determines the type of sensitivity index under study. In the following, several dissimilarity measures and their associated sensitivity indices are presented. The interested reader is invited, for any further information, to refer to both Da Veiga (2015) and Rahman (2016).

Another possible definition of the Sobol indices. As a first dissimilarity measure, one can choose a comparison between the mean values of the two probability distributions:

$$\mathcal{D}(P_Y, P_{Y|X_i}) = (\mathbb{E}[Y] - \mathbb{E}[Y|X_i])^2 \tag{4.18}$$

which leads, after some calculations, to the non-normalized first-order Sobol index:

$$S_i^{\mathcal{D}} = \mathrm{Var}\left[\mathbb{E}[Y|X_i]\right]. \tag{4.19}$$

Consequently, Sobol indices can be seen as a particular case of a class of more general sensitivity indices defined through dissimilarity measures. As one can see herebelow, one can thus define *moment-independent sensitivity indices* which do not rely on the variance of the output as a QoI.

Sensitivity indices derived from Csiszár $\mathrm{f_C}$-divergences. A wide class of dissimilarity measures is given by the family of *Csiszár* $\mathrm{f_C}$*-divergences* [8]. The dissimilarity measure, if chosen

[8] Note that the notation $\mathrm{f_C}$ instead of "Csiszár f-divergences" is adopted here to avoid any confusion with PDFs.

among the class of Csiszár $\mathrm{f_C}$-divergences (denoted $\mathcal{D}_{\mathrm{f_C}}(\cdot,\cdot)$) is given by [9]:

$$\mathcal{D}_{\mathrm{f_C}}(P_Y, P_{Y|X_i}) = \int_{\mathbb{R}} \mathrm{f_C}\left(\frac{f_Y(y)}{f_{Y|X_i}(y|x_i)}\right) f_{Y|X_i}(y|x_i)\mathrm{d}y \tag{4.20}$$

where $\mathrm{f_C}(\cdot)$ is a convex function defined such that the normalization condition $\mathrm{f_C}(1) = 0$ is verified [10]. The divergence function $\mathrm{f_C}(\cdot)$ can be chosen among a wide list of functions. For instance, one can mention:

- the *Kullback-Leibler divergence*: $\mathrm{f_C}(t) = -\ln(t)$ or $\mathrm{f_C}(t) = t\ln(t)$;
- the *Kolmogorov total variation distance*: $\mathrm{f_C}(t) = |t-1|$;
- the *Pearson* χ^2 *divergence*: $\mathrm{f_C}(t) = (t-1)^2$ or $\mathrm{f_C}(t) = t^2 - 1$.

As a consequence, combining Eq. (4.20) and Eq. (4.17), one can build the following generic $\mathrm{f_C}(\cdot)$-dependent sensitivity index:

$$S_i^{\mathcal{D}_{\mathrm{f_C}}} = \int_{\mathcal{D}_{X_i}\times\mathcal{D}_Y} \mathrm{f_C}\left(\frac{f_Y(y)f_{X_i}(x_i)}{f_{X_i,Y}(x_i,y)}\right) f_{X_i,Y}(x_i,y)\mathrm{d}x_i\mathrm{d}y. \tag{4.21}$$

The motivation for creating such a wide class of indices can be summed up as: an input X_i has a strong influence on the model output Y if, when one fixes this input, one can measure a strong change in the distribution of Y, and not only on the second-order-moment of Y (i.e., the variance, as for Sobol indices). This type of index has the fundamental properties of being nonnegative and reducing to zero if X_i and Y are independent. Finally, it can be shown that, choosing a particular function $\mathrm{f_C}(\cdot)$ in the previous list allows to reconstruct [11] several indices proposed in the literature in various contexts (Da Veiga, 2015; Rahman, 2016). As a few examples, one can cite:

- the *Kullback-Leibler discriminator* from Park and Ahn (1994) and *Relative entropy index* proposed by Liu et al. (2006a) both rely on the use of the Kullback-Leibler divergence with $\mathrm{f_C}(t) = t\ln(t)$;
- the *Entropy index* proposed by Krzykacz-Hausmann (2001) is a normalized version of the hereabove index assuming a Kullback-Leibler divergence with $\mathrm{f_C}(t) = -\ln(t)$;
- the *Moment-independent sensitivity index* (a.k.a. the *Borgonovo index*) proposed by Borgonovo (2007) relies on the use of the Kolmogorov total variation distance with $\mathrm{f_C}(t) = |t-1|$.

All these indices presented hereabove are not detailed in this manuscript for the sake of conciseness, but more information about them can be found in Caniou (2012) and Lemaître (2014) for an overview of their respective classical formulations. The major interest of all these indices is that they provide a better insight about sensitivities when the variance of the output is no longer relevant, and thus outperform the Sobol indices. For instance, a comparison between Sobol indices and both the "Entropy index" and "Relative entropy index" is proposed in Auder

[9] Formally, one needs to assume that, for any $i = 1,\ldots,d$, the couple (X_i, Y) has an absolutely continuous distribution w.r.t. the Lebesgue measure on $\mathbb{R}^2$. Thus, one can reasonably assume that the PDFs f_Y, $f_{Y|X_i}$ and $f_{X_i,Y}$ do exist.

[10] Note that this condition ensures that the smallest possible value for $\mathcal{D}_{\mathrm{f_C}}(P_Y, P_{Y|X_i})$ is zero, which is a useful property for the sensitivity indices.

[11] The term "reconstruct" here denotes the fact that the way these indices are presented in this manuscript, i.e., through their common underlying framework should not be misleading for the reader. Several sensitivity indices have been proposed several years before this common interpretation framework.

and Iooss (2009). As for "Moment-independent sensitivity index / Borgonovo index", much effort has been done to propose efficient estimation strategies (see, e.g., Wei et al., 2013; Derennes et al., 2018a; Derennes et al., 2018b) which could replace the initial "double-loop sampling" strategy (Borgonovo, 2007) which can be cumbersome for complex computer codes.

Sensitivity indices derived from other dissimilarity measures. Other dissimilarity measures can be used to extend the previous indices. In Da Veiga (2015), *dependence measures* such as the *mutual information* (which, when combined with specific Csiszár f_C-divergences, leads to a non-normalized version of the Entropy index presented hereabove), *distance correlation* (dCor) and the *Hilbert-Schmidt independence criterion* (HSIC). Starting from the two last dependence measures (dCor and HSIC), and working in the dedicated theoretical framework of *Reproducing Kernel Hilbert Spaces* (RKHS, see, e.g., Berlinet and Thomas-Agnan (2004)), two indices and their pick-and-freeze estimators are proposed and tested over a large panel of examples. A few advantages, among others, remain their low computational cost compared to Sobol indices and their ability to deal with large number of inputs. Finally, the possible use of these indices for screening purposes has been recently investigated in De Lozzo and Marrel (2016b) and their extension to SA of spatial model outputs has been studied in De Lozzo and Marrel (2016c). However, the accurate estimation of dependence measures in high-dimension remains a challenge for indices such as those defined using Csiszár f_C-divergences or other dependence measures.

4.2.3.3 Sensitivity indices based on contrast functions

Another class of sensitivity indices, called *goal-oriented sensitivity indices* has been introduced by Fort et al. (2016) [12]. These indices are based on the use of *contrast functions*.

As a first point, one can recall the wide variety of existing QoIs mentioned in Section 2.5.1 and the associated "goal-oriented point-of-view". Based on this analysis, Fort et al. (2016) propose to consider that all of the QoIs listed in Section 2.5.1 (i.e., the PDF of the model output f_Y, the mean value $\mathbb{E}[Y]$ or an exceedance probability $\mathbb{P}(Y \geq y_{\text{th}})$) can be considered as various different *features*, denoted by the generic quantity $\rho_{\mathcal{Z}} \in \mathcal{Z}$, with $\mathcal{Z}$ the *feature space*. Then, a *contrast function* (assuming that P_Y is some probability measure on the space $\mathcal{D}_Y$) is defined as any function ψ given by:

$$\psi : \left| \begin{array}{ccl} \mathcal{Z} & \longrightarrow & L^1(P_Y) \\ \rho_{\mathcal{Z}} & \longmapsto & \psi(\cdot, \rho_{\mathcal{Z}}) : y \in \mathcal{D}_Y \longmapsto \psi(y, \rho_{\mathcal{Z}}) \end{array} \right. \tag{4.22}$$

and such that $\rho^*_{\mathcal{Z}} = \underset{\rho_{\mathcal{Z}} \in \mathcal{Z}}{\arg\min}\ \Psi(Y, \rho_{\mathcal{Z}})$, where $\Psi : \rho_{\mathcal{Z}} \mapsto \mathbb{E}_Y[\psi(Y, \rho_{\mathcal{Z}})]$ is called the *average contrast function*. As an example, by choosing $\mathcal{Z} = \mathbb{R}$ as the feature space, thus one gets $\rho_{\mathcal{Z}} = \mathbb{E}[Y] \in \mathbb{R}$ and finally one gets the mean contrast given by $\psi(y, \rho_{\mathcal{Z}}) = (y - \rho_{\mathcal{Z}})^2$. Another example consists in choosing $\mathcal{Z} = [0,1]$, then $\rho_{\mathcal{Z}} = \mathbb{P}(Y \geq y_{\text{th}}) \in [0,1]$. As a result, the contrast function is given by $\psi(y, \rho_{\mathcal{Z}}) = (\mathbb{1}_{\{y > y_{\text{th}}\}}(y) - \rho_{\mathcal{Z}})^2$. Other examples can be found in Rachdi (2011, Chap. 2). Finally, the associated sensitivity index (called *ψ-index*) is given by:

$$S_i^{\psi} = \frac{\mathbb{E}[\psi(Y, \rho^*_{\mathcal{Z}})] - \mathbb{E}_{(X_i,Y)}[\psi(Y, \rho_{\mathcal{Z},i}(X_i))]}{\mathbb{E}[\psi(Y, \rho^*_{\mathcal{Z}})] - \mathbb{E}[\min_{\rho_{\mathcal{Z}}} \psi(Y, \rho_{\mathcal{Z}})]} \tag{4.23}$$

[12] Note that, in their paper, Fort et al. (2016) aim at developing a general approach for SA, named "*Goal Oriented Sensitivity Analysis*" (GOSA). The term "*Reliability-oriented sensitivity analysis*" (ROSA) used in this manuscript (not dedicated to a single method but to a wider class of methods) has been mainly borrowed and adapted from this reference and from the recent work of Perrin and Defaux (2019).

where $\rho_{\mathcal{Z},i}(x_i) = \arg\min_{\rho_{\mathcal{Z}}} \mathbb{E}[\psi(Y,\rho_{\mathcal{Z}})|X_i = x_i]$ is a feature of interest about Y conditionally to $X_i = x_i$ (which can be computed analytically for special cases of interest, see Rachdi (2011, Chap. 2)). Moreover, as mentioned in Fort et al. (2016), for specific cases, the second term in the denominator satisfies $\mathbb{E}[\min_{\rho_{\mathcal{Z}}} \psi(Y,\rho_{\mathcal{Z}})] = 0$. For any further details about practical implementation of these indices (e.g., MC estimators have been derived), the reader should refer to Rachdi (2011) and Fort et al. (2016). As a final remark, one should notice that, when choosing the *mean contrast* $\psi(y,\rho_{\mathcal{Z}}) = (y-\rho_{\mathcal{Z}})^2$, the ψ-indices correspond to the first-order Sobol indices (Fort et al., 2016).

Among several properties, one can mention that the ψ-indices are nonnegative and satisfy $S_i^{\psi} \in [0,1]$ and $S_i^{\psi} = 0$ if Y and X_i are independent. A major advantage remains their adaptability w.r.t. the chosen goal (i.e., the feature of interest) and their ability to provide more information than variance-based indices. However, for some specific contrasts (e.g., quantile-contrasts), their estimation remains difficult (see, e.g., Browne (2017, Chap. 7,8) and Maume-Deschamps and Niang (2018)).

4.2.3.4 Shapley effects

Shapley effects (a.k.a. *Shapley values*) have been introduced in game theory by Shapley (1953). The basic idea of Shapley values is, in the context of game theory, to find a way to fairly reward the players by splitting the gains resulting from a team effort. Thinking now in terms of variance-based SA, it appears that the idea of attributing a part of the output variance to each input contributor has some similarities. This similarity has been pointed out and brought to the SA community, in the context of variance-based SA, by Owen (2014).

Theoretically, the Shapley effects are not based on the Hoeffding-Sobol decomposition such as presented in Paragraph 4.2.3.1, but following a direct allocation of a part of the output variance to each input. As a preliminary remark, one should notice that, contrary to the way Sobol indices have been introduced in Paragraph 4.2.3.1, i.e., in the context of independent inputs [13], Shapley effects have been studied in the context of dependent inputs in Song et al. (2016) and Owen and Prieur (2017). As a consequence, the formulation of the Shapley effect associated with the i-th input variable X_i, while considering a set of inputs indexed by $v \subseteq \{1,\dots,d\}$, is given by:

$$Sh_i = \sum_{v \subseteq -\{i\}} \frac{(d-|v|-1)!\,|v|!}{d!}[c(v\cup\{i\}) - c(v)] \tag{4.24}$$

where $-\{i\} \equiv \{1,\dots,i-1,i+1,\dots,d\}$, $|v|$ stands for the cardinality of v and $c(\cdot)$ is a cost function. To make the link with Sobol indices, Song et al. (2016) and Iooss and Prieur (2017) propose to use the following cost function:

$$c(v) = \frac{\mathrm{Var}\left[\mathbb{E}[Y|\mathbf{X}_v]\right]}{\mathrm{Var}\left[Y\right]} \equiv S_v^{\mathrm{clo}} \tag{4.25}$$

with $\mathbf{X}_v$ the group of input variables whose indices correspond to those in v. Finally, this cost function corresponds to the so-called *closed Sobol index*, denoted by S_v^{clo}, and defined for a group of variables (Prieur and Tarantola, 2017). Consequently, the underlying idea of the Shapley effect Sh_i associated with X_i is that it intrinsically contains the possible interactions and/or correlations with other inputs X_j, for $j \in \{1,\dots,d\}, j \neq i$. Thus, to clarify the link between Shapley effects and Sobol indices, one can discriminate two cases:

[13] Note that, a wide literature about Sobol indices in the context of dependent inputs can be found, e.g., in Chastaing (2013) and in the first section of Iooss and Prieur (2017) for a comprehensive review.

- if the inputs are independent, the following equation holds:

$$S_i \leq Sh_i \leq S_{T_i} \tag{4.26}$$

  which makes the Shapley value be a "midpoint" between Sobol indices (Owen, 2014);

- if the inputs are dependent, then the previous equation does not hold anymore and multiple cases (Gaussian inputs or not, linear correlation vs. interaction between inputs) have been investigated (see Iooss and Prieur (2017), Benoumechiara and Elie-Dit-Cosaque (2018), and Broto et al. (2018)). However, if $Sh_i \approx 0$, one can still deduce that the input X_i does not contribute to the variance of the output, which meets the FF-setting.

Consequently, Shapley effects may provide relevant information in a context of dependent inputs compared to Sobol indices. As a key example, Iooss and Prieur (2017) show that an input, not directly involved in the numerical model $\mathcal{M}(\cdot)$, may have a non-zero effect if it is correlated with another influential input of the model. The main drawback concerns the estimation of Shapley effects. As pointed out in Owen (2014), Song et al. (2016), and Iooss and Prieur (2017), if one is able to compute the complete set of Sobol indices, then Shapley effects can be obtained as a simple post-treatment. Conversely, computing, in a direct way, Shapley effects may be prohibitive for general complex computer models (e.g., see the algorithms proposed by Song et al. (2016)). Finally, Iooss and Prieur (2017) and Benoumechiara and Elie-Dit-Cosaque (2018) investigate the use of surrogate-model-based strategies to avoid the computational burden.

4.3 Synthesis about SAMO and motivations for reliability-oriented sensitivity analysis

4.3.1 Synthesis and discussion about SAMO methods

Several SAMO methods (but only a limited panel of them) have been reviewed in the previous section. They rely on various underlying assumptions and mathematical frameworks. As a result, they provide a wide panel of qualitative and/or quantitative information in terms of sensivitity indices and potential ranking. However, the interpretation of these results remain a challenging task for the analyst who has to compare and contrast these results as much as possible, and take care of the multiple underlying constraints which might have an impact and lead to an erroneous interpretation.

A few constraints for the analyst. SAMO may suffer from various constraints the analyst should be aware of before performing such an analysis. A few examples are listed below:

- type of QoI (e.g., mean value of Y, variance of Y, full CDF of Y);
- goal of the study (e.g., fast screening vs. importance ranking);
- maximum allowable simulation budget (e.g., computational time or number of calls to the computer code);
- characteristics of the inputs (e.g., independent or not, functional input, input dimension) and of the outputs (e.g., single vs. multiple, functional output);
- available information about the model (e.g., monotonic, linear vs. nonlinear, complexity, multidisciplinary workflow, inner stochasticity);
- additional sources of uncertainties (e.g., on the input probabilistic model, on the model $\mathcal{M}(\cdot)$ itself or induced by the use of a surrogate model).

Some of the constraints mentioned above can be moderated in practice by using, when it is possible, the complementarity of several SAMO methods. Then, if the results from one method corroborates partially or totally the results obtained by another one, and if these methods rely on different assumptions, then one can consider they provide relevant results. As a synthesis, the interested reader may refer to the the decision diagram in De Rocquigny et al. (2008) and the concept map proposed in Iooss and Lemaître (2015) dedicated to global SAMO methods.

As announced at the beginning of this chapter, only a few SAMO methods have been presented. The priority has been put on SAMO methods which would exhibit a direct or indirect link with ROSA methods presented later in this chapter. For any further information about other SAMO methods, the interested reader is invited to refer to the various survey papers dedicated to this topic (see, e.g., Helton et al., 2006; Morio, 2011a; Iooss and Lemaître, 2015; Wei et al., 2015b; Borgonovo and Plischke, 2016).

4.3.2 Motivations for considering reliability-oriented sensitivity analysis

As highlighted in Figure 4.1, *reliability-oriented sensitivity analysis* (ROSA) differs from SAMO for two main reasons. The first one is due to the strong difference in the nature of the various QoIs under study (i.e., a reliability/safety measure vs. the model output). The second reason concerns the fact that, estimating a reliability measure (e.g., a failure probability p_f) requires dedicated methods, as presented in Chapter 3 which may provide reusable ingredients or features which can be relevant in the ROSA context (as thoroughly explained and illustrated in Zio and Pedroni (2012)).

Before introducing the methods, the following subsection aims at presenting the motivations for considering ROSA methods.

Restrictions about the QoI. The first reason mentioned hereabove is related to an issue which has already been pointed out and discussed in the SA literature. To make it simple, the idea is to not focus on the variability of Y over its whole support $\mathcal{D}_Y$, but on a more restrictive domain such as an interval (e.g., $[y_a, y_b]$ with $y_a < y_b$), the left/right tail of the distribution (e.g., $\{y \in \mathcal{D}_Y \mid y > y_{\text{th}}\}$), or more generally any *critical domain* $\mathcal{C}_Y$ such that $\mathcal{C}_Y \subset \mathcal{D}_Y$ (Raguet and Marrel, 2018).

This problem has been early addressed, for instance, in Spear and Hornberger (1980) and is denoted as "*regional* SA" [14]. Regional SA regroups methods whose goal is to identify specific regions in the input space corresponding to particular values (e.g., based on a binary classification of model outputs regarding if they belong to a constrained domain) of the output. Such a goal is deeply related to the FM-setting as defined in Section 4.1. Several authors derived sensitivity estimators based on SAMO methods, dedicated to perform regional SA (see, e.g., Liu et al., 2006b; Wei et al., 2015a; Pianosi et al., 2016).

At the same time, a large variety of works has been proposed in the reliability community to perform both local and global SA, but on the specific QoIs that are the failure probability p_f or the reliability index β, which are quantities which, obviously, can be related to the notion of critical domain $\mathcal{C}_Y \subset \mathcal{D}_Y$ such as described hereabove. However, it is important to notice that the estimation of the sensitivity indices with these methods is often related to the underlying technique used to get the reliability measure. These works have been gathered under the generic name "*reliability* SA". These methods are described in the next subsections and are thus not discussed here to avoid redundancy. However, one needs to mention that, a first thorough review specifically dedicated to reliability SA can be found in Lemaître (2014).

[14] Note that "*regional* SA" is also denoted sometimes as "*Monte Carlo filtering*" in some references, see, e.g., Saltelli et al. (2004, Chap. 6) and Pianosi et al. (2016) for a review. This second name is somewhat related to the fact that regional SA is linked to the FM-setting, which plays a major role not only in SA, but also in calibration of computer models and thus illustrates a link between "model vs. data/observations" as usually described in filtering theory.

Restrictions due to rare event probability estimation. The second reason mentioned in the introductory paragraph hereabove is related to the fact that performing ROSA implies first to get "access" to the reliability measure. In the context of rare event probability estimation, this specific task can be difficult and/or computationally expensive to achieve and may require dedicated techniques as presented in Chapter 3. Very recently, in a thorough review proposed by Raguet and Marrel (2018), the authors suggest to adopt a new paradigm to describe and generalize both "regional SA" and "reliability SA". They advocate the fact that one should consider, in addition to traditional global SA, two other SA families:

- first, "*target* SA", which still considers the entire input domain but aims at studying their impact over the critical domain $\mathcal{C}_Y$, and more specifically, over the occurrence of the critical event [15].
- second, "*conditional* SA", whose aim is to study the influence of the input exclusively within the critical domain $\mathcal{C}_Y$.

Consequently, following Raguet and Marrel (2018), one will see that some ROSA methods fit the definition of "target SA" while others are related to "conditional SA". Finally, as highlighted several times in their paper, the key challenge for target SA concerns the difficulties induced by the rareness of the critical event. This problem is typically a matter of efficient rare event estimation. Thus, the following review aims at presenting methods which stem from the reliability community and are thus adapted to rare event estimation.

"SA-settings" revisited. As highlighted in Lemaître (2014, Chap. 1) and illustrated in Zio and Pedroni (2012), in the specific context of ROSA, the traditional SA-settings as stated in Section 4.1 have to be reinterpreted. Moreover, it appears that in the ROSA context, two levels are of interest in input: the basic variables and the probabilistic model (i.e., the distribution type and the distribution parameters). Assuming that a parametric model has been set up (see Subsection 2.4.2), only the distribution parameters remain in the second level of input uncertainty. As an illustration, one can propose the following causal chain:

$$\boldsymbol{\theta} \mapsto \mathbf{X}_{\boldsymbol{\theta}} \mapsto g(\mathbf{X}_{\boldsymbol{\theta}}) \mapsto \mathbb{1}_{\mathcal{F}_x}(\mathbf{X}_{\boldsymbol{\theta}}) \mapsto p_{\mathrm{f}}(\boldsymbol{\theta}) \tag{4.27}$$

where $\boldsymbol{\theta} = (\theta_1, \ldots, \theta_{n_\theta})^\top \in \mathcal{D}_{\boldsymbol{\Theta}} \subseteq \mathbb{R}^{n_\theta}$ is the vector of distribution parameters, $\mathbf{X}_{\boldsymbol{\theta}}$ denotes the implicit dependence between $\mathbf{X}$ and $\boldsymbol{\theta}$ through the PDF $f_{\mathbf{X}}(\cdot;\boldsymbol{\theta})$, and $p_{\mathrm{f}}(\boldsymbol{\theta})$ denoting the resulting scalar mapping between the input of the chain, $\boldsymbol{\theta}$, and the output, p_{f}. As a result, in the ROSA context, one can consider the following ojectives:

- Objective #1

  $\hookrightarrow$ Quantify the sensitivity of a reliability measure w.r.t. the input distribution type.

- Objective #2

  $\hookrightarrow$ Determine which inputs are the most influential w.r.t. the occurence of the failure event.

These objectives should reflect important motivations to perform ROSA.

To sum up, in this section, the aim is to provide a review of ROSA methods, gathering methods developed in both fields of reliability and sensitivity analysis. To do so, one need to distinguish between two sorts of ROSA methods regarding the two input levels:

[15] Note that earlier works in SAMO (see, e.g., Da Veiga, 2015; Fort et al., 2016) have already foreseen the potential difficulties/differences regarding the FP- or FF-settings if one focuses on the occurrence of a critical event (e.g., by considering the indicator function of the critical event, such that $\mathbb{1}_{\mathcal{C}_Y}(y)$) instead of the whole distribution of Y.

- ROSA w.r.t. distribution parameters (i.e., ROSA w.r.t. $\boldsymbol{\theta}$);
- ROSA w.r.t. input variables (i.e., ROSA w.r.t. $\mathbf{X}$).

These two input levels correspond to two different kinds of *variables of interest* (VoIs): either the distribution parameters in $\boldsymbol{\theta}$ or the input variables in $\mathbf{X}$. As a result, due to the causal chain given in Eq. (4.27), the first type of ROSA methods is of major interest when one desires to focus on a reliability measure as a QoI (i.e., p_f or β). Thus, depending on the formalism used to treat the uncertainty in $\boldsymbol{\theta}$, both local, screening or global methods can be envisaged. As for the second type of ROSA methods, various QoIs can be envisaged in addition to the traditional reliability measures (e.g., the LSFs $g(\cdot)$ / $\mathring{g}(\cdot)$ or the indicator function of the failure domain $\mathbb{1}_{\mathcal{F}_\bullet}(\cdot)$). Then, depending on the objectives, constraints (computational cost) and the available information about the input distributions, both local, screening or global methods can be envisaged.

4.4 Reliability-oriented sensitivity analysis with respect to distribution parameters

4.4.1 Local ROSA methods with respect to distribution parameters

4.4.1.1 Sensitivities through MPFP-based techniques

Gradients of the reliability index and the failure probability. A set of local derivative-based indices have been proposed by Hohenbichler and Rackwitz (1986), Bjerager and Krenk (1987), and Bjerager and Krenk (1989) to locally assess the impact on the reliability index due to a change in the input distribution parameters, denoted as $\boldsymbol{\theta} \in \mathbb{R}^{n_{\boldsymbol{\theta}}}$. Starting from the expression of the Hasofer-Lind reliability index, the gradients are given by:

$$\nabla_{\boldsymbol{\theta}} \beta = \mathbf{J}_{\mathbf{u},\boldsymbol{\theta}}(\mathbf{u}^*;\boldsymbol{\theta})^\top \boldsymbol{\alpha} \tag{4.28}$$

where $\mathbf{J}_{\mathbf{u},\boldsymbol{\theta}}(\mathbf{u};\boldsymbol{\theta}) = [\partial u_i / \partial \theta_j]_{d \times n_{\boldsymbol{\theta}}}$ is the Jacobian matrix of the transformation $T(\cdot)$ w.r.t. the distribution parameters $\boldsymbol{\theta}$. The detailed derivations can be found in Bjerager and Krenk (1989) and Ditlevsen and Madsen (2007, Chap. 8). As a result, the gradient of the FORM estimate for the failure probability can be derived as follows:

$$\nabla_{\boldsymbol{\theta}} p_\mathrm{f}^{\mathrm{FORM}} = -\varphi(\beta) \nabla_{\boldsymbol{\theta}} \beta. \tag{4.29}$$

These gradients are useful, not only from a sensitivity perspective (see, e.g., the study of parameter sensitivity in finite element reliability analysis by Haukaas and Der Kiureghian (2005)), but also for reliability-based design optimization (Hou et al., 2004). However, these derivations are performed under the assumption of the uniqueness of the MPFP, which may be erroneous for a large variety of applications. Nonetheless, extensions to system reliability problems with multiple MPFPs (e.g., involving series and/or parallel systems), can be found in Karamchandani and Cornell (1992). When the LSS is nonlinear, one can still improve FORM sensitivities by considering the *multi-hyperplane combination method* (MHCM) and its associated sensitivity indices as proposed by Dong et al. (2014). Another possibility is to use the sensitivities derived in a SORM-like fashion (called *novel* SORM) as proposed in Yoo et al. (2014).

As a remark, one should notice that the Jacobian matrix appearing in Eq. (4.28) is obtained by differentiating the terms within the Nataf transformation (presented briefly in Appendix C). This differentiation makes appear two terms which may be, depending on the nature of $\boldsymbol{\theta}$ (i.e., a

moment, a linear correlation parameter or any other distribution parameter), negligible or not. Details about these derivations can be found in Bourinet (2018) [16].

Elasticities. For a comparison purpose, one can obtain normalized sensitivities, called *elasticities* (Lemaire et al., 2009, Chap. 6). These elasticities can be obtained according to various normalization formulas. A common way used in ROSA w.r.t. distribution parameters is to consider the following formula, here given for the reliability index:

$$e_{\theta_k} = \frac{\theta_k}{\beta} \frac{\partial \beta}{\partial \theta_k}. \tag{4.30}$$

Elasticities can be used to efficiently compare, at a low cost, the relative influence of inputs as illustrated in Chocat et al. (2016). However, as explained further in Chapter 6, several formulas for elasticities are available in literature and the scaled values obtained may vary from one formula to another (see, e.g., Wu, 1994b; Der Kiureghian, 1999; Lemaire et al., 2009; Millwater and Wieland, 2010).

4.4.1.2 Sensitivities through sampling-based techniques

In a similar manner as for MPFP-based techniques, local reliability-oriented sensitivity indices can be obtained through the use of sampling-based techniques. In the following, the idea is to present the underlying principle of the indices. Then, the interested reader is invited to refer to several references for details concerning a specific technique.

Sensitivities with CMC using the score function. To assess local sensivitities of the failure probability w.r.t. distribution parameters, one can consider the following partial derivative, for any distribution parameter $\theta_k \in \boldsymbol{\theta}$:

$$\frac{\partial p_\mathrm{f}}{\partial \theta_k} = \frac{\partial}{\partial \theta_k} \int_{\mathcal{D}_\mathbf{X}} \mathbb{1}_{\mathcal{F}_\mathbf{x}}(\mathbf{x}) f_\mathbf{X}(\mathbf{x}) \mathrm{d}\mathbf{x}. \tag{4.31}$$

Then, assuming that (i) the joint PDF $\mathbf{X}$ is continuously differentiable w.r.t. θ_k and (ii) the integration domain $\mathcal{D}_\mathbf{X}$ does not depend on θ_k, one can write [17]:

$$\frac{\partial p_\mathrm{f}}{\partial \theta_k} = \int_{\mathcal{D}_\mathbf{X}} \mathbb{1}_{\mathcal{F}_\mathbf{x}}(\mathbf{x}) \frac{\partial f_\mathbf{X}(\mathbf{x})}{\partial \theta_k} \mathrm{d}\mathbf{x}. \tag{4.32}$$

By simply manipulating this integral, using an *importance sampling trick* (here, with the initial density $f_\mathbf{X}$) as in Section 3.4, one gets:

$$\begin{aligned} \frac{\partial p_\mathrm{f}}{\partial \theta_k} &= \int_{\mathcal{D}_\mathbf{X}} \mathbb{1}_{\mathcal{F}_\mathbf{x}}(\mathbf{x}) \frac{\partial f_\mathbf{X}(\mathbf{x}) / \partial \theta_k}{f_\mathbf{X}(\mathbf{x})} f_\mathbf{X}(\mathbf{x}) \mathrm{d}\mathbf{x} \\ &= \int_{\mathcal{D}_\mathbf{X}} \mathbb{1}_{\mathcal{F}_\mathbf{x}}(\mathbf{x}) \frac{\partial \ln f_\mathbf{X}(\mathbf{x})}{\partial \theta_k} f_\mathbf{X}(\mathbf{x}) \mathrm{d}\mathbf{x} \\ &= \mathbb{E}_{f_\mathbf{X}}[\mathbb{1}_{\mathcal{F}_\mathbf{x}}(\mathbf{X})\ \kappa_{\theta_k}(\mathbf{X})] \end{aligned} \tag{4.33}$$

where $\kappa_{\theta_k}(\mathbf{X}) \overset{\text{def}}{=} \frac{\partial \ln f_\mathbf{X}(\mathbf{x})}{\partial \theta_k}$ is called the *score function* (SF). This way of deriving sensitivities in the CMC setting has been first introduced by Rubinstein (1986) and then popularized by many other

[16] Note that, for the specific topic of sensitivity w.r.t. linear correlation parameters, one can refer to Žanić and Žiha (1998), Žanić and Žiha (2001), Bourinet and Lemaire (2008), and Bourinet (2017). A synthesis of these works is given in Bourinet (2018).

[17] Note that this equality holds if one applies the *Lebesgue's dominated convergence theorem* (Jacod and Protter, 2004).

works such as Wu (1994b), Rahman (2009), Millwater (2009), Millwater et al. (2011), Millwater et al. (2012), and Garza and Millwater (2016a) [18].

The CMC estimator of the quantity $\partial p_f / \partial \theta_k$, for a N-sample $\{\mathbf{X}^{(j)}\}_{j=1}^{N} \overset{\text{i.i.d.}}{\sim} f_{\mathbf{X}}$, is given by:

$$\widehat{\frac{\partial p_f}{\partial \theta_k}} = \frac{1}{N} \sum_{j=1}^{N} \mathbb{1}_{\mathcal{F}_{\mathbf{x}}}(\mathbf{X}^{(j)}) \, \kappa_{\theta_k}(\mathbf{X}^{(j)}) \tag{4.34}$$

which highlights the fact that, using this estimator enables to reuse the same samples for estimating both p_f and its gradients w.r.t. distribution parameters. This simple *post-processing / post-treatment* step made the SF popular for various applications, from rare event estimation to reliability-based design optimization (see, e.g., Jha et al., 2009; Taflanidis and Beck, 2009; Millwater and Wieland, 2010; Chowdhury and Adhikari, 2010; Dubourg and Sudret, 2011; Dubourg and Sudret, 2014; Garza and Millwater, 2016b).

As a remark, one should mention that, when the condition (ii) mentioned hereabove is not fulfilled, i.e., when one considers finite supports such as for truncated probability distributions (e.g., uniform distribution, truncated Gaussian), the derivations are not straightforward as presented above, and one needs to apply *Leibniz integral rule for differentiation* for parameter-dependent integrals. For the sake of consiseness (and due to the fact that an adaptation of these derivations will be detailed in Chapter 6), the interested reader should refer to Millwater and Feng (2011) and Lee et al. (2011).

Finally, in a similar manner, Breitung (1991) derived asymptotic approximation formulas (i.e., valid for $\beta \to +\infty$) of both the failure probability and its sensitivities, in the cases of unbounded and bounded distributions (see, e.g., Cherng and Wen (1994) for an application of the method).

As a final remark, one can notice that, similarly to what has been done in Eq. (4.30), elasticities can also be derived based on the SF estimates.

Sensitivities derived for other sampling techniques. In the literature, several rare event techniques allow to derive, either using a SF-like method, or directly using partial derivatives, a set of sensitivities of p_f w.r.t. distribution parameters. Without going deeper into details, this paragraph aims at providing a brief overview of these multiple variants associated to well-known rare event estimation techniques:

- *Adaptive importance sampling*: see, e.g., Wu (1994a);
- *Stratified importance sampling*: see, e.g., Feng et al. (2010);
- *Subset sampling*: see, e.g., Song et al. (2009b) and Bourinet (2018, Chap. 1) for a detailed review;
- *Line sampling*: see, e.g., Lu et al. (2008), Song et al. (2009a), and Valdebenito et al. (2018);
- *Directional sampling*: see, e.g., Song et al. (2011);
- *Method of moments*: see, e.g., Song et al. (2010).

Finally, one should point out the work of Zio and Pedroni (2012) in which the authors compare sensitivity estimates obtained from both subset and line sampling mentioned hereabove in a context of reliability assessment of a complex nuclear engineering thermal-hydraulic passive system.

[18] Note that the name instead of the traditional name "*score function*", one can also encounter sometimes the terms "*kernel function*" such as in Millwater (2009).

4.4.1.3 Hybrid strategies mixing MPFP-based techniques and sampling

Another class of methods may combine some tools from both MPFP-based techniques and sampling techniques. As an example, one can cite the proposed method by Melchers and Ahammed (2004) which uses MC simulations to fit an hyperplane by least-square regression and then treat the problem in a FORM-like fashion, by deriving analytical sensitivities, but avoiding any transformation to the $\mathbf{u}$-space. However, the efficiency of the method greatly depends on the accuracy of the tangent hyperplane estimation. Moreover, this method is still limited regarding the possible strong nonlinearity of the true LSS. An extension of this work to non-normal random variables and constrained LSF can be found in Ahammed and Melchers (2006). Conversely, Sues and Cesare (2005) propose a method (for system reliability problems) which combines FORM to get the failure probability and MC simulations over the hyperplane to calculate analytical sensitivities using traditional partial derivative formulas.

4.4.2 Screening-like ROSA methods with respect to distribution parameters

As presented before, local ROSA methods, mainly through the use of partial derivatives, study the impact of a local change in the distribution parameters on the reliability measure which can be either the reliability index or the faillure probability. A possible way to generalize the study of the sensitivities w.r.t. distribution parameters, in a global sense, is to repeat a local sensitivity calculation for several different values $\{\boldsymbol{\theta}^{(j)}\}_{j=1}^{N}$. This is the main aim of screening methods as presented in the SAMO context in Section 4.2.2. Doing so implies, either to embrace the idea that *epistemic* uncertainty (i.e., lack-of-knowledge) does affect the input probabilistic modeling, or to desire to test the *robustness* of the reliability assessment regarding possible variations in the input probabilistic model. However, such parameter values may arise from three different but complementary processes:

- firstly, by adopting a *deterministic* point of view, which consists in sampling over a regular grid-based DOE;
- secondly, by adopting a *Bayesian* point of view, which implies to consider a prior density $f_{\boldsymbol{\Theta}} : \mathcal{D}_{\boldsymbol{\Theta}} \subseteq \mathbb{R}^{n_{\boldsymbol{\theta}}} \to \mathbb{R}_+$;
- thirdly, by adopting an *extra / imprecise probabilistic* point of view, which consists in considering other frameworks (e.g., intervals, fuzzy sets, etc.) [19].

In the following, two screening ROSA methods are presented.

4.4.2.1 A Morris method for ROSA

Following the same principles as those introduced in Subsection 4.2.2.1, Xiao et al. (2016) proposed to adapt the modified Morris' elementary effects method proposed by Campolongo et al. (2007) (i.e., using the $\mu^*_{|\Delta_i^{\mathrm{EE}}|}$ instead of the $\mu_{\Delta_i^{\mathrm{EE}}}$ one) to the ROSA context. Here, the inputs are independent epistemic uncertain distribution parameters gathered in the vector $\boldsymbol{\theta} = (\theta_1, \ldots, \theta_{n_{\boldsymbol{\theta}}})^\top \in \mathcal{D}_{\boldsymbol{\Theta}} \subseteq \mathbb{R}^{n_{\boldsymbol{\theta}}}$. The idea is to consider the following elementary effect (for $k \in \{1, \ldots, n_{\boldsymbol{\theta}}\}$):

$$\Delta_k^{\mathrm{EE}}(\boldsymbol{\theta}^{(j)}) = \frac{p_{\mathrm{f}}(\boldsymbol{\theta}^{(j)} + \delta_{\mathrm{EE}}\, \mathbf{e}_k) - p_{\mathrm{f}}(\boldsymbol{\theta}^{(j)})}{\delta_{\mathrm{EE}}} \overset{\mathsf{def}}{=} \Delta_k^{\mathrm{EE},(j)} \tag{4.35}$$

[19] Note that, in some references, Bayesian approaches are considered as being part of imprecise probabilities (see, e.g., Schöbi, 2017). In this manuscript, the choice of distinguishing these two families is made, not to break with the previous point of view, but because the Bayesian framework is more familiar due to its probabilistic roots than many other frameworks belonging to imprecise probabilities

where the failure probability p_f is estimated for each grid-point $\boldsymbol{\theta}^{(j)}$ using a particular rare event estimation technique [20]. However, any other technique such as those presented in Chapter 3 could be, in theory, used here. Finally, one can compute the set of two indices $(\mu^*_{|\Delta_k^{\text{EE}}|}, \sigma_{|\Delta_k^{\text{EE}}|})$ following formulas given in Eq. (4.5). The main drawback here remains that one needs to estimate several times (i.e., for all the grid-points) a possibly expensive-to-evaluate rare event probability which can be cumbersome.

4.4.2.2 Derivative-based global sensitivity measures for ROSA

Following what has been presented in Subsection 4.2.2.2, another way of thinking consists in deriving a global sensitivity measure based on the integral of local derivatives. Thus, a DGSM-like index has been proposed in the ROSA context by Wang et al. (2013a). The formulation of this index is as follows (for $k \in \{1, \dots, n_{\boldsymbol{\theta}}\}$) [21]:

$$\nu_k = \int_{\mathcal{D}_{\boldsymbol{\Theta}}} \left| \frac{\partial p_f(\boldsymbol{\theta})}{\partial \theta_k} \right| f_{\boldsymbol{\Theta}}(\boldsymbol{\theta}) \mathrm{d}\boldsymbol{\theta} \tag{4.36}$$

where $\partial p_f(\boldsymbol{\theta})/\partial \theta_k$ is obtained using the SF estimator given in Eq. (4.34). Finally, numerical estimation results are obtained using QMC and point estimate techniques. If the relative ranking of the most important parameters may be correctly estimated for screening purposes, the values obtained seem to be difficult to interpret in terms of absolute ranking for factor fixing purposes.

4.4.3 Importance measures for global ROSA with respect to distribution parameters

4.4.3.1 Variance-based importance measures for ROSA

Sobol indices on the conditional failure probability. Morio (2011b) proposed to consider that the change in a failure probability estimate due to epistemic uncertainty affecting distribution parameters can be seen in a functional relationship such that $P_f = \Gamma(\boldsymbol{\theta})$, whith $\Gamma : \mathbb{R}^{n_{\boldsymbol{\theta}}} \to \mathbb{R}$ (one can consider, for instance, a single parameter per input variable, e.g., the mean, which leads to $n_{\boldsymbol{\theta}} = d$). The distribution parameters $\boldsymbol{\theta}$ are assumed to be distributed according to a prior density $f_{\boldsymbol{\Theta}}$. Then, one can use a similar F-ANOVA as in Subsection 4.2.3.1 and get the following indices:

$$S_i^{P_f} = \frac{\mathrm{Var}\left[\mathbb{E}[P_f|\theta_i]\right]}{\mathrm{Var}\left[P_f\right]} \tag{4.37}$$

$$S_{T_i}^{P_f} = 1 - \frac{\mathrm{Var}\left[\mathbb{E}[P_f|\boldsymbol{\theta}^{-i}]\right]}{\mathrm{Var}\left[P_f\right]} \tag{4.38}$$

where $\boldsymbol{\theta}^{-i}$ stands for the vector $\boldsymbol{\theta}$ of distribution parameters without the i-th component. The numerical estimation of these indices can be achieved as a *by-product* if one considers small perturbations of the distribution parameters. To do so, one can use the so-called "*reverse/inverse importance sampling trick*" (see, e.g., Beckman and McKay, 1987; Hesterberg, 1996) described hereafter. Indeed, if one considers the IS estimator given by:

$$\widehat{P}_f(\boldsymbol{\theta}) = \frac{1}{N} \sum_{j=1}^{N} \mathbb{1}_{\mathcal{F}_{\mathbf{x}}}(\mathbf{X}^{(j)}) \frac{f_{\mathbf{X}|\boldsymbol{\Theta}}(\mathbf{X}^{(j)}|\boldsymbol{\theta})}{h_{\mathbf{X}}(\mathbf{X}^{(j)})} \tag{4.39}$$

[20] This technique, proposed by Zhang and Pandey (2013), is called the *multiplicative dimensional reduction method* (M-DRM) and is based on maximum entropy principle, fractional moments and dimensional reduction method.

[21] Note that this index is built using the absolute value of the partial derivative, in a similar fashion as the modified Morris index proposed by Campolongo et al. (2007). However, some links exist between the absolute value index and the square index as explained in Kucherenko and Iooss (2017).

then, one can assume that the failure domain does not depend on $\boldsymbol{\theta}$ (e.g., under small perturbations around mean values), and that $h_{\mathbf{X}}(\cdot)$ is a quasi-optimal density that still can be used to sample efficiently within the failure domain. Thus, to compute the Sobol indices, one just needs to recalculate the weights without evaluating the complex computer code again.

Finally, these Sobol indices on the conditional failure probability have been further investigated by Wang et al. (2013b) and Wang et al. (2013c) by considering efficient surrogate-based estimation (using GP and moving least-squares). Very recently, Ehre et al. (2018) proposed a slightly different version of the indices presented above by considering the logarithmic transformation $\ln(P_{\mathrm{f}})$ instead of P_{f} in their formulation. Then, efficient estimation is proposed through a double stage sampling strategies relying on the use of surrogate models (both PCE and LRA have been tested).

4.4.3.2 Perturbed-law indices

Perturbed-law indices (PLI) have been first proposed by Lemaître (2014) and Lemaître et al. (2015) [22]. The idea is to consider that, for any input variable X_i, $\forall i \in \{1,\ldots,d\}$, of density $f_{X_i} \overset{\mathsf{def}}{=} f_i$, a perturbation δ applied to this input leads to a pertubed density $f_{i\delta}$. Then, the failure probability is perturbed from its initial value P_{f} to $P_{\mathrm{f},i\delta}$ given by:

$$P_{\mathrm{f},i\delta} = \int_{\mathcal{D}_{\mathbf{X}}} \mathbb{1}_{\mathcal{F}_{\mathbf{x}}}(\mathbf{x}) \frac{f_{i\delta}(x_i)}{f_i(x_i)} f_{\mathbf{X}}(\mathbf{x}) \mathrm{d}\mathbf{x}. \tag{4.40}$$

Then, the PLI index is defined as follows:

$$S_{i\delta}^{\mathrm{PLI}} = \left[\frac{P_{\mathrm{f},i\delta}}{P_{\mathrm{f}}} - 1\right] \mathbb{1}_{\{P_{\mathrm{f},i\delta} \geq P_{\mathrm{f}}\}} + \left[1 - \frac{P_{\mathrm{f}}}{P_{\mathrm{f},i\delta}}\right] \mathbb{1}_{\{P_{\mathrm{f},i\delta} < P_{\mathrm{f}}\}} \tag{4.41}$$

$$= \frac{P_{\mathrm{f},i\delta} - P_{\mathrm{f}}}{P_{\mathrm{f}}\, \mathbb{1}_{\{P_{\mathrm{f},i\delta} \geq P_{\mathrm{f}}\}} + P_{\mathrm{f},i\delta}\, \mathbb{1}_{\{P_{\mathrm{f},i\delta} < P_{\mathrm{f}}\}}}. \tag{4.42}$$

Thus, when $S_{i\delta}^{\mathrm{PLI}} = 0 \Longleftrightarrow P_{\mathrm{f}} = P_{\mathrm{f},i\delta}$, one can conclude that, either X_i is a noninfluential variable, or δ is negligible (e.g., robustness of the probability estimation regarding the input perturbation). Moreover, the sign of $S_{i\delta}^{\mathrm{PLI}}$ may indicate whether the perturbation increases or decreases the reliability.

As for numerical estimation, considering a sample $\{\mathbf{X}^{(j)}\}_{j=1}^{N} \overset{\text{i.i.d.}}{\sim} f_{\mathbf{X}}$, P_{f} can be estimated, for instance, using the following traditional CMC estimator as given in Eq. (3.4) and recalled below:

$$\widehat{P}_{\mathrm{f}} = \frac{1}{N} \sum_{j=1}^{N} \mathbb{1}_{\mathcal{F}_{\mathbf{x}}}(\mathbf{X}^{(j)}). \tag{4.43}$$

Then, to avoid any supplementary call to the computer code, one can estimate the perturbed failure probability $P_{\mathrm{f},i\delta}$ using the "*reverse/inverse importance sampling trick*" (see, e.g., Beckman and McKay, 1987; Hesterberg, 1996) as in the previous ROSA method proposed by Morio (2011b):

$$\widehat{P}_{\mathrm{f},i\delta} = \frac{1}{N} \sum_{j=1}^{N} \mathbb{1}_{\mathcal{F}_{\mathbf{x}}}(\mathbf{X}^{(j)}) \, \frac{f_{i\delta}(X_i^{(j)})}{f_i(X_i^{(j)})}. \tag{4.44}$$

[22] Note that these indices have been initially named "*Density Modification based Reliability Sensitivity Indices*" (DMBRSI) in Lemaître et al. (2015) and then renamed "*Perturbed-law indices*" (PLI) in Sueur et al. (2017) and Iooss and Le Gratiet (2017).

Finally, the plug-in estimator for $S_{i\delta}^{\mathrm{PLI}}$ is given by:

$$\widehat{S}_{i\delta}^{\mathrm{PLI}} = \left[\frac{\widehat{P}_{\mathrm{f},i\delta}}{\widehat{P}_{\mathrm{f}}} - 1\right] \mathbb{1}_{\{\widehat{P}_{\mathrm{f},i\delta} \geq \widehat{P}_{\mathrm{f}}\}} + \left[1 - \frac{\widehat{P}_{\mathrm{f}}}{\widehat{P}_{\mathrm{f},i\delta}}\right] \mathbb{1}_{\{\widehat{P}_{\mathrm{f},i\delta} < \widehat{P}_{\mathrm{f}}\}}. \tag{4.45}$$

Theoretical convergence proofs are provided in Lemaître (2014) and Lemaître et al. (2015). Moreover, input perturbation strategies are investigated for several input distributions in Lemaître (2014) and Lemaître et al. (2015). Recent works extended the definition and the use of PLI indices to quantiles in Sueur et al. (2017) and probability of detection curves in Iooss and Le Gratiet (2017).

4.5 Reliability-oriented sensitivity analysis with respect to input variables

4.5.1 Local ROSA methods with respect to input variables

4.5.1.1 Sensitivities through MPFP-based techniques

Importance factors via FORM and SORM. During a FORM analysis (assuming the use of FORM is relevant regarding the linearity of the LSS and the uniqueness of the MPFP), the variance of the LSF in the **u**-space as expressed in Eq. (3.15) (see, e.g., Ditlevsen and Madsen (2007, Chap. 8) and Lemaire et al. (2009, Chap. 6)):

$$\begin{aligned} \mathrm{Var}\left[\mathring{g}_1(\mathbf{U})\right] &= \mathrm{Var}\left[-\left\|\nabla_{\mathbf{u}}\, \mathring{g}(\mathbf{u}^*)\right\|_2 \left(\boldsymbol{\alpha}^\top \mathbf{U} - \beta\right)\right] \\ &= \left\|\nabla_{\mathbf{u}}\, \mathring{g}(\mathbf{u}^*)\right\|_2^2 \mathrm{Var}\left[\boldsymbol{\alpha}^\top \mathbf{U}\right] \end{aligned} \tag{4.46}$$

with $\mathrm{Var}\left[\boldsymbol{\alpha}^\top \mathbf{U}\right] = \boldsymbol{\alpha}^\top \boldsymbol{\alpha} = \alpha_1^2 + \alpha_2^2 + \cdots + \alpha_d^2$. As a result, when the input variables are independent, the α_i^2-values measure the relative influence of input variables regarding the variability of the LSF response in the vicinity of the MPFP. These indices are denoted as *importance factors* (Paloheimo and Hannus, 1974; Hohenbichler and Rackwitz, 1986) and verify the following feature:

$$\sum_{i=1}^{d} \alpha_i^2 = 1 \tag{4.47}$$

which enables an easy interpretation of such normalized indices. As a remark, these sensitivity indices are just a *by-product* (i.e., post-processing) of a FORM reliability analysis (obtained directly from Eq. (3.12)). A recent illustration of the use of these two sensitivity indices can be found in Kouassi et al. (2016).

When the inputs are not independent (e.g., linearly correlated), Der Kiureghian (1999) proposed, instead of using the α_i^2-values, to consider another set of importance factors. To do so, one needs to introduce first an "equivalent" normal vector in the **x**-space at the MPFP $\mathbf{x}^*$, denoted by $\widehat{\mathbf{X}}$ and such that $\mathbf{u} = \mathbf{u}^* + \mathbf{J}_T(\widehat{\mathbf{x}} - \mathbf{x}^*)$, with $\mathbf{J}_T = \mathbf{J}_{\mathbf{u},\mathbf{x}}$ the Jacobian matrix of the transformation $T(\cdot)$ evaluated at $\mathbf{x}^*$. Thus, these new importance factors, denoted γ_i^2-factors, are defined as follows:

$$\boldsymbol{\gamma}^\top = \frac{\boldsymbol{\alpha}^\top \mathbf{J}_T \widehat{\mathbf{D}}}{\left\|\boldsymbol{\alpha}^\top \mathbf{J}_T \widehat{\mathbf{D}}\right\|_2} \tag{4.48}$$

where $\widehat{\mathbf{D}} = [\widehat{D}_{ii}]_{d\times d}$ is a diagonal square matrix such that $\widehat{D}_{ii} = \sqrt{J_{2,ii}}$, $\forall i \in \{1,\ldots,d\}$ and $J_{2,ii}$ is the i-th diagonal term of $\mathbf{J}_2 = [J_{2,ij}]_{d\times d} = \mathbf{J}_{T^{-1}} \mathbf{J}_{T^{-1}}^\top$, with $\mathbf{J}_{T^{-1}} = \mathbf{J}_{\mathbf{x},\mathbf{u}}$ is the Jacobian matrix of the

inverse transformation $T^{-1}(\cdot)$ evaluated at $\mathbf{u}^*$.
Finally, note that, in the specific case of independent input variables X_i, then $\boldsymbol{\alpha} = \boldsymbol{\gamma}$.

When dealing with nonlinear LSS, one can use SORM to estimate the failure probability. In this case, Kouassi (2017, Chap. 4) proposed in a recent work to derive importance factors based on the SORM-cf technique (assuming that the inputs X_i are independent). It can be shown, after some derivations to get Var $\left[\mathring{g}_2(\mathbf{U})\right]$, that on can obtain the following sensitivity index:

$$\delta_i = \frac{\widetilde{\delta}_i}{\text{Var}\left[\widetilde{\mathring{g}}_2(\mathbf{U})\right]} \tag{4.49}$$

where $\widetilde{\mathring{g}}_2(\mathbf{U}) = \frac{\mathring{g}_2(\mathbf{U})}{\left\|\nabla_{\mathbf{u}} \mathring{g}(\mathbf{u}^*)\right\|_2}$. Both quantities Var $\left[\widetilde{\mathring{g}}_2(\mathbf{U})\right]$ and $\widetilde{\delta}_i$ can be computed using detailed expressions given in Kouassi (2017, Chap. 4) [23]. Moreover, the author proposed to consider two higher order indices, denoted by δ_{ij} and δ_{ijk}, to take into account possible interactions between variables. Finally, one can notice that these indices follow the normalization property (i.e., they sum to one if considering all orders of indices) but may take negative values.

Omission sensitivity factors. In the context of reliability analysis, other sensitivity indices, called *omission sensitivity factors*, have been introduced by Madsen (1988). The basic idea is to consider the conditional ratio:

$$\zeta_i = \frac{\beta_{|X_i}}{\beta} \tag{4.50}$$

where $\beta_{|X_i}$ is the Hasofer-Lind reliability index conditional to the fixed input $X_i = x_i$ [24]. For instance, Madsen (1988) advocates to replace any input X_i by its mean or its median. More information about these indices can be found in Ditlevsen and Madsen (2007, Chap. 8).

4.5.2 Importance measures for global ROSA with respect to input variables

4.5.2.1 Distance-based importance measures for ROSA

Entropy-based indices. To account for variability in the failure probability estimate (e.g., due to sampling variability), several methods relying on the notion of "entropy" have been investigated. Reid (2002) proposed to consider the *entropy* $\mathcal{E}$, defined such that $\mathcal{E} = -\sum_i p_i \ln p_i$, where p_i is a probability mass associated to a range of discrete outcomes o_i. In the reliability context, this can be used as a measure for the "Fail / Safe" binary outcomes. Thus, Reid (2002) proposed to consider the following measure:

$$\mathcal{E}(p_\text{f}) = -[p_\text{f} \ln p_\text{f} + (1 - p_\text{f}) \ln(1 - p_\text{f})]. \tag{4.51}$$

Finally, for a range of input designs (i.e., a range of input probabilistic models), leading to various failure probability values, the entropy index can be characterized by the expected value $\mathbb{E}[\mathcal{E}(P_\text{f})]$ (where P_f denotes the fact that the failure probability becomes a random variable).

Following this idea, Liu et al. (2004) and Liu et al. (2006b) developed a Kullback-Leibler-entropy-based index (called *relative entropy index*) for failure probability defined as follows [25]:

$$\mathcal{D}_{\text{KL}}(P_{\text{f}|X_i}, P_\text{f}) = P_{\text{f}|X_i} \ln\left(\frac{P_{\text{f}|X_i}}{P_\text{f}}\right) + (1 - P_{\text{f}|X_i}) \ln\left(\frac{1 - P_{\text{f}|X_i}}{1 - P_\text{f}}\right) \tag{4.52}$$

[23] Note that these expressions rely on the components of the vector $\boldsymbol{\alpha}$ and on the components of the Hessian matrix $\mathbf{H} = \nabla^2_{\mathbf{u},\mathbf{u}} \mathring{g}(\mathbf{u}^*)$.
[24] Note that the formulation of the omission sensitivity factor can be stated either in the $\mathbf{x}$-space or the $\mathbf{u}$-space.
[25] Note that the index in Eq. (4.52) is proposed in Liu et al. (2006b) as an extension of their SAMO index discussed in Subsection 4.2.3.2.

where $P_{\mathrm{f}|X_i}$ is the failure probability conditional to the fixed input $X_i = x_i$. This index is called *total effect index* for X_i, while the *main effect index* is given by $-\mathcal{D}_{\mathrm{KL}}(P_{\mathrm{f}|\mathbf{X}^{-i}}, P_{\mathrm{f}})$, where $P_{\mathrm{f}|\mathbf{X}^{-i}}$ corresponds to the failure probability estimated while all input random variables are fixed, e.g., to their mean value, except X_i. Finally, Jiang et al. (2016) proposed an extension of these relative entropy indices under mixed aleatory and epistemic uncertainties in the context of multidisciplinary systems.

Moment-independent indices. Another class of indices are based in a similar fashion as the *Borgonovo index* for SAMO (by Borgonovo (2007), as introduced in Subsection 4.2.3.2) but considering failure probabilities instead of the model output. Cui et al. (2010) introduced two different ROSA importance measures, defined such that:

$$\eta_i^{P_{\mathrm{f}}} = \frac{1}{2}\int_{-\infty}^{+\infty} |P_{\mathrm{f}} - P_{\mathrm{f}|X_i}| f_{X_i}(x_i)\mathrm{d}x_i = \frac{1}{2}\mathbb{E}_{f_{X_i}}[|P_{\mathrm{f}} - P_{\mathrm{f}|X_i}|] \tag{4.53}$$

and a second one defined such that:

$$\delta_i^{P_{\mathrm{f}}} = \frac{1}{2}\int_{-\infty}^{+\infty} (P_{\mathrm{f}} - P_{\mathrm{f}|X_i})^2 f_{X_i}(x_i)\mathrm{d}x_i = \frac{1}{2}\mathbb{E}_{f_{X_i}}[(P_{\mathrm{f}} - P_{\mathrm{f}|X_i})^2]. \tag{4.54}$$

These indices have been then investigated in several papers (see, e.g., Li et al., 2012; Ruan and Lu, 2014; Yun et al., 2016) and, independently in Lemaître (2014). Their formulation can be easily extended to groups of input variables as shown in the previous references. Finally, one should notice that the case of correlated inputs has been studied in Li et al. (2016) and that a local parametric sensitivity analysis w.r.t. input distribution parameters applied to the index in Eq. (4.54), has been proposed in Zhang et al. (2015) to monitor the effect of this second level on the importance measures.

4.5.2.2 Variance-based importance measures for ROSA

Sobol indices on the indicator function. Another set of Sobol indices has been proposed in the ROSA context. These indices have not been introduced through a F-ANOVA decomposition but as a rewriting of the moment-independent index in Eq. (4.54). Indeed, following Li et al. (2012), one can notice the link between failure probabilities and mathematical expectations:

$$P_{\mathrm{f}} - P_{\mathrm{f}|X_i} = \mathbb{E}[\mathbb{1}_{\mathcal{F}_{\mathbf{x}}}(\mathbf{X})] - \mathbb{E}[\mathbb{1}_{\mathcal{F}_{\mathbf{x}}}(\mathbf{X})|X_i]. \tag{4.55}$$

which leads to write (omitting the scalar factor $1/2$):

$$\begin{aligned}
\delta_i^{P_{\mathrm{f}}} &\propto \mathbb{E}_{f_{X_i}}[(P_{\mathrm{f}} - P_{\mathrm{f}|X_i})^2] \\
&= \mathbb{E}_{f_{X_i}}\left[(\mathbb{E}[\mathbb{1}_{\mathcal{F}_{\mathbf{x}}}(\mathbf{X})] - \mathbb{E}[\mathbb{1}_{\mathcal{F}_{\mathbf{x}}}(\mathbf{X})|X_i])^2\right] &(4.56)\\
&= \mathrm{Var}\left[\mathbb{E}[\mathbb{1}_{\mathcal{F}_{\mathbf{x}}}(\mathbf{X})|X_i]\right]. &(4.57)
\end{aligned}$$

Thus, by dividing the last equation by the total variance $\mathrm{Var}[\mathbb{1}_{\mathcal{F}_{\mathbf{x}}}(\mathbf{X})]$, one gets the following set of Sobol indices:

$$S_i^{\mathbb{1}_{\mathcal{F}}} = \frac{\mathrm{Var}\left[\mathbb{E}[\mathbb{1}_{\mathcal{F}_{\mathbf{x}}}(\mathbf{X})|X_i]\right]}{\mathrm{Var}\left[\mathbb{1}_{\mathcal{F}_{\mathbf{x}}}(\mathbf{X})\right]} \tag{4.58}$$

$$S_{T_i}^{\mathbb{1}_{\mathcal{F}}} = 1 - \frac{\mathrm{Var}\left[\mathbb{E}[\mathbb{1}_{\mathcal{F}_{\mathbf{x}}}(\mathbf{X})|\mathbf{X}^{-i}]\right]}{\mathrm{Var}\left[\mathbb{1}_{\mathcal{F}_{\mathbf{x}}}(\mathbf{X})\right]} \tag{4.59}$$

where $\mathrm{Var}\left[\mathbb{1}_{\mathcal{F}_\mathbf{x}}(\mathbf{X})\right] = P_\mathrm{f}(1-P_\mathrm{f})$. Moreover, note that, similarly to traditional Sobol indices in the SAMO context, the total index can be rewritten as (Saltelli et al., 2008):

$$S_{T_i}^{\mathbb{1}_\mathcal{F}} = \frac{\mathbb{E}\left[\mathrm{Var}\left[\mathbb{1}_{\mathcal{F}_\mathbf{x}}(\mathbf{X})|\mathbf{X}^{-i}\right]\right]}{\mathrm{Var}\left[\mathbb{1}_{\mathcal{F}_\mathbf{x}}(\mathbf{X})\right]}. \tag{4.60}$$

Efficient estimation schemes (e.g., using FORM-IS or TIS, see Chapter 3) for these Sobol indices have been investigated in Wei et al. (2012), Wei et al. (2016), and Yun et al. (2018).

Very recently, another way of deriving these indices (i.e., both the $\delta_i^{P_\mathrm{f}}$ and the $(S_i^{\mathbb{1}_\mathcal{F}}, S_{T_i}^{\mathbb{1}_\mathcal{F}})$, following a Bayesian view of the problem, has been proposed respectively in Wang et al. (2018) for $\delta_i^{P_\mathrm{f}}$ and in Perrin and Defaux (2019) for the Sobol indices. To avoid any redundancy, this latter work will be further detailed in Chapter 7 as it will be a core ingredient of the proposed method.

As a remark, one can notice that Eq. (4.56) is linked to the remark made in Subsection 4.2.3.2 about dissimilarity measures and Sobol indices as shown in Murangira et al. (2015). In such a case, dealing with the indicator function of the failure domain can be linked to the χ^2-divergence by noticing that:

$$S_i^{\mathbb{1}_\mathcal{F}} = \frac{P_\mathrm{f}(Q_i - 1)}{1 - P_\mathrm{f}} \tag{4.61}$$

with $Q_i = \int_\mathbb{R} \frac{(f_{X_i|\mathcal{F}}(x_i|\mathcal{F}))^2}{f_{X_i}(x_i)} \mathrm{d}x_i$ and $f_{X_i|\mathcal{F}}(\cdot|\mathcal{F})$ is the marginal PDF of the sample points that led to failure (i.e., conditional to the failure event denoted by $\mathcal{F}$ here). Therefore, the hereabove numerator in Eq. (4.61) is subject to the link $(Q_i - 1) = \mathcal{D}_{\chi^2}(f_{X_i|\mathcal{F}}, f_{X_i})$. Similar results can be obtained for the total index and the major issue is thus to correctly and efficiently estimate this χ^2-divergence (see Murangira et al., 2015).

4.5.2.3 A hybrid strategy mixing MPFP-based techniques and sampling: generalized reliability importance measure

Importance factors obtained via FORM (i.e., $\boldsymbol{\alpha}$ and γ), as presented in 4.5.1.1, provide measures of the relative influence of the input variables on the LSF variability at the MPFP. However, they fall under two FORM assumptions: the linearity of the LSF and the uniqueness of the MPFP. As a result, in many real cases, these importance factors obtained may be not relevant. To overcome this issue, a new type of importance measure, called *generalized reliability importance measure* (GRIM) has been recently proposed by Kim and Song (2018a) and Kim and Song (2018b). GRIM indices are based on the underlying idea that one can identify, among the whole failure domain, some *critical subdomains* which correspond to the most probable failure regions (i.e., failure regions corresponding to different MPFPs such as illustrated in Figure 3.4). Such an identification is based on the *law of total variance*, which states that, assuming a partition $A_1, \ldots, A_K$ over the whole outcome space (i.e., they are *mutually exclusive and exhaustive* events), one gets the following decomposition:

$$\begin{aligned}
\mathrm{Var}\left[Y\right] &= \sum_{k=1}^{K} \mathrm{Var}\left[Y|A_k\right] \mathbb{P}(A_k) + \sum_{k=1}^{K} \mathbb{E}[Y|A_k]^2 \mathbb{P}(A_k) - \left(\sum_{k=1}^{K} \mathbb{E}[Y|A_k]\mathbb{P}(A_k)\right)^2 \\
&= \sum_{k=1}^{K} \left(\mathrm{Var}\left[Y|A_k\right] \mathbb{P}(A_k) + \mathbb{E}[Y|A_k]^2 \mathbb{P}(A_k) - \mathbb{E}[Y|A_k]\mathbb{P}(A_k)\mathbb{E}[Y]\right) \\
&= \sum_{k=1}^{K} \mathrm{Var}_k[Y]
\end{aligned} \tag{4.62}$$

with $\mathrm{Var}_k[Y] \overset{\text{def}}{=} \mathrm{Var}\left[Y|A_k\right]\mathbb{P}(A_k) + \mathbb{E}[Y|A_k]^2\mathbb{P}(A_k) - \mathbb{E}[Y|A_k]\mathbb{P}(A_k)\mathbb{E}[Y]$. This decomposition leads to consider the following *regional participation factor* of each k-th subdomain:

$$\mathrm{rp}_k = \frac{\mathrm{Var}_k[Y]}{\mathrm{Var}\left[Y\right]} = \frac{\mathrm{Var}_k[Y]}{\sum_{k=1}^{K}\mathrm{Var}_k[Y]}. \tag{4.63}$$

One can notice that the normalization property $\sum_{k=1}^{K}\mathrm{rp}_k = 1$ is verified. Going back to FORM approximation, one can apply the linearization of the LSF similarly to Eq. (3.14) at any point of coordinate vector $\mathbf{a}$ lying in the failure domain (i.e., verifying $\mathring{g}(\mathbf{a}) \leq 0$). Thus, one gets the following expression for the variance:

$$\mathrm{Var}\left[\mathring{g}_1(\mathbf{U}=\mathbf{A})\right] = \left\|\nabla_{\mathbf{u}}\,\mathring{g}(\mathbf{a})\right\|_2^2 \sum_{i=1}^{d}\alpha_i^2(\mathbf{a}) \tag{4.64}$$

where $\boldsymbol{\alpha}(\mathbf{a}) = -\frac{\nabla_{\mathbf{u}}\,\mathring{g}(\mathbf{a})}{\left\|\nabla_{\mathbf{u}}\,\mathring{g}(\mathbf{a})\right\|_2}$. Consequently, assuming that $A_1, \ldots, A_K$ represents a partition of the failure domain with $\mathbf{a}_1, \ldots, \mathbf{a}_K$ their respective representative points, one can notice that:

$$\sum_{k=1}^{K}\mathrm{rp}_k\|\boldsymbol{\alpha}(\mathbf{a}_k)\|_2^2 = \sum_{k=1}^{K}\|\mathrm{rp}_k\,\boldsymbol{\alpha}(\mathbf{a}_k)\|_2^2 = 1. \tag{4.65}$$

Finally, the GRIM index accounting for the contribution of the random variables of the k-th failure subdomain A_k is given by:

$$\boldsymbol{\alpha}_{\mathrm{GRIM}}^{k} = \sqrt{\mathrm{rp}_k}\,\boldsymbol{\alpha}(\mathbf{a}_k). \tag{4.66}$$

As a result, the GRIM index can be seen as an extension of the FORM importance factors by taking into account the contributions of random variables to the variability of the LSF at several failure regions and within the failure regions. In that sense, following Raguet and Marrel (2018), the GRIM index can be seen as a conditional SA index. In their papers, the authors consider two other quantities, namely a *participation matrix* and a *variable participation factor* which allows to identify the relative contribution of the failure regions, or the participation rate of a given variable. A last extension is proposed for correlated input variables by adapting the γ factor given in Eq. (4.48) in a similar fashion. As a last remark, one can highlight that identifying the failure subdomains may be difficult in practice. To efficiently estimate these indices, the authors use a AIS-CE which is based on the use of *Gaussian mixtures* (called "AIS-CE-GM" and proposed in Kurtz and Song (2013)). The use of such a method is also constrained by several tuning parameters such as the number of Gaussian mixtures K_{GM} which should be enough to find the possible K failure subdomains. For more information, the interested reader should refer to Kim and Song (2018a) and Kim and Song (2018b) and Kurtz and Song (2013) and Geyer et al. (2019) for the AIS-CE-GM technique.

4.6 Synthesis about reliability-oriented sensitivity analysis

The QoI vs. the VoI. In the ROSA context, several QoIs can be considered: reliability measures (i.e., p_{f} or β), the LSF (i.e., $g(\cdot)$ or $\mathring{g}(\cdot)$) or the indicator function (i.e., $\mathbb{1}_{\mathcal{F}_{\mathbf{x}}}(\cdot)$ or $\mathbb{1}_{\mathcal{F}_{\mathbf{u}}}(\cdot)$). As highlighted in this chapter, ROSA allows a two-way interpretation so as to find the relevant method to a given problem: either one starts from the available QoI, or one chooses the *variable of interest* (VoI), which can be either a basic variable (respectively, a group of variables) or a distribution parameter. Then, the analyst has to choose among several tools regarding this choice about the VoI.

Local vs. global ROSA. As shown in this chapter, the paradigm "local vs. global" is still relevant in the ROSA context. Several methods are available for both types of analyses and regarding the two types of VoI. However, as a remark, one should notice that the notion of "local" should be considered carefully. Indeed, one can study the local choice of a specific value (e.g., like in derivative-based SA) or be more interested in a "regional" point of view, e.g., by considering the variability within a specific region. In this sense, ROSA indices such as FORM importance factors are typical examples of ambiguous "local-global" indices: on the one hand, they can be considered as global since they are based on the variance of the LSF regarding the variability of the inputs over their entire support, but, on the other hand, they can be considered as local in the sense of regional SA since they are based on the local approximation at the MPFP in the $\mathbf{u}$-space.

Byproduct vs. standalone ROSA methods. A major difference one can mention between SAMO and ROSA consists in the fact that ROSA contains various methods directly issued from rare event probability estimation techniques. Thus, one can distinguish between the *by-product* methods and *standalone* ones. By-product methods provide indices which are directly (considering, at most, a supplementary post-processing phase) derived from the samples used to get the failure probability, or to the mathematical formulation as set in the rare event estimation problem (e.g., in the case of FORM). The main advantage of these methods is the relative moderate simulation cost required to get the sensitivity indices. However, as a drawback, the limits of the rare event probability estimation technique used may directly impact the sensitivity indices in terms of both accuracy and representativeness. Standalone methods are, for most of them, SAMO methods adapted to the ROSA context. They often consist in adding a extra-loop over a probability estimation one. This can be cumbersome and inefficient in the context of rare event probability estimation. Nonetheless, several tools available to achieve standalone ROSA may be not available yet as by-product methods.

Standard space vs. physical space. Another key characteristic of ROSA concerns the duality of spaces where such a type of analysis can be performed. In the $\mathbf{x}$-space, the results can be easily interpreted and compared with the underlying phenomenon under study. Nevertheless, $\mathbf{x}$-space is directly affected by the heterogeneity (e.g., in terms of probability distributions and range of values or units) from the input vector $\mathbf{X}$. Moreover, if any dependence characterizes the input vector, one needs to take into account in the ROSA, which is still a challenge in SA. In the $\mathbf{u}$-space, sensitivities are scaled by nature. Independence between the inputs is set by definition. Thus, computing and analyzing sensitivity indices in such a space is easier. The counterpart is a loss in terms of representativeness of the results, especially if the original input vector $\mathbf{X}$ is made of dependent inputs. Finally, performing ROSA with multiple indices in both spaces could be the safest practice. However, such a thorough analysis might be often impracticable in an industrial context regarding the tremendous computational effort required.

Single-level vs. bi-level. As a final remark, one should notice that, depending on the choice of the VoI, ROSA methods imply to consider either a *single-level* of input uncertainty (on the basic variables in $\mathbf{X}$), or a *bi-level* of input uncertainty as explained in Subsection 4.4.2. This second level on the distribution parameters $\boldsymbol{\theta}$ can be seen from the deterministic/parametric viewpoint (e.g., through the use of a regular grid-based DOE) or a stochastic one (e.g., through considering a prior distribution). If these two viewpoints differ on the fundamental hypotheses, the underlying idea is still practically the same: testing the robustness of the failure probability estimation w.r.t. $\boldsymbol{\theta}$. Thus, considering ROSA methods which take these two levels into account seems relevant both from a theoretical and a pragmatic point of view.

4.7 Conclusion

This chapter provided a review of sensitivity analysis methods according to the following distinction:

- sensitivity analysis of model output (a.k.a. SAMO) methods when the QoI is related to the model output;
- reliability-oriented sensitivity analysis (a.k.a. ROSA) methods when the QoI is related to a reliability measure.

Concerning SAMO, the basic principles of a few methods have been presented so as to highlight the common trends and differences between them. A synthesis has been provided about SAMO and the core motivations for considering ROSA have been presented. Then, a thorough review of ROSA methods has been proposed. Such a survey enabled to highlight the major trends and shortcomings about ROSA methods. Moreover, a discussion about a few key characteristics of ROSA methods the analyst should pay attention is provided in a final synthesis. Among others, the problem of checking the robustness of the failure probability estimation w.r.t. the distribution parameters has been mentioned.

Thus, in the next chapter, the problem of reliability assessment under distribution parameter uncertainty is discussed in the light of this last topic.

CHAPTER 5

Reliability assessment under distribution parameter uncertainty

Contents

This chapter is adapted from the following reference:

Chabridon V., M. Balesdent, J.-M. Bourinet, J. Morio, and N. Gayton (2017). "Evaluation of failure probability under parameter epistemic uncertainty: application to aerospace system reliability assessment". In: *Aerospace Science and Technology* 69, pp. 526–537.

5.1 Introduction and motivations

Rare event probability estimation techniques presented in Chapter 3 suppose a *perfect state of knowledge* about the input probabilistic model (Der Kiureghian, 1988), i.e., that the joint PDF $f_{\mathbf{X}}$ is perfectly determined. As recalled in Chapter 2, under the parametric hypothesis, this implies to be able to perfectly identify and model the marginal distributions (i.e., the shape/family of the PDF and the distribution parameters) and the stochastic dependence structure (i.e., the copula). However, in practice, this input probabilistic model relies on multiple sources of information which entail, themselves, their respective uncertainties. For instance, one can list the following sources of information:

- experimental data (see, e.g., BIPM, 2008);
- numerical simulation data (e.g., issued from high-fidelity computer codes);
- expert judgments or opinions (see, e.g., Ayyub, 2001; Meyer and Booker, 2001; O'Hagan et al., 2006);
- literature-based data (e.g., extracted values from references);
- standards and guides (see, e.g., AIAA, 1998; ASME, 2009; NASA, 2009);
- common sense, daily engineering practice (a.k.a. "Good Engineering Practices" (GEPs)) and traditions.

All of the sources mentioned above affect the input probabilistic model by including a part of *epistemic uncertainty*. Epistemic uncertainty [1] can be understood as the part of "reducible uncertainty" regarding a certain effort (e.g., gathering more data, using a more refined computer model for simulations, using more test specimens, elicitating more experts' judgments). When data is lacking, statistical uncertainty may play a major role by affecting the input probabilistic model. Thus, one can distinguish between the following two types of uncertainties:

- *distribution type uncertainty* which is related to choosing a relevant probability distribution to the input random variables (see, e.g., Ditlevsen, 1993; Sankararaman, 2012; Sankararaman and Mahadevan, 2013a);
- *distribution parameter uncertainty* which is related to the statistical estimation of the available data and thus impacts the choice of distribution parameters' values (see, e.g., Der Kiureghian, 1989; Pendola et al., 1999; Pendola, 2000).

In this thesis, and especially in the present chapter, one only focuses on the second type of uncertainty, i.e., the distribution parameter uncertainty, assuming that the distribution type has been preliminary chosen based on sufficient knowledge about the system, as explained in the parametric assumption given in Chapter 2.

[1] Note that, following Ditlevsen and Madsen (2007), *epistemic uncertainty* can be split into *statistical uncertainty*, related to the construction of the input probabilistic model, and *model uncertainty* related either to $\mathcal{M}(\cdot)$ or to the LSF $g(\cdot)$. In this thesis, the model is supposed to be set and black-box, so that only statistical uncertainty is of concern.

As a consequence, if the input probabilistic model (i.e., the joint PDF $f_{\mathbf{X}}$) can be affected by epistemic uncertainty (here, distribution parameter uncertainty), the input probabilistic model now consists of two uncertainty levels: on the basic variables $\mathbf{X}$ and on the distribution parameters $\boldsymbol{\theta}$. Moreover, there is a functional link between these two quantities. In this thesis, one calls this structure a *bi-level input uncertainty*. Thus, one can formulate the following questions:

Q1 – How to model this second level of uncertainty?

Q2 – How does this bi-level input uncertainty impact the reliability measure?

Q3 – How to link the variability of the reliability measure to this bi-level input uncertainty?

This chapter deals with the first two questions (**Q1** and **Q2**) while **Q3** will be progressively addressed in the next two chapters. This chapter is organized as follows. Section 5.2 aims at presenting a short bibliography review of reliability assessment under distribution parameter uncertainty and introducing the formal concepts and notations. Section 5.3 describes two approaches used to practically estimate into a common framework and provides generic algorithms for both of them. Section 5.4 illustrates the benefits of such an augmented approach through a numerical comparison between the two approaches on two test-cases of increasing complexity. Section 5.5 discusses limitations of those approaches and evokes possible perspectives. A conclusion gathering the most important results of this chapter is finally given in Section 5.6.

5.2 Reliability analysis under distribution parameter uncertainty

5.2.1 Distribution parameter uncertainty and the Bayesian framework

In this chapter, two levels of uncertainty are considered: the first one represents the variability in the basic input variables and thus affects the input random vector $\mathbf{X}$ when the second one represents the lack of knowledge affecting the distribution parameters $\boldsymbol{\Theta}$. To do so, the following *Bayesian hierarchical model* (Gelman et al., 2006) is considered:

$$\mathbf{X} \sim f_{\mathbf{X}|\boldsymbol{\Theta}}(\mathbf{x}|\boldsymbol{\theta}) : \mathcal{D}_{\mathbf{X}} \subseteq \mathbb{R}^d \to \mathbb{R}_+ \quad \text{(uncertainty level \#1)} \tag{5.1a}$$

$$\boldsymbol{\Theta} \sim f_{\boldsymbol{\Theta}|\boldsymbol{\xi}}(\boldsymbol{\theta}|\boldsymbol{\xi}) : \mathcal{D}_{\boldsymbol{\Theta}} \subseteq \mathbb{R}^{n_\theta} \to \mathbb{R}_+ \quad \text{(uncertainty level \#2)} \tag{5.1b}$$

$$\boldsymbol{\xi} = (\xi_1, \xi_2, \ldots, \xi_{n_\xi})^\top \in \mathcal{D}_{\boldsymbol{\xi}} \subseteq \mathbb{R}^{n_\xi} \quad \text{(deterministic level).} \tag{5.1c}$$

In this hierarchical representation, one can distinguish three layers of inputs:

- the first layer is constituted by the random vector $\mathbf{X}$ gathering the basic stochastic variables. Based on prior knowledge, a probability distribution can be assumed through the choice of a parametric model. This random vector can be possibly high-dimensional and may involve a complex dependence structure (Lebrun and Dutfoy, 2009b);
- the second layer is constituted by uncertain and deterministic (i.e., supposed to be known accurately enough) distribution parameters. Adding such a layer is consistent with the Bayesian point of view of modeling either "uncertain" (in the sense of stochastic) or "unknown but fixed" parameters (Gelman et al., 2006). If one can theoretically consider a possible dependence structure for the vector $\boldsymbol{\Theta}$, such a vector is often, from a pragmatic point of view (by omitting the deterministic parameters in it), of rather small dimension compared to the basic random vector and structured such that quadrature schemes or quasi-random sampling can be easily used to sample over the space $\mathcal{D}_{\boldsymbol{\Theta}}$. Other techniques,

such as the association of a rank correlation procedure developed in Iman and Davenport (1982) and quasi-random sampling have been successfully used in literature (see, e.g., Helton and Davis, 2003). In the present chapter, the prior distribution is mostly assumed to be derived from expert judgment or from a limited set of data. Thus, despite the fact that Bayes' theorem is not used as an updating procedure (but could be, if more data or a better characterization was available), one can consider that this prior distribution characterizes epistemic uncertainty affecting the distribution parameters;

- the third layer is composed of fixed hyper-parameters gathered in $\boldsymbol{\xi}$. These hyper-parameters, which can be either some moments or bounds, characterize the prior distributions of uncertain stochastic parameters $\boldsymbol{\Theta}$.

In the following, one will only focus on the first two layers, i.e., $\mathbf{X}$ and $\boldsymbol{\Theta}$. Thus, for the sake of clarity and conciseness, the third layer (i.e., the hyper-parameters $\boldsymbol{\xi}$) will be omitted such that one will denote the prior density over the distribution parameters by $f_{\boldsymbol{\Theta}}(\boldsymbol{\theta})$ instead of $f_{\boldsymbol{\Theta}|\boldsymbol{\xi}}(\boldsymbol{\theta}|\boldsymbol{\xi})$. The dependence on $\boldsymbol{\xi}$ will be introduced in the next chapter when dealing with sensitivity analysis.

As an illustration of the bi-level input uncertainty structure, Figure 5.1 represents a family of Gaussian PDFs. Indeed, assuming that a basic variable X is distributed according to a standard Gaussian density, one considers that the distribution parameters $\boldsymbol{\theta} = (\mu_X, \sigma_X)^\top$ are not precisely known. As a result, several densities for various pairs of distribution parameters are sketched. Finally, one can consider the *prior predictive* PDF of X, i.e., the PDF that both incorporates the variability in X and the prior distribution over $\boldsymbol{\Theta}$. This PDF is defined as follows:

$$\widetilde{f}_X(x) = \int_{\mathcal{D}_{\boldsymbol{\Theta}}} f_{X|\boldsymbol{\Theta}}(x|\boldsymbol{\theta}) f_{\boldsymbol{\Theta}}(\boldsymbol{\theta}) \mathrm{d}\boldsymbol{\theta}. \tag{5.2}$$

In Figure 5.1, $\widetilde{f}_X$ is sketched using KDE.

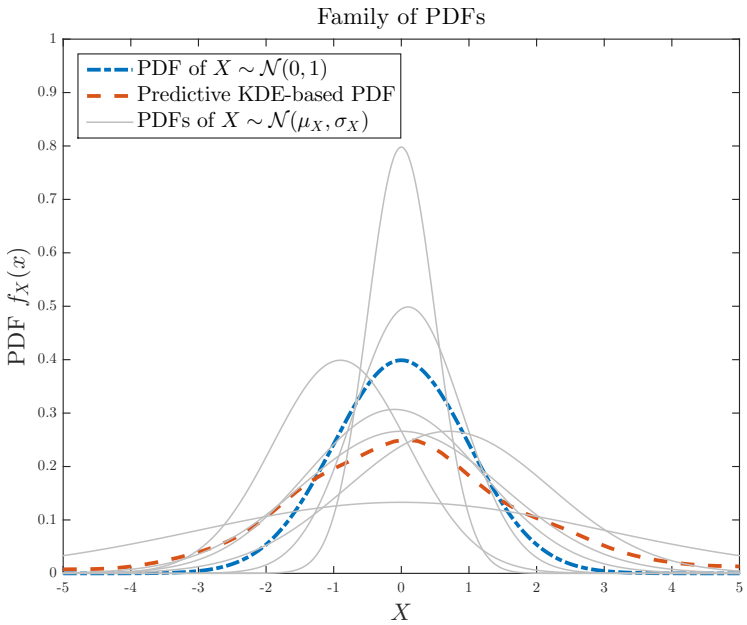

FIGURE 5.1: Illustration of a family of PDFs for a single Gaussian random variable under distribution parameter uncertainty.

5.2.2 Predictive failure probability

Such a topic has been early discussed among the structural reliability community, mainly in the first investigations led by Der Kiureghian (see, e.g., Der Kiureghian, 1988; Der Kiureghian, 1989; Der Kiureghian, 1996; Der Kiureghian, 2008) and Ditlevsen (see, e.g., Ditlevsen, 1979a; Ditlevsen, 1979b; Ditlevsen, 1982; Ditlevsen and Madsen, 2007). In their common paper, Der Kiureghian and Ditlevsen (2009) stress the need of a reliability measure that takes into account parameter uncertainty (Der Kiureghian (1988) proposed to call it "*predictive reliability measure*", following Bayesian analysis vocabulary, and provided a formal definition that will be recalled later).

Assuming now that $\mathbf{X}$ is distributed according to the parametric joint PDF $f_{\mathbf{X}|\boldsymbol{\Theta}}$, each random variable X_i is distributed according to the marginal PDF $f_{X_i|\boldsymbol{\Theta}_i}$. In the case of dependent inputs, in the normal copula case, uncertainty affecting the correlation matrix could easily be considered in this framework. However, from a more general point of view, uncertainty affecting the dependence structure (i.e., the copula) is not a widely studied topic in literature. Moreover, from an engineering perspective, this problem is really difficult to assess due to the crucial lack of information. In this chapter, only distribution parameter uncertainty is treated and copula structure uncertainty is not considered. Indeed the vector $\boldsymbol{\Theta}$ gathers all distribution parameters of the corresponding marginals such that $\boldsymbol{\Theta} = (\boldsymbol{\Theta}_1, \boldsymbol{\Theta}_2, \dots, \boldsymbol{\Theta}_d)^\top$, where each $\boldsymbol{\Theta}_i, i \in [\![1, d]\!]$ is a set of distribution parameters for the i-th marginal (for instance, if $X_i \sim \mathcal{N}(\mu_{X_i}, \sigma_{X_i})$, then $\boldsymbol{\Theta}_i = (\mu_{X_i}, \sigma_{X_i})^\top$). One can notice that, depending on the distribution type, all the marginal PDFs will not be defined with the same number of parameters. In this chapter, it is assumed that only a set of independent distribution parameters are uncertain which leads to consider a general collection of univariate random parameters given by $\boldsymbol{\Theta} = (\Theta_1, \Theta_2, \dots, \Theta_{n_\theta})^\top \in \mathcal{D}_{\boldsymbol{\Theta}} \subseteq \mathbb{R}^{n_\theta}$ (which can be either moments or bounds). Consequently, without any loss of generality, one can assume the existence of a joint PDF $f_{\boldsymbol{\Theta}} = \prod_{j=1}^{n_\theta} f_{\Theta_j}$ as a product of the marginal PDFs of each Θ_j (see, e.g., Vergé et al. (2016) for a similar assumption). Note here that one could also consider a dependence structure between the distribution parameters. However, the problem would be far more difficult and would imply to have, at minimum, a prior information about such a dependence structure. This topic is beyond the scope of this chapter. To get a deeper insight about the practical characterization of $f_{\boldsymbol{\Theta}}(\boldsymbol{\theta})$ based on available data (which is not the scope of this chapter), the reader may refer to Robert (2007). To sum up, in this chapter, only a *prior probability distribution* (for instance, following an expert-based judgment) will be assumed for $\boldsymbol{\Theta}$ without any purpose of Bayesian reliability updating (see, e.g., Pendola et al. (1999), Straub (2011), and Straub and Papaioannou (2015) for more information about this topic).

Consequently, a new formulation for the failure probability can be proposed, following Der Kiureghian (2008). Indeed, due to this bi-level uncertainty (on the vector of basic variables $\mathbf{X}$ and on the vector of distribution parameters $\boldsymbol{\Theta}$), the failure probability p_f is no longer a deterministic value. It becomes a random variable, denoted by P_f, which depends on the realization $\boldsymbol{\theta}$ of the random vector of uncertain parameters such that:

$$P_\mathrm{f}(\boldsymbol{\theta}) = \mathbb{P}(g(\mathbf{X}) \leq 0 \mid \boldsymbol{\Theta} = \boldsymbol{\theta}) \tag{5.3a}$$

$$= \int_{\mathcal{D}_\mathbf{X}} \mathbb{1}_{\mathcal{F}_\mathbf{x}}(\mathbf{x}) f_{\mathbf{X}|\boldsymbol{\Theta}}(\mathbf{x}|\boldsymbol{\theta}) \mathrm{d}\mathbf{x} \tag{5.3b}$$

$$= \mathbb{E}_{f_{\mathbf{X}|\boldsymbol{\Theta}}} \left[\mathbb{1}_{\mathcal{F}_\mathbf{x}}(\mathbf{X}) \mid \boldsymbol{\Theta} = \boldsymbol{\theta} \right]. \tag{5.3c}$$

Hence, by integrating over $\mathcal{D}_{\boldsymbol{\Theta}}$, one gets the so-called "*predictive failure probability*" $\widetilde{P}_\mathrm{f}$ which is a

measure of reliability taking into account the effect of the uncertain characterization of distribution parameters:

$$\widetilde{P}_{\mathrm{f}} = \mathbb{E}_{f_{\boldsymbol{\Theta}}}\left[P_{\mathrm{f}}(\boldsymbol{\Theta})\right] \tag{5.4a}$$

$$= \int_{\mathcal{D}_{\boldsymbol{\Theta}}} P_{\mathrm{f}}(\boldsymbol{\theta}) f_{\boldsymbol{\Theta}}(\boldsymbol{\theta}) \mathrm{d}\boldsymbol{\theta} \tag{5.4b}$$

$$= \int_{\mathcal{D}_{\boldsymbol{\Theta}}} \left(\int_{\mathcal{D}_{\mathbf{X}}} \mathbb{1}_{\mathcal{F}_{\mathrm{x}}}(\mathbf{x}) f_{\mathbf{X}|\boldsymbol{\Theta}}(\mathbf{x}|\boldsymbol{\theta}) \mathrm{d}\mathbf{x} \right) f_{\boldsymbol{\Theta}}(\boldsymbol{\theta}) \mathrm{d}\boldsymbol{\theta}. \tag{5.4c}$$

Eq. (5.4c) is the key equation whose solution is under consideration in this chapter. The idea is that it can be numerically solved by two different approaches. Indeed, using the Fubini-Tonelli theorem, one can show that:

$$\widetilde{P}_{\mathrm{f}} = \int_{\mathcal{D}_{\mathbf{X}}} \mathbb{1}_{\mathcal{F}_{\mathrm{x}}}(\mathbf{x}) \left(\int_{\mathcal{D}_{\boldsymbol{\Theta}}} f_{\mathbf{X}|\boldsymbol{\Theta}}(\mathbf{x}|\boldsymbol{\theta}) f_{\boldsymbol{\Theta}}(\boldsymbol{\theta}) \mathrm{d}\boldsymbol{\theta} \right) \mathrm{d}\mathbf{x} \tag{5.5a}$$

$$= \int_{\mathcal{D}_{\mathbf{X}}} \mathbb{1}_{\mathcal{F}_{\mathrm{x}}}(\mathbf{x}) \widetilde{f}_{\mathbf{X}}(\mathbf{x}) \mathrm{d}\mathbf{x} \tag{5.5b}$$

which makes appear the prior predictive PDF of $\mathbf{X}$ as defined in Eq. (5.2).

From a numerical point of view, a first way of computing this integral relies on evaluating pointwise the inner integral for each realization $\boldsymbol{\theta}$ of $\boldsymbol{\Theta}$ (Limbourg et al., 2010; Gayton et al., 2011; Balesdent et al., 2014): this leads to the nested reliability approach (presented in subsection 5.3.1). The second way consists in evaluating it by treating both basic variables and uncertain distribution parameters together and by integrating simultaneously on both domains (under a conditioning constraint) as suggested in Der Kiureghian (2008): this is the augmented reliability approach (presented in subsection 5.3.2). This second approach implies to sample according to prior predictive PDF. The next section describes these approaches in details. As a remark, one can notice that this Bayesian framework provides here a single reliability measure (the predictive failure probability). Nevertheless, this quantity can help engineers to make more informed decisions during the design process and can be coupled with the usual single-level reliability measure so as to analyze properly the risk undertaken with a design choice. Decision can be then enlightened by such additional information (Pasanisi et al., 2009; Keller et al., 2011; Pasanisi et al., 2012).

Up to now, several researchers deployed efforts to carry on the way of other approaches to compute this predictive failure probability (see another approach by Wen and Chen (1987), used in Der Kiureghian (1988) and in Hong (1996) only with FORM calculations). Nevertheless, the track of exploring the *augmented space* has not been over-exploited yet. In Pendola (2000), the author recommended and implemented this strategy on a fracture mechanics test-case but limited his study to the FORM algorithm. All these works mainly focused on providing a global reliability index, robust to parameter uncertainty, in the specific context of FORM. The use of an augmented space has also been exploited by Au (2005) for design sensitivity purpose while considering uncertain design parameters. More recently, in Sankararaman and Mahadevan (2013b), the authors proposed a broader view and an interpretation of the different levels of uncertainty involved in these calculations and advocated to use an augmented approach to solve a similar integral problem given in Eq. (5.4c). However, their study did not aim at performing reliability assessment for rare event failure probabilities of some complex simulation codes which is the scope of the present chapter.

5.3 Nested vs. augmented reliability approaches

5.3.1 The nested reliability approach (NRA)

This approach is based on nested loops since it involves the numerical estimation of two different quantities. The first (nested or inside) loop aims at computing a "conditional" failure probability whose numerical estimator is denoted by $\widehat{P}_{\mathrm{f}}(\boldsymbol{\theta})$. This estimator is a measure of reliability given a realization $\boldsymbol{\theta}$ of the random vector $\boldsymbol{\Theta}$. The second (outside) loop aims at computing an estimator of the predictive failure probability, denoted by $\widehat{\widehat{P}}_{\mathrm{f}}$. In practice, it consists in computing several $\widehat{P}_{\mathrm{f}}(\boldsymbol{\theta})$ for samples of the uncertain parameters $\boldsymbol{\Theta}$. It has been widely used in literature, in various contexts, such as for uncertainty propagation in monotonic models in Limbourg et al. (2010), probability-based tolerance analysis of products in Gayton et al. (2011) and rare event probability estimation using a Kriging surrogate model in Balesdent et al. (2014).

Algorithm 1 – Nested reliability approach (NRA) with CMC box for probability estimation.

1: **Start**
2: **Define**: $\mathbf{X}$, $\boldsymbol{\Theta}$, $N_{\mathbf{x}}$ and $N_{\boldsymbol{\theta}}$ (resp. the sampling budgets over the domain $\mathcal{D}_{\mathbf{X}}$ and the domain $\mathcal{D}_{\boldsymbol{\Theta}}$)
3: **For** $k = 1 : N_{\boldsymbol{\theta}}$
4: Sample $\boldsymbol{\Theta}^{(k)}$;
5: **For** $j = 1 : N_{\mathbf{x}}$
6: Sample $\mathbf{X}_{(k)}^{(j)}$ given $\boldsymbol{\Theta}^{(k)} = \boldsymbol{\theta}^{(k)}$;
7: Limit-state function evaluation: $g(\mathbf{x}_{(k)}^{(j)})$;
8: **Conditional failure probability estimator**:
9: $\widehat{P}_{\mathrm{f}}^{(k)}(\boldsymbol{\theta}^{(k)}) = \frac{1}{N_{\mathbf{x}}} \sum_{j=1}^{N_{\mathbf{x}}} \mathbb{1}_{\mathcal{F}_{\mathbf{x}}}(\mathbf{X}_{(k)}^{(i)})$;
10: **Predictive failure probability estimator**:
11: $\widehat{\widehat{P}}_{\mathrm{f}}^{\,\mathrm{NRA}} = \frac{1}{N_{\boldsymbol{\theta}}} \sum_{k=1}^{N_{\boldsymbol{\theta}}} \widehat{P}_{\mathrm{f}}^{(k)}(\boldsymbol{\theta}^{(k)})$;
12: **End**

Algorithm 2 – NRA generic box (FORM / SS / AIS-CE / NAIS).

...
Define: usual transformation T to the $\mathbf{u}$-space
$\mathbf{U} = T(\mathbf{X})$ (Nataf or Rosenblatt) and its inverse T^{-1} (see Appendix C)
Start
FORM / SS / AIS-CE / NAIS Algorithm
(see Appendix D for a full description of these algorithms)
End
Get: $\widehat{P}_{\mathrm{f}}^{(k)}(\boldsymbol{\theta}^{(k)})$
...

A generic implementation of NRA framework coupled with a nested CMC sampling technique is given in Algorithm 1. In the rectangular box at lines $5-9$, one can choose any available rare event probability estimation technique to estimate the conditional failure probability $\widehat{P}_{\mathrm{f}}(\boldsymbol{\theta})$,

from approximation techniques (FORM, SORM) to most advanced sampling techniques (IS, SS). However, for the sake of conciseness, one will only focus on the application of three techniques, i.e., CMC, FORM and SS, while IS will be extensively used in the next chapter. Indeed CMC is still considered as the reference rare event probability estimation technique for validation. Then, FORM is widely used in an industrial context as it enables practitioners to perform reliability assessment at a low computational cost. Finally, SS appeared to be a very powerful technique to reach estimation of rare event failure probabilities, under the constraint of nonlinear LSFs, with a rather moderate computational effort (Au et al., 2007). In brief, the rectangular box can be seen as a non-intrusive plug-in uncertainty propagation code for reliability assessment. An example of a plug-in box (for FORM, IS or SS) is given in the Algorithm 2. For specific cases (e.g., FORM or SS), an additional step may be required: the transformation to the **u**-space (see Appendix C). In the nested case, the transformation is already included in the plug-in reliability rectangular box, i.e., usual transformations such as Nataf or Rosenblatt ones can be both used, and the distribution parameter uncertainty does not change anything to their implementation. Nevertheless, one should notice that for each sampled parameter, the algorithm needs to rebuild and recalculate the transformation since it depends on the parameter value. Thus, for complicated transformations, with a large number of basic variables, the simulation cost induced can be increased. Finally, in this nested case, one can consider the following proposition.

Proposition 1 (NRA estimator)**.** *The NRA estimator* $\widehat{\widetilde{P}}_{\mathrm{f}}^{\,\mathrm{NRA}}$ *is unbiased.*

Proof. Consider that $\{\mathbf{X}_{(k)}^{(j)}\}_{j=1}^{N_{\mathbf{x}}} \overset{\text{i.i.d.}}{\sim} f_{\mathbf{X}|\boldsymbol{\Theta}^{(k)}}$ *and* $\{\boldsymbol{\Theta}^{(k)}\}_{k=1}^{N_{\boldsymbol{\theta}}} \overset{\text{i.i.d.}}{\sim} f_{\boldsymbol{\Theta}}$.

$$\mathbb{E}\left[\widehat{\widetilde{P}}_{\mathrm{f}}^{\,\mathrm{NRA}}\right] = \mathbb{E}\left[\frac{1}{N_{\boldsymbol{\theta}}}\sum_{k=1}^{N_{\boldsymbol{\theta}}}\left(\frac{1}{N_{\mathbf{x}}}\sum_{j=1}^{N_{\mathbf{x}}}\mathbb{1}_{\mathcal{F}_{\mathbf{x}}}(\mathbf{X}_{(k)}^{(j)})\right)\right] \tag{5.6a}$$

$$= \frac{1}{N_{\boldsymbol{\theta}}N_{\mathbf{x}}}\sum_{k=1}^{N_{\boldsymbol{\theta}}}\sum_{j=1}^{N_{\mathbf{x}}}\mathbb{E}_{f_{\boldsymbol{\Theta}}}\left[\mathbb{E}_{f_{\mathbf{X}|\boldsymbol{\Theta}^{(k)}}}[\mathbb{1}_{\mathcal{F}_{\mathbf{x}}}(\mathbf{X}_{(k)}^{(j)})|\boldsymbol{\Theta}^{(k)}]\right] \tag{5.6b}$$

$$= \frac{1}{N_{\boldsymbol{\theta}}N_{\mathbf{x}}}\sum_{k=1}^{N_{\boldsymbol{\theta}}}\sum_{j=1}^{N_{\mathbf{x}}}\mathbb{E}_{f_{\boldsymbol{\Theta}}}[P_{\mathrm{f}}(\boldsymbol{\Theta}^{(k)})] \tag{5.6c}$$

$$= \widetilde{P}_{\mathrm{f}} \tag{5.6d}$$

□

The simulation budget allocation defined in terms of the two domains, $\mathcal{D}_{\mathbf{X}}$ and $\mathcal{D}_{\boldsymbol{\Theta}}$, can be an obstacle for the accurate estimation of the predictive failure probability when using sampling techniques. For instance, for a fixed simulation budget, one needs to decide whether to allow a substantial budget to get a better precision over the integral on $\mathcal{D}_{\mathbf{X}}$ or over the integral on $\mathcal{D}_{\boldsymbol{\Theta}}$. On the one hand, because the simulation budget over $\mathcal{D}_{\mathbf{X}}$ is not easily reducible as it directly affects the estimation accuracy of the failure probability, it comes that adding a second integration budget over $\mathcal{D}_{\boldsymbol{\Theta}}$ can be computationally critical. On the other hand, sampling with only a few number of points over $\mathcal{D}_{\boldsymbol{\Theta}}$ may introduce a bias in the final measure of reliability by advantaging some parameter values which influence the final probability measure without taking their relative weight into account. For all these reasons, efficient *design of experiments* (DOE) may be used so as to optimize the sampling over $\mathcal{D}_{\boldsymbol{\Theta}}$. As an example, one can mention the *quadrature scheme*-based DOE over $\mathcal{D}_{\boldsymbol{\Theta}}$. The idea is to approximate a k-variate integral over $\mathcal{D}_{\boldsymbol{\Theta}} \subseteq \mathbb{R}^{n_\theta}$ of the form:

$$\mathcal{I}[P_{\mathrm{f}}(\boldsymbol{\theta})] = \int_{\mathcal{D}_{\boldsymbol{\Theta}}} P_{\mathrm{f}}(\boldsymbol{\theta}) f_{\boldsymbol{\Theta}}(\boldsymbol{\theta}) \mathrm{d}\boldsymbol{\theta} \tag{5.7}$$

where $f_{\boldsymbol{\Theta}}(\boldsymbol{\theta}) \equiv w(\boldsymbol{\theta})$ is a density (or weight) function which is evaluated at gridpoints. The quadrature rule provides an approximation using a combination of these weight functions such

that (Davis and Rabinowitz, 1984):

$$\mathcal{I}[P_{\mathrm{f}}(\boldsymbol{\theta})] \approx \sum_{j_1=1}^{M_1} \sum_{j_2=1}^{M_2} \cdots \sum_{j_{n_{\boldsymbol{\theta}}}=1}^{M_{n_{\boldsymbol{\theta}}}} (w_{j_1} \otimes w_{j_2} \otimes \cdots \otimes w_{j_{n_{\boldsymbol{\theta}}}}) P_{\mathrm{f}}(\theta_1^{(j_1)}, \theta_2^{(j_2)}, \ldots, \theta_{n_{\boldsymbol{\theta}}}^{(j_k)}) \tag{5.8}$$

with w_j the weights and $\otimes$ the tensor product operator. The indices $M_1, \ldots, M_k$ represent the number of points in each dimension. Such a strategy can be used with complex computer codes (e.g., as for the launcher fallout case presented in Chapter 8).

5.3.2 The augmented reliability approach (ARA)

Another approach is to consider an *augmented input random vector* $\mathbf{Z} \overset{\text{def}}{=} (\boldsymbol{\Theta}, \mathbf{X})^\top$ composed of the basic variables and their distribution parameters as it appears in Eq. (5.4c) (see Schöbi and Sudret (2015) for a similar definition). Thus, this augmented input space has a dimension of $n_{\boldsymbol{\theta}} + d$ ($n_{\boldsymbol{\theta}}$ uncertain distribution parameters and d random basic variables). The predictive failure probability can be then rewritten as follows:

$$\widetilde{P}_{\mathrm{f}} = \int_{\mathcal{D}_{\boldsymbol{\Theta}}} \int_{\mathcal{D}_{\mathbf{X}}} \mathbb{1}_{\mathcal{F}_{\mathbf{x}}}(\mathbf{x}) f_{\mathbf{X}|\boldsymbol{\Theta}}(\mathbf{x}|\boldsymbol{\theta}) f_{\boldsymbol{\Theta}}(\boldsymbol{\theta}) \mathrm{d}\mathbf{x} \mathrm{d}\boldsymbol{\theta} = \int_{\mathcal{D}_{\mathbf{Z}}} \mathbb{1}_{\mathcal{F}_{\mathbf{z}}}(\mathbf{z}) f_{\mathbf{Z}}(\mathbf{z}) \mathrm{d}\mathbf{z} = \mathbb{E}_{f_{\mathbf{Z}}}\left[\mathbb{1}_{\mathcal{F}_{\mathbf{z}}}(\mathbf{Z})\right] \tag{5.9}$$

where $\mathcal{F}_{\mathbf{z}} = \{\mathbf{z} \in \mathcal{D}_{\mathbf{Z}} \mid g(\mathbf{z}) \leq 0\}$ and $\mathcal{D}_{\mathbf{Z}} = \mathcal{D}_{\mathbf{X}} \times \mathcal{D}_{\boldsymbol{\Theta}}$ (where $\times$ is the Cartesian product). Note that this definition is similar to the one given in Eq. (5.5b) with the prior predictive distribution, however, to clearly distinguish between the single-level uncertainty involving only the $\mathbf{X}$ variables and the bi-level uncertainty involving both $\mathbf{X}$ and $\boldsymbol{\Theta}$, the notation $\widetilde{f}_{\mathbf{X}}$ is replaced by $f_{\mathbf{Z}}$. However, as an important remark, one should notice that using the notation "$\mathbf{Z}$" as inputs of the functions $\mathbb{1}_{\mathcal{F}_{\mathbf{z}}}(\mathbf{Z})$ and $g(\mathbf{Z})$ is an abuse of notation since, in practice, only the basic variables $\mathbf{X}$ do play a role in the computer code as physical variables. Such a notation is just used to denote that the derivations are achieved under bi-level uncertainty. In the literature, FORM has been the first technique that has been coupled to ARA as proposed in Hong (1996) and Pendola (2000).

A generic implementation framework is given in Algorithm 3. Again, in this algorithm, the rectangular box can be replaced by any non-intrusive plug-in uncertainty propagation code for reliability assessment as the ones cited previously for the NRA (see Algorithm 4 as an example). This shows that the ARA does not suffer from any major difference with the classical nested approach in terms of the variety of applicable techniques. Again, as for the NRA, one can consider the following proposition.

Proposition 2 (ARA estimator)**.** *The ARA estimator* $\widehat{\widetilde{P}}_{\mathrm{f}}^{\,\mathrm{ARA}}$ *is unbiased.*

Proof. Consider that $\{\mathbf{Z}^{(j)}\}_{j=1}^{N_{\mathbf{x},\boldsymbol{\theta}}} \overset{\text{i.i.d.}}{\sim} f_{\mathbf{Z}}$ *with* $f_{\mathbf{Z}} = f_{(\mathbf{X},\boldsymbol{\Theta})}$.

$$\mathbb{E}\left[\widehat{\widetilde{P}}_{\mathrm{f}}^{\,\mathrm{ARA}}\right] = \mathbb{E}\left[\frac{1}{N_{\mathbf{x},\boldsymbol{\theta}}} \sum_{j=1}^{N_{\mathbf{x},\boldsymbol{\theta}}} \mathbb{1}_{\mathcal{F}_{\mathbf{z}}}(\mathbf{Z}^{(j)})\right] \tag{5.10a}$$

$$= \frac{1}{N_{\mathbf{x},\boldsymbol{\theta}}} \sum_{j=1}^{N_{\mathbf{x},\boldsymbol{\theta}}} \mathbb{E}[\mathbb{1}_{\mathcal{F}_{\mathbf{z}}}(\mathbf{Z}^{(j)})] \tag{5.10b}$$

$$= \frac{1}{N_{\mathbf{x},\boldsymbol{\theta}}} \sum_{j=1}^{N_{\mathbf{x},\boldsymbol{\theta}}} \widetilde{P}_{\mathrm{f}} \tag{5.10c}$$

$$= \widetilde{P}_{\mathrm{f}} \tag{5.10d}$$

□

Algorithm 3 – Augmented reliability approach (ARA) with CMC box for probability estimation.

Start
Define: $\mathbf{X}$, $\boldsymbol{\Theta}$, $N_{\mathbf{x},\boldsymbol{\theta}}$ (sampling budget)
For $i = 1 : N_{\mathbf{x},\boldsymbol{\theta}}$
    Sample $\boldsymbol{\Theta}^{(i)}$;
    Sample $\mathbf{X}^{(i)}$ given $\boldsymbol{\Theta}^{(i)} = \boldsymbol{\theta}^{(i)}$;
    Consider $\mathbf{Z}^{(i)} = (\mathbf{X}^{(i)}, \boldsymbol{\Theta}^{(i)})$;
    Limit-state function evaluation: $g(\mathbf{z}^{(i)})$;
Predictive failure probability estimator:
$\widehat{\widehat{P}}_{\mathrm{f}}^{\,\mathrm{ARA}} = \frac{1}{N_{\mathbf{x},\boldsymbol{\theta}}} \sum_{i=1}^{N_{\mathbf{x},\boldsymbol{\theta}}} \mathbb{1}_{\mathcal{F}_{\mathbf{z}}}(\mathbf{Z}^{(i)})$;
End

Algorithm 4 – ARA generic box (FORM / SS / AIS-CE / NAIS).

...
Define: new transformation $T_{\mathrm{aug}}^{\mathrm{Ros}}$ for the augmented space
$\mathbf{U} = T_{\mathrm{aug}}^{\mathrm{Ros}}(\mathbf{Z})$
(see Eq. (5.11), but not compulsory for all techniques)
Start
    FORM / SS / AIS-CE / NAIS Algorithm
    (see Appendix D)
End
Get: $\widehat{\widehat{P}}_{\mathrm{f}}^{\,\mathrm{ARA}}$
...

One major difference concerns the transformation to the $\mathbf{u}$-space: since there exists a conditioning between the distribution parameters and the basic input variables, Nataf transformation cannot be used anymore and Rosenblatt transformation is the only one that can handle this constraint.

Under the bi-level input uncertainty, one needs to adapt the usual Rosenblatt transformation (see Appendix C for the traditional formulation of the transformation). It is assumed that the joint PDF $f_{\mathbf{X}|\boldsymbol{\Theta}}$ is known since all the marginal PDFs and the correlation matrix (or the covariance matrix) giving the linear correlation structure between the basic input variables (normal or Gaussian copula case (Lebrun, 2013)) are known. In addition, the joint PDF $f_{\boldsymbol{\Theta}}$, as explained previously in Subsection 5.2.1, is supposed to be known. In this case, under the consideration of the *augmented space* of dimension $n_{\boldsymbol{\theta}} + d$, one can apply the Rosenblatt transformation, first to

the $n_{\boldsymbol{\theta}}$ components of $\boldsymbol{\Theta}$, and second to the d ones of the vector $\mathbf{X}|\boldsymbol{\Theta}$ such that:

$$T_{\text{aug}}^{\text{Ros}}: \left| \begin{array}{ccc} \mathbb{R}^{n_{\boldsymbol{\theta}}+d} & \longrightarrow & \mathbb{R}^{n_{\boldsymbol{\theta}}+d} \\ \mathbf{z} & \longmapsto & \mathbf{u} = \begin{pmatrix} \Phi^{-1}\left(F_{\Theta_1}(\theta_1)\right) \\ \vdots \\ \Phi^{-1}\left(F_{\Theta_{n_{\boldsymbol{\theta}}}}(\theta_{n_{\boldsymbol{\theta}}})\right) \\ \vdots \\ \Phi^{-1}\left(F_{X_1|\Theta_1,\ldots,\Theta_{n_{\boldsymbol{\theta}}}}(x_1|\theta_1,\ldots,\theta_{n_{\boldsymbol{\theta}}})\right) \\ \vdots \\ \Phi^{-1}\left(F_{X_d|\Theta_1,\ldots,\Theta_{n_{\boldsymbol{\theta}}},X_1,\ldots,X_{d-1}}(x_d|\theta_1,\ldots,\theta_{n_{\boldsymbol{\theta}}},x_1,\ldots,x_{d-1})\right) \end{pmatrix} \end{array} \right. \tag{5.11}$$

where $\Phi^{-1}(\cdot)$ is the normal inverse CDF and $F_{\Theta_i}(\cdot)$, $F_{X_i|\Theta_i}(\cdot|\cdot)$ respectively the marginal CDFs of the parameters and the conditional marginal CDFs of the basic variables. In the case of correlated inputs, one can implement this regular transformation following and adapting general formulas given in Rosenblatt (1952). As a remark, one should notice that from a numerical point of view, the inverse transformation $\left(T_{\text{aug}}^{\text{Ros}}\right)^{-1}(\cdot)$ (from the $\mathbf{u}$-space to the $\mathbf{z}$-space) can be the most useful (especially when FORM, SORM or SS techniques are used).

5.3.3 Illustration

From a numerical point of view, NRA and ARA can be illustrated through a two-dimensional example with one uncertain distribution parameter. Let us call X_1 and X_2 the two basic input variables modeled as two Gaussian variates such that $X_1 \sim \mathcal{N}(\mu_{X_1} = 7, \sigma_{X_1} = 5/\sqrt{3})$ and $X_2 \sim \mathcal{N}(\Theta = \mu_{X_2}, \sigma_{X_2} = 2/\sqrt{3})$. The mean of X_2 is considered as being uncertain (for example, $\Theta \sim \mathcal{N}(2, 1.5)$). For the sake of clarity, in Figure 5.2a, only three clouds of samples are plotted for three different values of θ (200 points per cloud). Indeed such a sequential sampling is the underlying principle of NRA.

As for ARA, graphical results plotted in Figure 5.2b bring out the underlying principle of this approach: covering in one algorithm step the augmented input space (for the sake of comparison, 600 points are used, instead of 3×200 points for NRA). One can clearly notice the same trend between NRA and ARA, the first one by a sequential sampling strategy, the second one by a simultaneous sampling over all the dimensions of the augmented input space.

5.4 Numerical comparison between the two approaches

To evaluate the efficiency of the ARA, a numerical validation benchmark has been performed with a systematic comparison to the classical NRA. Two academic test-cases of increasing complexity have been chosen to check the validity of the two approaches. Numerical application on a realistic aerospace test-case is further proposed in Chapter 8. Moreover, three reliability techniques have been tested to calculate the failure probability: CMC, FORM and SS. The following numerical applications have been implemented in Matlab® and performed using the open source toolbox FERUM v4.1 (Bourinet et al., 2009).

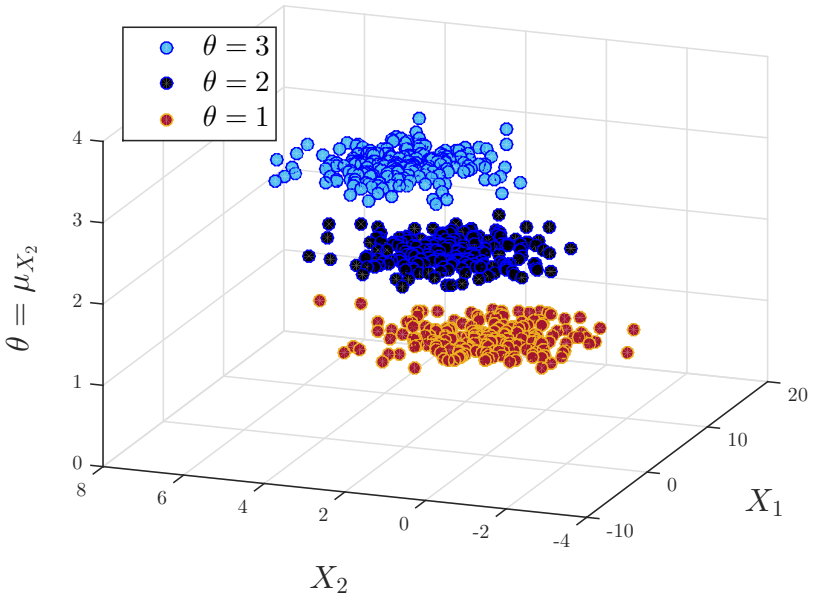

(a) NRA (200 points/cloud, indeed 600 points in total).

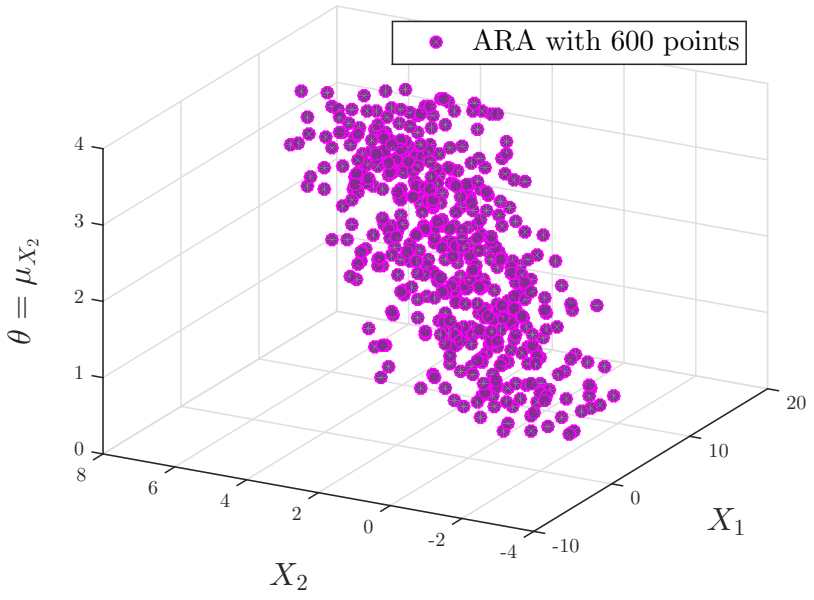

(b) ARA (600 points in the augmented space).

FIGURE 5.2: Illustration of NRA and ARA simulation procedures on a two-dimensional problem.

5.4.1 Methodology and comparison metrics

This section aims at comparing results obtained for both NRA and ARA. For each type of approach, two reliability techniques, FORM (when LSF is linear) and SS, will be used to estimate the predictive failure probability $\widetilde{P}_{\mathrm{f}}$. These combined approaches (NRA/FORM, NRA/SS, ARA/FORM, ARA/SS) will be respectively compared to a reference estimation performed using CMC (most of the time, a NRA/CMC with a large number of samples on both domains). These three techniques (CMC, FORM and SS) have been chosen for their representativeness of both reference, approximation and advanced sampling techniques. As for IS techniques (either

nonadaptive and adaptive ones), they could also be used here. However, they will be extensively studied in the next chapter. Table 5.1 gives a brief overview of the methodology.

TABLE 5.1: Overall methodology for the numerical comparison between NRA and ARA.

Test-case		**Ref.**	**NRA**			**ARA**		
		Ref. CMC	CMC	FORM	SS	CMC	FORM	SS
Ex. #1: Correlated $R-S$ [a]	(cf. 5.4.2)	■	■	■	■	■	■	■
Ex. #2: Nonlinear oscillator [b]	(cf. 5.4.3)	■	■	×	■	■	×	■

[a] 2 correlated basic variables, 1 uncertain parameter, $g(\cdot)$ linear, low single-level p_{f}.
[b] 8 independent basic variables, 1 uncertain parameter, $g(\cdot)$ nonlinear, low single-level p_{f}.

In Table 5.1, the black squares ■ stand for successful calculations of the test-cases and the crosses $\times$ indicate that FORM is clearly inappropriate since the LSF is known explicitly to be nonlinear. As a remark, one can notice that some specific cases are denoted by computationally "intractable". Indeed, to overcome such a difficulty and to get a reference result to make the comparison viable, specific computational strategies have been set up. For the sake of clarity and to avoid any confusion, these strategies are presented and discussed in the dedicated subsections of the test-cases.

One needs to introduce the comparison metrics used in the following numerical benchmarks. As proposed in Morio and Balesdent (2015), characterizing the quality of a rare event probability estimation by a given "method" M (considering the estimator $\widehat{\widetilde{P}}_{\mathrm{f}}^{\mathrm{M}}$ of $\widetilde{P}_{\mathrm{f}}$), can be achieved by the use of three performance metrics computed w.r.t. some reference estimation (here, those obtained by CMC). These metrics are detailed below.

Relative standard error. The *relative standard error* (RE) is defined as follows:

$$\mathrm{RE}\left[\widehat{\widetilde{P}}_{\mathrm{f}}^{\mathrm{M}}\right] = \frac{\sqrt{\mathrm{Var}\left[\widehat{\widetilde{P}}_{\mathrm{f}}^{\mathrm{M}}\right]}}{\mathbb{E}\left[\widehat{\widetilde{P}}_{\mathrm{f}}^{\mathrm{M}}\right]} \tag{5.12}$$

where $\mathbb{E}\left[\widehat{\widetilde{P}}_{\mathrm{f}}^{\mathrm{M}}\right]$ and $\mathrm{Var}\left[\widehat{\widetilde{P}}_{\mathrm{f}}^{\mathrm{M}}\right]$ are estimated on the sample obtained by replication of the analysis (see Eq. (5.15) and Eq. (5.16)).

Relative bias. The *relative bias* (RB) is defined as follows:

$$\mathrm{RB}\left[\widehat{\widetilde{P}}_{\mathrm{f}}^{\mathrm{M}}\right] = \frac{\mathbb{E}\left[\widehat{\widetilde{P}}_{\mathrm{f}}^{\mathrm{M}}\right] - \widehat{\widetilde{P}}_{\mathrm{f}}^{\mathrm{CMC}}}{\widehat{\widetilde{P}}_{\mathrm{f}}^{\mathrm{CMC}}}. \tag{5.13}$$

It gives a description of how close the estimate $\widehat{\widetilde{P}}_{\mathrm{f}}^{M}$ is close to the reference value $\widehat{\widetilde{P}}_{\mathrm{f}}^{\mathrm{CMC}}$. In the following (see Table 5.3 and Table 5.4), RB for NRA is computed with reference to the quantity $\widehat{\widetilde{P}}_{\mathrm{f,ref}}$ (estimated by a reference CMC or another technique when CMC is intractable) while RB for ARA is computed with reference to $\widehat{\widetilde{P}}_{\mathrm{f}}^{\mathrm{ARA/CMC}}$ to make the comparison representative.

Efficiency. The *efficiency* ν^{M} relatively to a CMC estimate (respectively obtained by NRA/CMC or ARA/CMC) can be defined such that:

$$\nu^{\mathrm{M}} = \frac{N_{\mathrm{sim}}^{\mathrm{CMC}}}{N_{\mathrm{sim}}^{\mathrm{M}}} \tag{5.14}$$

where $N_{\mathrm{sim}}^{\mathrm{CMC}}$ is the required number of CMC simulations to get $\mathrm{RE}\left[\widehat{\widehat{P}}_{\mathrm{f}}^{\mathrm{CMC}}\right] = \mathrm{RE}\left[\widehat{\widehat{P}}_{\mathrm{f}}^{\mathrm{M}}\right]$. A value of $\nu^{\mathrm{M}} > 1$ indicates that the method M is more efficient than CMC for the given test-case. In other words, ν^{M} indicates the quantity by which one can divide the initial CMC simulation budget for a same level of accuracy.

Statistics of the predictive failure probability estimator. In the following numerical studies, the mean and variance of $\widehat{\widehat{P}}_{\mathrm{f}}$ are estimated by replication of the algorithm, using the following usual statistics:

$$m_{\widehat{\widehat{P}}_{\mathrm{f}}} = \frac{1}{N_{\mathrm{rep}}} \sum_{i=1}^{N_{\mathrm{rep}}} \widehat{\widehat{P}}_{\mathrm{f}}^{(i)} \tag{5.15}$$

which is the *sample mean* with N_{rep} the number of replications of the predictive failure probability estimation and $S^2_{\widehat{\widehat{P}}_{\mathrm{f}}}$ the *unbiased sample variance* defined by:

$$S^2_{\widehat{\widehat{P}}_{\mathrm{f}}} = \frac{1}{N_{\mathrm{rep}} - 1} \sum_{i=1}^{N_{\mathrm{rep}}} \left(\widehat{\widehat{P}}_{\mathrm{f}}^{(i)} - m_{\widehat{\widehat{P}}_{\mathrm{f}}} \right)^2 . \tag{5.16}$$

5.4.2 Example #1: a resistance – demand toy-case with correlated basic variables and low failure probability

Description. The aim of this first academic test-case is to check the validity of the two approaches regarding two difficulties: assuming a strong correlation in the input probabilistic model and trying to estimate a low failure probability w.r.t. a given simulation budget. Table 5.2 gives the input data. The reference failure probability without parameter uncertainty is $p_{\mathrm{f,ref}} = 8.84 \times 10^{-8}$ (because of the linear LSF, the true conditional failure probability $P_{\mathrm{f}}(\boldsymbol{\theta})$ can be obtained using FORM). The correlation coefficient $\rho = 0.9$ expresses the linear correlation between the two basic variables. The failure is considered when the demand S exceeds the resource R. The LSF thus reads:

$$g(\mathbf{X}) = R - S = X_1 - X_2. \tag{5.17}$$

The conditional failure probability, i.e., $P_{\mathrm{f}}(\Theta = \theta)$, can be written in its integral form since the joint conditional PDF $f_{\mathbf{X}|\boldsymbol{\Theta}}$ can be analytically derived. One gets:

$$\begin{aligned} P_{\mathrm{f}}(\theta = \mu_{X_2}) = \int_{\mathcal{F}_{\mathbf{x}}} & \frac{1}{2\pi\sigma_{X_1}\sigma_{X_2}\sqrt{1-\rho^2}} \\ & \times \exp\left[-\frac{1}{2(1-\rho^2)} \left(\frac{(x_1 - \mu_{X_1})^2}{\sigma_{X_1}^2} - \frac{2\rho(x_1 - \mu_{X_1})(x_2 - \theta)}{\sigma_{X_1}\sigma_{X_2}} \right.\right. \\ & \left.\left. + \frac{(x_2 - \theta)^2}{\sigma_{X_2}^2} \right) \right] \mathrm{d}\mathbf{x}. \end{aligned} \tag{5.18}$$

In the specific case of two correlated normal variables and a linear LSF, the probability of failure becomes:

$$P_{\mathrm{f}}(\theta = \mu_{X_2}) = \Phi\left(-\beta_C\right) = \Phi\left(-\frac{\mu_{X_1} - \theta}{\sqrt{\sigma_{X_1}^2 + \sigma_{X_2}^2 - 2\rho\sigma_{X_1}\sigma_{X_2}}}\right). \tag{5.19}$$

where β_C is the *Cornell reliability index* (Madsen et al., 1986). This simple closed-form solution can be used to check and validate numerical results obtained for this elementary test-case.

TABLE 5.2: Input probabilistic model for Example #1.

Variable X_i [a]	**Distribution**	**Mean** μ_{X_i}	**S.d.** σ_{X_i}
$X_1 = R$	Normal	12	$5/\sqrt{3}$
$X_2 = S$	Normal	μ_{X_2} ***uncertain*** [b]	$2/\sqrt{3}$
$\Theta = \mu_{X_2}$	Normal	2	1.5

[a] Linear correlation between X_1 and X_2: $\rho = 0.9$.
[b] For a fixed value $\mu_{X_2} = 2$, $p_{\mathrm{f,ref}} = 8.84 \times 10^{-8}$.

Results. Table 5.3 illustrates that NRA and ARA give similar results for estimating the predictive failure probability. Moreover, for almost all the techniques (except NRA/CMC which suffers here from a lack of points while computing the integral over $\mathcal{D}_{\boldsymbol{\Theta}}$) it demonstrates that ARA can handle both rare event probabilities and strong correlation between basic input variables. On the one hand, ARA/FORM seriously challenges other techniques since it has a very small number of simulation code evaluations compared to CMC and SS and it gives exact results since the LSF is linear. On the other hand, ARA/SS definitely gives promising results compared to ARA/CMC since the ν value ($\nu = 54.44$) is high. In a classical context of rare event (often encountered in aerospace engineering), one can see the superiority of ARA (coupled with FORM or SS) compared to other NRA-coupled techniques. It also reveals how high can be the variations between the single-level failure probability estimate and the predictive one considering parameter uncertainty (here, it varies from 10^{-8} to 10^{-5}). Note that a similar test-case treating both μ_{X_i} and σ_{X_i} as uncertain distribution parameters is treated in Chabridon et al. (2017b) but are not recalled here for the sake of conciseness.

TABLE 5.3: Results for Example #1.

Approach	**CMC** [a]			**FORM**					**SS** [b]				
	$m_{\widehat{\widehat{P}}_f}$	$S^2_{\widehat{\widehat{P}}_f}$	RE	$m_{\widehat{\widehat{P}}_f}$	$S^2_{\widehat{\widehat{P}}_f}$	RE	RB	ν	$m_{\widehat{\widehat{P}}_f}$	$S^2_{\widehat{\widehat{P}}_f}$	RE	RB	ν
NRA [c]	2.57×10^{-5}	2.79×10^{-11}	0.21	1.99×10^{-5}	7.38×10^{-11}	0.43	-2.10×10^{-3}	–	1.99×10^{-5}	5.68×10^{-11}	0.38	-1.99×10^{-3}	48.03
ARA	1.95×10^{-5}	1.89×10^{-12}	7.03×10^{-2}	1.97×10^{-5}	–	–	7.84×10^{-3}	–	1.99×10^{-5}	7.26×10^{-11}	0.43	1.91×10^{-2}	54.44

[a] NRA: $N_{\boldsymbol{\theta}} = 10^3$ samples, $N_{\mathbf{x}} = 10^3$ samples | ARA: $N_{\mathbf{x},\boldsymbol{\theta}} = 10^6$ samples.
[b] NRA: $N_{\boldsymbol{\theta}} = 10^3$ samples, $N_{\mathbf{x}} = 10^3$ samples/step | ARA: $N_{\mathbf{x},\boldsymbol{\theta}} = 10^3$ samples/step.
[c] **Ref. (NRA/CMC, $N_{\boldsymbol{\theta}} = 10^6$ samples, $N_{\mathbf{x}} = 10^6$ samples):** $\widehat{\widehat{P}}_{f,\text{ref}} = 1.99 \times 10^{-5}$.

TABLE 5.4: Results for Example #2.

Approach	**CMC** [a]			**SS** [b]				
	$m_{\widehat{\widehat{P}}_f}$	$S^2_{\widehat{\widehat{P}}_f}$	RE	$m_{\widehat{\widehat{P}}_f}$	$S^2_{\widehat{\widehat{P}}_f}$	RE	RB	ν
NRA [c]	1.41×10^{-4}	1.41×10^{-10}	8.39×10^{-2}	1.59×10^{-4}	2.18×10^{-10}	9.27×10^{-2}	2.77×10^{-2}	0.18
ARA	1.53×10^{-4}	1.51×10^{-10}	8.00×10^{-2}	1.52×10^{-4}	3.31×10^{-9}	0.38	-1.08×10^{-2}	11.5

[a] NRA: $N_{\boldsymbol{\theta}} = 10^3$ samples, $N_{\mathbf{x}} = 10^3$ samples | ARA: $N_{\mathbf{x},\boldsymbol{\theta}} = 10^6$ samples.
[b] NRA: $N_{\boldsymbol{\theta}} = 10^3$ samples, $N_{\mathbf{x}} = 10^3$ samples/step | ARA: $N_{\mathbf{x},\boldsymbol{\theta}} = 10^3$ samples/step.
[c] **Ref. (NRA/CMC, $N_{\boldsymbol{\theta}} = 10^6$ samples, $N_{\mathbf{x}} = 10^6$ samples):** $\widehat{\widehat{P}}_{f,\text{ref}} = 1.55 \times 10^{-4}$.

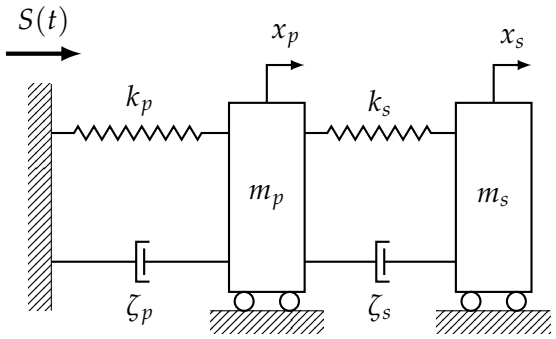

FIGURE 5.3: Two-degree-of-freedom damped oscillator with primary and secondary systems.

5.4.3 Example #2: a two d.o.f. primary/secondary damped oscillator

Description. This nonlinear oscillator is a well-known structural reliability test-case firstly proposed in Der Kiureghian and De Stefano (1991) and then used for benchmarking purposes in Bourinet et al. (2011), Bourinet (2016) and Dubourg (2011). The aim here, is to assess reliability of a two-degree-of-freedom primary-secondary system, as shown in Figure 5.3, under a white noise base acceleration. The basic variables characterizing the physical behavior are the masses m_p and m_s, spring stiffnesses k_p and k_s, natural frequencies $\omega_p = (k_p/m_p)^{1/2}$ and $\omega_s = (k_s/m_s)^{1/2}$ and damping ratios ζ_p and ζ_s, where the subscripts p and s respectively refer to the primary and secondary oscillators. If F_s denotes the force capacity of the secondary spring, then the reliability of the system can be evaluated using the following LSF (Der Kiureghian and De Stefano, 1991; Igusa and Der Kiureghian, 1985):

$$g(\mathbf{X}) = F_s - 3k_s \sqrt{\frac{\pi S_0}{4\zeta_s\omega_s^3}\left[\frac{\zeta_a\zeta_s}{\zeta_p\zeta_s\left(4\zeta_a^2+r^2\right)+\gamma\zeta_a^2}\frac{\left(\zeta_p\omega_p^3+\zeta_s\omega_s^3\right)\omega_p}{4\zeta\omega_a^4}\right]} = F_s - F_{\text{acc}}. \tag{5.20}$$

This equation defines the potential failure event $\{F_s \leq F_{\text{acc}}\}$ occuring if the force induced by the white noise base acceleration overcomes the force capacity in the secondary spring. Moreover, S_0 is the intensity of the white noise, $\gamma = m_s/m_p$ the mass ratio, $\omega_a = (\omega_p + \omega_s)/2$ the average frequency ratio, $\zeta_a = (\zeta_p + \zeta_s)/2$ the average damping ratio and $r = (\omega_p - \omega_s)/\omega_a$ a tuning parameter. The probabilistic model for $\mathbf{X}$ is detailed in Table 5.5.

The two interesting characteristics of this application test-case are its set of non-normal basic random variables and the fact that it suffers from a highly nonlinear limit-state surface (such a strong nonlinearity prevents from using any FORM-based approach, as illustrated by Bourinet (2016)). Moreover, following Dubourg (2011), under single-level uncertainty, it appears that the mean value of the force capacity μ_{X_7} is the most influential distribution parameter on the single-level failure probability. However, it is assumed here that this distribution parameter is not perfectly known. Thus one considers a prior distribution over μ_{X_7} as presented in Table 5.5.

TABLE 5.5: Input probabilistic model for Example #2.

Variable X_i [a]	**Distribution**	**Mean** μ_{X_i}	**C.v.** δ_{X_i}
$X_1 = m_p$ (kg)	Lognormal	1.5	10%
$X_2 = m_s$ (kg)	Lognormal	0.01	10%
$X_3 = k_p$ (N.m^{-1})	Lognormal	1	20%
$X_4 = k_s$ (N.m^{-1})	Lognormal	0.01	20%
$X_5 = \zeta_p$ (1)	Lognormal	0.05	40%
$X_6 = \zeta_s$ (1)	Lognormal	0.02	50%
$X_7 = F_s$ (N)	Lognormal	μ_{X_7} ***uncertain*** [b]	10%
$X_8 = S_0$ (m.s^{-2})	Lognormal	100	10%
$\Theta = \mu_{X_7}$ (N)	Normal	21.5	10%

[a] The basic variables are independent.
[b] For a fixed value $\mu_{X_7} = 21.5$, $p_{\text{f,ref}} = 4.78 \times 10^{-5}$.

Results. Numerical results summarized in Table 5.4 show that, for the same simulation budget, ARA/CMC is more accurate than NRA/CMC to estimate the predictive failure probability (the reference result $\widehat{\widetilde{P}}_{\text{f,ref}}$ is provided below the table). As for ARA/SS, a significant gain is noticeable referring to the high ν values compared to unity ($\nu > 10$). In brief, that means the ARA/SS is very efficient to treat this problem compared to a classical Monte Carlo approach. A final remark concerns the comparison between the two reference probabilities $p_{\text{f,ref}} = 4.78 \times 10^{-5}$ and $\widehat{\widetilde{P}}_{\text{f,ref}} = 1.55 \times 10^{-4}$: one can see that, in this case, considering uncertainty on a distribution parameter makes the system less safe, which can be, for example, an important indicator for design or re-design purposes.

5.4.4 Synthesis about numerical results

The aim of this subsection is to give a synthesis about the main advantages and drawbacks of both NRA and ARA. According to the numerical results, one can make the following remarks:

- ARA leads to more accurate results than NRA with respect to a given simulation budget;
- only ARA, coupled with dedicated rare event probability estimation techniques, is able to handle very expensive simulation codes;
- NRA suffers from the "budget allocation" problem;
- ARA requires to adapt the Rosenblatt transformation so as to use the usual rare event probability estimation techniques in the **u**-space.

As a final remark concerning the coupling between ARA and rare event probability estimation techniques, one can notice that large efficiencies can be attained with advanced sampling techniques such as ARA/SS (here, only SS is used but in the next chapter, similar efficiencies are demonstrated with IS) seems to be a very promising technique since it can handle most of the difficulties encountered in complex simulation codes. However, other techniques can be used if some specific characteristics are preponderant. For instance, if one knows that the LSF is linear, one should use ARA/FORM instead (whatever the rareness of the failure probability). Combining several characteristics lead to deduce which optimal technique should be used regarding all these simulation constraints.

5.5 Discussion and perspectives

As described in the previous sections, reliability assessment under parameter uncertainty involves mainly two components: the choice of an estimator for the failure probability (here, the predictive failure probability $\widetilde{P}_f$) and the choice of a numerical strategy to get an estimate of it (i.e., NRA vs. ARA). Concerning the first point, $\widetilde{P}_f$ corresponds to the mean failure probability over all the conditional failure probabilities $P_f(\boldsymbol{\theta})$. As discussed in Keller et al. (2011) and Pasanisi et al. (2012), such a predictive estimator appears to be, from the *statistical decision theory* point of view (Berger, 1985), associated to a *quadratic cost function* whose aim is to quantify the impact of a mis-estimation through $\widetilde{P}_f$ with respect to the true failure probability p_f (probability obtained with a full knowledge of the probability distribution of $\mathbf{X}$ and with a perfect computer model). However, as pointed out in Pasanisi et al. (2012), since the associated quadratic cost function is symmetric, both under- and over-estimations have the same costs, theoretically speaking. Nevertheless, this symmetry of costs may have asymmetric consequences from a risk management perspective. Thus, a more conservative estimate (e.g., a quantile) could be combined with $\widetilde{P}_f$ to characterize more accurately the probability of interest. However, estimating such an indicator is possible with NRA but, as mentioned previously, with a computational cost which might be incompatible with industrial considerations. Further investigations are required to make the calculation of quantiles possible with ARA. A first track could be to use the *reverse importance sampling trick* in a similar fashion as in Morio (2011b) and Lemaître et al. (2015) so as to avoid the naive sampling strategy imposed by NRA. In the recent work of Zhao et al. (2018), a point-estimate technique is used to either approximate the mean and a quantile of the conditional failure probability. This approximation technique seems promising but presents some limitations, mainly due to the use of point-estimate approximation techniques which can introduce some bias in the estimates.

Further enhancements can be envisaged from reliability updating process, especially by coupling the proposed approaches with reliability updating schemes such as those proposed in Straub (2011) and Straub and Papaioannou (2015). Indeed, one could consider either getting more information about the basic input variables (e.g., more data) or even more information about distribution parameters (see, e.g., the discussion about the topic of statistical tolerancing for mass production in Chabridon et al., 2017c).

Finally, in order to reduce the computational cost of these estimations, one possible enhancement track could be to use a surrogate model coupled with ARA in order to reduce the computational cost of these estimations. However, one needs to ensure first that the accuracy of the surrogate model is high enough so as to avoid adding noise to the already existing bi-level input uncertainty.

5.6 Conclusion

In this chapter, a coupling between rare event probability estimation techniques (e.g., CMC, FORM, SS) and two existing strategies, namely the nested reliability approach (NRA) and the augmented reliability approach (ARA), is investigated to handle reliability assessment of black-box computer codes under distribution parameter uncertainty. If the first one, the NRA, is widely used and simple to set up, it definitely crashes with both the curse of dimensionality and simulation budget considerations. The second one, the ARA, relies on the definition of an augmented input vector of uncertain distribution parameters and the basic input variables. For ARA, numerical sampling and integration can be carried simultaneously on both basic random variables conditioned on uncertain distribution parameters. The main principles of both techniques have been presented into a unified common framework. Specific attention has been given

to the algorithmic links and differences existing between these approaches. Specificities concerning the use of Rosenblatt transformation with ARA have been evoked. Then, a comparison between NRA and ARA has been carried out through application on two academic test-cases. Numerical application on a realistic aerospace test-case will be further studied in Chapter 8. This study showed the benefits of using ARA with dedicated rare event probability estimation techniques for complex models. Several enhancements raised in Section 5.5 are currently open research tracks.

In the next chapter, a first way to study the variability of the reliability measure (i.e., the predictive failure probability) w.r.t. the bi-level input uncertainty is investigated. It relies on the proposition of local derivative-based sensitivity estimators of the predictive failure probability regarding the deterministic hyper-parameters of the prior probability distribution of $\boldsymbol{\Theta}$.

CHAPTER 6

Local ROSA under distribution parameter uncertainty

Contents

This chapter is adapted from the following reference:

Chabridon V., M. Balesdent, J.-M. Bourinet, J. Morio, and N. Gayton (2017). "Reliability-based sensitivity estimators of rare event probability in the presence of distribution parameter uncertainty". In: *Reliability Engineering and System Safety* 178, pp. 164–178.

6.1 Introduction and motivations

In this chapter, one considers the same Bayesian hierarchical model as that presented in Chapter 5:

$$\begin{aligned}
\mathbf{X} &\sim f_{\mathbf{X}|\boldsymbol{\Theta}}(\mathbf{x}|\boldsymbol{\theta}) : \mathcal{D}_{\mathbf{X}} \subseteq \mathbb{R}^d \to \mathbb{R}_+ \quad \text{(uncertainty level \#1)} \\
\boldsymbol{\Theta} &\sim f_{\boldsymbol{\Theta}|\boldsymbol{\xi}}(\boldsymbol{\theta}|\boldsymbol{\xi}) : \mathcal{D}_{\boldsymbol{\Theta}} \subseteq \mathbb{R}^{n_\theta} \to \mathbb{R}_+ \quad \text{(uncertainty level \#2)} \\
\boldsymbol{\xi} &= (\xi_1, \xi_2, \ldots, \xi_{n_\xi})^\top \in \mathcal{D}_{\boldsymbol{\xi}} \subseteq \mathbb{R}^{n_\xi} \quad \text{(deterministic level)}.
\end{aligned}$$

In the present chapter, contrarily to the previous one, the third level is considered in an explicit way. This is due to the fact that, in the context of a lack of information about $\boldsymbol{\Theta}$, the epistemic uncertainty is characterized through the use of a prior distribution. This prior can be elicited from experts' judgments. As a result, the choice of the prior distribution hyper-parameters (e.g., choice of moments or bounds) might have an impact on the safety measure. The idea is to check the robustness of the safety measure w.r.t. the local choice of specific values for the hyper-parameters.

Moreover, as described in Chapter 5, under this *bi-level input uncertainty*, the chosen QoI is the *predictive failure probability* defined such that:

$$\widetilde{P}_{\mathrm{f}}(\boldsymbol{\xi}) \overset{\text{def}}{=} \mathbb{E}_{f_{\boldsymbol{\Theta}|\boldsymbol{\xi}}}\left[P_{\mathrm{f}}(\boldsymbol{\Theta})\right] = \mathbb{E}_{f_{\boldsymbol{\Theta}|\boldsymbol{\xi}}}\left[\mathbb{E}_{f_{\mathbf{X}|\boldsymbol{\Theta}}}\left[\mathbb{1}_{\mathcal{F}_{\mathbf{x}}}(\mathbf{X})|\boldsymbol{\Theta}\right]|\boldsymbol{\xi}\right] \tag{6.2a}$$

$$= \int_{\mathcal{D}_{\boldsymbol{\Theta}}} P_{\mathrm{f}}(\boldsymbol{\theta}) f_{\boldsymbol{\Theta}|\boldsymbol{\xi}}(\boldsymbol{\theta}|\boldsymbol{\xi}) \mathrm{d}\boldsymbol{\theta} \tag{6.2b}$$

where $P_{\mathrm{f}}(\boldsymbol{\theta})$ is the *conditional failure probability* given by:

$$P_{\mathrm{f}}(\boldsymbol{\theta}) = \mathbb{P}(g(\mathbf{X}) \leq 0 \mid \boldsymbol{\Theta} = \boldsymbol{\theta}) = \int_{\mathcal{D}_{\mathbf{X}}} \mathbb{1}_{\mathcal{F}_{\mathbf{x}}}(\mathbf{x}) f_{\mathbf{X}|\boldsymbol{\Theta}}(\mathbf{x}|\boldsymbol{\theta}) \mathrm{d}\mathbf{x} \tag{6.3a}$$

$$= \mathbb{E}_{f_{\mathbf{X}|\boldsymbol{\Theta}}}\left[\mathbb{1}_{\mathcal{F}_{\mathbf{x}}}(\mathbf{X}) \mid \boldsymbol{\Theta} = \boldsymbol{\theta}\right]. \tag{6.3b}$$

As demonstrated in the previous chapter (see also Chabridon et al. (2017a) and Chabridon et al. (2017c)), an efficient way to estimate such a QoI can be achieved by considering a so-called "augmented" random vector $\mathbf{Z} \overset{\text{def}}{=} (\mathbf{X}, \boldsymbol{\Theta})^\top$ defined on $\mathcal{D}_{\mathbf{Z}} = \mathcal{D}_{\mathbf{X}} \times \mathcal{D}_{\boldsymbol{\Theta}}$ (where $\times$ is the Cartesian product) with joint PDF $f_{\mathbf{Z}|\boldsymbol{\xi}}(\mathbf{z}|\boldsymbol{\xi}) \overset{\text{def}}{=} f_{(\mathbf{X},\boldsymbol{\Theta})|\boldsymbol{\xi}}((\mathbf{x},\boldsymbol{\theta})|\boldsymbol{\xi}) = f_{\mathbf{X}|\boldsymbol{\Theta}}(\mathbf{x}|\boldsymbol{\theta}) f_{\boldsymbol{\Theta}|\boldsymbol{\xi}}(\boldsymbol{\theta}|\boldsymbol{\xi})$ such that the expression in Eq. (6.2b) can be rewritten as follows:

$$\widetilde{P}_{\mathrm{f}}(\boldsymbol{\xi}) = \int_{\mathcal{D}_{\boldsymbol{\Theta}}} \int_{\mathcal{D}_{\mathbf{X}}} \mathbb{1}_{\mathcal{F}_{\mathbf{x}}}(\mathbf{x}) f_{\mathbf{X}|\boldsymbol{\Theta}}(\mathbf{x}|\boldsymbol{\theta}) f_{\boldsymbol{\Theta}|\boldsymbol{\xi}}(\boldsymbol{\theta}|\boldsymbol{\xi}) \mathrm{d}\mathbf{x}\mathrm{d}\boldsymbol{\theta} = \int_{\mathcal{D}_{\mathbf{Z}}} \mathbb{1}_{\mathcal{F}_{\mathbf{z}}}(\mathbf{z}) f_{\mathbf{Z}|\boldsymbol{\xi}}(\mathbf{z}|\boldsymbol{\xi}) \mathrm{d}\mathbf{z} \tag{6.4a}$$

$$= \mathbb{E}_{f_{\mathbf{Z}|\boldsymbol{\xi}}}\left[\mathbb{1}_{\mathcal{F}_{\mathbf{z}}}(\mathbf{Z}) \mid \boldsymbol{\xi}\right] \tag{6.4b}$$

where $\mathcal{F}_{\mathbf{z}} = \{\mathbf{z} \in \mathcal{D}_{\mathbf{Z}} \mid g(\mathbf{z}) \leq 0\}$. This augmented formulation (a.k.a. ARA) numerically implies to estimate the expected value in Eq (6.4b).

In this chapter, the aim is to propose a possible answer to the **Q3** recalled herebelow:

Q3 – How to link the variability of the reliability measure to this bi-level input uncertainty?

This chapter is organized as follows. Section 6.2 describes both the derived sensitivity estimators and their implementation within the augmented Adaptive Importance Sampling strategy. Section 6.3 illustrates the benefits of such a methodology on different test-cases of increasing complexity and a synthesis gathering the key aspects and issues of the proposed approach is provided at the end of this section. A conclusion gathering the most important results of this chapter is finally given in Section 6.4.

6.2 Sensitivity analysis of predictive failure probability with respect to distribution hyper-parameters

The use of local sensitivities in this study is motivated mainly by two reasons. The first one corresponds to the way the problem is set as explained above (i.e., one wants to measure the sensitivity w.r.t. a local choice of $\boldsymbol{\xi}$). Finally, the second reason, which is a key constraint in this work, remains the limited allowable extra simulation budget one can afford to get sensitivities while the rare event probability estimation can be very expensive too (without any consideration here of any use of a metamodel).

The gradient of the predictive failure probability $\widetilde{P}_\mathrm{f}$ w.r.t. the vector of the hyper-parameters $\boldsymbol{\xi}$ is defined as follows:

$$\boldsymbol{\nabla}_{\boldsymbol{\xi}} \widetilde{P}_\mathrm{f}(\boldsymbol{\xi}) = \left(\frac{\partial \widetilde{P}_\mathrm{f}(\boldsymbol{\xi})}{\partial \xi_j}, j = 1, \ldots, n_\xi \right)^\top . \tag{6.5}$$

Depending on the nature of the hyper-parameter ξ_j, two cases are considered:

- Case #1: ξ_j is an hyper-parameter of a prior distribution with an unbounded support;
- Case #2: ξ_j is an hyper-parameter of a prior distribution with a bounded/truncated support.

6.2.1 Sensitivity estimators for Case #1 in the augmented framework

The partial derivative of the predictive failure probability w.r.t. the j-th component of $\boldsymbol{\xi}$ is given by:

$$\frac{\partial \widetilde{P}_\mathrm{f}(\boldsymbol{\xi})}{\partial \xi_j} = \frac{\partial}{\partial \xi_j} \left[\int_{\mathcal{D}_{\boldsymbol{\Theta}}} P_\mathrm{f}(\boldsymbol{\theta}) f_{\boldsymbol{\Theta}|\boldsymbol{\xi}}(\boldsymbol{\theta}|\boldsymbol{\xi}) \mathrm{d}\boldsymbol{\theta} \right] = \int_{\mathcal{D}_{\boldsymbol{\Theta}}} P_\mathrm{f}(\boldsymbol{\theta}) \frac{\partial f_{\boldsymbol{\Theta}|\boldsymbol{\xi}}(\boldsymbol{\theta}|\boldsymbol{\xi})}{\partial \xi_j} \mathrm{d}\boldsymbol{\theta}. \tag{6.6}$$

Note that, in the previous derivations, the differential and integral operators are switched due to Lebesgue's dominated convergence theorem (Jacod and Protter, 2004). Following the idea given in Rubinstein (1986), one can use the so-called *importance sampling trick* so as to get an expectation w.r.t. the same probability measure as that used for the failure probability estimation. It thus comes:

$$\begin{aligned}
\frac{\partial \widetilde{P}_\mathrm{f}(\boldsymbol{\xi})}{\partial \xi_j} &= \int_{\mathcal{D}_{\boldsymbol{\Theta}}} P_\mathrm{f}(\boldsymbol{\theta}) \frac{\frac{\partial}{\partial \xi_j} f_{\boldsymbol{\Theta}|\boldsymbol{\xi}}(\boldsymbol{\theta}|\boldsymbol{\xi})}{f_{\boldsymbol{\Theta}|\boldsymbol{\xi}}(\boldsymbol{\theta}|\boldsymbol{\xi})} f_{\boldsymbol{\Theta}|\boldsymbol{\xi}}(\boldsymbol{\theta}|\boldsymbol{\xi}) \mathrm{d}\boldsymbol{\theta} && \text{(6.7a)} \\
&= \int_{\mathcal{D}_{\boldsymbol{\Theta}}} \left(\int_{\mathcal{D}_{\mathbf{X}}} \mathbb{1}_{\mathcal{F}_\mathbf{x}}(\mathbf{x}) f_{\mathbf{X}|\boldsymbol{\Theta}}(\mathbf{x}|\boldsymbol{\theta}) \mathrm{d}\mathbf{x} \right) \frac{\partial \ln f_{\boldsymbol{\Theta}|\boldsymbol{\xi}}(\boldsymbol{\theta}|\boldsymbol{\xi})}{\partial \xi_j} f_{\boldsymbol{\Theta}|\boldsymbol{\xi}}(\boldsymbol{\theta}|\boldsymbol{\xi}) \mathrm{d}\boldsymbol{\theta} && \text{(6.7b)} \\
&= \int_{\mathcal{D}_{\boldsymbol{\Theta}}} \left(\int_{\mathcal{D}_{\mathbf{X}}} \mathbb{1}_{\mathcal{F}_\mathbf{x}}(\mathbf{x}) \, \kappa_j(\boldsymbol{\theta}, \boldsymbol{\xi}) \, f_{\mathbf{X}|\boldsymbol{\Theta}}(\mathbf{x}|\boldsymbol{\theta}) \mathrm{d}\mathbf{x} \right) f_{\boldsymbol{\Theta}|\boldsymbol{\xi}}(\boldsymbol{\theta}|\boldsymbol{\xi}) \mathrm{d}\boldsymbol{\theta} && \text{(6.7c)} \\
&= \mathbb{E}_{f_{\mathbf{Z}|\boldsymbol{\xi}}} \left[\mathbb{1}_{\mathcal{F}_\mathbf{z}}(\mathbf{Z}) \, \kappa_j(\boldsymbol{\Theta}, \boldsymbol{\xi}) \right] && \text{(6.7d)}
\end{aligned}$$

where $\kappa_j(\boldsymbol{\theta}, \boldsymbol{\xi}) \overset{\text{def}}{=} \frac{\partial \ln f_{\boldsymbol{\Theta}|\boldsymbol{\xi}}(\boldsymbol{\theta}|\boldsymbol{\xi})}{\partial \xi_j}$ is called the "*score function*" (SF). As recalled in Chapter 4, the SF approach has been widely used in the ROSA literature under *single-level* uncertainty (see, e.g., Wu (1994b), Rahman (2009), and Millwater and Feng (2011)). It is used here, in the context of bi-level uncertainty, for three main reasons: first, it enables to provide the targeted local sensitivity in Eq. (6.6) as a simple derivation (assuming rather simple cases for the prior distribution); then, it fits naturally to an importance-sampling-based estimation framework; and finally, it provides an efficient sampling-based estimator which allows to avoid finite difference schemes. One should notice that, to avoid any confusion, in the above equations and in the rest of the chapter, the vector $\boldsymbol{\Theta}$ is explicitely written instead of $\mathbf{Z} = (\mathbf{X}, \boldsymbol{\Theta})^\top$ since the dependence w.r.t. $\boldsymbol{\xi}$ is through $\boldsymbol{\Theta}$. An example of a SF associated to an unbounded normal prior for an uncertain distribution parameter Θ_j is given in Table 6.1. Then, considering a sample $\{\mathbf{Z}^{(i)}\}_{i=1}^N$ of N i.i.d. copies of the augmented vector $\mathbf{Z}$, one can derive the following MC estimator:

$$\frac{\partial \widetilde{P}_{\text{f}}(\boldsymbol{\xi})}{\partial \xi_j} \underset{\text{MC}}{\approx} \frac{1}{N} \sum_{i=1}^{N} \mathbb{1}_{\mathcal{F}_{\mathbf{z}}}(\mathbf{Z}^{(i)})\, \kappa_j(\boldsymbol{\Theta}^{(i)}, \boldsymbol{\xi}). \tag{6.8}$$

As a remark, if the probability is estimated with ARA, its gradient in Eq. (6.8) may be estimated at a reduced cost. However, due to central limit theorem, one can show that the predictive failure probability and its sensitivities may have different convergence rates. Thus, the variance associated with the two asymptotic distributions will necessarily differ.

TABLE 6.1: Score functions for normal (Case #1) and uniform (Case #2) prior distributions on an uncertain parameter Θ_j.

Distribution	**PDF** $f_{\Theta_j\|\boldsymbol{\xi}}(\theta_j\|\xi_1,\xi_2)$	**Hyper-parameters**	**SF** $\kappa_1(\theta_j,\xi_1)$	**SF** $\kappa_2(\theta_j,\xi_2)$
Normal (Case #1)	$\frac{1}{\xi_2\sqrt{2\pi}} \exp\left[-\frac{1}{2}\left(\frac{\theta_j-\xi_1}{\xi_2}\right)^2\right]$	$\xi_1 = \mu_{\Theta_j}$, $\xi_2 = \sigma_{\Theta_j}$	$\frac{1}{\xi_2}\left(\frac{\theta_j-\xi_1}{\xi_2}\right)$	$\frac{1}{\xi_2}\left[\left(\frac{\theta_j-\xi_1}{\xi_2}\right)^2 - 1\right]$
Uniform (Case #2)	$\frac{1}{\xi_2-\xi_1}$	$\xi_1 = a_{\theta_j}$, $\xi_2 = b_{\theta_j}$	$\frac{1}{\xi_2-\xi_1}$	$-\frac{1}{\xi_2-\xi_1}$

6.2.2 Sensitivity estimators for Case #2 in the augmented framework

Here, at least, one of the basic variables X_j follows a parametrized distribution whose parameter Θ_j follows a bounded or truncated distribution denoted by $f_{\Theta_j|\boldsymbol{\xi}}(\theta_j|\boldsymbol{\xi})$, with $\boldsymbol{\xi} = (\xi_1, \xi_2, \ldots, \xi_{n_\xi})^\top$ the vector of the hyper-parameters. Here, $\xi_j \in \boldsymbol{\xi}$ could be either a bound or a moment. In the next derivations, one considers that the distribution parameters $\Theta_i, i = 1, \ldots, n_{\boldsymbol{\theta}}$ are independent, which leads to $f_{\boldsymbol{\Theta}|\boldsymbol{\xi}}(\boldsymbol{\theta}|\boldsymbol{\xi}) = \prod_{i=1}^{n_{\boldsymbol{\theta}}} f_{\Theta_i|\boldsymbol{\xi}}(\theta_i|\boldsymbol{\xi})$. Before deriving the sensitivities, one should notice that, in this case, the support $\mathcal{D}_{\boldsymbol{\Theta}}$ is a function of ξ_j as the support of Θ_j is either bounded or truncated (note that, without any loss of generality, the bounds are denoted by $a(\xi_j)$ and $b(\xi_j)$ in Eq. (6.9b)). In the following, the notation $\boldsymbol{\Theta}^{-j}$ (respectively $\boldsymbol{\theta}^{-j}$) denotes the vector without the j-th component Θ_j (repectively θ_j) which depends on the hyper-parameter ξ_j. Thus, one can

write:

$$\frac{\partial \widetilde{P}_{\mathrm{f}}(\boldsymbol{\xi})}{\partial \xi_j} = \frac{\partial}{\partial \xi_j}\left[\int_{\mathcal{D}_{\boldsymbol{\Theta}}(\xi_j)} P_{\mathrm{f}}(\boldsymbol{\theta}) f_{\boldsymbol{\Theta}|\boldsymbol{\xi}}(\boldsymbol{\theta}|\boldsymbol{\xi})\mathrm{d}\boldsymbol{\theta}\right] \tag{6.9a}$$

$$= \frac{\partial}{\partial \xi_j}\left[\int_{\mathbb{R}^{n_{\boldsymbol{\theta}}-1}} \int_{a(\xi_j)}^{b(\xi_j)} P_{\mathrm{f}}(\boldsymbol{\theta}) f_{\Theta_j|\boldsymbol{\xi}}(\theta_j|\boldsymbol{\xi}) f_{\boldsymbol{\Theta}^{-j}|\boldsymbol{\xi}}(\boldsymbol{\theta}^{-j}|\boldsymbol{\xi})\mathrm{d}\theta_j \mathrm{d}\boldsymbol{\theta}^{-j}\right] \tag{6.9b}$$

$$= \int_{\mathbb{R}^{n_{\boldsymbol{\theta}}-1}} \frac{\partial}{\partial \xi_j}\left[\int_{a(\xi_j)}^{b(\xi_j)} P_{\mathrm{f}}(\boldsymbol{\theta}) f_{\Theta_j|\boldsymbol{\xi}}(\theta_j|\boldsymbol{\xi})\mathrm{d}\theta_j\right] f_{\boldsymbol{\Theta}^{-j}|\boldsymbol{\xi}}(\boldsymbol{\theta}^{-j}|\boldsymbol{\xi})\mathrm{d}\boldsymbol{\theta}^{-j} \tag{6.9c}$$

$$= \int_{\mathbb{R}^{n_{\boldsymbol{\theta}}-1}} \frac{\partial}{\partial \xi_j}\left[\mathcal{I}\left(P_{\mathrm{f}}(\boldsymbol{\theta}), \boldsymbol{\xi}\right)\right] f_{\boldsymbol{\Theta}^{-j}|\boldsymbol{\xi}}(\boldsymbol{\theta}^{-j}|\boldsymbol{\xi})\mathrm{d}\boldsymbol{\theta}^{-j} \tag{6.9d}$$

where $\mathcal{I}\left(P_{\mathrm{f}}(\boldsymbol{\theta}), \boldsymbol{\xi}\right)$ is an integral whose bounds (denoted by a and b) depend on the parameter ξ_j. Indeed, using the Leibniz integral rule for differentiation of a definite integral whose limits are functions of the differential variables, one gets:

$$\frac{\partial}{\partial \xi_j}\left[\mathcal{I}\left(P_{\mathrm{f}}(\boldsymbol{\theta}), \boldsymbol{\xi}\right)\right] = \frac{\partial}{\partial \xi_j}\left[\int_{a(\xi_j)}^{b(\xi_j)} P_{\mathrm{f}}(\boldsymbol{\theta}) f_{\Theta_j|\boldsymbol{\xi}}(\theta_j|\boldsymbol{\xi})\mathrm{d}\theta_j\right] \tag{6.10a}$$

$$\begin{aligned} &= \int_{a(\xi_j)}^{b(\xi_j)} P_{\mathrm{f}}(\boldsymbol{\theta}) \frac{\partial f_{\Theta_j|\boldsymbol{\xi}}(\theta_j|\boldsymbol{\xi})}{\partial \xi_j}\mathrm{d}\theta_j \\ &+ P_{\mathrm{f}}\left(\boldsymbol{\theta}^{-j}, \theta_j = b(\xi_j)\right)\ f_{\Theta_j|\boldsymbol{\xi}}(b(\xi_j)|\boldsymbol{\xi})\ \frac{\partial b(\xi_j)}{\partial \xi_j} \\ &- P_{\mathrm{f}}\left(\boldsymbol{\theta}^{-j}, \theta_j = a(\xi_j)\right)\ f_{\Theta_j|\boldsymbol{\xi}}(a(\xi_j)|\boldsymbol{\xi})\ \frac{\partial a(\xi_j)}{\partial \xi_j} \end{aligned} \tag{6.10b}$$

where $P_{\mathrm{f}}\left(\boldsymbol{\theta}^{-j}, \theta_j = \bullet(\xi_j)\right)$ represents the failure probability estimated with θ_j fixed to one of the integration bounds (i.e., $\bullet(\xi_j) = a(\xi_j)$ or $b(\xi_j)$).

To illustrate the previous reasoning, one can apply these derivations to a test-case involving a distribution parameter Θ_j following a continuous uniform distribution such that $\Theta_j \sim \mathcal{U}([a, b])$. In this example, ξ_j can be either a bound (a or b) or even a moment (e.g., $\mu_{\Theta_j} = \frac{a+b}{2}$ or $\sigma_{\Theta_j} = \frac{b-a}{\sqrt{12}}$). Let us first assume that $\xi_j = a$:

$$\frac{\partial}{\partial a}\left[\mathcal{I}\left(P_{\mathrm{f}}(\boldsymbol{\theta}), \boldsymbol{\xi}\right)\right] = \int_a^b P_{\mathrm{f}}(\boldsymbol{\theta}) \frac{\partial f_{\Theta_j|\boldsymbol{\xi}}(\theta_j|\boldsymbol{\xi})}{\partial a}\mathrm{d}\theta_j + 0 - P_{\mathrm{f}}(\boldsymbol{\theta}^{-j}, \theta_j = a) f_{\Theta_j|\boldsymbol{\xi}}(a|\boldsymbol{\xi}) \times 1 \tag{6.11a}$$

$$= \int_a^b P_{\mathrm{f}}(\boldsymbol{\theta}) \frac{\partial f_{\Theta_j|\boldsymbol{\xi}}(\theta_j|\boldsymbol{\xi})}{\partial a}\mathrm{d}\theta_j - \frac{1}{b-a} P_{\mathrm{f}}(\boldsymbol{\theta}^{-j}, \theta_j = a). \tag{6.11b}$$

Hence, using the same trick as in paragraph 6.2.1, one gets:

$$\frac{\partial \widetilde{P}_{\mathrm{f}}(\boldsymbol{\xi})}{\partial a} = \int_{\mathbb{R}^{n_{\boldsymbol{\theta}}}} P_{\mathrm{f}}(\boldsymbol{\theta}) \frac{\frac{\partial}{\partial a} f_{\Theta_j|\boldsymbol{\xi}}(\theta_j|\boldsymbol{\xi})}{f_{\Theta_j|\boldsymbol{\xi}}(\theta_j|\boldsymbol{\xi})} f_{\Theta_j|\boldsymbol{\xi}}(\theta_j|\boldsymbol{\xi}) f_{\boldsymbol{\Theta}^{-j}|\boldsymbol{\xi}}(\boldsymbol{\theta}^{-j}|\boldsymbol{\xi}) \mathrm{d}\theta_j \mathrm{d}\boldsymbol{\theta}^{-j}$$

$$- \frac{1}{b-a} \int_{\mathbb{R}^{n_{\boldsymbol{\theta}}-1}} P_{\mathrm{f}}(\boldsymbol{\theta}^{-j}, \theta_j = a) f_{\boldsymbol{\Theta}^{-j}|\boldsymbol{\xi}}(\boldsymbol{\theta}^{-j}|\boldsymbol{\xi}) \mathrm{d}\boldsymbol{\theta}^{-j} \tag{6.12a}$$

$$= \int_{\mathbb{R}^{n_{\boldsymbol{\theta}}}} \left(\int_{\mathbb{R}^d} \mathbb{1}_{\mathcal{F}_{\mathbf{x}}}(\mathbf{x}) f_{\mathbf{X}|\boldsymbol{\Theta}}(\mathbf{x}|\boldsymbol{\theta}) \mathrm{d}\mathbf{x} \right) \frac{\partial \ln f_{\Theta_j|\boldsymbol{\xi}}(\theta_j|\boldsymbol{\xi})}{\partial a} f_{\boldsymbol{\Theta}|\boldsymbol{\xi}}(\boldsymbol{\theta}|\boldsymbol{\xi}) \mathrm{d}\boldsymbol{\theta}$$

$$- \frac{1}{b-a} \int_{\mathbb{R}^{n_{\boldsymbol{\theta}}-1}} \left(\int_{\mathbb{R}^d} \mathbb{1}_{\mathcal{F}_{\mathbf{x}}}(\mathbf{x}) f_{\mathbf{X}|\boldsymbol{\Theta}}(\mathbf{x}|\boldsymbol{\theta}^{-j}, \theta_j = a) \mathrm{d}\mathbf{x} \right) f_{\boldsymbol{\Theta}^{-j}|\boldsymbol{\xi}}(\boldsymbol{\theta}^{-j}|\boldsymbol{\xi}) \mathrm{d}\boldsymbol{\theta}^{-j} \tag{6.12b}$$

$$= \int_{\mathbb{R}^{n_{\boldsymbol{\theta}}}} \left(\int_{\mathbb{R}^d} \mathbb{1}_{\mathcal{F}_{\mathbf{x}}}(\mathbf{x}) \, \kappa_j(\theta_j, a) \, f_{\mathbf{X}|\boldsymbol{\Theta}}(\mathbf{x}|\boldsymbol{\theta}) \mathrm{d}\mathbf{x} \right) f_{\boldsymbol{\Theta}|\boldsymbol{\xi}}(\boldsymbol{\theta}|\boldsymbol{\xi}) \mathrm{d}\boldsymbol{\theta}$$

$$- \frac{1}{b-a} \int_{\mathbb{R}^{n_{\boldsymbol{\theta}}-1}} \left(\int_{\mathbb{R}^d} \mathbb{1}_{\mathcal{F}_{\mathbf{x}}}(\mathbf{x}) f_{\mathbf{X}|\boldsymbol{\Theta}}(\mathbf{x}|\boldsymbol{\theta}^{-j}, \theta_j = a) \mathrm{d}\mathbf{x} \right) f_{\boldsymbol{\Theta}^{-j}|\boldsymbol{\xi}}(\boldsymbol{\theta}^{-j}|\boldsymbol{\xi}) \mathrm{d}\boldsymbol{\theta}^{-j} \tag{6.12c}$$

$$= \mathbb{E}_{f_{\mathbf{Z}|\boldsymbol{\xi}}} \left[\mathbb{1}_{\mathcal{F}_{\mathbf{z}}}(\mathbf{Z}) \, \kappa_j(\Theta_j, \boldsymbol{\xi}) \right] - \frac{1}{b-a} \mathbb{E}_{f_{\mathbf{Z}|\Theta_j=a,\boldsymbol{\xi}}} \left[\mathbb{1}_{\mathcal{F}_{\mathbf{z}}}(\mathbf{Z}^{-j}) \mid \Theta_j = a \right] \tag{6.12d}$$

where $\mathbf{Z}^{-j}$ stands for $(\mathbf{X}, \boldsymbol{\Theta}^{-j})^\top$, which means that the integration is achieved over a $(n_{\mathrm{aug}} - 1)$-dimensional domain where $n_{\mathrm{aug}} = n_{\boldsymbol{\theta}} + d$. Using formulas given in Table 6.1 and the linearity of expectation, one obtains the following two sensitivities:

$$\frac{\partial \widetilde{P}_{\mathrm{f}}(\boldsymbol{\xi})}{\partial a} = \frac{1}{b-a} \left(\mathbb{E}_{f_{\mathbf{Z}|\boldsymbol{\xi}}} \left[\mathbb{1}_{\mathcal{F}_{\mathbf{z}}}(\mathbf{Z}) \right] - \mathbb{E}_{f_{\mathbf{Z}|\Theta_j=a,\boldsymbol{\xi}}} \left[\mathbb{1}_{\mathcal{F}_{\mathbf{z}}}(\mathbf{Z}^{-j}) \mid \Theta_j = a \right] \right) \tag{6.13a}$$

$$= \frac{1}{b-a} \left(\widetilde{P}_{\mathrm{f}}(\boldsymbol{\xi}) - P^a_{\mathrm{f,aux}} \right); \tag{6.13b}$$

$$\frac{\partial \widetilde{P}_{\mathrm{f}}(\boldsymbol{\xi})}{\partial b} = -\frac{1}{b-a} \left(\mathbb{E}_{f_{\mathbf{Z}|\boldsymbol{\xi}}} \left[\mathbb{1}_{\mathcal{F}_{\mathbf{z}}}(\mathbf{Z}) \right] - \mathbb{E}_{f_{\mathbf{Z}|\Theta_j=b,\boldsymbol{\xi}}} \left[\mathbb{1}_{\mathcal{F}_{\mathbf{z}}}(\mathbf{Z}^{-j}) \mid \Theta_j = b \right] \right) \tag{6.13c}$$

$$= \frac{1}{b-a} \left(P^b_{\mathrm{f,aux}} - \widetilde{P}_{\mathrm{f}}(\boldsymbol{\xi}) \right). \tag{6.13d}$$

where $P^a_{\mathrm{f,aux}}$ and $P^b_{\mathrm{f,aux}}$ are two "auxiliary" failure probabilities which have to be estimated. These derivations are consistent with those provided in Millwater and Feng (2011) and Lee et al. (2011) in the context of ROSA under single-level uncertainty (i.e., deterministic distribution parameters and traditional failure probability as a QoI). As for the interpretation, the sensitivity estimators obtained in Eqs. (6.13b) and (6.13d) are close to those derived in Millwater and Feng (2011) and similarly involve flux integrals, here $P^a_{\mathrm{f,aux}}$ and $P^b_{\mathrm{f,aux}}$, over a $(n_{\mathrm{aug}} - 1)$-dimensional space. As a further remark, one should highlight the fact that for uniform prior distributions, one can calculate the sensitivities of the predictive failure probability w.r.t. the moments $\mu_{\Theta_j} = \frac{a+b}{2}$ or $\sigma_{\Theta_j} = \frac{b-a}{\sqrt{12}}$ by combining the previous sensitivities w.r.t. the bounds such that:

$$\frac{\partial \widetilde{P}_{\mathrm{f}}(\boldsymbol{\xi})}{\partial \mu_{\Theta_j}} = \frac{\partial \widetilde{P}_{\mathrm{f}}(\boldsymbol{\xi})}{\partial a} \frac{\partial a(\mu_{\Theta_j})}{\partial \mu_{\Theta_j}} + \frac{\partial \widetilde{P}_{\mathrm{f}}(\boldsymbol{\xi})}{\partial b} \frac{\partial b(\mu_{\Theta_j})}{\partial \mu_{\Theta_j}} = 2 \left(\frac{\partial \widetilde{P}_{\mathrm{f}}(\boldsymbol{\xi})}{\partial a} + \frac{\partial \widetilde{P}_{\mathrm{f}}(\boldsymbol{\xi})}{\partial b} \right); \tag{6.14a}$$

$$\frac{\partial \widetilde{P}_{\mathrm{f}}(\boldsymbol{\xi})}{\partial \sigma_{\Theta_j}} = \frac{\partial \widetilde{P}_{\mathrm{f}}(\boldsymbol{\xi})}{\partial a} \frac{\partial a(\sigma_{\Theta_j})}{\partial \sigma_{\Theta_j}} + \frac{\partial \widetilde{P}_{\mathrm{f}}(\boldsymbol{\xi})}{\partial b} \frac{\partial b(\sigma_{\Theta_j})}{\partial \sigma_{\Theta_j}} = \sqrt{12} \left(\frac{\partial \widetilde{P}_{\mathrm{f}}(\boldsymbol{\xi})}{\partial b} - \frac{\partial \widetilde{P}_{\mathrm{f}}(\boldsymbol{\xi})}{\partial a} \right). \tag{6.14b}$$

As a final remark, one could notice that for Case #2, the computational cost (i.e., estimating two probabilities) is similar to that required by applying a finite difference method (FDM). However, using FDM can be difficult for several reasons: firstly, FDM is an approximation method

to compute the gradient; secondly, the type of finite difference scheme (forward, backward or centered) may influence the results; thirdly, choosing an optimal perturbation step can be problematic. The proposed method allows to overcome these difficulties by providing (assuming the SF is available for the prior distribution) an exact formulation to get the gradient of the predictive failure probability and estimate it independently of any choice for the perturbation step.

Up to now, the previous framework allows to estimate jointly, within the same sampling phase and with limited extra computational effort, a predictive failure probability and its derivatives w.r.t. a priori deterministic hyper-parameters. However, even with the ARA strategy, ARA/CMC is not able to handle rare event probability estimation regarding real engineering system safety assessment. The idea of the next subsection is to propose a dedicated numerical methodology combining efficient sampling strategy in the augmented space and the above sensitivity estimators.

6.2.3 Proposed methodology (ARA/AIS) for local ROSA under bi-level input uncertainty

Estimating a rare event probability with CMC can be cumbersome and can even become intractable for costly-to-evaluate computer codes. Importance Sampling (IS) is now a well-known variance-reduction technique (see Chapter 3). The idea is to use a so-called "auxiliary density" $h_{\mathbf{Z}}(\cdot)$ to generate samples such that, if this density is the optimal one, one gets a zero variance of the IS estimator of the rare event probability. To introduce it, one can start from the observation that the following equality holds:

$$\int_{\mathcal{D}_{\mathbf{Z}}} \mathbb{1}_{\mathcal{F}_z}(\mathbf{z}) f_{\mathbf{Z}|\xi}(\mathbf{z}|\boldsymbol{\xi}) \mathrm{d}\mathbf{z} = \int_{\mathcal{D}_{\mathbf{Z}}} \mathbb{1}_{\mathcal{F}_z}(\mathbf{z}) \frac{f_{\mathbf{Z}|\xi}(\mathbf{z}|\boldsymbol{\xi})}{h_{\mathbf{Z}}(\mathbf{z})} h_{\mathbf{Z}}(\mathbf{z}) \mathrm{d}\mathbf{z} = \int_{\mathcal{D}_{\mathbf{Z}}} \mathbb{1}_{\mathcal{F}_z}(\mathbf{z}) w(\mathbf{z}) h_{\mathbf{Z}}(\mathbf{z}) \mathrm{d}\mathbf{z} \tag{6.15}$$

where $w(\mathbf{z}) \overset{\text{def}}{=} \frac{f_{\mathbf{Z}|\xi}(\mathbf{z}|\boldsymbol{\xi})}{h_{\mathbf{Z}}(\mathbf{z})}$ is called the *likelihood ratio* (Rubinstein and Kroese, 2008). This weight is introduced in the probability estimator and takes into account the change in the sampling PDF. Thus, considering $\{\mathbf{Z}^{(i)}\}_{i=1}^{N} \overset{\text{i.i.d.}}{\sim} h_{\mathbf{Z}}$ of N i.i.d. copies of the augmented vector $\mathbf{Z}$, the IS estimators for both the probability and its sensitivities can be derived such that:

$$\widetilde{P}_{\mathrm{f}}(\boldsymbol{\xi}) \underset{\text{IS}}{\approx} \frac{1}{N} \sum_{i=1}^{N} \mathbb{1}_{\mathcal{F}_z}(\mathbf{Z}^{(i)})\ w(\mathbf{Z}^{(i)}) \tag{6.16a}$$

$$\frac{\partial \widetilde{P}_{\mathrm{f}}(\boldsymbol{\xi})}{\partial \xi_j} \underset{\text{IS}}{\approx} \frac{1}{N} \sum_{i=1}^{N} \mathbb{1}_{\mathcal{F}_z}(\mathbf{Z}^{(i)})\ w(\mathbf{Z}^{(i)})\ \kappa_j(\boldsymbol{\Theta}^{(i)}, \boldsymbol{\xi}). \tag{6.16b}$$

The estimator $\widehat{\widetilde{P}}_{\mathrm{f}}$ of $\widetilde{P}_{\mathrm{f}}$ given in the right hand side in Eq. (6.16a) is unbiased (i.e., one can show that $\mathbb{E}_{h_{\mathbf{Z}}}\left[\widehat{\widetilde{P}}_{\mathrm{f}}\right] = \widetilde{P}_{\mathrm{f}}$) and its variance $\mathrm{Var}\left[\widehat{\widetilde{P}}_{\mathrm{f}}\right]$ reduces to zero as the density $h_{\mathbf{Z}}(\cdot)$ equals the optimal auxiliary density $h^*_{\mathbf{Z}}(\cdot)$ given by:

$$h^*_{\mathbf{Z}}(\mathbf{z}) = \frac{\mathbb{1}_{\mathcal{F}_z}(\mathbf{z}) f_{\mathbf{Z}|\xi}(\mathbf{z}|\boldsymbol{\xi})}{\widetilde{P}_{\mathrm{f}}}. \tag{6.17}$$

Since this quantity depends on the predictive probability $\widetilde{P}_{\mathrm{f}}$ to estimate, this intricate problem can be solved by using *Adaptive Importance Sampling* (AIS) techniques (Tokdar and Kass, 2009). These techniques aim at, using different adaptive strategies, sequentially approximating the optimal auxiliary density.

In this chapter, it is proposed to adapt two existing AIS techniques (see Chapter 3), namely the *Nonparametric Adaptive Importance Sampling* (NAIS) and the *Adaptive Importance Sampling by*

Cross-Entropy (AIS-CE) to the ARA framework. The idea is to estimate both the predictive failure probability and its sensitivities w.r.t. deterministic hyper-parameters at a reduced cost compared to CMC. Thus, one presents in this chapter two different techniques which are called respectively "ARA/NAIS" and "ARA/AIS-CE". Two generic algorithms are given in Algorithm 5 (for ARA/NAIS) and Algorithm 6 (for ARA/AIS-CE). A complete description of these algorithms is provided in Appendix D. However, one should insist on the fact that these two rare event estimation algorithms rely on some assumptions and dedicated parameters (e.g., the choice of a given kernel $K(\cdot)$ for ARA/NAIS, the choice of an initial parametric family for the auxiliary PDF $h_{\boldsymbol{\lambda}}(\cdot)$ with $\boldsymbol{\lambda} \in \boldsymbol{\Lambda}$ for ARA/AIS-CE, the choice of the α-quantiles for both techniques) whose tuning and performance optimization are not treated in the core discussion of the present chapter (the interested reader may refer to Morio and Balesdent (2015) for more information about it). Note that the algorithms' parameters used in this chapter are given as footnotes of both algorithms (see Algorithms 5 and 6).

Algorithm 5 – Generic algorithm for **ARA/AIS**
(with an **ARA/NAIS** plug-in box in this example).

Start
Define: PDF $f_{\mathbf{Z}|\boldsymbol{\xi}}$, budget N, model $\mathcal{M}(\cdot)$, threshold $\mathrm{y_{th}}$,
quantile $\alpha \in [0,1]$ [a], kernel $K(\cdot)$ [b]
Set: $k = 1$ and $h_0 = f_{\mathbf{Z}|\boldsymbol{\xi}}$
Generate: i.i.d. samples $\mathbf{z}_1^{(i)}$ of $\{\mathbf{Z}_1^{(i)}\}_{i=1}^N \sim h_0$
Evaluate: $Y_1^{(1)} = \mathcal{M}(\mathbf{Z}_1^{(1)}), \ldots, Y_1^{(N)} = \mathcal{M}(\mathbf{Z}_1^{(N)})$
Compute: empirical α-quantile γ_1 of the samples $\{Y_1^{(i)}\}_{i=1}^N$
While $\gamma_k < \mathrm{y_{th}}$ **do**

Estimate: $l_k = \frac{1}{kN} \sum_{j=1}^{k} \sum_{i=1}^{N} \mathbb{1}_{\{\mathcal{M}(\mathbf{z}_j^{(i)}) \geq \gamma_k\}}(\mathbf{Z}_j^{(i)}) \frac{f_{\mathbf{Z}|\boldsymbol{\xi}}(\mathbf{Z}_j^{(i)})}{h_{j-1}(\mathbf{Z}_j^{(i)})}$

and set $w_j(\mathbf{Z}_j^{(i)}) = \mathbb{1}_{\{\mathcal{M}(\mathbf{z}_j^{(i)}) \geq \gamma_k\}}(\mathbf{Z}_j^{(i)}) \frac{f_{\mathbf{Z}|\boldsymbol{\xi}}(\mathbf{Z}_j^{(i)})}{h_{j-1}(\mathbf{Z}_j^{(i)})}$

Update [c]:
$h_{k+1}(\mathbf{z}) = \frac{1}{kNl_k \det(\mathbf{H}_k^{1/2})} \sum_{j=1}^{k} \sum_{i=1}^{N} w_j(\mathbf{Z}_j^{(i)}) K\left(\mathbf{H}_k^{-1/2}(\mathbf{z} - \mathbf{Z}_j^{(i)})\right)$

Set: $k = k + 1$
Generate: i.i.d. samples $\mathbf{z}_k^{(i)}$ of $\{\mathbf{Z}_k^{(i)}\}_{i=1}^N \sim h_k$
Evaluate: $Y_k^{(1)} = \mathcal{M}(\mathbf{Z}_k^{(1)}), \ldots, Y_k^{(N)} = \mathcal{M}(\mathbf{Z}_k^{(N)})$
Compute:
empirical α-quantile γ_k of the samples $\{Y_k^{(i)}\}_{i=1}^N$

Estimate:
$\widehat{\widetilde{P}}_{\mathrm{f}} = \frac{1}{N} \sum_{i=1}^{N} \mathbb{1}_{\{\mathcal{M}(\mathbf{z}_k^{(i)}) > \mathrm{y_{th}}\}}(\mathbf{Z}_k^{(i)}) \frac{f_{\mathbf{Z}|\boldsymbol{\xi}}(\mathbf{Z}_k^{(i)})}{h_k(\mathbf{Z}_k^{(i)})}$

$\widehat{\partial \widetilde{P}_{\mathrm{f}} / \partial \xi_j} = \frac{1}{N} \sum_{i=1}^{N} \mathbb{1}_{\{\mathcal{M}(\mathbf{z}_k^{(i)}) > \mathrm{y_{th}}\}}(\mathbf{Z}_k^{(i)}) \frac{f_{\mathbf{Z}|\boldsymbol{\xi}}(\mathbf{Z}_k^{(i)})}{h_k(\mathbf{Z}_k^{(i)})} \kappa_j(\boldsymbol{\Theta}_k^{(i)}, \boldsymbol{\xi})$

End

[a] **In this chapter:** $\alpha = 0.9$.
[b] **In this chapter: the Gaussian kernel is used**.
[c] $\mathbf{H}_k$ is a symmetric positive definite bandwidth matrix optimized with the asymptotic integrated square error (AMISE) criterion, see Morio and Balesdent (2015).

Algorithm 6 – Generic **ARA/AIS-CE** plug-in box.

Define: ..., parametric family of PDFs $h_\lambda(\cdot)$ with $\boldsymbol{\lambda} \in \boldsymbol{\Lambda}$ [a]
...
Set: $k = 1$
Generate: i.i.d. samples $\mathbf{z}^{(i)}$ of $\{\mathbf{Z}^{(i)}\}_{i=1}^N \sim h_{\lambda_0}$
...
While $\gamma_k < y_{th}$ **do**

Optimize [b]: the parameters of the auxiliary PDF family

$$\lambda_k = \arg\max_{\lambda \in \Lambda} \left\{ \frac{1}{N} \sum_{i=1}^N \left[\mathbb{1}_{\{\mathcal{M}(\mathbf{z}_j^{(i)}) \geq \gamma_k\}}(\mathbf{Z}_j^{(i)}) \frac{f_{\mathbf{Z}|\xi}(\mathbf{Z}^{(i)})}{h_{\lambda_{k-1}}(\mathbf{Z}^{(i)})} \ln[h_\lambda(\mathbf{Z}^{(i)})] \right] \right\}$$

Set: $k = k + 1$
Generate: i.i.d. samples $\mathbf{z}^{(i)}$ of $\{\mathbf{Z}^{(i)}\}_{i=1}^N \sim h_{\lambda_{k-1}}$
Evaluate: $Y^{(1)} = \mathcal{M}(\mathbf{Z}^{(1)}), \ldots, Y^{(N)} = \mathcal{M}(\mathbf{Z}^{(N)})$
Compute:
empirical α-quantile γ_k of the samples $\{Y^{(i)}\}_{i=1}^N$

...

[a] **In this chapter: the Gaussian parametric family is used**.
[b] For specific density families (e.g., Gaussian), the PDF optimal parameters have analytical formulas, see Morio and Balesdent (2015). **In this chapter: both mean and standard deviation are optimized.**

The proposed methodology is able to handle both Case #1 and Case #2 as detailed in Subsections 6.2.1 and 6.2.2. However, in Case #2, estimating the predictive failure probability is not enough to get the sensitivities w.r.t. bounds. An estimation of the auxiliary failure probability, as shown in Eqs. (6.13b) and (6.13d) for the uniform case, is required. To do so, one needs to apply a second time the ARA/AIS algorithm (with either NAIS or AIS-CE as the core algorithm) to estimate this quantity and allow an accurate estimation of the sensitivity.

As an illustration of the ARA/AIS sampling strategy, one can consider a simple test case involving two basic random variables, similar to a so-called "Resistance – Demand" problem (similar to that presented further in the numerical applications in Subsection 6.3.1). Assuming these variables are Gaussian, one can imagine that, due to limited data, their distribution parameters are affected by epistemic uncertainty: for instance, the standard deviation of the resistance variable and the mean value of the demand one are not perfectly known. Some prior distributions are considered to model the a priori knowledge about these parameters. The propagation of this bi-level uncertainty (to get an estimate of the predictive failure probability and its sensitivities) using the ARA/AIS strategy is presented only with the ARA/NAIS method in Figure 6.1 for the sake of conciseness.

In Figure 6.1a, one can see two sets of $N = 10^3$ realizations in the $\mathbf{x}$-space of the vector $\boldsymbol{\Theta} = (\Theta_1, \Theta_2)^\top$. The first set of samples corresponds to the first iteration of the ARA/NAIS algorithm. The second set corresponds to the final iteration of the algorithm. By comparing them, one can notice the modification between the initial sampling density and the final one. Such a modification is also noticeable in Figure 6.1b which represents the same samples in the $\mathbf{u}$-space. One can see the shrinkage of the initial standard normal density to the optimal one. Based on these samples, one can observe the corresponding realizations of the basic variables gathered in $\mathbf{X}$. Figure 6.1c and Figure 6.1d show the corresponding samples plotted respectively in the $\mathbf{x}$- and in $\mathbf{u}$-spaces. Again, from the first iteration to the final one, the convergence of the density towards the optimal one is noticeable. One can also highlight that considering a second

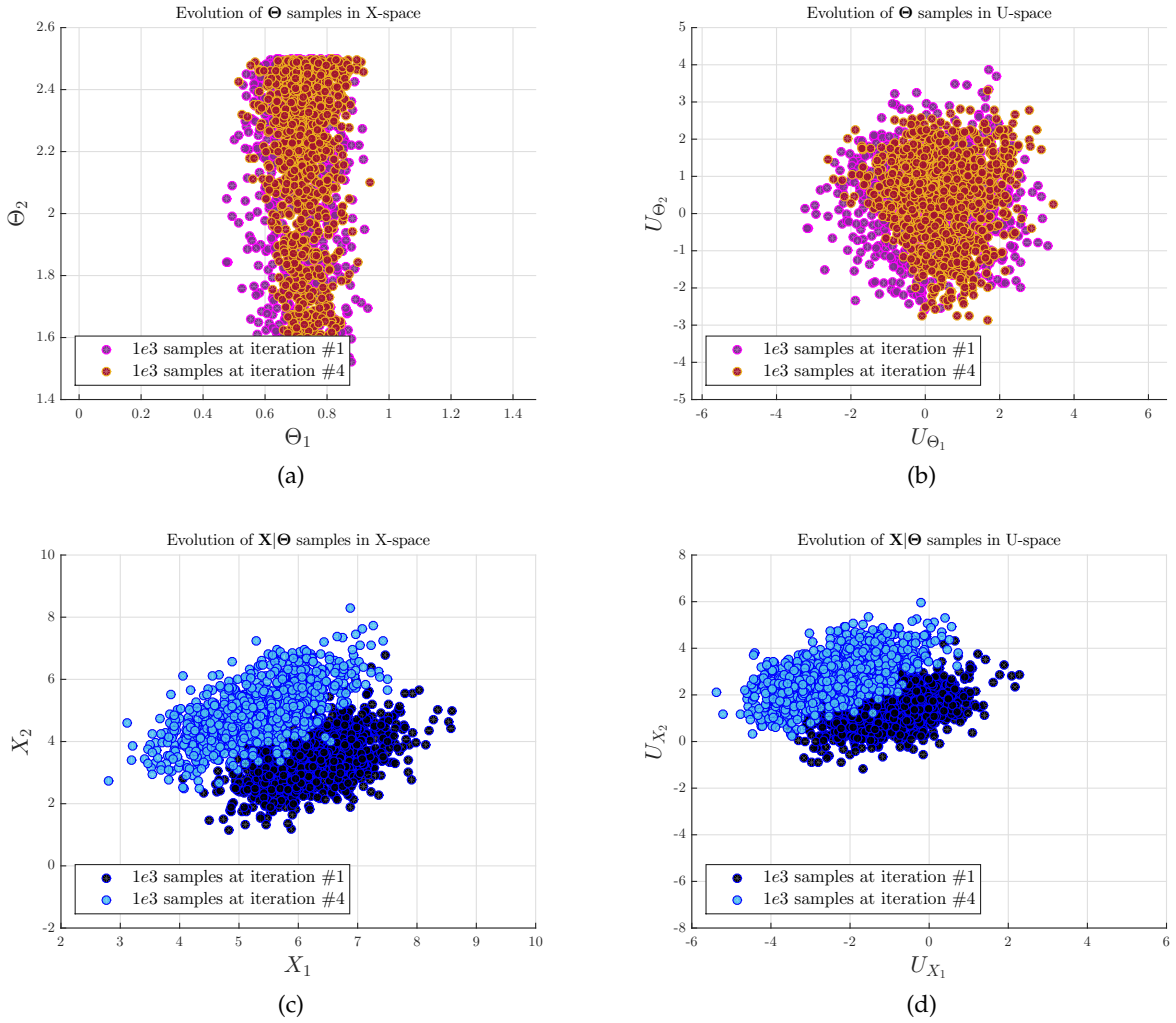

FIGURE 6.1: Illustration of the ARA/NAIS method on a Resistance – Demand test-case (similar to that described in Example #1 (cf. 6.3.1)). In this example, two different sets of samples, drawn at iterations #1 and #4 of the ARA/NAIS method (Algorithm 5) are presented. One can see the evolution of the samples showing the adaptive evolution of the augmented sampling density towards a near optimal one.

level of uncertainty does affect the realizations of the basic variables by changing the shape of the distribution of $\mathbf{X}$.

In the following section, the numerical efficiency of the ARA/AIS method is demonstrated on two numerical test-cases representative of various challenges in reliability assessment. A numerical application on a realistic aerospace test-case will be further proposed in Chapter 8.

6.3 Application examples

The following numerical applications have been implemented in Matlab® and performed using a rare event simulation toolbox developed at ONERA – The French Aerospace Lab.

The numerical testing of the methodology developed in this chapter, as summed up in Table 6.2, relies on the following settings:

- firstly, the ARA/AIS method has been implemented and tested on two different test-cases of increasing difficulty (see the first column and the footnotes below Table 6.2 for the specifications of each test-case);
- secondly, reference results for the estimation of the predictive failure probability and its sensitivities are obtained using a CMC with large sample size performed by ARA (see the second column denoted ARA/CMC, see Chapter 5 and Chabridon et al. (2017a) for details about the coupling between ARA and sampling techniques);
- thirdly, as shown in the third column of Table 6.2, the two different techniques, namely ARA/AIS-CE and ARA/NAIS are applied on the two test-cases for the sake of comparison, but also to illustrate the modular aspect of the methodology (the black squares ■ stand for the performed calculations). Finally, after validation of the method, the impact of the increasing rareness of the failure event (regarding a limited simulation budget available) is studied as an extension of the last two test-cases (see the four black stars ★). This last extension is called "rare event context" in the rest of the chapter. One should notice that, for these specific cases, the reference calculation by ARA/CMC is considered as computationally "intractable" (see the corresponding crosses ×).

TABLE 6.2: Overall strategy for the numerical tests of the proposed methodology.

Test-case		**Reference**	**ARA/AIS**	
		ARA/CMC	ARA/AIS-CE	ARA/NAIS
Ex. #1: Resistance – Demand [a]	(cf. 6.3.1)	■	■	■
Ex. #2: Nonlinear oscillator [b]	(cf. 6.3.2)	■ ×	■ ★	■ ★

[a] 2 basic variables, 2 uncertain parameters (1 unbounded & 1 bounded), $g(\cdot)$ linear.
[b] 8 basic variables, 2 uncertain parameters (1 unbounded & 1 bounded), $g(\cdot)$ nonlinear.

Finally, for a comparison in terms of numerical efficiency of the method w.r.t. CMC estimation, the following standard coefficient $\nu^{\mathrm{ARA/AIS}}$ is used:

$$\nu^{\mathrm{ARA/AIS}} = \frac{N_{\mathrm{sim}}^{\mathrm{ARA/CMC}}}{N_{\mathrm{sim}}^{\mathrm{ARA/AIS}}} \tag{6.18}$$

where $N_{\mathrm{sim}}^{\mathrm{ARA/CMC}}$ is the required number of CMC samples to reach the same coefficient of variation δ on the probability estimate for both techniques. A value of $\nu^{\mathrm{ARA/AIS}} > 1$ indicates that the method ARA/AIS is more efficient than CMC for the given test-case. In other words, $\nu^{\mathrm{ARA/AIS}}$ indicates the quantity by which one can divide the initial CMC simulation budget for a same level of accuracy.

6.3.1 Example #1: a resistance-demand toy-case

Description. The goal of this first academic test-case is to validate the method regarding the estimation accuracy of both the predictive failure probability and its sensitivities w.r.t. its hyperparameters. Table 6.3 gives the input data. The LSF $g(\mathbf{X}) = R - S = X_1 - X_2$ is linear and involves two independent Gaussian random variables. One assumes that both the standard deviation of the first variable and the mean of the second one are affected by epistemic uncertainty. Thus, two prior distributions (one unbounded and one bounded) are assumed for the uncertain parameters (e.g., based either on limited data, literature-based information or expert opinion). As a remark, one could argue that the choice of a normal prior for Θ_1 may be inappropriate regarding physical constraints and informativeness. In this chapter, common priors (i.e., normal

and uniform) are set for the sake of illustration to characterize epistemic uncertainty and for an easy sampling, without loss of generality. For a pure Bayesian approach (involving possible updating), the reader should refer to Gelman et al. (2006), Hamada et al. (2008), and Straub and Papaioannou (2015).

TABLE 6.3: Input probabilistic model for Example #1.

Variable	Distribution	Parameter #1	Parameter #2
$X_1 = R$	Normal	$\mu_{X_1} = 7$	σ_{X_1} ***uncertain***
$X_2 = S$	Normal	μ_{X_2} ***uncertain*** [a]	$\sigma_{X_2} = 1$
$\Theta_1 = \sigma_{X_1}$	Normal	$\xi_1 = \mu_{\sigma_{X_1}} = 0.7$	$\xi_2 = \sigma_{\sigma_{X_1}} = 0.07$
$\Theta_2 = \mu_{X_2}$	Uniform	$\xi_3 = a_{\mu_{X_2}} = 1.5$	$\xi_4 = b_{\mu_{X_2}} = 2.5$

[a] For fixed values $\sigma_{X_1} = 0.7$ and $\mu_{X_2} = 2$, $p_{\mathrm{f,ref}} = 2.50 \times 10^{-5}$.

TABLE 6.4: Results for Example #1.

	ARA/CMC ($N_{\mathrm{x},\boldsymbol{\theta}} = 10^8$ samples)		**ARA/AIS-CE** ($N_{\mathrm{x},\boldsymbol{\theta}} = 10^4$ samples/step)		**ARA/NAIS** ($N_{\mathrm{x},\boldsymbol{\theta}} = 10^4$ samples/step)	
	Estimate	cv	Estimate	cv	Estimate	cv
$\widehat{\widetilde{P}}_{\mathrm{f}}$	3.72×10^{-5}	(1.60 %)	3.73×10^{-5}	(4.39 %)	3.71×10^{-5}	(3.62 %)
$\widehat{\partial \widetilde{P}_{\mathrm{f}}/\partial \xi_1}$	2.77×10^{-4}	(3.50 %)	2.81×10^{-4}	(14.2 %)	2.75×10^{-4}	(13.7 %)
$\widehat{\partial \widetilde{P}_{\mathrm{f}}/\partial \xi_2}$	1.37×10^{-4}	(10.8 %)	1.45×10^{-4}	(62.9 %)	1.35×10^{-4}	(59.1 %)
$\widehat{\partial \widetilde{P}_{\mathrm{f}}/\partial \xi_3}$	3.30×10^{-5}	(1.91 %)	3.32×10^{-5}	(4.91 %)	3.30×10^{-5}	(4.06 %)
$\widehat{\partial \widetilde{P}_{\mathrm{f}}/\partial \xi_4}$	8.91×10^{-5}	(1.41 %)	8.87×10^{-5}	(5.99 %)	8.89×10^{-5}	(4.74 %)
$\widehat{\partial \widetilde{P}_{\mathrm{f}}/\partial \mu_{\Theta_2}}$ [a]	2.44×10^{-4}	–	2.44×10^{-4}	–	2.44×10^{-4}	–
$\widehat{\partial \widetilde{P}_{\mathrm{f}}/\partial \sigma_{\Theta_2}}$	1.94×10^{-4}	–	1.92×10^{-4}	–	1.94×10^{-4}	–
$\nu^{\mathrm{ARA/AIS}}$	–	–	103	–	158	–

[a] Cf. Eqs. (6.14a) and (6.14b) for the uniform case.

Results. Table 6.4 gathers the numerical values obtained for the probability estimates, sensitivities and efficiencies. For comparison purpose, a CMC with $N_{\mathrm{x},\boldsymbol{\theta}} = 10^8$ samples is performed. The coefficient of variation (cv) for any estimate is calculated using a hundred replicates of each algorithm. However, for the sake of conciseness, only the results associated to the highest numerical efficiency $\nu^{\mathrm{ARA/AIS}}$ are presented in Table 6.4 for the two proposed techniques (here, $N_{\mathrm{x},\boldsymbol{\theta}} = 10^4$ samples/step). As a remark, one can see that both the predictive failure probability and its sensitivities are well estimated with both techniques compared to ARA/CMC. Concerning the estimation of the predictive failure probability, one can see that $\widehat{\widetilde{P}}_{\mathrm{f}} = 3.72 \times 10^{-5}$ which shows that taking a second uncertainty level into account implies a slight increase compared to the failure probability under single-level uncertainty $p_{\mathrm{f}} = 2.50 \times 10^{-5}$ (see below Table 6.3). From these results, one can notice that the sensitivities w.r.t. bounds (i.e., $\widehat{\partial \widetilde{P}_{\mathrm{f}}/\partial \xi_3}$ and $\widehat{\partial \widetilde{P}_{\mathrm{f}}/\partial \xi_4}$) show a reduced coefficient of variation compared to those for the unbounded distribution (i.e., $\widehat{\partial \widetilde{P}_{\mathrm{f}}/\partial \xi_1}$ and $\widehat{\partial \widetilde{P}_{\mathrm{f}}/\partial \xi_2}$). This could be due to the fact that they are estimated as a difference of two probabilites estimated both by the method which lead to a reduced variance. In terms of comparison, since the problem involves two uncertain distribution parameters (Θ_1 unbounded and Θ_2 bounded), one can use Eqs. (6.14a) and (6.14b) to get sensitivities w.r.t. moments of Θ_2 instead of its bounds. Finally, in this case, the predictive failure probability seems to

be slightly more sensitivive to the a priori choice of the mean values of both distribution parameters than to the choice of the standard deviations. As for the $\nu^{\mathrm{ARA/AIS}}$ coefficients, they are very high compared unity for both techniques. This implies that, for the same level of accuracy, one can reduce the CMC simulation budget by 103 times if one uses ARA/AIS-CE and by 158 times if one uses ARA/NAIS. This gain can be of practical importance for applications involving rare event probabilities.

6.3.2 Example #2: a two d.o.f. primary/secondary damped oscillator

Description. This nonlinear oscillator is the same two-degree-of-freedom primary-secondary system, as presented in Chapter 5, in Subsection 5.4.3, excited by a white noise base acceleration (Der Kiureghian and De Stefano, 1991). Thus, one just recalls the LSF of the system:

$$g(\mathbf{X}) = F_s - 3k_s \sqrt{\frac{\pi S_0}{4\zeta_s\omega_s^3}\left[\frac{\zeta_a\zeta_s}{\zeta_p\zeta_s\left(4\zeta_a^2+r^2\right)+\gamma\zeta_a^2}\frac{\left(\zeta_p\omega_p^3+\zeta_s\omega_s^3\right)\omega_p}{4\zeta\omega_a^4}\right]} = F_s - F_{\mathrm{acc}}. \tag{6.19}$$

Table 6.5 gives the input data (the set of parameters here for the basic variables are mean values and coefficients of variation). The LSF $g(\cdot)$ is highly nonlinear and involves eight independent lognormal random variables. Moreover, one assumes that the mean of the second mass is not precisely known due to measure uncertainty and that the mean of the secondary spring force capacity is also affected by epistemic uncertainty. Thus, two prior distributions (Gaussian and uniform) are assumed for the uncertain parameters based on expert judgment.

TABLE 6.5: Input probabilistic model for Example #2.

Variable [a]	**Distribution**	**Parameter #1**	**Parameter #2**
$X_1 = m_p$ (kg)	Lognormal	$\mu_{X_1} = 1.5$	$\delta_{X_1} = 10\%$
$X_2 = m_s$ (kg)	Lognormal	μ_{X_2} ***uncertain*** [b]	$\delta_{X_2} = 10\%$
$X_3 = k_p$ (N.m^{-1})	Lognormal	$\mu_{X_3} = 1$	$\delta_{X_3} = 20\%$
$X_4 = k_s$ (N.m^{-1})	Lognormal	$\mu_{X_4} = 0.01$	$\delta_{X_4} = 20\%$
$X_5 = \zeta_p$ (1)	Lognormal	$\mu_{X_5} = 0.05$	$\delta_{X_5} = 40\%$
$X_6 = \zeta_s$ (1)	Lognormal	$\mu_{X_6} = 0.02$	$\delta_{X_6} = 50\%$
$X_7 = F_s$ (N)	Lognormal	μ_{X_7} ***uncertain***	$\delta_{X_7} = 10\%$
$X_8 = S_0$ (m.s^{-2})	Lognormal	$\mu_{X_8} = 100$	$\delta_{X_8} = 10\%$
$\Theta_1 = \mu_{X_7}$ (N)	Normal	$\xi_1 = \mu_{\mu_{X_7}} = 21.5$ / 27.5 (★) [c]	$\xi_2 = \sigma_{\mu_{X_7}} = 2.15$ / 2.75 (★)
$\Theta_2 = \mu_{X_2}$ (kg)	Uniform	$\xi_3 = a_{\mu_{X_2}} = 0.008$	$\xi_4 = b_{\mu_{X_2}} = 0.012$

[a] The basic variables are independent.
[b] For fixed values $\mu_{X_2} = 0.01$ and $\mu_{X_7} = 21.5$ / 27.5, $p_{\mathrm{f,ref}} = 4.78 \times 10^{-5}$ / 3.78×10^{-7}.
[c] The second value is for the rare event case, cf. Table 5.1.

Results. Numerical results summarized in Table 6.6 show that, for a moderately rare failure event, both ARA/AIS-CE and ARA/NAIS give accurate results in the predictive failure probability estimation compared to ARA/CMC. Again, the coefficient of variation (cv) for any estimate is calculated using a hundred replicates of each algorithm. It first reveals the variations between the failure probability under single-level uncertainty p_{f} and the predictive one $\widetilde{P}_{\mathrm{f}}$ (here, it increases from 4.78×10^{-5} to 2.35×10^{-4}) due to the bi-level uncertainty. In this case, considering uncertainty on a distribution parameter makes the system less safe, which can be an important indicator for design or re-design purposes. Concerning sensitivities, most of them are correctly estimated, except for $\widehat{\partial \widetilde{P}_{\mathrm{f}}/\partial \xi_2}$ for which one can observe a slight relative bias between

the proposed techniques and reference results. In terms of comparison, once again, since the problem involves two uncertain distribution parameters (Θ_1 unbounded and Θ_2 bounded), one can use Eqs. (6.14a) and (6.14b) to get sensitivities w.r.t. moments of Θ_2 instead of its bounds. Finally, in this case, the predictive failure probability seems to be slightly more sensitivive to the a priori choice modelling the uncertain mean of the secondary mass. Thus, the lack of knowledge about the mean value of the mass plays a key role in terms of system safety. As for the convergence of the results, Figure 6.2a compares the estimated sensitivities (to avoid any redundancy, only the ARA/NAIS plots are presented) to the reference results obtained by ARA/CMC. One can notice the convergence w.r.t. the increasing number of samples per step and a low variability of the two last sensitivities as mentioned previously. Finally, for a moderate rareness of the failure event, the efficiency of the method is promising: $\nu^{\mathrm{ARA/AIS}}$ is equal to 58 for ARA/AIS-CE and 50 for ARA/NAIS, meaning the equivalent ARA/CMC simulation budget can be still divided while ensuring a given target accuracy in the estimation.

In the rare event context (★) (see Table 6.7), reference results are supposed to be intractable. Again, a hundred replicates were used to get samples' statistics. One can first observe a slight increase for the predictive failure probability (around 7×10^{-6}) compared to the failure probability under single-level uncertainty (equals to 3.78×10^{-7} as given below Table 6.5). With the proposed method, one can notice that the estimated values show relatively low coefficient of variation. Comparing sensitivities leads to notice that the rareness of the failure event (i.e., between Table 6.6 and Table 6.7) does not impact the relative order in terms of influence. The moments of Θ_2 are still the most influential hyper-parameters of the predictive failure probability. The method ensures a higher efficiency as the rareness of the probability increases ($\nu^{\mathrm{ARA/AIS}}$ from 792 for ARA/AIS-CE to 830 for ARA/NAIS). Finally, the global convergence is observed on Figure 6.2b (for ARA/NAIS only).

TABLE 6.6: Results for Example #2.

	ARA/CMC		**ARA/AIS-CE**		**ARA/NAIS**	
	($N_{\mathrm{x},\boldsymbol{\theta}} = 10^8$ samples)		($N_{\mathrm{x},\boldsymbol{\theta}} = 10^4$ samples/step)		($N_{\mathrm{x},\boldsymbol{\theta}} = 10^4$ samples/step)	
	Estimate	cv	Estimate	cv	Estimate	cv
$\widehat{\widetilde{P}}_{\mathrm{f}}$	2.35×10^{-4}	(0.603 %)	2.36×10^{-4}	(4.69 %)	2.38×10^{-4}	(4.57 %)
$\widehat{\partial \widetilde{P}_{\mathrm{f}}/\partial \xi_1}$	-1.61×10^{-4}	(0.661 %)	-1.60×10^{-4}	(4.80 %)	-1.61×10^{-4}	(5.32 %)
$\widehat{\partial \widetilde{P}_{\mathrm{f}}/\partial \xi_2}$	9.04×10^{-3}	(0.602 %)	1.08×10^{-2}	(4.69 %)	1.09×10^{-2}	(4.57 %)
$\widehat{\partial \widetilde{P}_{\mathrm{f}}/\partial \xi_3}$	5.57×10^{-2}	(0.650 %)	5.58×10^{-2}	(4.89 %)	5.63×10^{-2}	(4.81 %)
$\widehat{\partial \widetilde{P}_{\mathrm{f}}/\partial \xi_4}$	1.36×10^{-1}	(0.525 %)	1.35×10^{-1}	(6.45 %)	1.34×10^{-1}	(6.22 %)
$\widehat{\partial \widetilde{P}_{\mathrm{f}}/\partial \mu_{\Theta_2}}$ [a]	3.82×10^{-1}	–	3.82×10^{-1}	–	3.82×10^{-1}	–
$\widehat{\partial \widetilde{P}_{\mathrm{f}}/\partial \sigma_{\Theta_2}}$	2.77×10^{-1}	–	2.75×10^{-1}	–	2.71×10^{-1}	–
$\nu^{\mathrm{ARA/AIS}}$	–	–	58	–	50	–

[a] Cf. Eqs. (6.14a) and (6.14b) for the uniform case.

TABLE 6.7: Results for Example #2 considering the influence of the failure event rareness.

	ARA/AIS-CE (★) ($N_{\mathrm{x},\boldsymbol{\theta}} = 10^4$ samples/step)		**ARA/NAIS (★)** ($N_{\mathrm{x},\boldsymbol{\theta}} = 10^4$ samples/step)	
	Estimate	cv	Estimate	cv
$\widehat{\widetilde{P}}_{\mathrm{f}}$	6.71×10^{-6}	(6.25 %)	6.82×10^{-6}	(5.97 %)
$\widehat{\partial \widetilde{P}_{\mathrm{f}}/\partial \xi_1}$	-4.95×10^{-6}	(6.58 %)	-4.98×10^{-6}	(5.56 %)
$\widehat{\partial \widetilde{P}_{\mathrm{f}}/\partial \xi_2}$	2.41×10^{-4}	(6.25 %)	2.45×10^{-4}	(5.97 %)
$\widehat{\partial \widetilde{P}_{\mathrm{f}}/\partial \xi_3}$	1.62×10^{-3}	(6.51 %)	1.65×10^{-3}	(6.14 %)
$\widehat{\partial \widetilde{P}_{\mathrm{f}}/\partial \xi_4}$	4.63×10^{-3}	(6.74 %)	4.59×10^{-3}	(9.01 %)
$\widehat{\partial \widetilde{P}_{\mathrm{f}}/\partial \mu_{\Theta_2}}$ [a]	1.25×10^{-2}	–	1.25×10^{-2}	–
$\widehat{\partial \widetilde{P}_{\mathrm{f}}/\partial \sigma_{\Theta_2}}$	1.04×10^{-2}	–	1.02×10^{-2}	–
$\nu^{\mathrm{ARA/AIS}}$	792	–	830	–

[a] Cf. Eqs. (6.14a) and (6.14b) for the uniform case.

6.3.3 Synthesis about numerical results and discussion

Synthesis about numerical results. The aim of this subsection is to give a synthesis about the main advantages and drawbacks of the proposed approach. According to the numerical results, one can sum up the following characteristics:

- ARA/AIS-CE and ARA/NAIS lead to similar results for the predictive failure probability and reliability-oriented sensitivities estimation compared with those of the reference approach, namely ARA/CMC. They both enable to reduce the variance of estimation and limit the number of calls to the black-box model;
- ARA/AIS-CE and ARA/NAIS, coupled to the derived sensitivity estimators, enable to estimate sensitivities w.r.t. distribution parameters appearing in both unbounded and bounded priors.

More generally, the proposed approach is dependent on the intrinsic performances of both AIS-CE and NAIS algorithms. Therefore, for specific cases, ARA/AIS-CE could suffer from the possible multimodality of the optimal auxiliary density (i.e., problem with multiple failure regions), which is a known issue of this method (Kurtz and Song, 2013). As for ARA/NAIS, it is able to handle multimodal densities but its use should be restricted to problems whose input dimensionality (including the stochastic distribution parameters) is around ten while ARA/AIS-CE could handle higher input dimensions.

Efficiency of the proposed methodology. Figure 6.3 summarizes the evolution of the numerical efficiency $\nu^{\mathrm{ARA/AIS}}$ (for both ARA/AIS-CE and ARA/NAIS) regarding the results obtained for the second example (i.e., the nonlinear oscillator). The two configurations, i.e., initial problem (■) and the problem under increased rareness of the failure event (★), are given as a function of the number of samples per step (from 10^3 to 10^4). As a remark, one can notice that the increasing curves as a function of the number of samples only represent the underlying tradeoff of the proposed method between accuracy (i.e., the coefficient of variation on the probability

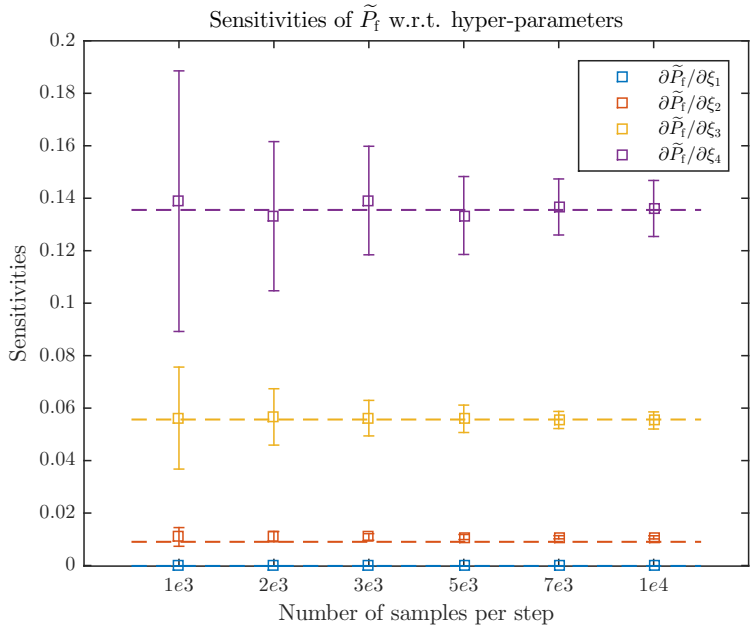

(a) Estimated sensitivities (error bars) vs. reference results obtained by ARA/CMC (dashed lines).

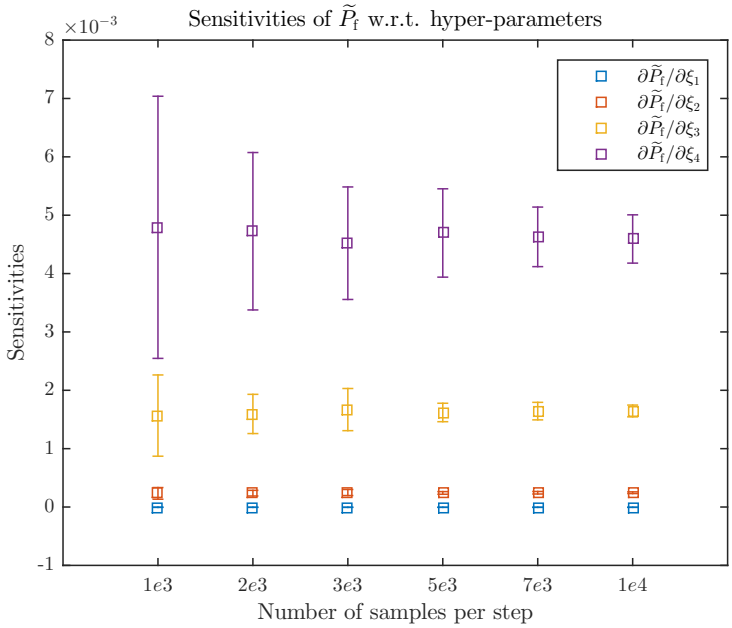

(b) Estimated sensitivities (error bars) in a context of rare event (★).

FIGURE 6.2: Convergence plots obtained by ARA/NAIS for Example #2.

decreasing as the number of samples increases) and the global computational cost. However, one should notice that these results are dependent on the tuning parameters of the underlying algorithms (AIS-CE and NAIS). Typically, the choice of the empirical quantile threshold value may affect the value of the efficiency (e.g., by modifying the value of the coefficient of variation on the probability and the total number of samples).

Interpretation of the estimated sensitivities. In terms of interpretation of the sensitivities derived in this chapter, one should remember that local sensitivities are not quantities that can be

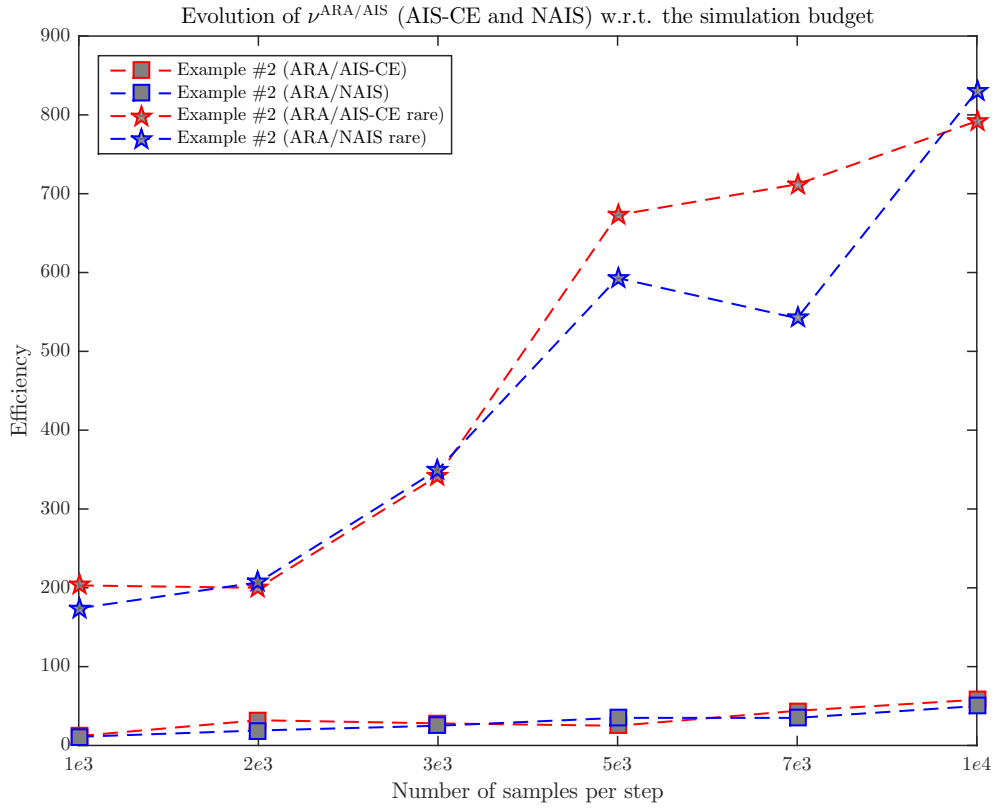

FIGURE 6.3: Efficiency.

easily ranked. Local sensitivities can only give a qualitative result which should be considered as an indication for the user to know whether he/she should get more information about the lack of knowledge affecting one or more distribution parameters. It cannot be used as a variable importance measure for factor fixing purposes (Wei et al., 2015b). However, they can be useful to highlight some features and underlying behaviors associated, either to the input probabilistic modeling, or to the model behavior at failure. To do so, one should compare sensitivities of the same nature, for instance sensitivities to a mean together, sensitivities to a standard deviation together, sensitivities to bounds together. Another possible solution is to build what is called an *elasticity* which is a normalized sensitivity (Lemaire et al., 2009). In reliability literature, several authors advocated different types of elasticities. For instance, Table 6.8 gathers three different formulas and the corresponding literature sources for computing elasticities (adapted here to the bi-level uncertainty framework). From the authors knowledge, there is no consensus about the elasticity formulation. For the sake of generality, the sensitivity indicator provided in this chapter do not take into account any normalization factor. All the derivative-based formulas (and associated numerical results) described in this chapter can be combined with the formulas given in Table 6.8 to obtain elasticities.

TABLE 6.8: Different formulas for elasticities.

	Formula	Hyper-parameters	Source
(f1)	$e_j = \frac{\partial \widetilde{P}_f}{\partial \xi_j} \times \frac{\sigma_{\Theta_j}}{\widetilde{P}_f}$	$\xi_j = \mu_{\Theta_j}$ or $\xi_j = \sigma_{\Theta_j}$	Wu (1994b)
(f2)	$e_j = \frac{\partial \widetilde{P}_f}{\partial \xi_j} \times \sigma_{\Theta_j}$	$\xi_j = \mu_{\Theta_j}$ or $\xi_j = \sigma_{\Theta_j}$	Der Kiureghian (1999)
(f3)	$e_j = \frac{\partial \widetilde{P}_f}{\partial \xi_j} \times \frac{\xi_j}{\widetilde{P}_f}$	$\xi_j = \mu_{\Theta_j}$ or $\xi_j = \sigma_{\Theta_j}$	Lemaire et al. (2009)
(f4)	$e_j = \frac{\partial \widetilde{P}_f}{\partial \xi_j} \times \xi_j$	$\xi_j = \mu_{\Theta_j}$ or $\xi_j = \sigma_{\Theta_j}$	Millwater and Wieland (2010)

It is important to notice that the choice of prior distributions is of utmost importance in practice and can achieved using various techniques (expert judgment, data analysis, experimental results). For the sake of conciseness, in this chapter, the sensitivity estimator formula (and application cases) are explicitely given using only normal and uniform probability distributions as priors. When facing more complex priors (e.g., truncated normal distribution to avoid unrealistic physical data), these formula can be adapted. Finally, for some priors, score functions may not be available (Rahman, 2009; Millwater and Feng, 2011; Lee et al., 2011).

6.4 Conclusion

In this chapter, new local reliability-oriented sensitivity estimators are proposed using the so-called "augmented reliability approach". The proposed derivative-based local sensitivity estimators of predictive failure probability, with respect to deterministic distribution hyper-parameters, are derived for two cases: firstly, when all the stochastic distribution parameters follow some unbounded prior probability distributions; secondly, when at least one distribution parameter follows a bounded prior. Thus, this method allows to get sensitivities with either none (in the unbounded case) or a moderate extra computational effort (in the bounded case). To enhance the efficiency of the method, these estimators are derived using an *adaptive importance sampling* scheme, either using a parametric algorithm (ARA/AIS-CE) or a nonparametric one (ARA/NAIS). Then, two numerical applications of increasing difficulty are considered. The comparison with a reference method (ARA/CMC) demonstrates the convergence and the efficiency of the proposed method. Finally, this study shows the benefits of using an ARA/AIS strategy when the failure event becomes very rare and the LSF is nonlinear.

A first enhancement track could be to study the possibility of enhancing ARA/AIS-CE strategy for reliability and sensitivity assessment under bi-level uncertainty by adapting recent works on AIS-CE (Kurtz and Song, 2013; Wang and Song, 2016) to handle both multiple failure regions and high-dimensionality. In order to further reduce the computational cost of these estimations, another possible enhancement track could be to couple the ARA/AIS strategy to a *metamodel* such as proposed in Dubourg and Sudret (2014) to possibly extend it to the bi-level uncertainty problem. However, metamodels also bring their own contribution to the overall uncertaintiy by adding some "model uncertainty". This type of uncertainty has to be handled and should not cover the uncertainty introduced by considering a prior on the distribution parameters. Some recent metamodel-based strategies also consider a so-called "augmented framework" by considering that the metamodel can handle all kinds of epistemic uncertainties in its own definition (Walter, 2015).

In the next chapter, one considers that the impact of the prior distribution hyper-parameters need to be studied. Then, a more global point of view is adopted by studying the impact of the entire support of the prior distribution over $\boldsymbol{\Theta}$ on the safety measure. Thus, one decides to investigate a particular set of global importance measures adapted to the ROSA context: the

Sobol indices on the indicator function. After a presentation of the main characteristics of these indices, an extension to the bi-level input uncertainty case is proposed, as well as an efficient estimation scheme based on the post-treatment of a reliability analysis phase.

CHAPTER 7

Global ROSA under distribution parameter uncertainty

Contents

7.1 Introduction and motivations

In this chapter, one still considers the same hierarchical structure of input variables as presented in Chapter 5 and Chapter 6. In the previous chapter, the goal was to study the impact of a local choice in terms of the hyper-parameters $\boldsymbol{\xi}$ characterizing the prior distribution $f_{\boldsymbol{\Theta}|\boldsymbol{\xi}}$ (e.g., following experts' judgments) on the predictive failure probability. Such a study is useful to investigate the robustness of the reliability measure regarding some prior choices about the input probabilistic model in the context of lack-of-information. In the present chapter, the idea is to consider that the probabilistic model of the second level is now fixed (i.e., that the hyper-parameters $\boldsymbol{\xi}$ of $f_{\boldsymbol{\Theta}|\boldsymbol{\xi}}$ have been set to a given value regarding the study conducted in Chapter 6). Thus, this second level is now representative of the lack-of-knowledge about the distribution parameters. Then, one would like to study how does this bi-level input uncertainty play a role in terms of system behavior at failure. More precisely, the idea is to provide an index which is as follows:

- it should be adapted to the bi-level input uncertainty;
- it should be an importance measure in the ROSA context such that it allows a ranking of the most influential inputs;
- it should distinguish between both aleatory uncertainty and epistemic uncertainty.
- it should be sufficiently cheap to estimate, especially in the context of rare event probability estimation and/or costly-to-evaluate black-box computer code.

Among the various indices listed in Chapter 4, it appears that the set of Sobol indices on the indicator function (denoted by "$S^{\mathbb{1}_F}$-indices" in the rest of this chapter) present several advantages, both in terms of interpretation and estimation. They correspond to a class of relevant importance measures in the reliability context as already demonstrated in several works (see, e.g., Wei et al., 2012; Lemaître, 2014).

In this chapter, the adaptation of these indices to the bi-level input uncertainty is investigated and a new methodology is proposed to efficiently estimate these global importance measures for ROSA under the constraint of the bi-level input uncertainty. To do so, a disaggregated version of the input augmented vector is proposed before the rare event probability estimation. Then, using an adapted version of the estimators recently proposed in Perrin and Defaux (2019) together with an advanced version of KDE proposed in Perrin et al. (2018), the $S^{\mathbb{1}_F}$-indices are estimated only by post-processing failure samples contained in the elite set obtained at the final step of an advanced sampling-based technique. Due to the disaggregated version of the augmented vector, either the stochastic distribution parameters and the basic variables are given a first and total index. To make it clear, the tools used in this chapter are methodological tools recently proposed in literature. The innovation remains in their adaptation to the bi-level input uncertainty and their intensive use so as to reach both some limits and open some perspectives for these tools.

This chapter is organized as follows. Section 7.2 describes briefly the Sobol indices on the indicator function and presents the set of estimators that will be adapted further. Section 7.3 proposes a disaggregated version of the augmented vector such that both aleatory and epistemic uncertainty can be treated separately in the context of ROSA under a bi-level uncertainty. Then, an extension of the $S^{\mathbb{1}_F}$-indices is proposed to handle the bi-level uncertainty and pick-freeze estimators are provided. Section 7.4 treats the problem of the efficient estimation of these indices and proposes a methodology based on the use of the recent *data-driven tensorized Gaussian* KDE proposed by Perrin et al. (2018). Section 7.5 illustrates the benefits of such a methodology on two test-cases of increasing complexity. Then, a synthesis gathering the key aspects and issues of the proposed approach is provided at the end of this section. A conclusion gathering the most important results of this chapter is finally given in Section 7.6.

7.2 Focus on Sobol indices applied to the indicator function

7.2.1 Basic formulation of the Sobol indices on the indicator function

As a reminder, one can recall that, in Chapter 4, $S^{\mathbb{1}_\mathcal{F}}$-indices have been presented in 4.5.2.2. These indices are variance-based importance measures which differ from traditional Sobol indices on model output as the QoI is the indicator function of the failure domain $\mathbb{1}_{\mathcal{F}_\mathbf{x}}(\cdot)$. As mentioned in 4.5.2.2, they arise from the following equality (Li et al., 2012):

$$\mathbb{E}_{f_{X_i}}[(P_\mathrm{f} - P_{\mathrm{f}|X_i})^2] = \mathrm{Var}\left[\mathbb{E}[\mathbb{1}_{\mathcal{F}_\mathbf{x}}(\mathbf{X})|X_i]\right]. \tag{7.1}$$

Thus, after normalizing by $\mathrm{Var}\left[\mathbb{1}_{\mathcal{F}_\mathbf{x}}(\mathbf{X})\right]$, the basic formulation of the sensitivity indices as introduced by Li et al. (2012) and Lemaître (2014) is given by:

$$S_i^{\mathbb{1}_\mathcal{F}} = \frac{\mathrm{Var}\left[\mathbb{E}[\mathbb{1}_{\mathcal{F}_\mathbf{x}}(\mathbf{X})|X_i]\right]}{\mathrm{Var}\left[\mathbb{1}_{\mathcal{F}_\mathbf{x}}(\mathbf{X})\right]} \tag{7.2}$$

$$S_{T_i}^{\mathbb{1}_\mathcal{F}} = 1 - \frac{\mathrm{Var}\left[\mathbb{E}[\mathbb{1}_{\mathcal{F}_\mathbf{x}}(\mathbf{X})|\mathbf{X}^{-i}]\right]}{\mathrm{Var}\left[\mathbb{1}_{\mathcal{F}_\mathbf{x}}(\mathbf{X})\right]} = \frac{\mathbb{E}\left[\mathrm{Var}\left[\mathbb{1}_{\mathcal{F}_\mathbf{x}}(\mathbf{X})|\mathbf{X}^{-i}\right]\right]}{\mathrm{Var}\left[\mathbb{1}_{\mathcal{F}_\mathbf{x}}(\mathbf{X})\right]} \tag{7.3}$$

where $S_i^{\mathbb{1}_\mathcal{F}}$ is the first-order index and $S_{T_i}^{\mathbb{1}_\mathcal{F}}$ the total index associated to the input variable X_i.

Efficient estimation schemes using a single-loop CMC, FORM-IS and TIS [1], have been investigated (see, e.g., Wei et al., 2012; Yun et al., 2018). Very recently, another efficient estimation scheme using subset sampling has been proposed by Perrin and Defaux (2019). This work is detailed hereafter.

7.2.2 Rewriting Sobol indices on the indicator function using Bayes' theorem

Following Perrin and Defaux (2019), it is proposed to rewrite the $S^{\mathbb{1}_\mathcal{F}}$-indices presented hereabove as in the following proposition. Note that similar derivations have been proposed in Wang et al. (2018) for the $\eta_i^{P_\mathrm{f}}$ index as defined in Eq. (4.53) (see Chapter 4).

Proposition 3 (Perrin and Defaux, 2018)**.** *The first and total order $S^{\mathbb{1}_\mathcal{F}}$-indices associated to each input X_i, $\forall i \in \{1\dots,d\}$, can be rewritten as follows:*

$$S_i^{\mathbb{1}_\mathcal{F}} = \frac{P_\mathrm{f}}{1-P_\mathrm{f}}\mathrm{Var}\left[\frac{f_{X_i|\mathcal{F}}(X_i)}{f_{X_i}(X_i)}\right] \tag{7.4}$$

$$S_{T_i}^{\mathbb{1}_\mathcal{F}} = 1 - \frac{P_\mathrm{f}}{1-P_\mathrm{f}}\mathrm{Var}\left[\frac{f_{\mathbf{X}^{-i}|\mathcal{F}}(\mathbf{X}^{-i})}{f_{\mathbf{X}^{-i}}(\mathbf{X}^{-i})}\right] \tag{7.5}$$

where:

$$f_{\mathbf{X}|\mathcal{F}}(\mathbf{x}) = \frac{\mathbb{1}_{\mathcal{F}_\mathbf{x}}(\mathbf{x})f_\mathbf{X}(\mathbf{x})}{P_\mathrm{f}} \tag{7.6a}$$

$$f_{X_i|\mathcal{F}}(x_i) = \int_{\mathcal{D}_{\mathbf{X}^{-i}}} f_{\mathbf{X}|\mathcal{F}}(\mathbf{x}) \prod_{\substack{j=1\\ j\neq i}}^{d} \mathrm{d}x_j, \quad \mathcal{D}_{\mathbf{X}^{-i}} = \bigtimes_{\substack{j=1\\ j\neq i}}^{d} \mathcal{D}_{X_j} \tag{7.6b}$$

$$f_{\mathbf{X}^{-i}|\mathcal{F}}(\mathbf{x}^{-i}) = \int_{\mathcal{D}_{X_i}} f_{\mathbf{X}|\mathcal{F}}(\mathbf{x})\, \mathrm{d}x_i. \tag{7.6c}$$

[1] As a reminder, TIS stands for *truncated importance sampling* as presented in Chapter 3, i.e., sampling outer the β-sphere (see, e.g., Harbitz, 1986; Grooteman, 2008; Grooteman, 2011).

Proof. A sketch of proof can be found in Perrin and Defaux (2019). However, more details are given below for the sake of clarity. Recalling that $\mathrm{Var}\left[\mathbb{1}_{\mathcal{F}_\mathbf{x}}(\mathbf{X})\right] = P_\mathrm{f}(1-P_\mathrm{f})$ *and applying Bayes' theorem to Eq. (7.1), one gets:*

$$\mathbb{E}_{f_{X_i}}[(P_\mathrm{f} - P_{\mathrm{f}|X_i})^2] = \mathbb{E}_{f_{X_i}}\left[\left(P_\mathrm{f} - P_\mathrm{f}\frac{f_{X_i|\mathcal{F}}(x_i)}{f_{X_i}(x_i)}\right)^2\right] \tag{7.7a}$$

$$= P_\mathrm{f}^2\,\mathbb{E}_{f_{X_i}}\left[\left(1 - \frac{f_{X_i|\mathcal{F}}(x_i)}{f_{X_i}(x_i)}\right)^2\right]. \tag{7.7b}$$

Hence, for the first order index, by applying the total variance theorem, one gets:

$$S_i^{\mathbb{1}_\mathcal{F}} = \frac{\mathbb{E}_{f_{X_i}}[(P_\mathrm{f} - P_{\mathrm{f}|X_i})^2]}{P_\mathrm{f}(1-P_\mathrm{f})} \tag{7.8a}$$

$$= \frac{P_\mathrm{f}}{1-P_\mathrm{f}}\left(\mathrm{Var}\left[1 - \frac{f_{X_i|\mathcal{F}}(x_i)}{f_{X_i}(x_i)}\right] + \mathbb{E}^2_{f_{X_i}}\left[1 - \frac{f_{X_i|\mathcal{F}}(x_i)}{f_{X_i}(x_i)}\right]\right) \tag{7.8b}$$

$$= \frac{P_\mathrm{f}}{1-P_\mathrm{f}}\left(\mathrm{Var}\left[\frac{f_{X_i|\mathcal{F}}(x_i)}{f_{X_i}(x_i)}\right] + 1 - \mathbb{E}^2_{f_{X_i}}\left[\frac{f_{X_i|\mathcal{F}}(x_i)}{f_{X_i}(x_i)}\right]\right). \tag{7.8c}$$

Moreover, one can notice that:

$$\mathbb{E}_{f_{X_i}}\left[\frac{f_{X_i|\mathcal{F}}(x_i)}{f_{X_i}(x_i)}\right] = \int_{\mathcal{D}_{X_i}} \frac{f_{X_i|\mathcal{F}}(x_i)}{f_{X_i}(x_i)} f_{X_i}(x_i)\mathrm{d}x_i \tag{7.9a}$$

$$= \int_{\mathcal{D}_{X_i}} \int_{\mathcal{D}_{\mathbf{X}^{-i}}} f_{\mathbf{X}|\mathcal{F}}(\mathbf{x}) \prod_{\substack{j=1 \\ j\neq i}}^{d} \mathrm{d}x_j \,\mathrm{d}x_i \tag{7.9b}$$

$$= \int_{\mathcal{D}_\mathbf{X}} \frac{1}{P_\mathrm{f}} \mathbb{1}_{\mathcal{F}_\mathbf{x}}(\mathbf{x}) f_\mathbf{X}(\mathbf{x})\mathrm{d}\mathbf{x} \tag{7.9c}$$

$$= 1 \tag{7.9d}$$

which finally allows to get the expected result. Similar derivations for the total index can be achieved starting from:

$$\mathbb{E}_{f_{\mathbf{X}^{-i}}}[(P_\mathrm{f} - P_{\mathrm{f}|\mathbf{X}^{-i}})^2] = P_\mathrm{f}^2\,\mathbb{E}_{f_{\mathbf{X}^{-i}}}\left[\left(1 - \frac{f_{\mathbf{X}^{-i}|\mathcal{F}}(\mathbf{x}^{-i})}{f_{\mathbf{X}^{-i}}(\mathbf{x}^{-i})}\right)^2\right] \tag{7.10a}$$

and noticing that $\mathbb{E}_{f_{\mathbf{X}^{-i}}}\left[\frac{f_{\mathbf{X}^{-i}|\mathcal{F}}(\mathbf{x}^{-i})}{f_{\mathbf{X}^{-i}}(\mathbf{x}^{-i})}\right] = 1.$ □

As a result, the two estimators associated to the indices are given by:

$$\widehat{S}_i^{\mathbb{1}_\mathcal{F}} = \frac{\widehat{P}_\mathrm{f}}{1-\widehat{P}_\mathrm{f}} \mathrm{Var}\left[\frac{\widehat{f}_{X_i|\mathcal{F}}(X_i)}{\widehat{f}_{X_i}(X_i)}\right] \tag{7.11}$$

$$\widehat{S}_{T_i}^{\mathbb{1}_\mathcal{F}} = 1 - \frac{\widehat{P}_\mathrm{f}}{1-\widehat{P}_\mathrm{f}} \mathrm{Var}\left[\frac{\widehat{f}_{\mathbf{X}^{-i}|\mathcal{F}}(\mathbf{X}^{-i})}{\widehat{f}_{\mathbf{X}^{-i}}(\mathbf{X}^{-i})}\right] \tag{7.12}$$

where $\widehat{f}_{X_i|\mathcal{F}}$ and $\widehat{f}_{X_i}$ are, respectively, the estimator of the marginal PDF of X_i conditioned to failure (i.e., the marginal PDF of X_i estimated on the elite set $\mathcal{E}_\mathbf{x}$ [2]) and the estimator of the initial marginal PDF.

This set of estimators present the main advantage of requiring only a post-processing phase of a single elite set $\mathcal{E}_\mathbf{x}$ obtained from a reliability analysis using any sampling-based technique mentioned in Chapter 3. Moreover, one could theoretically get all the $S^{\mathbb{1}_\mathcal{F}}$-indices at any order. However, the difficulty remains the accurate estimation of the densities, especially for the total indices which involve the estimation of a multivariate density at failure.

7.3 Sobol indices on the indicator function adapted to the bi-level input uncertainty

7.3.1 Bi-level input uncertainty: aggregated vs. disaggregated types of uncertainty

In this part, the same Bayesian hierarchical structure is considered as in the two previous chapters:

$$\begin{aligned}
&\mathbf{X} \sim f_{\mathbf{X}|\mathbf{\Theta}}(\mathbf{x}|\boldsymbol{\theta}) : \mathcal{D}_\mathbf{X} \subseteq \mathbb{R}^d \to \mathbb{R}_+ && \text{(uncertainty level \#1)}\\
&\mathbf{\Theta} \sim f_{\mathbf{\Theta}|\boldsymbol{\xi}}(\boldsymbol{\theta}|\boldsymbol{\xi}) : \mathcal{D}_\mathbf{\Theta} \subseteq \mathbb{R}^{n_\theta} \to \mathbb{R}_+ && \text{(uncertainty level \#2)}\\
&\boldsymbol{\xi} = (\xi_1, \xi_2, \ldots, \xi_{n_\xi})^\top \in \mathcal{D}_{\boldsymbol{\xi}} \subseteq \mathbb{R}^{n_\xi} && \text{(deterministic level).}
\end{aligned}$$

Moreover, it is assumed that the input variables X_i, for $i = 1, \ldots, d$, are independent. To be consistent with such a hypothesis, one can consider that, either the problem naturally involves independent input variables, or transformations like those presented in Appendix C can be used to set the problem in the $\mathbf{u}$-space. In the latter case, one should notice that, unfortunately, any results obtained by ROSA should be interpreted carefully as dependence between input variables is not taken into account.

When dealing with the bi-level input uncertainty, two cases can be considered:

- on the one hand, one might be interested in the combined effects of both aleatory and epistemic uncertainties at failure, i.e., one might want to "*aggregate*" both sources of uncertainty;
- on the other hand, one might be rather interested in distinguishing between the contributions of aleatory and epistemic uncertainties, i.e., one might want to "*disaggregate*" (or "*separate*") both sources of uncertainty.

Concerning the first problem, adapting the previous $S^{\mathbb{1}_\mathcal{F}}$-indices can be achieved by considering the equivalent indices evaluated on the augmented vector $\mathbf{Z} = (\mathbf{X}, \mathbf{\Theta})^\top$. Such indices would reflect the contribution of both the variables $\mathbf{X}|\mathbf{\Theta}$ and distribution parameters $\mathbf{\Theta}$.

[2] As a reminder, the elite set is defined such that $\mathcal{E}_\mathbf{x} = \{\mathbf{X}^{(j)}, 1 \leq j \leq N_\mathrm{fail} \mid \mathbb{1}_{\mathcal{F}_\mathbf{x}}(\mathbf{X}^{(j)}) = 1\}$, with N_fail the number of failure points.

In the second problem, the idea is to study the impact of aleatory and epistemic uncertainties separately. Indeed, as stressed in Hoffman and Hammonds (1994), Helton (1997), Helton et al. (2004), and Sankararaman and Mahadevan (2013b), separating both contributions of aleatory and epistemic uncertainties may be of utmost importance if one desires to get a deeper insight about which type of uncertainty plays a major role on the system at failure, and to start a well-informed decision process in terms of budget allocation to possibly reduce epistemic uncertainty if this one plays a significant role on the variability of the reliability measure.

In this chapter, it is proposed to consider a disaggregated version of the augmented input vector to separate both types of uncertainty. Moreover, the effects of both types of uncertainties on the indicator function (in other words, "at failure") are studied and taken into account in the ROSA context, as presented in the following sections.

7.3.2 Disaggregated random variables

One possible manner to study the effects of distribution parameter uncertainty and input variability separately is to transform the input variables as proposed in Schöbi and Sudret (2017) (in the context of p-boxes). As a preliminary example, one can consider the Gaussian case as an illustrative example. Thus, under a single-level type of uncertainty, a Gaussian random variable X can be split as follows:

$$X = \mu_X + \sigma_X \, U_X \tag{7.14}$$

where $\boldsymbol{\theta} = (\mu_X, \sigma_X)^\top$ are the distribution parameters and $U_X \sim \mathcal{N}(0,1)$ is a standard Gaussian variable which characterizes the inherent variability of X. Note that such a transformation is not limited to the Gaussian case. One can build similar transformations for random variables following, for instance, lognormal, Gumbel or Weibull distributions. The interested reader should refer to Schöbi and Sudret (2017) for the presentation of these cases.

Under a bi-level input uncertainty, the idea is to consider a prior distribution $f_{\boldsymbol{\Theta}}$ over the uncertain distribution parameters $\boldsymbol{\Theta} = (M_X, S_X)^\top$. As a consequence, the previous decomposition can be rewritten as follows:

$$X = M_X + S_X \, U_X \tag{7.15}$$

where $\mathbf{V}_{\text{dis}} = (M_X, S_X, U_X)^\top$ is a vector of independent variables denoted as the "*disaggregated augmented vector*". Note that, for some cases, only the mean value or the standard deviation could be considered as uncertain. In the following, the study will be limited to the Gaussian case as working in the $\mathbf{u}$-space will facilitate the calculations, without loss of generality. Finally, the augmented input vector under a bi-level uncertainty will be composed of two sorts of inputs, the inputs that are not affected by the bi-level uncertainty ones (gathered in the vector $\mathbf{X}_{\text{single}}$) and the disaggregated ones, such that $\mathbf{Z} = (\mathbf{V}_{\text{dis}}, \mathbf{X}_{\text{single}})^\top$ with $d_{\mathbf{Z}} = d_{\text{dis}} + d_{\text{single}}$ denotes the dimension of this vector. As a final remark, one should notice that, in a multivariate setting, one has $f_{\mathbf{Z}} = f_{\boldsymbol{\Theta}} \times f_{\mathbf{U}} \times f_{\mathbf{X}_{\text{single}}}$.

As a remark and to avoid any confusion for the reader, one should notice that, similarly to the remark mentioned in Chapter 6, despite the disaggregated inputs, only the basic variables $\mathbf{X}$ do play a role in the physical model. Thus, these disaggregated inputs are "re-aggregated" within the code such that only $\mathbf{X}$ variables play a role in the physical behavior. In the following, one will use the notation $\mathbf{Z}$ to deal with input variables, but the reader should be aware that only the $\mathbf{X}$ variables have a physical sense from the failure point of view.

7.3.3 Extension to the bi-level input uncertainty and pick-freeze estimators

In this chapter, it is proposed to extend the previous $S^{\mathbb{1}_{\mathcal{F}}}$-indices to the bi-level input uncertainty. To do so, the following pair of indices is proposed:

$$S_i^{\mathbb{1}_{\mathcal{F}}} = \frac{\mathrm{Var}\left[\mathbb{E}[\mathbb{1}_{\mathcal{F}_{\mathbf{z}}}(\mathbf{Z})|Z_i]\right]}{\mathrm{Var}\left[\mathbb{1}_{\mathcal{F}_{\mathbf{z}}}(\mathbf{Z})\right]} \tag{7.16}$$

$$S_{T_i}^{\mathbb{1}_{\mathcal{F}}} = 1 - \frac{\mathrm{Var}\left[\mathbb{E}[\mathbb{1}_{\mathcal{F}_{\mathbf{z}}}(\mathbf{Z})|\mathbf{Z}^{-i}]\right]}{\mathrm{Var}\left[\mathbb{1}_{\mathcal{F}_{\mathbf{z}}}(\mathbf{Z})\right]} = \frac{\mathbb{E}\left[\mathrm{Var}\left[\mathbb{1}_{\mathcal{F}_{\mathbf{z}}}(\mathbf{Z})|\mathbf{Z}^{-i}\right]\right]}{\mathrm{Var}\left[\mathbb{1}_{\mathcal{F}_{\mathbf{z}}}(\mathbf{Z})\right]}. \tag{7.17}$$

Pick-freeze estimators can be used to estimate these indices by MC simulations. In the following, these estimators will be used to get the reference results.

Computing $S_i^{\mathbb{1}_{\mathcal{F}}}$ and $S_{T_i}^{\mathbb{1}_{\mathcal{F}}}$ under a bi-level uncertainty using a single-loop CMC sampling can be achieved in four steps. The procedure presented herebelow is adapted from the one proposed by Wei et al. (2012).

Step #1. Generate $2N$ copies of the augmented vector $\{\mathbf{Z}^{(j)}\}_{j=1}^{2N} \overset{\text{i.i.d.}}{\sim} f_{\mathbf{Z}}$. These samples are stored in the following two matrices:

$$\mathbf{A} = \begin{array}{c} \\ 1 \\ 2 \\ \vdots \\ N \end{array} \begin{array}{c} \begin{array}{cccccc} Z_1 & Z_2 & \dots & Z_i & \dots & Z_{d_{\mathbf{Z}}} \end{array} \\ \begin{pmatrix} z_1^{(1)} & z_2^{(1)} & \dots & z_i^{(1)} & \dots & z_{d_{\mathbf{Z}}}^{(1)} \\ z_1^{(2)} & z_2^{(2)} & \dots & z_i^{(2)} & \dots & z_{d_{\mathbf{Z}}}^{(2)} \\ \vdots & \vdots & \ddots & \vdots & \ddots & \vdots \\ z_1^{(N)} & z_2^{(N)} & \dots & z_i^{(N)} & \dots & z_{d_{\mathbf{Z}}}^{(N)} \end{pmatrix} \end{array} \tag{7.18}$$

$$\mathbf{B} = \begin{array}{c} \\ N+1 \\ N+2 \\ \vdots \\ 2N \end{array} \begin{array}{c} \begin{array}{cccccc} Z_1 & Z_2 & \dots & Z_i & \dots & Z_{d_{\mathbf{Z}}} \end{array} \\ \begin{pmatrix} z_1^{(N+1)} & z_2^{(N+1)} & \dots & z_i^{(N+1)} & \dots & z_{d_{\mathbf{Z}}}^{(N+1)} \\ z_1^{(N+2)} & z_2^{(N+2)} & \dots & z_i^{(N+2)} & \dots & z_{d_{\mathbf{Z}}}^{(N+2)} \\ \vdots & \vdots & \ddots & \vdots & \ddots & \vdots \\ z_1^{(2N)} & z_2^{(2N)} & \dots & z_i^{(2N)} & \dots & z_{d_{\mathbf{Z}}}^{(2N)} \end{pmatrix} \end{array}. \tag{7.19}$$

Step #2. Generate a set of matrices $\mathbf{C}^{(i)}$, with $i \in \{1, \dots, d_{\mathbf{Z}}\}$ where the i-th column of $\mathbf{C}^{(i)}$ comes for $\mathbf{A}$ and all other $d_{\mathbf{Z}} - 1$ columns come from $\mathbf{B}$:

$$\mathbf{C}^{(i)} = \begin{array}{c} \begin{array}{cccccc} Z_1 & Z_2 & \dots & Z_i & \dots & Z_{d_{\mathbf{Z}}} \end{array} \\ \begin{pmatrix} z_1^{(N+1)} & z_2^{(N+1)} & \dots & z_i^{(1)} & \dots & z_{d_{\mathbf{Z}}}^{(N+1)} \\ z_1^{(N+2)} & z_2^{(N+2)} & \dots & z_i^{(2)} & \dots & z_{d_{\mathbf{Z}}}^{(N+2)} \\ \vdots & \vdots & \ddots & \vdots & \ddots & \vdots \\ z_1^{(2N)} & z_2^{(2N)} & \dots & z_i^{(N)} & \dots & z_{d_{\mathbf{Z}}}^{(2N)} \end{pmatrix} \end{array}. \tag{7.20}$$

Step #3. Compute the indicator function values for each sample in the matrices $\mathbf{A}$, $\mathbf{B}$ and $\mathbf{C}^(i)$. Finally, one gets the following set of N-dimensional column vectors:

$$\mathbb{1}_{\mathbf{A}} = \mathbb{1}_{\mathcal{F}_{\mathbf{z}}}(\mathbf{A}), \quad \mathbb{1}_{\mathbf{B}} = \mathbb{1}_{\mathcal{F}_{\mathbf{z}}}(\mathbf{B}), \quad \mathbb{1}_{\mathbf{C}^{(i)}} = \mathbb{1}_{\mathcal{F}_{\mathbf{z}}}(\mathbf{C}^{(i)}). \tag{7.21}$$

Step #4. The $S^{\mathbb{1}_{\mathcal{F}}}$-indices, for $i \in \{1, \ldots, d_{\mathbf{Z}}\}$, are computed using the following CMC estimators:

$$\widehat{S}_i^{\mathbb{1}_{\mathcal{F}}} = \frac{\widehat{D}_i - \widehat{\widetilde{P}}_{\mathrm{f}}^{\,2}}{\widehat{D}} \tag{7.22}$$

$$\widehat{S}_{T_i}^{\mathbb{1}_{\mathcal{F}}} = 1 - \frac{\widehat{D}_{-i} - \widehat{\widetilde{P}}_{\mathrm{f}}^{\,2}}{\widehat{D}} \tag{7.23}$$

where:

$$\widehat{\widetilde{P}}_{\mathrm{f}} = \frac{1}{2N} \sum_{j=1}^{N} (\mathbb{1}_{\mathbf{A}}^{(j)} + \mathbb{1}_{\mathbf{B}}^{(j)}) \tag{7.24}$$

$$\widehat{\widetilde{P}}_{\mathrm{f}}^{\,2} = \frac{1}{N} \sum_{j=1}^{N} \mathbb{1}_{\mathbf{A}}^{(j)} \mathbb{1}_{\mathbf{B}}^{(j)} \tag{7.25}$$

$$\widehat{D} = \widehat{\widetilde{P}}_{\mathrm{f}} - \widehat{\widetilde{P}}_{\mathrm{f}}^{\,2} \tag{7.26}$$

$$\widehat{D}_i = \frac{1}{N} \sum_{j=1}^{N} \mathbb{1}_{\mathbf{A}}^{(j)} \mathbb{1}_{\mathbf{C}^{(i)}}^{(j)} \tag{7.27}$$

$$\widehat{D}_{-i} = \frac{1}{N} \sum_{j=1}^{N} \mathbb{1}_{\mathbf{B}}^{(j)} \mathbb{1}_{\mathbf{C}^{(i)}}^{(j)} \tag{7.28}$$

where $\mathbb{1}_{\mathbf{A}}^{(j)}$, $\mathbb{1}_{\mathbf{B}}^{(j)}$ and $\mathbb{1}_{\mathbf{C}^{(i)}}^{(j)}$ are, respectively, the j-th component of the column vector $\mathbb{1}_{\mathbf{A}}$, $\mathbb{1}_{\mathbf{B}}$ and $\mathbb{1}_{\mathbf{C}^{(i)}}$.

In the following, reference values for $S^{\mathbb{1}_{\mathcal{F}}}$-indices will be estimated using this four-step procedure. Note that, following Homma and Saltelli (1996) and Wei et al. (2012), an extra step could be added to compute analytical formulas to get the estimation error. However, in the following, this error is controled by use of repetitions of the whole procedure. At this point, one should notice that this single-loop CMC sampling procedure may become inefficient in the context of rare event probability estimation as most of the indicator functions in Eq. (7.21) could be equal to zero. Moreover, the simulation cost associated to this single-loop procedure is $N_{\text{cost}} = N(d_{\mathbf{Z}} + 2)$ calls to the LSF. To avoid such a computational burden, Wei et al. (2012) proposes FORM-IS and TIS-based estimators of the above CMC estimators (in the context of single-level ROSA). In the next section, another way is investigated to efficiently obtain the indices under a bi-level uncertainty by an efficient estimation scheme coupling the estimators presented in Subsection 7.2.2, a subset sampling technique and kernel density estimation.

7.4 Efficient estimation using subset sampling and kernel density estimation

7.4.1 The problem of estimating the optimal distribution at failure

By adapting the expressions given in Eq. (7.11) and Eq. (7.12) to the bi-level uncertainty, one gets the following estimators:

$$\widehat{S}_i^{\mathbb{1}_{\mathcal{F}}} = \frac{\widehat{\widetilde{P}}_{\mathrm{f}}}{1-\widehat{\widetilde{P}}_{\mathrm{f}}} \mathrm{Var}\left[\frac{\widehat{f}_{Z_i|\mathcal{F}}(Z_i)}{\widehat{f}_{Z_i}(Z_i)}\right] \tag{7.29}$$

$$\widehat{S}_{T_i}^{\mathbb{1}_{\mathcal{F}}} = 1 - \frac{\widehat{\widetilde{P}}_{\mathrm{f}}}{1-\widehat{\widetilde{P}}_{\mathrm{f}}} \mathrm{Var}\left[\frac{\widehat{f}_{\mathbf{Z}^{-i}|\mathcal{F}}(\mathbf{Z}^{-i})}{\widehat{f}_{\mathbf{Z}^{-i}}(\mathbf{Z}^{-i})}\right] \tag{7.30}$$

where $\widehat{\widetilde{P}}_{\mathrm{f}}$ is the estimated value of the predictive failure probability as presented in Chapter 5, estimated here by ARA/SS. As suggested by these estimators adapted to the bi-level uncertainty, the first and total sensitivity indices require the estimation of $f_{Z_i|\mathcal{F}}$ and $f_{\mathbf{Z}^{-i}|\mathcal{F}}$. These densities correspond, respectively, to the marginal distribution w.r.t. Z_i and to the "joint minus one" (abbreviated as "joint-1", the one corresponding to the i-th marginal) distribution of the failure points. These two estimators exhibit a number of challenges that are detailed below in the dedicated paragraphs.

As a remark, one should notice that these densities $f_{Z_i|\mathcal{F}}$ and $f_{\mathbf{Z}^{-i}|\mathcal{F}}$ are closely related to the optimal ones discussed in Chapter 3 (see Eq. (3.27) and Eq. (3.28)) in the context of importance sampling and subset sampling. However, as explained all along Chapter 3, the optimal density at failure (without specifying the space, either $\mathbf{x}$-space or $\mathbf{u}$-space), may be challenging to estimate due to multiple reasons. Such a task can be achieved by means of KDE (see Appendix B and its use, e.g., in the NAIS technique as explained Chapter 3).

In the context defined hereabove, i.e., global ROSA with $S^{\mathbb{1}_{\mathcal{F}}}$-indices, under a bi-level input uncertainty, one needs to recall the major challenges arising from the estimation of the optimal distribution at failure using KDE, and the new challenges induced by the use of the estimators in Eq. (7.29) and Eq. (7.30).

Challenge #1: input dimension. It is known that the performance of KDE deteriorates with the input dimension. However, in the estimators presented above, this issue is predominantly affecting the total index $\widehat{S}_{T_i}^{\mathbb{1}_{\mathcal{F}}}$ as it requires the estimation of the joint-1 density $f_{\mathbf{Z}^{-i}|\mathcal{F}}$ at failure. However, this issue is intrinsically affected by the fact that, under a bi-level uncertainty, one considers the augmented vector $\mathbf{Z} = (\mathbf{V}_{\mathrm{dis}}, \mathbf{X}_{\mathrm{single}})^\top$ of size $d_{\mathbf{Z}} > d$ due to the disaggregated variables contained in $\mathbf{V}_{\mathrm{dis}}$. This increased input dimension is the counterpart of taking the bi-level input uncertainty into account.

Challenge #2: complex shape of the optimal density at failure. As explained in Chapter 3, the shape of the optimal density at failure may be complex. By complex, one means that it is a distribution truncated by the LSS, which can be multimodal and may thus arise from a complex combination of the inputs. Note that the multimodality can be either smooth (close modes) or very sharp, especially in the context of disconnected failure regions of almost equal importances.

Challenge #3: limited number of failure points in the elite set. In the context of rare event probability estimation, the number of failure points, i.e., samples that lie in the true failure domain, is often limited (e.g., with the CMC technique). Even if variance reduction techniques such as IS or SS can be used and may significantly increase the number of failure points in the

last iteration, the elite set $\mathcal{E}_{\mathbf{x}}$ (or $\mathcal{E}_{\mathbf{u}}$) is often of rather small size compared to the total number of simulations used to get an estimate of the failure probability. Finally, one can also add more samples by using *resampling* within this failure domain (e.g., by using MCMC techniques such as presented in Appendix D). In the context of costly-to-evaluate computer codes, resampling may even become untractable. As a result, the learning procedure of $f_{Z_i|\mathcal{F}}$ and $f_{\mathbf{Z}^{-i}|\mathcal{F}}$ by KDE has to be performed over a limited elite set composed of from a few hundreds to a few thousands of failure points.

Challenge #4: accuracy of the KDE. A last challenge concerns the fact that, in Eq. (7.29) and Eq. (7.30), not only the estimations of $f_{Z_i|\mathcal{F}}$ and $f_{\mathbf{Z}^{-i}|\mathcal{F}}$ are required but also their evaluations on samples Z_i and $\mathbf{Z}^{-i}$. Moreover, these indices are based on the variance of ratios of these density evaluations. Thus, one needs to ensure that the KDE provides sufficiently accurate estimations for the densities to avoid large estimation errors. Consequently, if a coarse KDE can be sufficient to get a sampling density able to generate samples within a certain region (e.g., a failure region, such as in the NAIS technique), getting a very accurate estimation of a multivariate density over a limited set of samples is far more challenging.

If the traditional KDE formulation such as presented in Appendix B may be sufficient for basic "*estimation-sampling*" tasks used in reliability assessment such as in the NAIS technique, it is definitely not efficient enough regarding the four challenges listed hereabove. To do so, one needs to focus on dedicated tools developed w.r.t. these challenges. Recently, a modified formulation based on Gaussian KDE (G-KDE, i.e., using Gaussian kernels) has been proposed in Perrin et al. (2018). This formulation is briefly reviewed below.

7.4.2 Data-driven tensorized kernel density estimation

Introduced in Perrin et al. (2018), a new *data-driven tensorized* G-KDE has been proposed so as to overcome a few difficulties of traditional G-KDE. For the sake of clarity and conciseness, only a few prerequisites and the core modifications are presented below. The interested reader is invited to refer to Perrin et al. (2018) for any further information.

Context and prerequisites. This data-driven tensorized G-KDE relies on the assumption that the maximum available information consists of a set of independent realizations $\{\mathbf{Z}\}_{j=1}^{N}$ of a random vector $\mathbf{Z}$. In the reliability context, such a dataset can be typically the elite set denoted by $\mathcal{E}_{\mathbf{z}}$, i.e., a N-dimensional vector of realizations of the input vector whose coordinates fall in the failure domain (which can be either in the $\mathbf{x}$-space or in the $\mathbf{u}$-space).

Another prerequisite consists in assuming that the unknown underlying distribution $f_{\mathbf{Z}}$ of these data samples might be concentrated on an unknown subset of $\mathbb{R}^d$. This assumption may be particularly true when the distribution of $\mathbf{Z}$ may exhibit a strong stochastic dependence structure. In the reliability context, this case typically corresponds to the case of the optimal density at failure for complex LSFs (even if the input vector of basic variables $\mathbf{X}$ is made of independent variables). This theoretical problem of probability concentration is strongly linked with mathematical concepts related to dimension reduction via *diffusion maps theory* (see, e.g., Coifman et al., 2015; Soize and Ghanem, 2016; Soize and Ghanem, 2017). The basic idea of diffusion maps is to identify the underlying manifold upon which the data is embedded (see, e.g., De La Porte et al., 2008). Nonetheless, this theoretical topic is beyond the scope of this thesis and the interested reader is invited to refer to the above references for any further information.

Main features of the data-driven tensorized G-KDE. Regarding the potential constraints and challenges mentioned above, Perrin et al. (2018) propose two main adaptations to the traditional G-KDE. These two features are detailed below:

- the *data-driven* feature: while considering a dataset $\mathcal{E}_{\mathbf{z}} = \{\mathbf{Z}^{(1)}, \ldots, \mathbf{Z}^{(N_{\text{fail}})}\}$, the idea is to modify the traditional G-KDE estimator so that the mean and covariance matrix are equal to the empirical moments $\widehat{\mathbf{m}}_{\mathcal{E}_{\mathbf{z}}}$ and $\widehat{\mathbf{\Sigma}}_{\mathcal{E}_{\mathbf{z}}}$ estimated from the dataset $\mathcal{E}_{\mathbf{z}}$. Moreover, it is proposed to replace the "*Silverman's rule of thumb*" (see Appendix B) characterized by the bandwidth matrix given in Eq. (B.14) parametrized by a single scalar bandwidth η_{Silv} given in Eq. (B.15). Instead, it is proposed to use the maximum likelihood estimate $\mathbf{H}^{\text{ML}}$ based on the available data;

- the *tensorization* feature: to take into account the possible complex dependence structure of the underlying distribution of interest, it is proposed to consider a *block-by-block decomposition* to separate the components of $\mathbf{Z}$ which can be reasonably assumed to be independent from those which can be assumed dependent. Thus, two dependent inputs should belong to the same block. This leads to consider a tensorized version of the bandwidth matrix $\mathbf{H}^{\text{ML}}$ parametrized by a set of bandwiths η_l with $l \in \{1, \ldots, n_{\text{block}}\}$.

7.4.3 Methodology based on subset sampling and data-driven tensorized G-KDE

The proposed methodology can be summarized as proposed in Figure 7.1. Thus, it can be decomposed into two major phases:

- **Phase #1**: the first phase (cf. the blue blocks in Figure 7.1) corresponds to a *reliability analysis phase*. The idea is to perform a rare event probability estimation using ARA/SS. To do so, one first needs to set the augmented problem by constructing the augmented vector using the disaggregated strategy. Then, one performs a SS-based rare event probability estimation (which implies to set several tuning algorithms for SS as explained in Appendix D) so as to get an *elite set*. A possible final step consists in resampling within the failure domain, if necessary;

- **Phase #2**: the second phase (cf. the orange blocks in Figure 7.1) corresponds to a *learning and sensitivity analysis phase*. To do so, one needs first to estimate empirical moments based on the available elite set. Then, one can run the procedure of *data-driven tensorized G-KDE* as set in Perrin et al. (2018). Note that, in this chapter, the algorithm used to find the block-dependence structure is a greedy algorithm. Another possibility could be to use a genetic algorithm as achieved in Perrin et al. (2018). Finally, one can evaluate the $S^{\mathbb{1}_{\mathcal{F}}}$-indices using estimators given in Eq. (7.29) and Eq. (7.30).

In the following, this methodology is applied and tested on two academic test-cases. A numerical application on a realistic aerospace test-case will be further studied in Chapter 8.

7.5 Application examples

The numerical applications presented in this section are based on the following tools:

- the rare event probability estimation has been implemented in Matlab® and performed using both a rare event simulation toolbox developed at ONERA;

- a Python™ implementation of the data-driven tensorized G-KDE procedure proposed by Perrin et al. (2018).

The numerical testing of the methodology developed in this chapter, as summed up in Table 7.1, relies on the following settings:

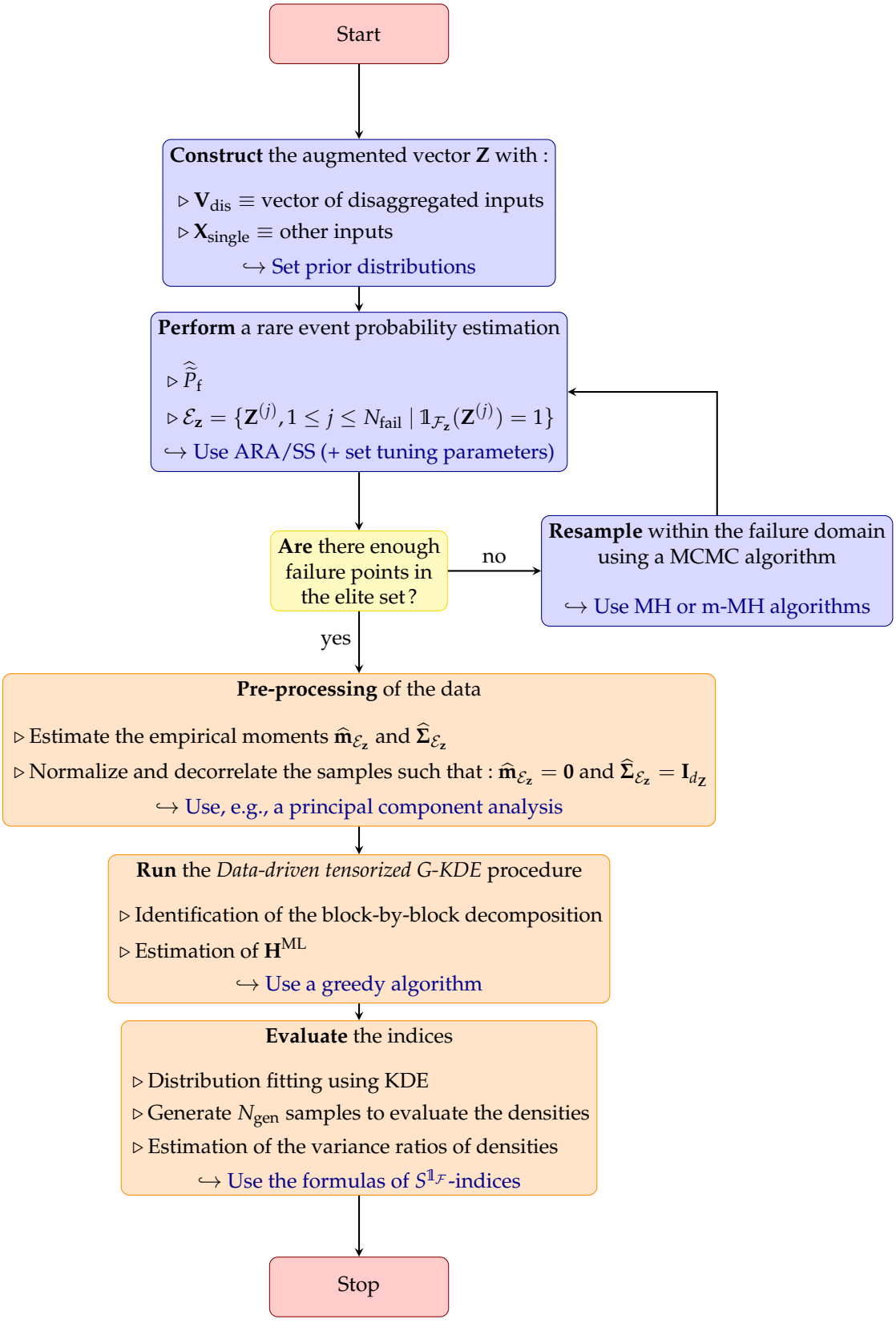

FIGURE 7.1: Flowchart of the proposed methodology to compute $S^{\mathbb{1}_{\mathcal{F}}}$-indices under a bi-level uncertainty.

- firstly, the idea is to highlight the fact that dealing with bi-level uncertainty, especially with disaggregated random variables, may provide more information about how epistemic uncertainty plays a role on the variability of the indicator function. To do so, one proposes a comparison of $S^{\mathbb{1}_{\mathcal{F}}}$-indices under single- and bi-level uncertainty, obtained using both CMC and ARA/CMC with large sample sizes;
- secondly, it is proposed to efficiently estimate the bi-level $S^{\mathbb{1}_{\mathcal{F}}}$-indices using the methodology described in Subsection 7.4.3 (i.e., the coupling between SS and the data-driven tensorized G-KDE, abbreviated as "SS + G-KDE" in the following), at a lower computational cost than CMC (see Subsection 7.3.3). To do so, one considers that several elite sets $\{\mathcal{E}_{\mathbf{z}}^{(j)}\}_{j=1}^{n_{\text{set}}}$ are obtained by repeating n_{set} times the SS algorithm. Then, based on these elite sets, one can repeat the overall procedure proposed in Subsection 7.4.3 so as to estimate the indices. However, due to possible numerical instabilities in the estimation of the $S^{\mathbb{1}_{\mathcal{F}}}$-indices (mainly due to the approximation of the PDFs), the mean estimate are given together with a "*success rate*" which indicates the percentage of estimated values that have been kept to get the mean estimate. The rejected ones correspond to negative values of the indices which are considered as outliers but are taken into account in the score provided by the success rate.
- thirdly, after validation of the method, the impact of the increasing rareness of the failure event (regarding a limited simulation budget available) is studied as an extension of the first test-case (see the three black stars ★).

TABLE 7.1: Overall strategy for the numerical tests of the proposed methodology.

Test-case		**Single-level**	**Bi-level**	
		CMC	Ref. ARA/CMC	ARA/SS
Ex. #1: Polynomial function [a]	(cf. 7.5.1)	■ ★	■ ★	■ ★
Ex. #2: Truss structure [b]	(cf. 7.5.2)	■	■	■

[a] $d_{\mathbf{Z}} = 5$.
[b] $d_{\mathbf{Z}} = 7$.

As shown in Table 7.1, the proposed methodology is applied on two test-cases, respectively a polynomial toy-case and the failure of a roof structure modeled by a truss (the black squares stand for the performed calculations). A numerical application on a realistic aerospace test-case will be further proposed in Chapter 8.

7.5.1 Example #1: a polynomial function toy-case

Description. In a first example (issued from Perrin and Defaux (2019)), one considers an analytical toy-case made of a polynomial function whose failure is given by the following LSF:

$$g(\mathbf{X}) = y_{\text{th}} - \mathcal{M}(\mathbf{X}) = y_{\text{th}} - (1 + X_1)(5 + X_2)(10 + X_3) \tag{7.31}$$

where the X_i, for $i = 1, \ldots, d$, are three independent standard Gaussian variables. The failure is supposed to occur as soon as the output value exceeds the threshold y_{th}. In the following, two cases are treated:

- $y_{\text{th}} = 250$: in this case, the reference failure probability estimated using CMC (with $N = 10^6$ samples and $N_{\text{rep}} = 100$ replications) is $p_{\text{f,ref}} = 8.55 \times 10^{-4}$);
- $y_{\text{th}} = 350$: in this case, the rareness of the failure event is increased so as to reach a reference failure probability under a single-level uncertainty of $p_{\text{f,ref}} = 1.17 \times 10^{-5}$ (estimated using

CMC with $N = 10^7$ samples and $N_{\text{rep}} = 100$ replications). For this case, the s.d. values of the prior distributions are increased so as to get stronger sensitivities (see the values marked with the symbol ★ in Table 7.2).

Under a bi-level uncertainty, one considers that the probabilistic model of the first input variable X_1 is not perfectly known (see Table 7.2). Thus, one considers the following decomposition:

$$X_1 = M_{X_1} + S_{X_1} U_{X_1} \tag{7.32}$$

where M_{X_1} and S_{X_1} follow respectively some prior distributions described in Table 7.2. As for U_{X_1}, it represents the natural variability of the input X_1.

TABLE 7.2: Input probabilistic model for Example #1.

Variable X_i	**Distribution**	**Mean** μ_{X_i}	**S.d.** σ_{X_i}
X_1	Normal	μ_{X_1} ***uncertain*** [a]	σ_{X_1} ***uncertain***
X_2	Normal	0	1
X_3	Normal	0	1
M_{X_1}	Normal	0	0.1/0.7(★)
S_{X_1}	Normal	1	0.1/0.7(★)
U_{X_1}	Normal	0	1

[a] For fixed values $\mu_{X_1} = 0$ and $\sigma_{X_1} = 1$, $p_{\text{f,ref}} = 8.55 \times 10^{-4}$.

Results. Figure 7.2a and Figure 7.2b provide the reference results for the estimation of both first-order and total $S^{\mathbb{1}_{\mathcal{F}}}$-indices under a single-level uncertainty. Based on these plots, one can notice firstly that X_1 is the most influential variable on the indicator function, and second, that all the three variables show high values for the total indices which indicates that these variables present strong interactions at failure (which is coherent with the results observed by Lemaître (2014, Chap. 1)).

Now, one can compare these results with the reference ones obtained under a bi-level uncertainty using the CMC pick-freeze estimators presented in Subsection 7.3.3. The most influential input variable X_1 has been disaggregated. Thus, Figure 7.3a and Figure 7.3b show that it is U_{X_1} which is the most influential regarding first-order indices. Then, looking at total indices, one can notice that, even if the ranking is still preserved ($U_{X_1} > X_2 > X_3$), S_{X_1} is most influential than M_{X_1} and is of the same order of magnitude as X_3. Consequently, considering an extra level of uncertainty plays, not only a role on the reliability assessment (here, the failure probability slighty increases from 8.55×10^{-4} to 1.0×10^{-3}), but also on the relative influence of the random variables at failure. Moreover, these results show that epistemic uncertainty affecting distribution parameters may play a non-negligible role compared to aleatory uncertainty of the basic variables.

Numerical results obtained by the proposed methodology are given in Table 7.3. These results have been obtained for the following settings: $n_{\text{set}} = 10$ elite sets of $N_{\text{fail}} = 2.5 \times 10^3$ failure samples have been obtained by repetition of the SS algorithm. In addition to that, one generates $N_{\text{gen}} = 5 \times 10^4$ samples on which one evaluates the densities and compute the variance of the ratio. Thus, one can notice, by comparing the second and third columns, that the first order indices are rather correctly estimated, at a relative moderate cost and with a high success rate. One can still note that the index associated to U_{X_1} is a little bit under-estimated. As for the total indices, even if the orders of magnitude are almost correct, most of them are a little bit over-estimated.

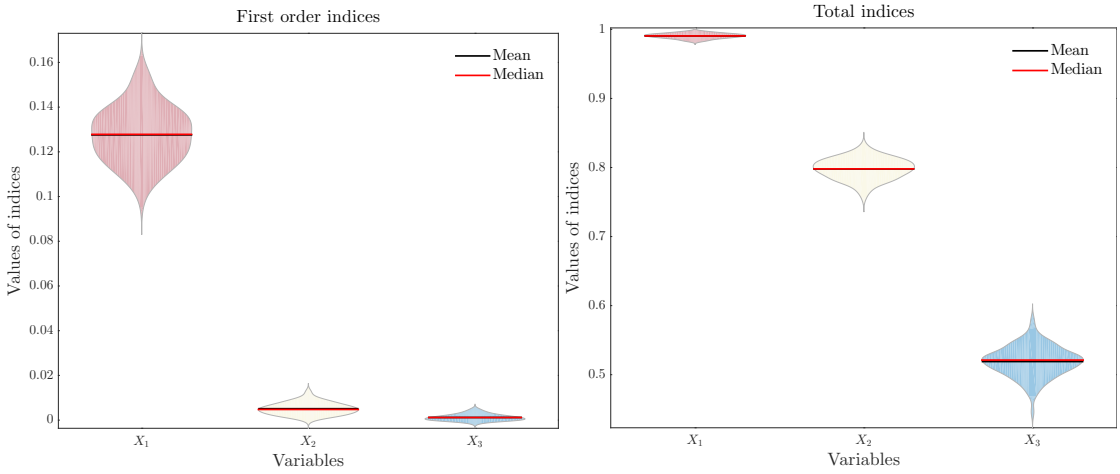

FIGURE 7.2: Reference $S^{\mathbb{1}_{\mathcal{F}}}$-indices estimated for the Example #1 under a single-level uncertainty (CMC of $N_{\text{sim}} = 10^6$ samples and $N_{\text{rep}} = 100$ repetitions, with $p_{\text{f,ref}} = 8.55 \times 10^{-4}$).

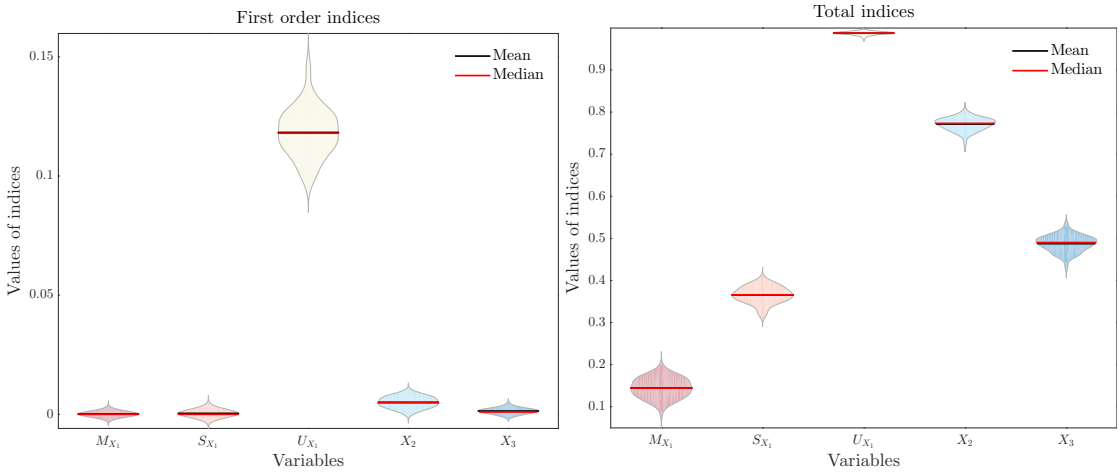

FIGURE 7.3: Reference $S^{\mathbb{1}_{\mathcal{F}}}$-indices estimated for the Example #1 under a bi-level uncertainty (CMC of $N_{\text{sim}} = 10^6$ samples and $N_{\text{rep}} = 100$ repetitions, with $\widetilde{P}_{\text{f,ref}} = 1.0 \times 10^{-3}$).

TABLE 7.3: Results for Example #1.

Variable	**First order indices**			**Total indices**		
	Ref. CMC	SS + G-KDE	Success rate	Ref. CMC	SS + G-KDE	Success rate
M_{X_1}	1.4×10^{-4}	8.4×10^{-5}	(100 %)	0.145	0.224	(90 %)
S_{X_1}	4×10^{-4}	5.8×10^{-4}	(100 %)	0.366	0.476	(100 %)
U_{X_1}	0.118	0.069	(100 %)	0.987	0.981	(100 %)
X_2	5.1×10^{-3}	4.1×10^{-3}	(100 %)	0.772	0.806	(100 %)
X_3	1.4×10^{-3}	1.5×10^{-3}	(100 %)	0.487	0.604	(100 %)

Considering the influence of the failure event rareness (i.e., for $y_{\text{th}} = 350$), numerical results are given in Table 7.4. For this case, the reference predictive failure probability is such that

$\widetilde{P}_{\text{f,ref}} = 2.05 \times 10^{-5}$. Reference values for $S^{\mathbb{1}_{\mathcal{F}}}$-indices have been obtained by CMC, with $N = 10^8$ samples and $N_{\text{rep}} = 100$ replications. Numerical results for the proposed methodology have been obtained for the following settings: $n_{\text{set}} = 10$ elite sets of $N_{\text{fail}} = 500$ failure samples have been obtained by repetition of the SS algorithm (with 5×10^3 samples/step, an α_{SS}-quantile set to 0.75 and a final MCMC-based resampling step of 5×10^3 samples whose only the first 10 % samples are kept). In addition to that, one generates $N_{\text{gen}} = 5 \times 10^5$ samples on which one evaluates the densities and compute the variance of the ratio. Thus, one can notice that the first order indices are rather correctly estimated, at a relative moderate cost compared to CMC and high success rates. As for the total indices, almost all of them have been correctly estimated. However, the smallest one, associated to M_{X_1}, is over-estimated at a low success rate of 50 %.

TABLE 7.4: Results for Example #1 (★).

Variable	First order indices			Total indices		
	Ref. CMC	SS + G-KDE	Success rate	Ref. CMC	SS + G-KDE	Success rate
M_{X_1}	7.8×10^{-8}	2.6×10^{-6}	(100 %)	0.176	0.394	(50 %)
S_{X_1}	2.0×10^{-5}	3.5×10^{-5}	(100 %)	0.539	0.517	(100 %)
U_{X_1}	0.026	0.016	(100 %)	0.998	0.990	(100 %)
X_2	4.6×10^{-4}	1.3×10^{-3}	(100 %)	0.902	0.906	(100 %)
X_3	7.4×10^{-5}	8.7×10^{-5}	(100 %)	0.659	0.700	(100 %)

7.5.2 Example #2: a truss structure

Description. The second example (issued from Wei et al. (2012)) is a roof structure whose behavior is modeled by a truss as sketched in Figure 7.4. For the bars, two different materials are assumed: the top boom and the compression bars are reinforced by concrete (denoted by the subscript c in the mechanical characteristics) while the bottom boom and the tension bars are made of steel (denoted by the subscript s in the mechanical characteristics). A uniformly distributed load q is applied to the roof. As a result of the modeling, one can reduce it to nodal loads $P = ql/4$ applied respectively on nodes C, D and F. The failure of such a structure can be attained if the deflection of node C (denoted by Δ_C) reaches a given threshold Δ_{th}. Such a scenario is given by the following LSF:

$$g(\mathbf{X}) = \Delta_{\text{th}} - \mathcal{M}(\mathbf{X}) = 0.025 - \Delta_C. \tag{7.33}$$

The analytical formulation of Δ_C can be derived from the basic principles of structural mechanics applied to trusses. As a result, one has the following deflection formula (Wei et al., 2012):

$$\Delta_C = \frac{ql^2}{2}\left(\frac{3.81}{A_c E_c} + \frac{1.13}{A_s E_s}\right) \tag{7.34}$$

where l denotes the total length of the basis of the truss, A_c and A_s the sectional areas of, respectively, the concrete and steel bars, and finally E_c and E_s the Young's modulus of concrete and steel. Thus, one has to consider a 6-dimensional input random vector, such that $\mathbf{X} = (q, l, A_s, A_c, E_s, E_c)^\top$, composed of independent Gaussian variables as described in Table 7.5.

Considering a single-level of uncertainty in input, the reference failure probability estimated using CMC (with $N = 10^6$ samples and $N_{\text{rep}} = 100$ replications) is $p_{\text{f,ref}} = 1.27 \times 10^{-2}$. Under a bi-level uncertainty, one assumes that the probabilistic model of the first input variable X_1 is not perfectly known (see Table 7.2). Thus, one considers the following decomposition:

$$X_1 = M_{X_1} + \sigma_{X_1} U_{X_1} \tag{7.35}$$

where M_{X_1} follow respectively a prior distribution described in Table 7.5, while σ_{X_1} is supposed to be well known. As for U_{X_1}, it represents the natural variability of the input X_1 and is thus modeled by a standard Gaussian random variable.

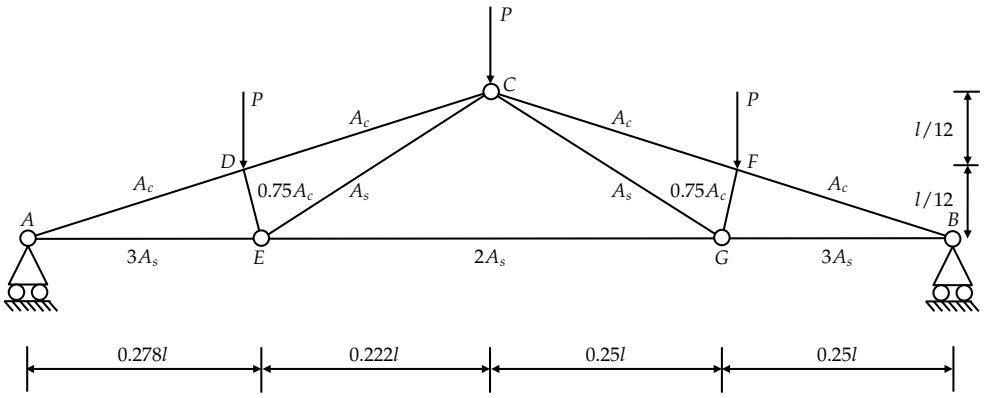

FIGURE 7.4: A roof truss.

TABLE 7.5: Input probabilistic model for Example #2.

Variable X_i	**Distribution**	**Mean** μ_{X_i}	**S.d.** σ_{X_i}
$X_1 = q$ (N.m^{-1})	Normal	μ_{X_1} ***uncertain*** [a]	$0.08 \times 20\,000$
$X_2 = l$ (m)	Normal	$\mu_{X_2} = 12$	$0.02 \times \mu_{X_2}$
$X_3 = A_s$ (m^2)	Normal	$\mu_{X_3} = 9.82 \times 10^{-4}$	$0.06 \times \mu_{X_3}$
$X_4 = A_c$ (m^2)	Normal	$\mu_{X_4} = 0.04$	$0.2 \times \mu_{X_4}$
$X_5 = E_s$ (N.m^{-2})	Normal	$\mu_{X_5} = 1.2 \times 10^{11}$	$0.07 \times \mu_{X_5}$
$X_6 = E_c$ (N.m^{-2})	Normal	$\mu_{X_6} = 3 \times 10^{10}$	$0.08 \times \mu_{X_6}$
M_{X_1}	Normal	20 000	$0.05 \times 20\,000$
U_{X_1}	Normal	0	1

[a] For the fixed value $\mu_{X_1} = 20\,000$, $p_{\text{f,ref}} = 1.27 \times 10^{-2}$.

Results. Figure 7.5a and Figure 7.5b provide the reference results for the estimation of both first-order and total $S^{\mathbb{1}_\mathcal{F}}$-indices under a single-level uncertainty. Based on these plots, one can notice first, that X_4 presents the largest first order index, and second, that the total indices indicate a partition into three groups of inputs: (X_4, X_1) show the strongest indices, then (X_2, X_3, X_5) have quasi-similar values for their indices, and finally X_6 (these results are coherent with those obtained by Wei et al. (2012)).

Under a bi-level uncertainty, it is assumed that the mean of X_1 is affected by epistemic uncertainty. Thus, X_1 has been desaggregated into M_{X_1} and U_{X_1}. As a result, Figure 7.6a and Figure 7.6b show that it is U_{X_1} is the second most influential input regarding first-order indices. As for total indices, one can see that the group (X_4, U_{X_1}) is the most influential, followed by (M_{X_1}, X_2, X_3, X_5) and finally X_6. Thus, again, the epistemic uncertainty affecting the mean of X_1 plays a non-negligible role on the variability of the indicator function, mainly due to interactions with other inputs.

The numerical results obtained by the proposed methodology are given in Table 7.6. These results have been obtained for the following settings: $n_{\text{set}} = 50$ elite sets of $N_{\text{fail}} = 2 \times 10^3$ failure samples have been obtained by repetition of the SS algorithm. In addition to that, one generates $N_{\text{gen}} = 1 \times 10^4$ samples on which one evaluates the densities and compute the variance of the

ratio. Thus, one can notice, by comparing the second and third columns, that the first order indices are almost perfectly estimated (only the strongest index associated to X_4 is moderately over-estimated), at a lower cost compared to CMC and with the highest success rates for all the indices. As for the total indices, some of them are perfectly estimated while others show a relative bias. Moreover, the ranking is slighty modified between M_{X_1} and X_3. However, the reference values are also very close. Thus, the proposed methodology is able to catch, at least, accurate orders of magnitude. Finally, one can see that the success rates of total indices do not reach values under 82 %.

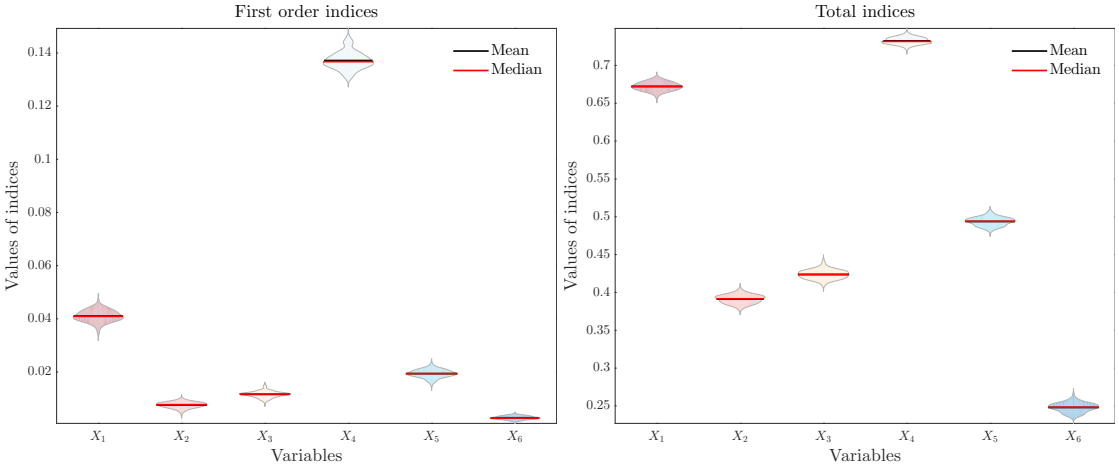

FIGURE 7.5: Reference $S^{\mathbb{1}_{\mathcal{F}}}$-indices estimated for the Example #2 under a single-level uncertainty (CMC of $N_{\text{sim}} = 10^6$ samples and $N_{\text{rep}} = 100$ repetitions, with $p_{\text{f,ref}} = 1.26 \times 10^{-2}$).

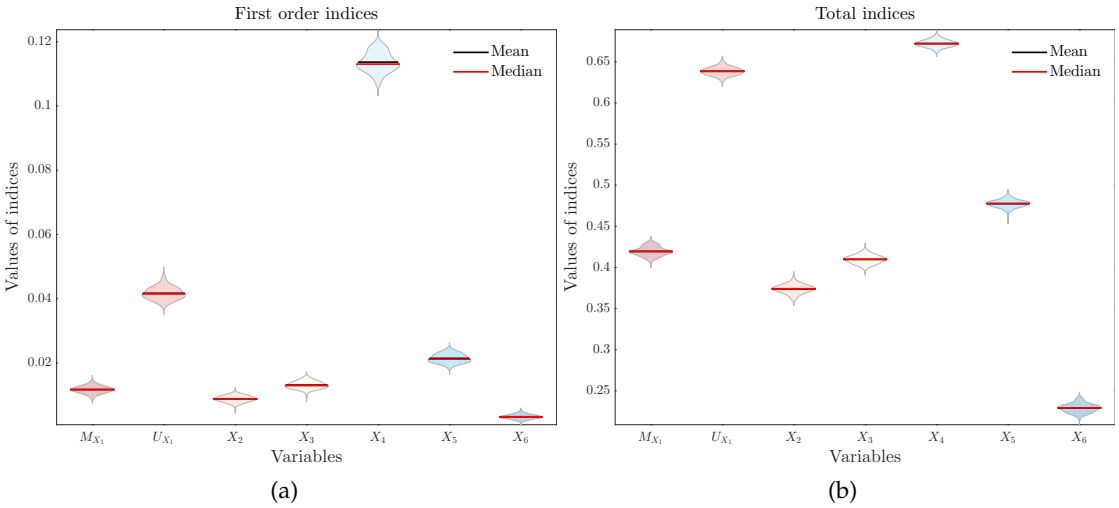

FIGURE 7.6: Reference $S^{\mathbb{1}_{\mathcal{F}}}$-indices estimated for the Example #2 under a bi-level uncertainty (CMC of $N_{\text{sim}} = 10^6$ samples and $N_{\text{rep}} = 100$ repetitions, with $\widetilde{P}_{\text{f,ref}} = 1.65 \times 10^{-2}$).

TABLE 7.6: Results for Example #2.

Variable	First order indices			Total indices		
	Ref. CMC	SS + G-KDE	Success rate	Ref. CMC	SS + G-KDE	Success rate
M_{X_1}	0.012	0.012	(100 %)	0.420	0.346	(98 %)
U_{X_1}	0.042	0.046	(100 %)	0.639	0.567	(100 %)
X_2	8.8×10^{-3}	9.1×10^{-3}	(100 %)	0.374	0.297	(94 %)
X_3	0.013	0.015	(100 %)	0.410	0.365	(94 %)
X_4	0.114	0.145	(100 %)	0.672	0.643	(100 %)
X_5	0.021	0.023	(100 %)	0.478	0.444	(100 %)
X_6	3.2×10^{-3}	3.4×10^{-3}	(100 %)	0.229	0.207	(82 %)

7.5.3 Synthesis about numerical results and discussion

As a synthesis, and according to the numerical results presented previously, one can highlight a few characteristics and perspectives about the proposed methodology:

- the proposed methodology allows to investigate the impact of the relative part of epistemic uncertainty and aleatory uncertainty to the variability of the indicator function (which is directly linked to the variability of the failure probability as showed in Eq. (7.1));
- the coupling between ARA/SS and the data-driven tensorized G-KDE seems to provide very promising results for global ROSA under a bi-level uncertainty, especially concerning the reduction in terms of computational cost compared to CMC, since this methodology only requires a post-treatment of an elite set obtained after a reliability analysis;
- the methodology seems able to handle moderate dimensions, at least, greater dimensions for which traditional KDE fails to estimate correctly multivariate densities;
- this methodology is driven by several tuning parameters which may influence drastically the results: the quality of the elite set (influenced by the tuning of the SS algorithm), the number N_{fail} of failure samples in the elite set and the number N_{gen} of generated samples to compute the variance. As for n_{set}, it is important to notice that, in practice, for costly-to-evaluate computer models (and rare event probability estimation), it might not be possible to get neither multiple not large-sample-size elite sets.

7.6 Conclusion

In this chapter, a new methodology is proposed to estimate, at a lower computational cost than CMC, a set of $S^{\mathbb{1}_{\mathcal{F}}}$-indices, in the context of bi-level input uncertainty. This methodology relies on the combination of three main components:

- first, a disaggregated structure of the inputs that are affected by epistemic uncertainty;
- second, the use of the SS algorithm to get an estimate of the predictive failure probability and, jointly, to use the final elite set of failure samples to estimate the $S^{\mathbb{1}_{\mathcal{F}}}$-indices;
- third, a data-driven tensorized G-KDE which allows to improve the density estimation required to compute the indices.

The combination of these three tools allows to propose a methodology whose efficiency has been observed on two numerical test-cases. Moreover, the influence of the failure event rareness has been investigated too. However, this work only provides promising preliminary results. Indeed

as mentioned in the results, some numerical experiments can lead to negative values of the $S^{\mathbb{1}_{\mathcal{F}}}$-indices as indicated by the "success rate" scores. Thus, the proposed methodology might be not suited to a use as a one-shot methodology. Its robustness should be improved, mainly by investigating the potential reasons for such a failure in terms of estimation (e.g., possible insufficiency in terms of budget allocation / inaccuracy of the KDE / inefficiency of the resampling phase using MCMC creating correlated samples).

In the next chapter, the methodologies developed in Chapter 5, Chapter 6 and in the present chapter, are applied on a real aerospace test-case, i.e., a launcher stage fallout test-case, to demonstrate both the applicability and the practical interests of the proposed methodologies when facing bi-level input uncertainty in both rare event probability estimation and ROSA contexts.

CHAPTER 8

Application to a launcher stage fallout test-case

Contents

8.1 Introduction and motivations

The role of a *launch vehicle* (a.k.a. *space launcher*) is to carry a payload (e.g., a satellite) from the Earth's surface to a given orbit. A traditional *expendable* space launcher is composed of multiple stages, equipped with their propulsion systems. An example of such a launch vehicle is given in Figure 8.1. During the flight, uncertainties can affect several variables in multiple disciplines (e.g., on the perturbation during trajectory or propellant combustion). For instance, focusing on the optimal trajectory assessment leads to consider the *separation point* (denoted by "stage separation" in Figure 8.1) as a key point in terms of uncertainty analysis. For instance, the first stage of a light VEGA type launcher is jettisoned at an altitude of around 61 km (Arianespace, 2014) while the solid rocket boosters of the heavy ARIANE 5 launcher are jettisoned at an altitude of around 69 km (Arianespace, 2016). Thus, such altitudes are still lower than the *Kármán line* [1] so that wind perturbations might affect their dynamics. As a consequence, the handling of uncertainties (e.g., arising from dynamic perturbations, error measurements due to sensors or varying unburned propellant left mass) plays a crucial role in the comprehension and prediction of the global system behavior. That is the reason why it is of prime importance to take it into account during the reliability analysis and the prediction of the fallout zone. A misestimation can have dramatic consequences in terms of launcher safety, human security and environmental impact.

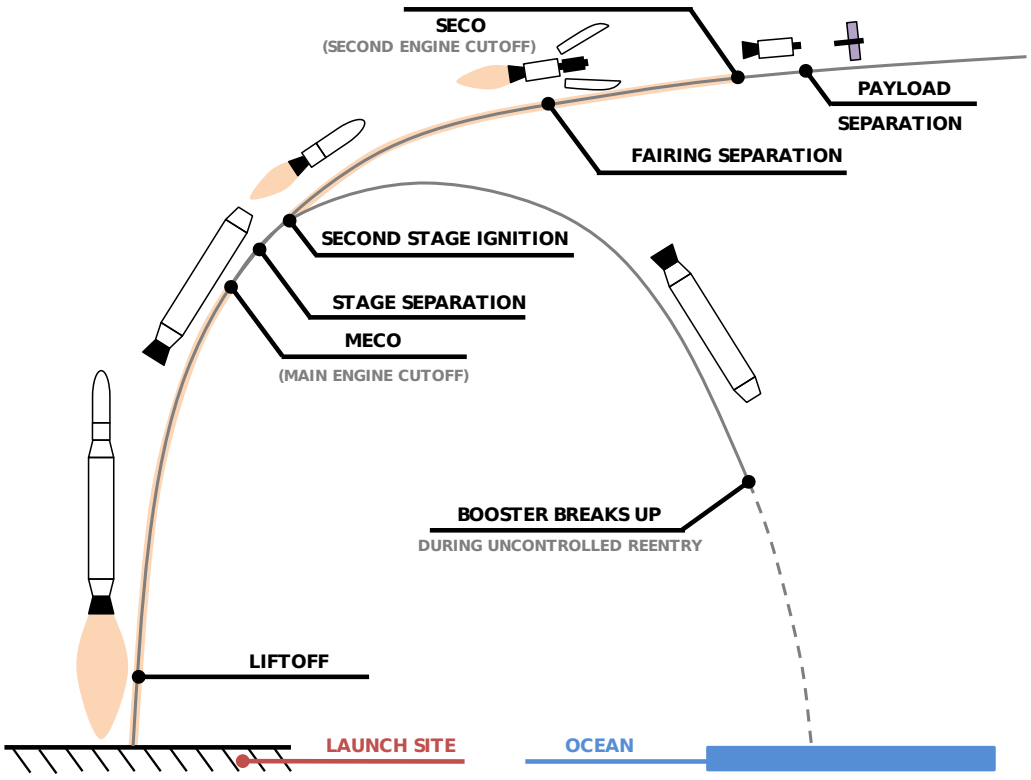

FIGURE 8.1: Illustration scheme of a first stage fallout phase (recreated and adapted from an infographic by Jon Ross, see http://www.zlsadesign.com).

[1] The Kármán line denotes the boundary between the Earth's atmosphere and outer space. The practical use of such a limit mainly appears to consider when the effects of the atmosphere might become negligible. Traditionally set to a 100 km altitude for common applications, some researchers recently advocated that a value of 80 km altitude would be more realistic (McDowell, 2018).

The goal of this chapter is to present a simplified, but representative, fallout trajectory simulation model. Indeed, this model is representative of the phenomena encountered but with a reduced simulation cost (e.g., use of mass point model) while remaining challenging enough regarding the use of advanced rare event estimation techniques and sensitivity analysis methods. For more realistic problems, one can refer to Ronse and Mooij (2014), Ridolfi and Mooij (2016), Hoogendoorn et al. (2018), and Geul et al. (2018). In these studies, other parameters are considered and investigated concerning the dynamics of the vehicle (e.g., perturbation of atmospheric density, winds). In the present chapter, they are not taken into account for the sake of simplicity and interpretation of the given results, but they remain parameters that should be incorporated in the model to get a full high-fidelity simulation model.

The launcher stage fallout simulation computer code may be represented as an input-output black-box model. The input variables are, among others, some characteristics of the launcher and some conditions (initial or arising during the flight) of the fallout phase. These inputs are affected by uncertainties and are gathered in a random vector with a given PDF. It is assumed that this PDF is described by a parametric model of density. The output corresponds to the position of fallout and is also a random variable because of the input randomness. A typical safety measure can be the probability that a stage (e.g., the first stage) falls at a distance greater than a given safety limit. Indeed this estimation is strategic for the qualification of such vehicles.

This chapter is organized as follows. Section 8.2 describes the physical model and describes the sources of uncertainties. Section 8.3 defines the input probabilistic model, the failure scenario and the associated LSF. Section 8.4 proposes a first preliminary analysis to get more insight about the behavior of the system at failure. Then, Section 8.5, Section 8.6 and Section 8.7 aim at applying the three methodologies presented in the three previous chapters (i.e., efficient estimation of the predictive failure probability, local ROSA and global ROSA, all of them within the ARA framework) to the aerospace test-case. Finally, a conclusion gathering the most important results of this chapter is given in Section 8.8.

8.2 Description of the physical model

Space launcher complexity arises from the coupling between several subsystems, such as stages or boosters and other embedded systems.

The simulation model used in this chapter can be considered as a black-box model denoted by $\mathcal{M} : \mathbb{R}^{d=6} \to \mathbb{R}$. Here, it is a simplified trajectory simulation code of the dynamic fallout phase of a generic launcher first stage. The avantage of a black-box model is to enlarge the applicability of the proposed statistical approaches illustrated in this chapter to any test-cases in this range of models. As a matter of fact, the following methods proposed in this chapter are said to be "non-intrusive" w.r.t. the model under study. The d-dimensional (here $d = 6$) input vector of the simulation code, denoted by $\mathbf{X}$, contains the following basic variables (i.e., physical variables) modeling some initial conditions, environmental variables and launch vehicle characteristics:

X_1: stage altitude perturbation at separation Δa (m);

X_2: velocity perturbation at separation Δv (m.s^{-1});

X_3: flight path angle perturbation at separation $\Delta\gamma$ (rad);

X_4: azimuth angle perturbation at separation $\Delta\psi$ (rad);

X_5: propellant mass residual perturbation at separation Δm (kg);

X_6: drag force error perturbation ΔC_d (dimensionless).

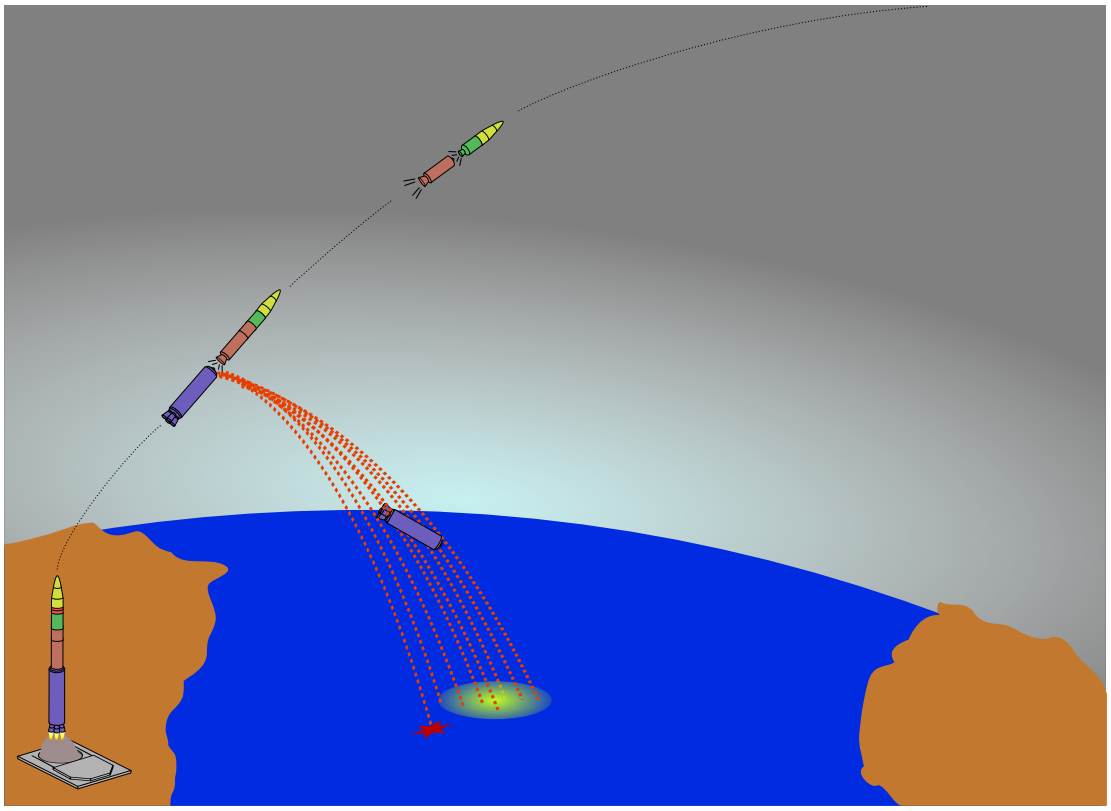

FIGURE 8.2: Illustration scheme of a launch vehicle first stage fallout phase into the Atlantic Ocean. Multiple fallout trajectories are drawn (red dotted lines), leading to the impact zone (yellow circular surface). Due to uncertainties, one fallout trajectory may lead to a failure impact point (red star).

These variables are assumed to be independent for the sake of simplicity. As an output, the code will give back the scalar distance $Y = \mathcal{M}(\mathbf{X})$ which represents the distance D_{code} between the theoretical fallout position into the ocean and the estimated one due to the uncertainty propagation.

8.3 Input probabilistic model and limit-state function

In the context of the launch vehicle fallout case, the input variables are known to be affected by uncertainties (e.g., , due to the natural variability of wind or due to lack-of-knowledge). Thus, applying UQ methodology leads to consider a probabilistic model for the input vector $\mathbf{X}$, i.e., by assuming the existence of a joint PDF $f_{\mathbf{X}} : \mathcal{D}_{\mathbf{X}} \subseteq \mathbb{R}^d \to \mathbb{R}_+$. Since the input variables are assumed to be independent, this joint PDF corresponds to the product of the marginal PDFs f_{X_i} of the input variables X_i, $i \in \{1, \ldots, d\}$. The input probabilistic model for the launch vehicle fallout case is given in Table 8.1. Note that the numerical values used in this test-case are hypothetic and should not be used for industrial applications.

TABLE 8.1: Input probabilistic model.

Variable X_i [a]	**Distribution**	**Mean** μ_{X_i}	**S.d.** σ_{X_i}
$X_1 = \Delta a$ (m)	Normal	0	1650
$X_2 = \Delta v$ (m.s^{-1})	Normal	0	3.7
$X_3 = \Delta\gamma$ (rad)	Normal	0	0.001
$X_4 = \Delta\psi$ (rad)	Normal	0	0.0018
$X_5 = \Delta m$ (kg)	Normal	0	70
$X_6 = \Delta C_d$ (1)	Normal	0	0.1

[a] The input variables are independent.

The input probabilistic model is given in Table 8.1. The code output is the distance D_{code} between the theoretical fallback position into the ocean and the estimated one. For the sake of clarity, one recalls that the LSF $g(\cdot)$ can be written as follows:

$$g(\mathbf{X}) = d_{\text{safe}} - \mathcal{M}(\mathbf{X}) = d_{\text{safe}} - D_{\text{code}} \tag{8.1}$$

for which the rareness of the failure event depends on the safety threshold distance d_{safe}.

8.4 Preliminary analysis of the limit-state surface

As a preliminary analysis of the black-box model, one can transform the problem set in the original physical space (a.k.a. **x**-space) into the standard Gaussian space (a.k.a. **u**-space) by using one of the transformations recalled in Appendix C. Then, one can use FORM in the first place (see Chapter 3). The idea is not only to get a first estimate of the failure probability (whose value may be completely wrong if the LSS turns out to be nonlinear), but, above all, to find a first MPFP. Based on this first MPFP, one can use it to visualize the shape of the failure domain, i.e., how the LSS behaves. Indeed, in the **u**-space, one can consider *two-dimensional cross-cuts* by fixing all the inputs but two and solving the LSF equation on a regular grid (e.g., as performed in Dubourg (2011) and Bourinet (2016)). These cross-cuts may be helpful to get a first insight about the behavior of the LSS within the **u**-space, where visualization is the easiest one. Similar cross-cuts in the **x**-space could be, for heteregeneous input random vector $\mathbf{X}$ (i.e., different probability distributions with very different ranges of values), complicated to get and not easy to plot.

As an example, Figure 8.3 provides the cross-cuts in the (u_i, u_j)-plane for the launcher stage fallout test case. The black cross is the origin and the black square represents the MPFP found by applying FORM. The black line is the limit-state surface (LSS), formally defined by the set $\mathcal{F}_{\mathbf{u}}^0 = \{\mathbf{u} \in \mathbb{R}^d \mid \mathring{g}(\mathbf{u}) = 0\}$, which highlights the separation between the safe domain (in green/light grey) and the failure domain (in orange/dark grey). By definition, the LSS belongs to the failure domain.

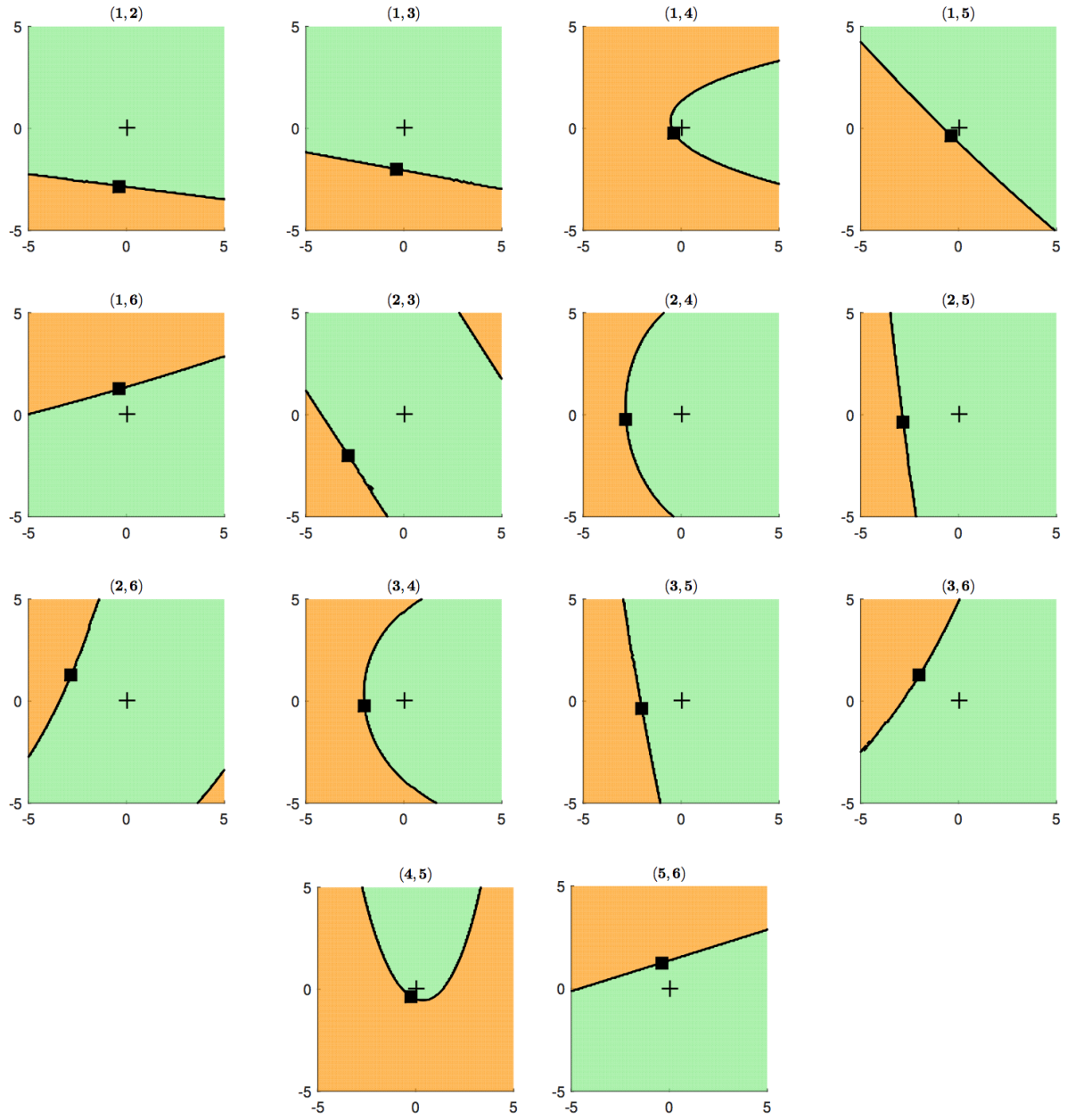

FIGURE 8.3: Illustration of cross-cuts in the **u**-space.

By analyzing these cross-cuts, one can formulate the following remarks:

- firstly, one can notice that, for some combinations, the LSS is highly nonlinear (e.g., for the pairs (u_1, u_4), (u_2, u_4), (u_3, u_4), (u_4, u_5)). Moreover, one can see that these nonlinearities seem to be specific to the variable X_4, i.e., the azimuth angle perturbation at separation. Such nonlinearities indicate that any method relying on a linear assumption of the LSS (such as FORM) should be avoided for reliability assessment in this specific case;

- secondly, one can notice that the two cross-cuts $((u_2, u_3), (u_2, u_6))$ present possible multiple MPFPs. In particular, (u_2, u_3) would suggest the presence of a second MPFP of opposite coordinates.

As explained in Chapter 3, tracking multiple MPFPs can be achieved using the "*multi*-FORM" algorithm proposed by Der Kiureghian and Dakessian (1998). Briefly, this method consists in repeating a FORM analysis with a modified LSF which triggers the search outside the area where a MPFP has been found. Here, by applying this method, one can find that a second MFPF exists with the coordinates in the **u**-space given by $(u_2, u_3) = (3.084, 2.058)$ and $(u_2, u_6) = (3.084, -1.798)$. This result is just a qualitative example which should highlight that, MPFP-based techniques can be useful to learn some key characteristics of a black-box model (e.g., non-linearity of the LSS, curvatures, possible multiple MPFPs). These key characteristics can then be taken into account to choose a dedicated technique to correctly estimate the failure probability. For instance, if one knows that the problem presents multiple MPFPs of possible almost equal importance, one should, for example, avoid FORM-IS and recourse to advanced sampling techniques such as adaptive IS techniques or subset sampling.

As highlighted in the present section, the black-box model under study present a few key characteristics which have to be kept in mind in the following phases:

- it is of moderate input dimension ($d = 6$);
- the inputs are independent Gaussian variables;
- the rareness of the failure event depends on the safety threshold d_{safe};
- the LSS is highly nonlinear in the **u**-space and might present multiple MPFPs (i.e., mutliple failure regions);

In the following, one will investigate the impact of the lack-of-knowledge (i.e., epistemic uncertainty arising from lack of data or measurement uncertainty) about a few distribution parameters set in Table 8.1. The idea is then to evaluate the impact of such a bi-level uncertainty through a three-step long study: firstly, on the reliability assessment (called **Step #1**); secondly, by testing the robustness of the reliability assessment w.r.t. to the local prior parametrization (called **Step #2**); and thirdly, by investigating the impact of the bi-level uncertainty level at failure (called **Step #3**). As a remark, one should notice that the same comparison metrics such as those described in Chapter 5 are used in the numerical applications.

8.5 Step #1: reliability assessment under distribution parameter uncertainty

In this first step, it is assumed that the mean values of the basic variables X_2 (i.e., the velocity perturbation at separation) and X_3 (i.e., the flight path angle perturbation at separation) are uncertain. As they are related to physical quantities which are very difficult to measure and to control in reality, it is supposed that they are affected by epistemic uncertainty and modeled using prior distributions detailed in Table 8.2.

8.5.1 Simulation settings

For the numerical experiments, simulation settings have been defined as follows. Firstly, the threshold safety distance d_{safe} is set to 20 km so as to reach a reference probability without parameter uncertainty $p_{\text{f,ref}}$ equal to 2.31×10^{-7} (estimated by CMC with 10^8 samples and confirmed by SS with 10^3 samples/step). Then, for both NRA and ARA (see Chapter 5), three rare event probability estimation techniques are investigated:

- CMC as a reference technique;

- FORM as it is widely used in daily industrial practice and to be consistent with the results presented in Chapter 5. As a remark, even if, in this case, one already knows from the analysis conducted in Section 8.4 that the LSS is highly nonlinear in the **u**-space and that FORM is not adapted to this problem, conducted FORM analysis still provides a worst-case estimation comparison which can still be relevant during the reliability analysis phase;
- SS as it is a widely used advanced sampling technique which will be considered as sufficiently representative of the most advanced variance reduction techniques.

TABLE 8.2: Input probabilistic model under bi-level input uncertainty.

Variable [a]	**Distribution**	**Mean**	**S.d.**
$X_1 = \Delta h$ (m)	Normal	$\mu_{X_1} = 0$	$\sigma_{X_1} = 1650$
$X_2 = \Delta v$ (m.s^{-1})	Normal	μ_{X_2} ***uncertain*** [b]	$\sigma_{X_2} = 3.7$
$X_3 = \Delta\gamma$ (rad)	Normal	μ_{X_3} ***uncertain***	$\sigma_{X_3} = 0.001$
$X_4 = \Delta\psi$ (rad)	Normal	$\mu_{X_4} = 0$	$\sigma_{X_4} = 0.0018$
$X_5 = \Delta m$ (kg)	Normal	$\mu_{X_5} = 0$	$\sigma_{X_5} = 70$
$X_6 = \Delta C_d$ (1)	Normal	$\mu_{X_6} = 0$	$\sigma_{X_6} = 0.1$
$\Theta_2 = \mu_{X_2}$ (m.s^{-1})	Normal	$\xi_1 = \mu_{\mu_{X_2}} = 0$	$\xi_2 = \sigma_{\mu_{X_2}} = 3.7$
$\Theta_3 = \mu_{X_3}$ (rad)	Normal	$\xi_3 = \mu_{\mu_{X_3}} = 0$	$\xi_4 = \sigma_{\mu_{X_3}} = 0.001$

[a] The basic variables are independent.
[b] For fixed values $\mu_{X_2} = 0$ and $\mu_{X_3} = 0$, one has:
▷ for $d_{\text{safe}} = 15$ km, $p_{\text{f,ref}} = 1.36 \times 10^{-4}$;
▷ for $d_{\text{safe}} = 20$ km, $p_{\text{f,ref}} = 2.31 \times 10^{-7}$.

8.5.2 Results and discussion

Numerical results gathered in Table 8.3 show that both NRA/CMC and ARA/CMC give similar results and manage to correctly estimate the predictive failure probability (whose reference value is given below Table 8.3). NRA/SS and ARA/SS provide close results even if one can notice a significant value of the efficiency ($\nu > 20$) for ARA/SS which indicates how promising is the use of ARA/SS with such an industrial test-case. As for NRA/FORM and ARA/FORM, they both give poor results. ARA/FORM manages to give, at least, an order of magnitude of the predictive failure probability quite close to the reference one. A possible explanation for this could be that, adding a second uncertainty level on μ_{X_2} and μ_{X_2}, one made one of the MPFPs be more dominant than the other one.

As explained in Chapter 5 (see Subsection 5.3.1), the launcher fallout case is a complex computer model for which adding an extra sampling loop could be cumbersome. Here, two uncertain distribution parameters are considered, which means that the integration domain is $\mathbb{R}^2$. The quadrature type is chosen to be a *Gauss-Hermite quadrature scheme*, which means that one uses Gaussian weights (see, e.g., Heiss and Winschel, 2007; Heiss and Winschel, 2008). Depending on the problem dimensionality, one can choose an accuracy level M_{acc} which allows to integrate complete polynomials of total order $2M_{acc} - 1$ exactly. Here, an accuracy level $M_{acc} = 14$ is chosen so as to provide enough samples (here, it corresponds exactly to 1009 samples) to cover the domain $\mathcal{D}_{\boldsymbol{\Theta}}$. Such a choice is constrained by the expensive aspect of the computer code. However, for different applications, one could choose another accuracy level. Finally, coupling this DOE with a SS technique with 10^4 samples/step allows to estimate the reference predictive failure probability $\widehat{\widetilde{P}}_{\text{f,ref}}$. A last remark concerns the fact that taking only two parameters out of six basic variables as being uncertain implies to increase the failure probability of three logarithmic decades in terms of magnitude compared to the single-level reference estimate. Again,

that emphasizes how crucial taking distribution parameters uncertainty is during the reliability analysis phase.

TABLE 8.3: Results for Step #1.

Approach	**Estimates** [a]				
	$m_{\widehat{\widehat{P}}_f}$	$S^2_{\widehat{\widehat{P}}_f}$	RE	RB	ν
NRA/CMC [b]	1.18×10^{-4}	8.82×10^{-11}	7.97×10^{-2}	–	–
ARA/CMC	1.27×10^{-4}	1.05×10^{-10}	8.07×10^{-2}	–	–
NRA/FORM	9.16×10^{-3}	1.11×10^{-4}	1.15	75.32	–
ARA/FORM	8.28×10^{-5}	–	–	-0.35	–
NRA/SS [c]	1.13×10^{-4}	4.98×10^{-9}	0.63	-6.09×10^{-2}	5.65×10^{-2}
ARA/SS	1.25×10^{-4}	1.52×10^{-9}	0.31	-1.57×10^{-2}	20.6

[a] **Ref. (Gauss-Hermite with $N_{\boldsymbol{\theta}} = 1009$ samples + SS with $N_{\mathbf{x}} = 10^4$ samples/step):** $\widehat{\widehat{P}}_{\text{f,ref}} = 1.20 \times 10^{-4}$.
[b] NRA: $N_{\boldsymbol{\theta}} = 10^3$ samples, $N_{\mathbf{x}} = 10^3$ samples | ARA: $N_{\mathbf{x},\boldsymbol{\theta}} = 10^6$ samples.
[c] NRA: $N_{\boldsymbol{\theta}} = 10^3$ samples, $N_{\mathbf{x}} = 10^3$ samples/step | ARA: $N_{\mathbf{x},\boldsymbol{\theta}} = 10^3$ samples/step.

8.6 Step #2: local ROSA under distribution parameter uncertainty

In this second step, the same input probabilistic model as set in Table 8.2 is considered. In this section, the idea is to investigate the local robustness of the predictive failure probability estimate w.r.t. the choice of the hyper-parameters $\boldsymbol{\xi}$.

8.6.1 Simulation settings

For the numerical experiments, simulation settings have been defined as follows. Firstly, concerning the LSF, two cases are treated to investigate the influence of the rareness of the failure event:

- in the first place, the safety threshold distance is set to $d_{\text{safe}} = 15$ km;
- then, it is set to $d_{\text{safe}} = 20$ km (denoted by the sign ★).

Secondly, using the ARA framework solely (see Chapter 5), three rare event probability estimation techniques are investigated in this part:

- ARA/CMC as the reference technique;
- ARA/AIS-CE, i.e., a parametric adaptive IS technique based on cross-entropy optimization;
- ARA/NAIS, i.e., a nonparametric adaptive IS technique based on kernel density estimation.

Note that, in the following, the term "ARA/AIS" (see, e.g., for the efficiency $\nu^{\text{ARA/AIS}}$) symbolizes a generic denomination for both adaptive IS sampling techniques, ARA/AIS-CE and ARA/NAIS.

8.6.2 Results and discussion

Numerical results gathered in Table 8.4 show that both techniques manage to correctly estimate the predictive failure probability. As a first remark, this predictive failure probability is slightly greater than the failure probability under single-level uncertainty whose reference

value $p_{\mathrm{f,ref}}$ recalled below Table 8.2. This emphasizes how taking uncertainty on the distribution parameters into account can be relevant regarding system safety. Then, one can highlight the fact that ARA/NAIS gets closer results to reference ones (obtained by ARA/CMC) than ARA/AIS-CE. The problem here is inherent to the cross-entropy method as it shows some difficulty to converge with a correct accuracy when the problem involves multiple failure regions. In terms of comparison, the predictive failure probability seems to be more sensitivive to the hyper-parameters ξ_4 and ξ_3 which are respectively the standard deviation and the mean of $\Theta_3 = \mu_{X_3}$. Here, the lack of knowledge affecting the mean value of the flight path angle perturbation really plays a key role on the final predictive failure probability. This can be a relevant information for refining the a priori probabilistic model for Θ_3 (especially in terms of variance reduction) and set up an investigation policy about the possible reduction of epistemic (statistical) uncertainty affecting Θ_3. Concerning the efficiencies, while ARA/AIS-CE is inefficient in this specific case where AIS-CE is not accurate enough, ARA/NAIS manages to provide a precise estimation for both the probability and the sensitivities. The convergence plot in Figure 8.4a illustrates these results. Note that, due to the small values for the sensitivities, the two curves for $\widehat{\partial \widetilde{P}_{\mathrm{f}}}/\partial\xi_1$ and $\widehat{\partial \widetilde{P}_{\mathrm{f}}}/\partial\xi_2$ are superimposed so that one cannot differentiate them.

In the rare event context (★, as given in Table 8.5, one can still see that ARA/NAIS provides better results than ARA/AIS-CE, even if this one still manages to get relevant orders of magnitude for both the probability and the sensitivities. However, the efficiency of ARA/AIS-CE is annealed by the poor accuracy of the estimation while ARA/NAIS outperforms ARA/CMC by allowing to reduce the simulation budget by 207. Similar comparisons can be drawn to the previous case regarding the relative influence of the hyper-parameters. However, one can still notice that increasing the rareness of the failure event decreased, in proportion, the relative influence of ξ_4. Finally, the global convergence of ARA/NAIS sensitivity estimation is represented in Figure 8.4b. Again, note that, due to the small values for the sensitivities, the two curves for $\widehat{\partial \widetilde{P}_{\mathrm{f}}}/\partial\xi_1$ and $\widehat{\partial \widetilde{P}_{\mathrm{f}}}/\partial\xi_2$ are superimposed so that one cannot differentiate them.

TABLE 8.4: Results for Step #2.

	ARA/CMC		**ARA/AIS-CE**		**ARA/NAIS**	
	($N_{\mathrm{x},\boldsymbol{\theta}} = 10^6$ samples)		($N_{\mathrm{x},\boldsymbol{\theta}} = 10^4$ samples/step)		($N_{\mathrm{x},\boldsymbol{\theta}} = 10^4$ samples/step)	
	Estimate	cv	Estimate	cv	Estimate	cv
$\widehat{\widetilde{P}}_{\mathrm{f}}$	4.40×10^{-3}	(1.38 %)	4.41×10^{-3}	(10.3 %)	4.40×10^{-3}	(2.08 %)
$\widehat{\partial \widetilde{P}_{\mathrm{f}}}/\partial\xi_1$	-9.13×10^{-4}	(3.44 %)	-8.68×10^{-4}	(27.7 %)	-9.12×10^{-4}	(5.90 %)
$\widehat{\partial \widetilde{P}_{\mathrm{f}}}/\partial\xi_2$	2.95×10^{-3}	(2.32 %)	3.02×10^{-3}	(14.8 %)	2.95×10^{-3}	(3.22 %)
$\widehat{\partial \widetilde{P}_{\mathrm{f}}}/\partial\xi_3$	-2.31	(3.88 %)	-2.29	(25.7 %)	-2.30	(5.82 %)
$\widehat{\partial \widetilde{P}_{\mathrm{f}}}/\partial\xi_4$	6.43	(2.18 %)	6.26	(14.6 %)	6.41	(3.77 %)
$\nu^{\mathrm{ARA/AIS}}$	–	–	0.5	–	13	–

TABLE 8.5: Results for Step #2 considering the influence of the failure event rareness.

	ARA/AIS-CE (★) ($N_{\mathrm{x},\boldsymbol{\theta}} = 10^4$ samples/step)		**ARA/NAIS (★)** ($N_{\mathrm{x},\boldsymbol{\theta}} = 10^4$ samples/step)	
	Estimate	cv	Estimate	cv
$\widehat{\widetilde{P}}_{\mathrm{f}}$	1.00×10^{-4}	(29.7 %)	1.19×10^{-4}	(2.85 %)
$\widehat{\partial \widetilde{P}_{\mathrm{f}}/\partial \xi_1}$	-4.65×10^{-5}	(46.9 %)	-3.66×10^{-5}	(7.00 %)
$\widehat{\partial \widetilde{P}_{\mathrm{f}}/\partial \xi_2}$	1.21×10^{-4}	(40.3 %)	1.41×10^{-4}	(3.62 %)
$\widehat{\partial \widetilde{P}_{\mathrm{f}}/\partial \xi_3}$	-1.19×10^{-1}	(34.4 %)	-9.18×10^{-2}	(7.67 %)
$\widehat{\partial \widetilde{P}_{\mathrm{f}}/\partial \xi_4}$	2.51×10^{-1}	(25.2 %)	3.10×10^{-1}	(4.24 %)
$\nu^{\mathrm{ARA/AIS}}$	2	–	207	–

8.7 Step #3: global ROSA under distribution parameter uncertainty

In this third step, the idea is to investigate the global impact of the bi-level input uncertainty of the system at failure. To do so, one focuses on the Sobol indices on the indicator function (denoted by "$S^{\mathbb{1}_{\mathcal{F}}}$-indices") adapted to the bi-level input uncertainty, as presented in Chapter 7.

8.7.1 Simulation settings

Due to the presence of a bi-level input uncertainty and following the methodology proposed in Subsection 7.3.2, it is proposed to consider the following disaggregated inputs:

$$X_2 = M_{X_2} + \sigma_{X_2} U_{X_2} \tag{8.2}$$

$$X_3 = M_{X_3} + \sigma_{X_3} U_{X_3} \tag{8.3}$$

where M_{X_2} and M_{X_3} follow the same prior distributions as previously presented in Table 8.2, U_{X_2} and U_{X_3} are two standard Gaussian variables, and σ_{X_2} and σ_{X_3} are the two standard deviations defined in Table 8.2. Finally, one considers the following augmented input vector:

$$\mathbf{Z} = (\mathbf{V}_{\mathrm{dis}}, \mathbf{X}_{\mathrm{single}})^{\top} = (X_1, M_{X_2}, U_{X_2}, M_{X_3}, U_{X_3}, X_4, X_5, X_6)^{\top} \tag{8.4}$$

For the numerical experiments, simulation settings have been defined as follows. Firstly, concerning the LSF, two cases are treated to investigate the influence of the rareness of the failure event:

- in the first place, the safety threshold distance is set to $d_{\mathrm{safe}} = 11$ km (associated to a reference failure probability under single-level input uncertainty such that $p_{\mathrm{f,ref}} = 6.10 \times 10^{-3}$). This case is used to obtain reference results (using CMC) in order to have a better insight of what is at stake in terms of sensitivity indices.
- then, the safety threshold distance is set to $d_{\mathrm{safe}} = 15$ km. In such a case, only reference results in bi-level are provided and compared to those obtained from the proposed methodology.

Finally, concerning the proposed methodology, mean estimates of the sensitivity indices are provided together with a "success rate" which indicates, in percentage of the total number of

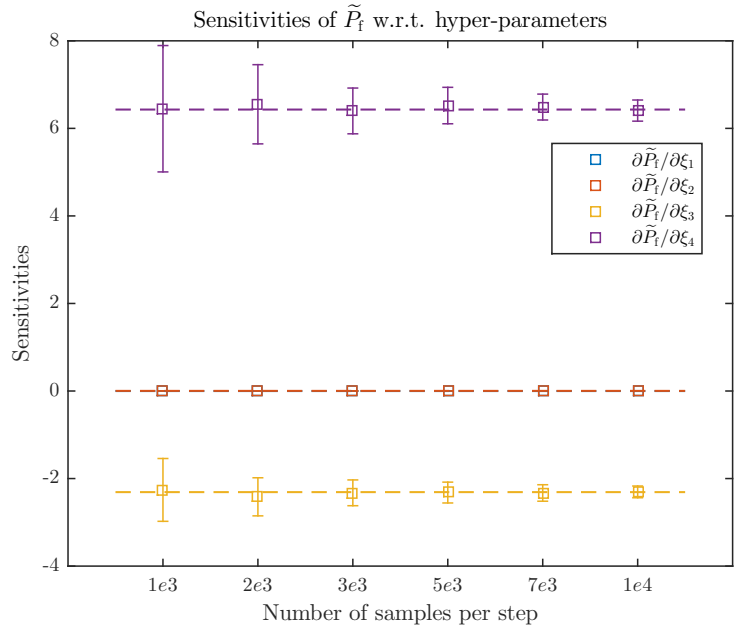

(a) Estimated sensitivities (error bars) vs. reference results obtained by ARA/CMC (dashed lines).

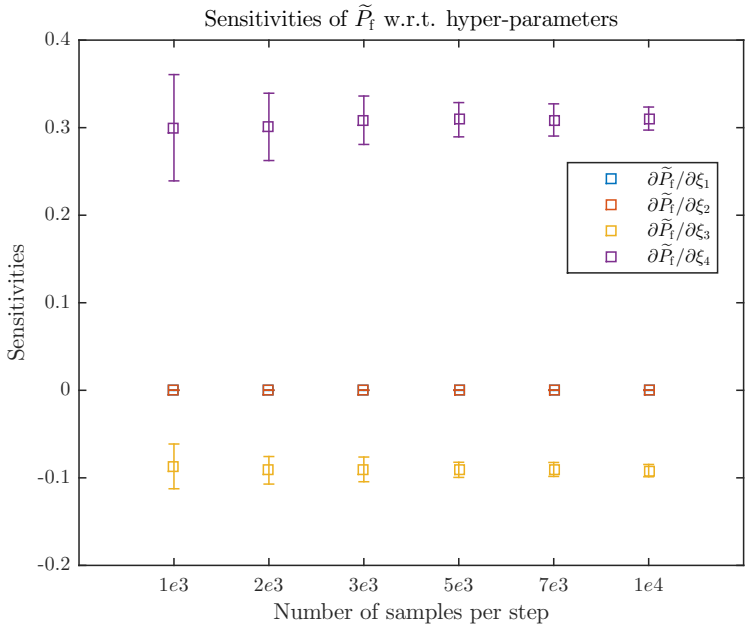

(b) Estimated sensitivities (error bars) in a context of rare event (★).

FIGURE 8.4: Convergence plots obtained by ARA/NAIS for Step #2.

repetitions, the number of experiments that have provided positive values of indices. If the index value is negative, the numerical experiment is considered as "failed" and the estimated value is removed.

8.7.2 Results and discussion

Figure 8.5a and Figure 8.5b provide the reference results for the estimation of both first-order and total $S^{\mathbb{1}_{\mathcal{F}}}$-indices under single-level uncertainty. Based on these plots, one can notice first,

that X_2 presents the largest first order index, and second, that the total indices indicate a partition into two groups of inputs: (X_2, X_3, X_6) show the strongest indices (above 0.50) while (X_1, X_4, X_5) have rather moderate values (around 0.15). Moreover, one can see that first-order indices are, for most of them, very low while total order indices are much stronger. This clearly indicates that variables interact a lot at failure but do not contribute that much on their own to the variability of the indicator function. Such a remark has been already pointed out in the work of Lemaître (2014).

Under bi-level uncertainty, Figure 8.6a shows that, for X_2, U_{X_2} is more influential than M_{X_2}, while for X_3, it is M_{X_3} which is more influential than U_{X_3}. This clearly highlights that, due to the disaggregated version of the augmented vector, one can analyze both effects from aleatory and epistemic uncertainties. Again, the first order indices are low which indicates a poor contribution of each variable to the overall variability of the indicator. As for total indices displayed in Figure 8.6b, one can observe the same ranking as for first-order indices. However, one can see the epistemic uncertainties affecting the mean value of X_2 and X_3 play a major role on the variability of the indicator function and have thus to be taken into account.

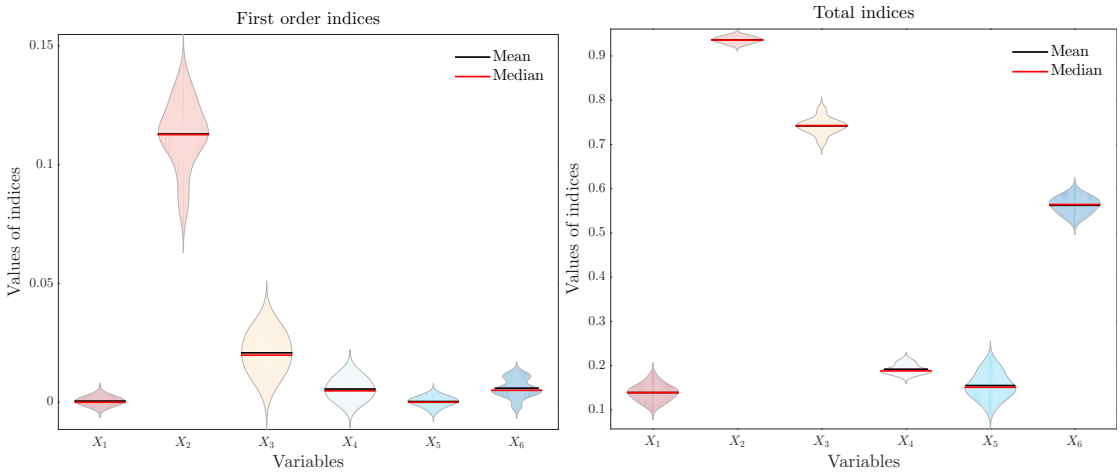

FIGURE 8.5: $S^{\mathbb{1}_{\mathcal{F}}}$-indices estimated under single-level uncertainty (CMC of $N_{\text{sim}} = 10^5$ samples and $N_{\text{rep}} = 10$ repetitions, with $p_{\text{f,ref}} = 6.10 \times 10^{-3}$).

When considering the case where d_{safe} is set to 15 km, numerical results obtained by the proposed methodology are given in Table 8.6. These results have been obtained for the following settings:

- $n_{\text{set}} = 35$ elite sets obtained after 35 repetitions of the SS algorithm;
- each elite set contains $N_{\text{fail}} = 2 \times 10^3$ failure samples resampled at the end of each application of SS;
- in addition to that, one generates $N_{\text{gen}} = 1 \times 10^5$ samples on which one evaluates the densities and compute the variance of the ratio;
- the reference CMC is obtained by $N_{\text{rep}} = 10$ repetitions of $N_{\text{sim}} = 10^5$ samples;
- the "success rate" is obtained by counting the number of negative-valued indices removed from the statistics.

Concerning the first-order indices, one can see that, most of them are correctly estimated (despite the fact they have small values). The strongest first-order indices (i.e., those associated to M_{X_2}

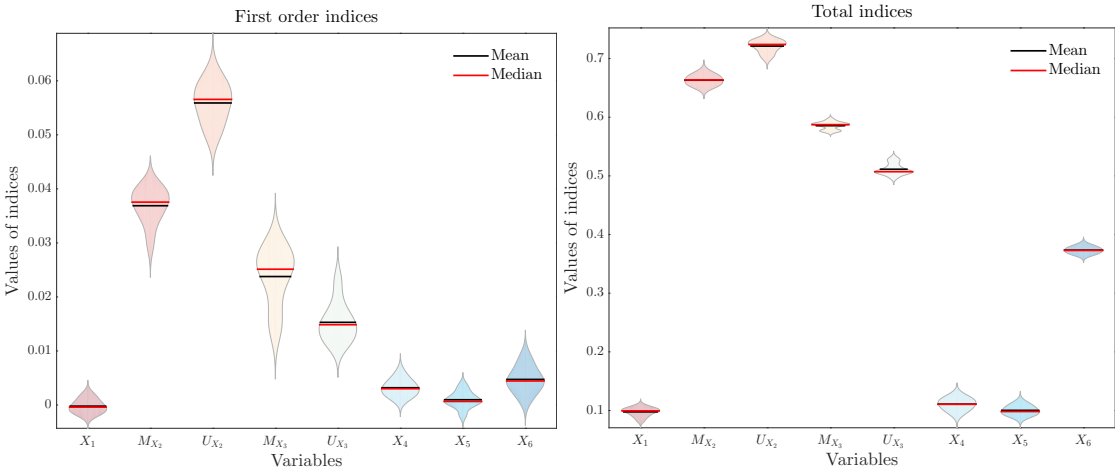

(a) (b)

FIGURE 8.6: $S^{\mathbb{1}_{\mathcal{F}}}$-indices estimated under bi-level uncertainty (ARA/CMC of $N_{\text{sim}} = 10^5$ samples and $N_{\text{rep}} = 10$ repetitions, with $\widetilde{P}_{\text{f,ref}} = 3.98 \times 10^{-2}$).

and U_{X_2}) are rather well estimated. As for the total order indices, the results show that the indice associated to X_1 can be correctly estimated but with a very low success rate. As for X_6, its total index is well estimated but with a moderate success rate. The group $(M_{X_2}, U_{X_2}, M_{X_3}, U_{X_3})$ are estimated in terms of order of magnitude but not accurately. Finally, the indices associated to (X_4, X_5) are completely over-estimated.

TABLE 8.6: Results for Step #3.

Variable	**First order indices**			**Total indices**		
	Ref. CMC	SS + G-KDE	Success rate	Ref. CMC	SS + G-KDE	Success rate
X_1	2.3×10^{-3}	1.1×10^{-4}	(100 %)	0.155	0.135	**(3 %)**
M_{X_2}	0.014	0.022	(100 %)	0.776	0.598	**(66 %)**
U_{X_2}	0.028	0.038	(100 %)	0.792	0.511	**(77 %)**
M_{X_3}	9.3×10^{-3}	0.012	(100 %)	0.697	0.523	**(60 %)**
U_{X_3}	4.7×10^{-3}	5.6×10^{-3}	(100 %)	0.620	0.540	**(60 %)**
X_4	0	5.3×10^{-4}	(100 %)	0.137	0.608	**(63 %)**
X_5	0	1.2×10^{-4}	(100 %)	0.132	0.407	**(49 %)**
X_6	2.3×10^{-3}	2.0×10^{-3}	(100 %)	0.524	0.518	**(51 %)**

8.8 Conclusion

In this chapter, the methodologies proposed in the three previous chapters have been applied to a launcher stage fallout test-case issued from aerospace research. Despite the fact this model is a simplified version, the underlying difficulties of the model are still representative of the difficulties encountered in reliability assessment of such complex systems.

In a first part, the presentation and its key characteristic have been presented or identifies from a preliminary analysis of its LSF. Then, in a second part, the three main methodologies developed in this manuscript have been applied to the case. As a result, one can set up the following synthesis:

- About **Step #1**: ARA/SS demonstrated a good efficiency compared to NRA/CMC and ARA/CMC for the estimation of a rare predictive faillure probability;
- About **Step #2**: ARA/NAIS demonstrated a very high efficiency compared to ARA/CMC in terms of probability estimation. Moreover, local sensitivities w.r.t. distribution hyper-parameters can be obtained by simple post-processing (in the case of unbounded prior distributions) which makes the approach tractable and efficient for both complex computer models and rare event probability estimation;
- About **Step #3**: the proposed methodology demonstrated, on the one hand, promising results in terms of cost reduction compared to a single-loop CMC to get the $S^{\mathbb{1}_{\mathcal{F}}}$-indices, but on the other hand, still lack of robustness regarding the accuracy of the estimates.

Consequently, the three steps are partially validated regarding such a complex aerospace test-case. This motivates further improvements and perspectives for the proposed methodologies, especially regarding the last step. These perspectives are gathered in the following concluding chapter. Nonetheless, this step is also the most challenging one as it involves well-known issues related to KDE and high-dimension as stated in Chapter 7.

CHAPTER 9

Conclusion and perspectives

Summary of the main contributions

The underlying theme of this thesis was to develop numerical strategies to handle the *bi-level input uncertainty* (i.e., the aleatory uncertainty characterizing the basic variables and the epistemic uncertainty on their probabilistic modeling) all along the UQ methodology process, i.e., starting from the uncertainty modeling step to the inverse analysis one as presented in Figure 1.1.

As a first step, it has been proposed to adopt a Bayesian viewpoint such that the distribution parameters affected by epistemic uncertainty follow some prior distributions. A hierarchical prior structure is thus considered in input. Then, it has been decided to focus on the predictive failure probability. Such a QoI appears to be relevant for reliability purposes as it incorporates both levels of uncertainty.

Nested vs. augmented reliability approaches

The first technical contribution of this work has consisted in investigating the coupling between several rare event probability estimation techniques and two distinct approaches to estimate the predictive failure probability: the nested reliability approach (NRA) and the augmented reliability approach (ARA). The NRA relies on a double-loop estimation scheme while the ARA relies on a single-loop one. A numerical comparison between these two approaches has been conducted on several test-cases of increasing complexity. When coupled with advanced rare event sampling techniques (e.g., adaptive importance sampling techniques, subset sampling), ARA outperforms NRA in terms of numerical efficiency, especially for rare failure probabilities. Finally, this contribution is linked to the following publications:

- Chabridon V., M. Balesdent, J.-M. Bourinet, J. Morio and N. Gayton (2017). "Evaluation of failure probability under parameter epistemic uncertainty: application to aerospace system reliability assessment". In: *Aerospace Science and Technology* 69, pp. 526–537.
- Chabridon V., N. Gayton, J.-M. Bourinet, M. Balesdent and J. Morio (2017). "Some Bayesian insights for statistical tolerance analysis". In: *Actes du 23ème Congrès Français de Mécanique (CFM 2017)*, Lille, France.

Local reliability-oriented sensitivity estimators under bi-level uncertainty

The second technical contribution of this work focused on proposing local reliability-oriented sensitivity estimators within the augmented framework. These estimators are based on the

first-order partial derivative of the predictive failure probability w.r.t. deterministic distribution hyper-parameters. The underlying idea has been to take advantage of the use of the prior distribution score functions. Finally, two cases have been treated: firstly, when all the uncertain distribution parameters follow some unbounded prior probability distributions and secondly, when at least one distribution parameter follows a bounded prior. Then, an efficient adaptive importance sampling scheme has been proposed to estimate these sensitivities along with the predictive failure probability at a reduced simulation cost. A numerical comparison between the proposed methodology and a reference CMC approach has been conducted on several test-cases of increasing complexity. Finally, this contribution is linked to the following publications:

- Chabridon V., M. Balesdent, J.-M. Bourinet, J. Morio and N. Gayton (2018). "Reliability-based sensitivity estimators of rare event probability in the presence of distribution parameter uncertainty". In: *Reliability Engineering and System Safety* 178, pp. 164–178.
- Chabridon V., M. Balesdent, J.-M. Bourinet, J. Morio and N. Gayton (2017). "Reliability-based sensitivity analysis of aerospace systems under distribution parameter uncertainty using an augmented approach". In: *Proc. of the 12th International Conference on Structural Safety & Reliability (ICOSSAR 2017)*, Vienna, Austria.

Global reliability-oriented sensitivity estimators under bi-level uncertainty

The third technical contribution of this work aimed at adapting global reliability-oriented sensitivity estimators (i.e., the Sobol indices on the indicator function) within the augmented framework. The underlying idea was to allow a quantitative analysis of the impact of both types of uncertainties (i.e., aleatory and epistemic) on the indicator function of the failure domain. To do so, the augmented vector has been modified to a disaggregated version allowing to separate both aleatory and epistemic uncertainties. Then, a coupling between recently proposed tools (i.e., Bayesian sensitivity estimators and a data-driven tensorized kernel density estimation) has been proposed so as to be able to estimate these indices at a lower cost compared to CMC. The main advantage is that the indices can be obtained just by post-processing an elite set of failure points in the augmented space, obtained in the final step of any advanced sampling technique (e.g., adaptive importance sampling techniques, subset sampling). Finally, the possible publication of these results in a scientific book chapter is considered and currently under writing process.

Application to a realistic aerospace computer model

The fourth contribution of this work is focused on applications. All the previous technical contributions have been applied to a representative aerospace test-case issued from a launch vehicle trajectory simulation model. This case is based on the dynamical modeling of the ballistic fallout phase of the first stage of an expendable space launcher. A complete uncertainty-oriented study of this test case has been conducted. Moreover, both advantages and limits of the proposed methodologies have been investigated. The intrinsic difficulties (rareness of the failure event together with multimodality of the optimal density at failure, strong influence of some key variables) appearing in this test-case have been highlighted and led to consider several open issues and perspectives. Finally, this contribution is linked to the following publications:

- Derennes P., V. Chabridon, J. Morio, M. Balesdent, F. Simatos, J.-M. Bourinet and N. Gayton (2018). "Nonparametric importance sampling techniques for sensitivity analysis and reliability assessment of a launcher stage fallout". In: *Optimization in Space Engineering*. Ed. by G. Fasano and J. Pintér. Springer International Publishing. (To Appear).

▷ Chabridon V., M. Balesdent, J.-M. Bourinet, J. Morio and N. Gayton (2018). "Nonparametric adaptive importance sampling strategy for reliability assessment and sensitivity analysis under distribution parameter uncertainty – Application to launch vehicle fallback zone estimation". In: *Actes des 10èmes Journées Fiabilité des Matériaux et des Structures (JFMS 2018)*, Bordeaux, France.

Perspectives

A few possible extensions about the thesis' contributions

About the Bayesian framework. A first research track could consist in studying the impact on data gathering process in the proposed methodologies. Due to the Bayesian framework, *reliability updating* could be possible, especially using existing methologies (see, e.g., Papadimitriou et al., 2001; Straub, 2011; Straub and Papaioannou, 2015; Straub et al., 2016). Moreover, recent tools developed in the context of Bayesian calibration could be used too (see, e.g., Nagel and Sudret, 2016). Another track could be to go beyond the parametric assumption for the basic variables and to study the impact of the distribution type through the use of *Bayesian model averaging* (BMA) (see, e.g., Sankararaman and Mahadevan, 2013a).

About the predictive failure probability and risk analysis. From the Bayesian decision theory, the predictive failure probability is not suited for risk analysis as this measure is not conservative enough (Pasanisi et al., 2012). However, reconstructing the entire distribution of the conditional failure probability might be cumbersome using naive NRA. A first research track could be to use a surrogate model of the black-box model so as to reduce the computational burden of nested calls to the computer model and to efficiently get the distribution of the conditional failure probability. A second track could be to use the reverse importance sampling trick as used in Beckman and McKay (1987), Hesterberg (1996), and Morio (2011b) so as to reconstruct the distribution of the conditional failure probability w.r.t. the uncertain distribution parameters. A third track could be to replace the predictive measure so as to consider a more conservative measure, e.g., a penalized reliability measure.

A few methodological perspectives

Exploring the possibilities offered by new sensitivity indices. One resulting research track at the end of this thesis concerns the dependence of the inputs at failure. Such a key feature could be specifically handled by SAMO indices which could be adapted to the ROSA context and, if possible, to the bi-level input uncertainty. For instance, one can cite the *sensitivity indices based on dependence measures* (see Chapter 4). As already proposed in Da Veiga (2015) and then extended by Raguet and Marrel (2018), these indices seem to be more informative than traditional variance-based indices. Recently, the adaptation of these indices (in their SAMO version) to the bi-level input uncertainty has been proposed in Meynaoui et al. (2018). Other indices such as the *GOSA indices* (see Chapter 4) seem to not have been investigated regarding the bi-level input uncertainty. Finally, recently proposed indices in literature, such as *Sobol indices with constraints* by Kucherenko et al. (2017) or *support indices* by Fruth et al. (2018) might present interesting features which could be investigated w.r.t. the ROSA context.

Exploring the possibilities offered by surrogate modeling. Surrogate modeling is definitely a powerful tool for efficient reliability assessment and sensitivity analysis of computer models. However, the counterpart remains the difficulty to catch and measure the impact of the modeling errors induced by the surrogate model itself. In the context of bi-level input uncertainty, one

needs to ensure that such an extra type of uncertainty will not exceed the probabilistic model uncertainty.

Exploring the possibilities offered by kernel density estimation. The topic of kernel density estimation for high-dimensional problems is still an open issue. In the ROSA context, it has been demonstrated that the optimal density was likely to be concentrated on an unknown subset of $\mathbb{R}^d$. Thus, new methodologies tackling this problem of probability concentration (see, e.g., Soize and Ghanem, 2016; Soize and Ghanem, 2017) might be a relevant research track for ROSA. In that sense, the *data-driven tensorized* G-KDE proposed by Perrin et al. (2018) seems a promising tool which can outperform usual KDE in this specific context, and thus should be further investigated.

Exploring the effects of incomplete information about the dependence structure. Studying the impact of epistemic uncertainty affecting the dependence structure is a fundamental topic which has not been widely studied. For instance, one can mention the works by Tang et al. (2013), Tang et al. (2015), and Benoumechiara et al. (2018). Developing sensitivity indices for ROSA adapted to this specific issue could be valuable and would allow to get a full insight about the lack-of-knowledge that could affect the input probabilistic model.

Exploring the links between the Bayesian framework and imprecise probabilities. As a final methodological research track, one should stress the need to fill the gap between Bayesian approaches and imprecise probabilities. As stated in Beer et al. (2014), these frameworks are complementary and should be both investigated so as to combine advantages from both. As an example, one can mention the work of Schöbi and Sudret (2017) which fills the gap between traditional SAMO using Sobol indices and their "imprecise version" when dealing with probability-boxes.

A few perspectives about the applications

About complex aerospace computer models. Dealing with aerospace computer models may imply to develop complex computational workflows such as those encountered in multidisciplinary design optimization (MDO). As a result, these workflows may combine several sources and types of uncertainties (see, e.g., Jaeger et al., 2013; Dubreuil et al., 2016). Combining the several sources of uncertainties while assessing the reliability of multidisciplinary systems has been investigated in Brevault (2015). Performing SAMO regarding multidisciplinary systems has been both addressed in Sankararaman (2012) and Jiang et al. (2016). Proposing efficient ROSA indices in such a context could be a challenging perspective.

About aerospace systems' safety facing uncertain conditions. Aerospace systems are now designed and controled so that they can be able to manage uncertain conditions. Research topics such as *time-dependent reliability*, *online reliability updating*, *predictive maintenance* or *prognostics* are active fields of research (see, e.g., Karandikar et al., 2012; Wang et al., 2016; Chiachío et al., 2017; Robinson et al., 2018). For these topics, contrary to usual static reliability analysis, the uncertainty management has to be performed *online*. Both aleatory and epistemic uncertainties appear in such a state-space dynamic evolution. Thus, these several uncertainty sources have to be taken into account so as to guarantee the accuracy of the predictions and to ensure the system safety. Developing methodological tools to handle the bi-level uncertainty and to perform online sensitivities for time-dependent processes (see, e.g., Alexanderian et al., 2017) in such a context is a real challenge as the computational constraints are drastic.

Bibliography

Ahammed, M. and R. E. Melchers (2006). "Gradient and parameter sensitivity estimation for systems evaluated using Monte Carlo analysis". In: *Reliability Engineering and System Safety* 91, pp. 594–601.

AIAA (1998). *Guide for the Verification and Validation of Computational Fluid Dynamics Simulations (AIAA G-077-1998)*. Tech. rep. The American Institute of Aeronautics and Astronautics.

Alexanderian, A., P. A. Gremaud, and R. C. Smith (2017). "Variance-based sensitivity analysis for time-dependent processes". In: *ArXiv e-prints*, pp. 1–23. arXiv: 1711.08030 [stat.CO].

Allaire, G. (2015). "A review of adjoint methods for sensitivity analysis, uncertainty quantification and optimization in numerical codes". In: *Actes du Congrès Simulation SIA*. Montigny-le-Bretonneux, France.

Apostolakis, G. (1990). "The Concept of Probability in Safety Assessments of Technological Systems". In: *Science* 250, pp. 1359–1364.

Arianespace (2014). *Vega User's Manual, Issue 4 Revision 0*. http://www.arianespace.com/vehicle/vega/. Arianespace.

— (2016). *Ariane 5 User's Manual, Issue 5 Revision 2*. http://www.arianespace.com/vehicle/ariane-5/. Arianespace.

ASME (2009). *Standard for Verification and Validation in Computational Fluid Dynamics and Heat Transfer (ASME V&V 20-2009)*. Tech. rep. The American Society of Mechanical Engineers.

Asmussen, S. and P. W. Glynn (2007). *Stochastic Simulation: Algorithms and Analysis*. Stochastic Modelling and Applied Probability. Springer Science+Business Media.

Au, S. K. (2005). "Reliability-based design sensitivity by efficient simulation". In: *Computers & Structures* 83, pp. 1048–1061.

Au, S.-K. and J. L. Beck (1999). "A new adaptive importance sampling scheme for reliability calculations". In: *Structural Safety* 21, pp. 135–158.

— (2001). "Estimation of small failure probabilities in high dimensions by subset simulation". In: *Probabilistic Engineering Mechanics* 16.4, pp. 263–277.

— (2003). "Important sampling in high dimensions". In: *Structural Safety* 25, pp. 139–163.

Au, S.-K. and Y. Wang (2014). *Engineering Risk Assessment with Subset Simulation*. Wiley.

Au, S.-K., J. Ching, and J. L. Beck (2007). "Application of subset simulation methods to reliability benchmark problems". In: *Structural Safety* 29, pp. 183–193.

Auder, B. and B. Iooss (2009). "Global sensitivity analysis based on entropy". In: *Proc. of the 20th European Safety and Reliability Conference (ESREL 2009)*. Prague, Czech Republic.

Ayyub, B. M. (2001). *Elicitation of Expert Opinions for Uncertainty and Risks*. CRC Press LLC.

Balesdent, M. (2011). "Multidisciplinary Design Optimization of Launch Vehicles". PhD thesis. École Centrale de Nantes.

Balesdent, M., J. Morio, and J. Marzat (2013). "Kriging-based adaptive Importance Sampling algorithms for rare event simulation". In: *Structural Safety* 44, pp. 1–10.

Balesdent, M., J. Morio, and L. Brevault (2014). "Rare Event Probability Estimation in the Presence of Epistemic Uncertainty on Input Probability Distribution Parameters". In: *Methodology and Computing in Applied Probability* 18.1, pp. 197–216.

Balesdent, M., J. Morio, and J. Marzat (2015). "Recommendations for the tuning of rare event probability estimators". In: *Reliability Engineering and System Safety* 133, pp. 68–78.

Barbe, P. and M. Ledoux (2007). *Probabilité*. (in French). EDP Sciences.

Baudin, M. and J.-M. Martinez (2014). *Introduction to sensitivity analysis with NISP, Version 0.5*.

Beckman, R. J. and M. D. McKay (1987). "Monte Carlo Estimation under Different Distributions Using the Same Simulation". In: *Technometrics* 29.2, pp. 153–160.

Bect, J., D. Ginsbourger, L. Li, V. Picheny, and E. Vazquez (2012). "Sequential design of computer experiments for the estimation of a probability of failure". In: *Statistics and Computing* 22, pp. 773–793.

Bect, J., L. Li, and E. Vazquez (2017). "Bayesian Subset Simulation". In: *SIAM/ASA Journal of Uncertainty Quantification* 5.1, pp. 762–786.

Beer, M., S. Ferson, and V. Kreinovich (2013). "Imprecise probabilities in engineering analyses". In: *Mechanical Systems and Signal Processing* 37, pp. 4–29.

Beer, M., F. A. DiazDelaO, E. Patelli, and S. K. Au (2014). "Conceptual comparison of Bayesian approaches and imprecise probabilities". In: *Computational Technology Reviews* 9, pp. 1–29.

Benjamin, J. R. and C. A. Cornell (1970). *Probability, statistics, and decision for civil engineers*. McGraw-Hill.

Benoumechiara, N. and K. Elie-Dit-Cosaque (2018). "Shapley effects for sensitivity analysis with dependent inputs: bootstrap and kriging-based algorithms". In: *ArXiv e-prints*, pp. 1–30. arXiv: 1801.03300 [math.ST].

Benoumechiara, N., B. Michel, P. Saint-Pierre, and N. Bousquet (2018). "Detecting and modeling worst-case dependence structures between random inputs of computational reliability models". In: *ArXiv e-prints*, pp. 1–42. arXiv: 1804.10527 [stat.ME].

Berger, J. O. (1985). *Statistical Decision Theory and Bayesian Analysis*. Second ed. Springer Series in Statistics. Springer-Verlag New York.

Berlinet, A. and C. Thomas-Agnan (2004). *Reproducing Kernel Hilbert Spaces in Probability and Statistics*. Springer US.

Bernard, P. and M. Fogli (1986). "Un calcul probabiliste en génie civil. Évaluation de la probabilité de ruine des structures par une méthode de Monte-Carlo fondée sur une technique de conditionnement". In: *Annales scientifiques de l'Université de Clermont-Ferrand 2, Série Mathématiques* 89.23. (in French), pp. 47–90.

BIPM (2008). *Evaluation of measurement data – Guide to the expression of uncertainty in measurement*. Tech. rep. GUM 100:2008. Bureau International des Poids et Mesures (BIPM), Joint Committee for Guides in Metrology (JCGM).

Bjerager, P. (1988). "Probability integration by directional simulation". In: *Journal of Engineering Mechanics* 114.8, pp. 1288–1302.

Bjerager, P. and S. Krenk (1987). "Sensitivity measures in structural reliability analysis". In: *Reliability and Optimization of Structural Systems '87: Proceedings of the 1st IFIP WG 7.5 Conference, Aalborg, Denmark, 1987*. Ed. by P. Thoft-Christensen. Berlin Heidelberg: Springer-Verlag, pp. 459–470.

— (1989). "Parametric Sensitivity in First Order Reliability Theory". In: *Journal of Engineering Mechanics* 115, pp. 1577–1582.

Bolado-Lavin, R. and A. Costescu Badea (2008). *Review of sensitivity analysis methods and experience for geological disposal of radioactive waste and spent nuclear fuel, JRC Scientific and Technical Reports EUR 23712 EN - 2008*. Tech. rep. Joint Research Center, Petten, The Netherlands.

Borgonovo, E. (2007). "A bew uncertainty importance measure". In: *Reliability Engineering and System Safety* 92, pp. 771–784.

— (2017). *Sensitivity Analysis. An Introduction for the Management Scientist*. International Series in Operations Research & Management Science. Springer International Publishing.

Borgonovo, E. and E. Plischke (2016). "Sensitivity analysis: a review of recent advances". In: *European Journal of Operational Research* 248, pp. 869–887.

Botev, Z. I., D. P. Kroese, and T. Taimre (2007). "Generalized Cross-Entropy methods with applications to rare-event simulation and optimization". In: *Simulation* 83.11, pp. 785–806.

Botev, Z. I., J. F. Grotowski, and D. P. Kroese (2010). "Kernel density estimation via diffusion". In: *The Annals of Statistics* 38.5, pp. 2916–2957.

Bourinet, J.-M. (2016). "Rare-event probability estimation with adaptive support vector regression surrogates". In: *Reliability Engineering and System Safety* 150, pp. 210–221.

— (2017). "FORM Sensitivities to Distribution Parameters with the Nataf Transformation". In: *Risk and Reliability Analysis: Theory and Applications. In Honor of Prof. Armen Der Kiureghian*. Ed. by P. Gardoni. Springer Series in Reliability Engineering. Springer International Publishing, pp. 277–302.

— (2018). "Reliability analysis and optimal design under uncertainty – Focus on adaptive surrogate-based approaches". 245 pages. HDR (French Accreditation to Supervise Research). Université Clermont Auvergne.

Bourinet, J.-M. and M. Lemaire (2008). "FORM sensitivities to correlation: application to fatigue crack propagation based on Virkler data". In: *Proc. of the 4th International ASRANet Colloquium*. Athens, Greece.

Bourinet, J.-M., C. Mattrand, and V. Dubourg (2009). "A review of recent features and improvements added to FERUM software". In: *Proc. of the 10th International Conference on Structural Safety and Reliability (ICOSSAR'09)*. Osaka, Japan.

Bourinet, J.-M., F. Deheeger, and M. Lemaire (2011). "Assessing small failure probabilities by combined subset simulation and Support Vector Machines". In: *Structural Safety* 33.6, pp. 343–353.

Breitung, K. (1984). "Asymptotic Approximations for Multinormal Integrals". In: *Journal of Engineering Mechanics* 110.3, pp. 357–366.

— (1991). "Parameter sensitivity of failure probabilities". In: *Reliability and Optimization of Structural Systems '90: Proceedings of the 3rd IFIP WG 7.5 Conference, Berkeley, CA, USA, 1990*. Ed. by A. Der Kiureghian and P. Thoft-Christensen. Berlin Heidelberg: Springer-Verlag, pp. 43–51.

— (2019). "The geometry of limit state function graphs and subset simulation: Counterexamples". In: *Reliability Engineering and System Safety* 182, pp. 98–106.

Brevault, L. (2015). "Contributions to Multidisciplinary Design Optimization under uncertainty, application to launch vehicle design". PhD thesis. École Nationale Supérieure des Mines de Saint-Étienne.

Broto, B., F. Bachoc, M. Depecker, and J.-M. Martinez (2018). "Sensitivity indices for independent groups of variables". In: *ArXiv e-prints*, pp. 1–16. arXiv: 1801.04095 [math.ST].

Browne, T. (2017). "Regression models and sensitivity analysis for stochastic simulators: applications to non-destructive examination". PhD thesis. Université Paris Descartes.

Bucklew, J. A. (2004). *Intoduction to Rare Event Simulation*. Springer Series in Statistics. Springer-Verlag New York, Inc.

Bungartz, H.-J. and M. Griebel (2004). "Sparse grids". In: *Acta Numerica* 13, pp. 147–269.

Cacuci, D. G. (1981). "Sensitivity theory for nonlinear systems. I. Nonlinear functional analysis approach". In: *Journal of Mathematical Physics* 22.12, pp. 2794–2802.

— (2003). *Sensitivity and Uncertainty Analysis, Volume I: Theory*. Chapman and Hall/CRC.

Cacuci, D. G., M. Ionescu-Bujor, and I. M. Navon (2005). *Sensitivity and Uncertainty Analysis, Volume II: Applications to Large-Scale Systems*. Chapman and Hall/CRC.

Campolongo, F., J. Cariboni, and A. Saltelli (2007). "An effective screening design for sensitivity analysis of large models". In: *Environmental Modelling & Software* 22, pp. 1509–1518.

Caniou, Y. (2012). "Global sensitivity analysis for nested and multiscale modelling". PhD thesis. Université Blaise Pascal – Clermont II.

Cannaméla, C. (2007). "Apport des méthodes probabilistes dans la simulation du comportement sous irradiation du combustible à particules". (in French). PhD thesis. Université Paris Diderot – Paris VII.

Caron, V., A. Guyader, M. Munoz Zuniga, and B. Tuffin (2014). "Some recent results in rare event estimation". In: *ESAIM Proceedings* 44, pp. 239–259.

Castillo, E., R. Mínguez, and C. Castillo (2008). "Sensitivity analysis in optimization and reliability problems". In: *Reliability Engineering and System Safety* 93, pp. 1788–1800.

Cérou, F. and A. Guyader (2007). "Adaptive Multilevel Splitting for Rare Event Analysis". In: *Stochastic Analysis and Applications* 25.3, pp. 417–443.

Cérou, F., P. Del Moral, T. Furon, and A. Guyader (2012). "Sequential Monte Carlo for rare event estimation". In: *Statistics and Computing* 22, pp. 795–808.

Chabridon, V., M. Balesdent, J.-M. Bourinet, J. Morio, and N. Gayton (2017a). "Evaluation of failure probability under parameter epistemic uncertainty: application to aerospace system reliability assessment". In: *Aerospace Science and Technology* 69, pp. 526–537.

— (2017b). "Reliability-based sensitivity analysis of aerospace systems under distribution parameter uncertainty using an augmented approach". In: *Proc. of the 12th International Conference on Structural Safety and Reliability (ICOSSAR'17)*. Vienna, Austria.

Chabridon, V., N. Gayton, M. Balesdent, J.-M. Bourinet, and J. Morio (2017c). "Some Bayesian insights for statistical tolerance analysis". In: *Actes du 23ème Congrès Français de Mécanique (CFM 2017)*. Lille, France.

Chan, K. (2008). *Spacecraft Collision Probability*. The Aerospace Press. American Institute of Aeronautics and Astronautics.

Chan, K., A. Saltelli, and S. Tarantola (1997). "Sensitivity analysis of model output: variance-based methods make the difference". In: *Proc. of the 1997 Winter Simulation Conference (WSC'97)*. Atlanta, GA, USA.

Chastaing, G. (2013). "Indices de Sobol généralisés pour variables dépendantes". (in French). PhD thesis. Université de Grenoble.

Cherng, R.-H. and Y. K. Wen (1994). "Reliability of Uncertain Nonlinear Trusses under Random Excitation. II". In: *Journal of Engineering Mechanics* 120.4, pp. 748–757.

Chiachío, M., J. Chiachío, S. Sankararaman, K. Goebel, and J. Andrews (2017). "A new algorithm for prognostics using Subset Simulation". In: *Reliability Engineering and System Safety* 168, pp. 189–199.

Chocat, R., P. Beaucaire, L. Debeugny, J.-P. Lefebvre, C. Sainvitu, P. Breitkopf, and E. Wyart (2016). "Reliability analysis in fracture mechanics according to combined failure criteria". In: *Proc. of the VII European Congress on Computational Methods in Applied Sciences and Engineering (ECCOMAS Congress 2016)*. Crete Island, Greece.

Chowdhury, R. and S. Adhikari (2010). "Stochastic sensitivity analysis using preconditioning approach". In: *Engineering Computations* 27.7, pp. 841–862.

Coifman, R. R., S. Lafon, A. B. Lee, M. Maggioni, B. Nadler, F. Warner, and S. W. Zucker (2015). "Geometric Diffusions as a Tool for Harmonic Analysis and Structure Definition of Data: Diffusion Maps". In: *Proceedings of the National Academy of Sciences of the United States of America* 102.21, pp. 7426–7431.

Cornell, C. A. (1969). "A Probability-Based Structural Code". In: *Journal of the American Concrete Institute* 66.12, pp. 974–985.

Cui, L., Z. Lu, and X. Zhao (2010). "Moment-independent importance measure of basic random variable and its probability density evolution solution". In: *Science China Technical Sciences* 53.10, pp. 1138–1145.

Da Veiga, S. (2015). "Global sensitivity analysis with dependence measures". In: *Journal of Statistical Computation and Simulation* 85.7, pp. 1283–1305.

Damblin, G. (2015). "Contributions statistiques au calage et à la validation des codes de calcul". PhD thesis. Université Paris-Saclay.

Davis, P. J. and P. Rabinowitz (1984). *Methods of Numerical Integration*. Second ed. Computer Science and Applied Mathematics. Academic Press Limited.

De Boer, P.-T., D. P. Kroese, S. Mannor, and R. Y. Rubinstein (2005). "A Tutorial on the Cross-Entropy Method". In: *Annals of Operations Research* 134, pp. 19–67.

De La Porte, J., B. M. Herbst, W. Hereman, and S. J. Van Der Walt (2008). "An Introduction to Diffusion Maps". In: *Proc. of the 19th Symposium of the Pattern Recognition Association of South Africa (PRASA 2008)*. Cape Town, South Africa.

De Lozzo, M. and A. Marrel (2016a). "Estimation of the Derivative-Based Global Sensitivity Measures Using a Gaussian Process Metamodel". In: *SIAM/ASA Journal of Uncertainty Quantification* 4.1, pp. 708–738.

— (2016b). "New improvements in the use of dependence measures for sensitivity analysis and screening". In: *Journal of Statistical Computation and Simulation* 86.15, pp. 3038–3058.

— (2016c). "Sensitivity analysis with dependence and variance-based measures for spatio-temporal numerical simulators". In: *Stochastic Environmental Research and Risk Assessment* 31, pp. 1437–1453.

De Rocquigny, E. (2006a). "La maîtrise des incertitudes dans un contexte industriel. 1ère partie : une approche méthodologique globale basée sur des exemples". In: *Journal de la Société Française de Statistique* 147.3, pp. 33–71.

— (2006b). "La maîtrise des incertitudes dans un contexte industriel. 2ème partie : revue des méthodes de modélisation statistique physique et numérique". In: *Journal de la Société Française de Statistique* 147.3, pp. 73–106.

De Rocquigny, E., N. Devictor, and S. Tarantola (2008). *Uncertainty in industrial practice: a guide to quantitative uncertainty management*. Wiley.

Der Kiureghian, A. (1988). *Measures of Structural Safety Under Imperfect States of Knowledge, Report No. UCB/SEMM-88/06*. Tech. rep. Department of Civil and Environmental Engineering, University of California, Berkeley.

— (1989). "Measures of Structural Safety Under Imperfect States of Knowledge". In: *Journal of Structural Engineering ASCE* 115.5, pp. 1119–1140.

— (1996). "Structural reliability methods for seismic safety assessment: a review". In: *Engineering Structures* 18.6, pp. 412–424.

— (1999). *Introduction to Structural Reliability, Class Notes for CE229, Structural Reliability*.

— (2008). "Analysis of structural reliability under parameter uncertainties". In: *Probabilistic Engineering Mechanics* 23.4, pp. 351–358.

Der Kiureghian, A. and T. Dakessian (1998). "Multiple design points in first and second-order reliability". In: *Structural Safety* 20.1, pp. 37–49.

Der Kiureghian, A. and M. De Stefano (1991). "Efficient Algorithm for Second-Order Reliability Analysis". In: *Journal of Engineering Mechanics ASCE* 117.12, pp. 2904–2923.

Der Kiureghian, A. and O. Ditlevsen (2009). "Aleatory or epistemic? Does it matter?" In: *Structural Safety* 31.2, pp. 105–112.

Der Kiureghian, A. and P.-L. Liu (1986). "Structural Reliability Under Incomplete Probability Information". In: *Journal of Engineering Mechanics ASCE* 112.1, pp. 85–104.

Derennes, P., J. Morio, and F. Simatos (2018a). "A nonparametric importance sampling estimator for moment independent importance measures". In: *Reliability Engineering and System Safety*. (In Press), pp. 1–27.

— (2018b). "Estimation of moment independent importance measures using a copula and maximum entropy framework". In: *Proc. of the 2018 Winter Simulation Conference (WSC'18)*. Gothenburg, Sweden.

Ditlevsen, O. (1979a). "Generalized Second Moment Reliability Index". In: *Journal of Structural Mechanics* 7.4, pp. 435–451.

Ditlevsen, O. (1979b). "Narrow Reliability Bounds for Structural Systems". In: *Journal of Structural Mechanics* 7.4, pp. 453–472.
— (1982). "Model uncertainty in structural reliability". In: *Structural Safety* 1.1, pp. 73–86.
— (1993). "Distribution arbitrariness in structural reliability". In: *Proc. of the 6th International Conference on Structural Safety and Reliability (ICOSSAR'93)*. Innsbruck, Austria.
Ditlevsen, O. and H. O. Madsen (2007). *Structural Reliability Methods*. Internet ed. 2.3.7.
Dong, Y.-G., H.-T. Lu, and L.-L. Li (2014). "Reliability sensitivity analysis based on multi-hyperplane combination method". In: *Defence Technology* 10, pp. 354–359.
Dubourg, V. (2011). "Adaptive surrogate models for reliability analysis and reliability-based design optimization". PhD thesis. Université Blaise Pascal – Clermont II.
Dubourg, V. and B. Sudret (2011). "Reliability-based design optimization using kriging surrogates and subset simulation". In: *Structural and Multidisciplinary Optimization* 44, pp. 673–690.
— (2014). "Metamodel-based importance sampling for reliability sensitivity analysis". In: *Structural Safety* 49, pp. 27–36.
Dubourg, V., B. Sudret, and F. Deheeger (2013). "Metamodel-based importance sampling for structural reliability analysis". In: *Probabilistic Engineering Mechanics* 33, pp. 45–57.
Dubreuil, S., N. Bartoli, C. Gogu, and T. Lefebvre (2016). "Propagation of modeling uncertainty by polynomial chaos expansion in multidisciplinary analysis". In: *Journal of Mechanical Design* 138, pp. 111411–1–111411–11.
Durrett, R. (2010). *Probability: Theory and Examples*. Fourth ed. Cambridge University Press.
Dussault, J. P., D. Labrecque, P. L'Ecuyer, and R. Y. Rubinstein (1997). "Combining the Stochastic Counterpart and Stochastic Approximation Methods". In: *Discrete Event Dynamic Systems: Theory and Applications* 7, pp. 5–28.
Dutfoy, A. and R. Lebrun (2009). "Practical approach to dependence modelling using copulas". In: *Proceedings of the Institution of Mechanical Engineers, Part O: Journal of Risk and Reliability* 223.4, pp. 347–361.
Echard, B., N. Gayton, and M. Lemaire (2011). "AK-MCS: An active learning reliability method combining Kriging and Monte Carlo Simulation". In: *Structural Safety* 33.2, pp. 145–154.
Echard, B., N. Gayton, M. Lemaire, and N. Relun (2013). "A combined Importance Sampling and Kriging reliability method for small failure probabilities with time-demanding numerical models". In: *Reliability Engineering and System Safety* 111, pp. 232–240.
Ehre, M., I. Papaioannou, and D. Straub (2018). "Efficient estimation of variance-based reliability sensitivities in the presence of multi-uncertainty". In: *Proc. of the 2018 IFIP WG 7.5 Working Conference on Reliability and Optimization of Structural Systems*. Zurich, Switzerland.
Ekström, P.-A. and R. Broed (2006). *Sensitivity analysis methods and a biosphere test case implemented in EIKOS, Posiva Working Report 2006-31*. Tech. rep. Posiva Oy, Eurajoki, Finland.
Engelund, S. and R. Rackwitz (1993). "A benchmark study on importance sampling techniques in structural reliability". In: *Structural Safety* 12, pp. 255–276.
Feng, Z., Z. Lu, L. Cui, and S. Song (2010). "Reliability sensitivity algorithm based on stratified importance sampling method for multiple failure modes systems". In: *Chinese Journal of Aeronautics* 23, pp. 660–669.
Ferson, S. and L. R. Ginzburg (1996). "Different methods are needed to propagate ignorance and variability". In: *Reliability Engineering and System Safety* 54, pp. 133–144.
Ferson, S. and W. L. Oberkampf (2009). "Validation of imprecise probability models". In: *International Journal of Reliability and Safety* 3.1, pp. 3–22.
Fort, J.-C., T. Klein, and N. Rachdi (2016). "New sensitivity analysis subordinated to a contrast". In: *Communications in Statistics - Theory and Methods* 45.15, pp. 4349–4364.
Fruth, J., O. Roustant, and S. Kuhnt (2018). "Support indices: Measuring the effects of input variables over their supports". In: *Reliability Engineering and System Safety*. (In Press).

Gamboa, F., A. Janon, T. Klein, A. Lagnoux, and C. Prieur (2015). "Statistical inference for Sobol pick freeze Monte Carlo method". In: *Statistics*, pp. 1–22.

Garza, J. and H. R. Millwater (2016a). "Higher-order probabilistic sensitivity calculations using the multicomplex score function method". In: *Probabilistic Engineering Mechanics* 45, pp. 1–12.

— (2016b). "Sensitivity of the probability of failure of detection curve regions". In: *International Journal of Pressure Vessels and Piping* 141, pp. 26–39.

Gayton, N., P. Beaucaire, J.-M. Bourinet, E. Duc, M. Lemaire, and L. Gauvrit (2011). "APTA: advanced probability-based tolerance analysis of products". In: *Mechanics & Industry* 12, pp. 71–85.

Gelman, A., J. B. Carlin, H. S. Stern, D. B. Dunson, A. Vehtari, and D. B. Rubin (2006). *Bayesian Data Analysis*. Third ed. Texts in Statistical Science. Chapman and Hall/CRC.

Gentle, J. E. (2003). *Random number generation and Monte Carlo methods*. Second ed. Statistics and Computing. Springer Science+Business Media.

Geul, J., E. Mooij, and R. Noomen (2018). "Analysis of Uncertainties and Modeling in Short-Term Reentry Predictions". In: *Journal of Guidance, Control, and Dynamics*. (In Press), pp. 1–14.

Geyer, S., I. Papaioannou, and D. Straub (2019). "Cross entropy-based importance sampling using Gaussian densities revisited". In: *Structural Safety* 76, pp. 15–27.

Ghanem, R., D. Higdon, and H. Owhadi, eds. (2017). *Handbook of Uncertainty Quantification*. Springer International Publishing.

Givens, G. H. and A. E. Raftery (1996). "Local Adaptive Importance Sampling for Multivariate Densities With Strong Nonlinear Relationships". In: *Journal of the American Statistical Association* 91.433, pp. 132–141.

Glasserman, P., P. Heidelberger, P. Shahabuddin, and T. Zajic (1999). "Multilevel splitting for estimating rare event probabilities". In: *Operations Research* 47.4, pp. 585–600.

Grooteman, F. (2008). "Adaptive radial-based importance sampling method for structural reliability". In: *Structural Safety* 30, pp. 533–542.

— (2011). "An adaptive directional importance sampling method for structural reliability". In: *Probabilistic Engineering Mechanics* 26, pp. 134–141.

Gut, A. (2009). *An Intermediate Course in Probability*. Second ed. Springer Texts in Statistics. Springer Science+Business Media.

Guyader, A., N. Hengartner, and E. Matzner-Løber (2011). "Simulation and Estimation of Extreme Quantiles and Extreme Probabilities". In: *Applied Mathematics and Optimization* 64, pp. 171–196.

Hamada, M. S., A. G. Wilson, C. S. Reese, and H. F. Martz (2008). *Bayesian Reliability*. Springer Science+Business Media.

Harbitz, A. (1986). "An efficient sampling method for probability of failure calculation". In: *Structural Safety* 3, pp. 109–115.

Hasofer, A. M. and N. C. Lind (1974). "Exact and Invariant Second-Moment Code Format". In: *Journal of the Engineering Mechanics Division ASCE* 100.1, pp. 111–121.

Hastings, W. K. (1970). "Monte Carlo sampling methods using Markov chains and their applications". In: *Biometrika* 57.1, pp. 97–109.

Haukaas, T. and A. Der Kiureghian (2005). "Parameter Sensitivity and Importance Measures in Nonlinear Finite Element Reliability Analysis". In: *Journal of Engineering Mechanics* 131, pp. 1013–1026.

Heiss, F. and V. Winschel (2007). *Quadrature on sparse grids: Code to generate and readily evaluated nodes and weights (Matlab toolbox)*. http://www.sparse-grids.de.

— (2008). "Likelihood approximation by numerical integration on sparse grids". In: *Journal of Econometrics* 144, pp. 62–80.

Helton, J. C. (1997). "Uncertainty and sensitivity analysis in the presence of stochastic and subjective uncertainty". In: *Journal of Statistical Computation and Simulation* 57, pp. 3–76.

Helton, J. C. and F. J. Davis (2003). "Latin hypercube sampling and the propagation of uncertainty in analyses of complex systems". In: *Reliability Engineering and System Safety* 81, pp. 23–69.

Helton, J. C., J. D. Johnson, and W. L. Oberkampf (2004). "An exploration of alternative approaches to the representation of uncertainty in model predictions". In: *Reliability Engineering and System Safety* 85, pp. 39–71.

Helton, J. C., J. D. Johnson, C. J. Sallaberry, and C. B. Storlie (2006). "Survey of sampling-based methods for uncertainty and sensitivity analysis". In: *Reliability Engineering and System Safety* 91, pp. 1175–1209.

Hesterberg, T. C. (1996). "Estimates and Confidence Intervals for Importance Sampling Sensitivity Analysis". In: *Mathematical and Computer Modelling* 23, pp. 79–85.

Hoeffding, W. (1948). "A class of statistics with asymptotically normal distribution". In: *The Annals of Mathematical Statistics* 19.3, pp. 293–325.

Hoffman, F. O. and J. S. Hammonds (1994). "Propagation of uncertainty in risk assessments: the need to distinguish between uncertainty due to lack of knowledge and uncertainty due to variability". In: *Risk Analysis* 14.35, pp. 707–712.

Hohenbichler, M. and R. Rackwitz (1981). "Non-Normal Dependent Vectors in Structural Safety". In: *Journal of the Engineering Mechanics Division ASCE* 107.6, pp. 1227–1238.

— (1986). "Sensitivity and importance measures in structural reliability". In: *Civil Engineering Systems* 3, pp. 203–209.

Homem-de-Mello, T. (2007). "A study on the Cross-Entropy method for rare-event probability estimation". In: *INFORMS Journal on Computing* 19.3, pp. 381–394.

Homem-de-Mello, T. and R. Y. Rubinstein (2002). "Estimation of rare event probabilities using cross-entropy". In: *Proc. of the 2002 Winter Simulation Conference (WSC'02)*. San Diego, CA, USA.

Homma, T. and A. Saltelli (1996). "Importance measures in global sensitivity analysis of nonlinear models". In: *Reliability Engineering and System Safety* 52, pp. 1–17.

Hong, H. P. (1996). "Evaluation of the Probability of Failure with Uncertain Distribution Parameters". In: *Civil Engineering Systems* 13, pp. 157–168.

Hoogendoorn, R., E. Mooij, and J. Geul (2018). "Uncertainty propagation for statistical impact prediction of space debris". In: *Advances in Space Research* 61, pp. 167–181.

Hou, G. J.-W., C. R. Gumbert, and P. A. Newman (2004). "A most probable point-based method for reliability analysis, sensitivity analysis and design optimization". In: *Proc. of the 9th ASCE Specialty Conference on Probabilistic Mechanics and Structural Reliability (PMC2004)*. Albuquerque, NM, USA.

Hurtado, J. E. (2012). "Dimensionality reduction and visualization of structural reliability problems using polar features". In: *Probabilistic Engineering Mechanics* 29, pp. 16–31.

Igusa, T. and A. Der Kiureghian (1985). "Dynamic characterization of two-degree-of-freedom equipment-structure systems". In: *Journal of Engineering Mechanics ASCE* 111.1, pp. 1–19.

Iman, R. L. and J. M. Davenport (1982). "Rank correlation plots for use with correlated input variables". In: *Communications in Statistics: Simulation and Computation* 11, pp. 335–360.

Iooss, B. (2009). "Contributions au traitement des incertitudes en modélisation numérique : propagation d'ondes en milieu aléatoire et analyse statistique d'expériences simulées". 120 pages, (in French). HDR (French Accreditation to Supervise Research). Université Toulouse III – Paul Sabatier.

Iooss, B. and L. Le Gratiet (2017). "Uncertainty and sensitivity analysis of functional risk curves based on Gaussian processes". In: *Reliability Engineering and System Safety*. (In Press), pp. 1–9.

Iooss, B. and P. Lemaître (2015). "A Review on Global Sensitivity Analysis Methods". In: *Uncertainty Management in Simulation-Optimization of Complex Systems: Algorithms and Applications*. Ed. by G. Dellino and C. Meloni. Boston, MA: Springer US. Chap. 5, pp. 101–122.

Iooss, B. and C. Prieur (2017). "Shapley effects for sensitivity analysis with dependent inputs: comparisons with Sobol' indices, numerical estimation and applications". In: *(Submitted to: Reliability Engineering and System Safety)*, pp. 1–37.

Iott, J., R. T. Haftka, and H. M. Adelman (1985). *Selecting step sizes in sensitivity analysis by finite differences, NASA Technical Memorandum 86382*. Tech. rep. National Aeronautics, Space Administration, Scientific, and Technical Information Branch, Langley Research Center Hampton, Virginia.

Jacod, J. and P. E. Protter (2004). *Probability Essentials*. Second ed. Universitext. Springer-Verlag Berlin Heidelberg.

Jaeger, L., C. Gogu, S. Segonds, and C. Bes (2013). "Aircraft multidisciplinary design optimization under both model and design variables uncertainty". In: *Journal of Aircraft* 50.2, pp. 528–538.

Jha, S. K., H. R. Millwater, and J. M. Larsen (2009). "Probabilistic sensitivity analysis in life-prediction of an $\alpha + \beta$ titanium alloy". In: *Fatigue & Fracture of Engineering Materials & Structures* 32, pp. 493–504.

Jiang, Z., W. Chen, and B. J. German (2016). "Multidisciplinary Statistical Sensitivity Analysis Considering Both Aleatory and Epistemic Uncertainties". In: *AIAA Journal* 54.4, pp. 1326–1338.

Jones, M. C., J. S. Marron, and S. J. Sheather (1996). "A Brief Survey of Bandwidth Selection for Density Estimation". In: *Journal of the American Statistical Association* 91.433, pp. 401–407.

Kahn, H. and T. E. Harris (1951). "Estimation of particle transmission by random sampling". In: *National Bureau of Standards Applied Mathematics Series* 12, pp. 27–30.

Karamchandani, A. and C. A. Cornell (1992). "Sensitivity estimation within first and second order reliability methods". In: *Structural Safety* 11, pp. 95–107.

Karandikar, J. M., N. H. Kim, and T. L. Schmitz (2012). "Prediction of remaining useful life for fatigue-damaged structures using Bayesian inference". In: *Engineering Fracture Mechanics* 96, pp. 588–605.

Katafygiotis, L. S. and K. M. Zuev (2008). "Geometric insight into the challenges of solving high-dimensional reliability problems". In: *Probabilistic Engineering Mechanics* 23, pp. 208–218.

Keller, M., A. Pasanisi, and E. Parent (2011). "On uncertainty analysis in an industrial context: Or, how to combine available information with decisional stakes". In: *Journal de la Société Française de Statistique* 152.4. (in French), pp. 60–77.

Kim, T. and J. Song (2018a). "Development of generalized reliability importance measure (GRIM) using Gaussian mixture". In: *Proc. of the 2018 IFIP WG 7.5 Working Conference on Reliability and Optimization of Structural Systems*. Zurich, Switzerland.

— (2018b). "Generalized Reliability Importance Measure (GRIM) using Gaussian mixture". In: *Reliability Engineering and System Safety* 173, pp. 105–115.

Kim, Y. B., D. S. Roh, and M. Y. Lee (2000). "Nonparametric adaptive importance sampling for rare event simulation". In: *Proc. of the 2000 Winter Simulation Conference (WSC'00)*. Orlando, FL, USA.

Klinkrad, H. (2006). *Space Debris – Models and Risk Analysis*. Springer Science+Business Media.

Konakli, K. and B. Sudret (2016). "Global sensitivity analysis using low-rank tensor approximations". In: *Reliability Engineering and System Safety* 156, pp. 64–83.

Kouassi, A. (2017). "Propagation d'incertitudes en CEM. Application à l'analyse de fiabilité et de sensibilité de lignes de transmission et d'antennes". (in French). PhD thesis. Université Clermont Auvergne.

Kouassi, A., J.-M. Bourinet, S. Lalléchère, P. Bonnet, and M. Fogli (2016). "Reliability and sensitivity analysis of transmission lines in a probabilistic EMC context". In: *IEEE Transactions on Electromagnetic Compatibility* 58.2, pp. 561–572.

Krzykacz-Hausmann, B. (2001). "Epistemic sensitivity analysis based on the concept of entropy". In: *Proc. of the Sensitivity Analysis on Model Output (SAMO) Conference 2001*. Madrid, Spain.

Kucherenko, S and B. Iooss (2017). "Derivative-Based Global Sensitivity Measures". In: *Handbook of Uncertainty Quantification*. Ed. by R. Ghanem, D. Higdon, and H. Owhadi. Springer International Publishing. Chap. 36, pp. 1241–1263.

Kucherenko, S., M. Rodriguez-Fernandez, C. Pantelides, and N. Shah (2009). "Monte Carlo evaluation of derivative-based global sensitivity measures". In: *Reliability Engineering and System Safety* 94, pp. 1135–1148.

Kucherenko, S., O. V. Klymenko, and N. Shah (2017). "Sobol' indices for problems defined in non-rectangular domains". In: *Reliability Engineering and System Safety* 167, pp. 218–231.

Kullback, S. and R. A. Leibler (1951). "On information and sufficiency". In: *The Annals of Mathematical Statistics* 22.1, pp. 79–86.

Kurtz, N. and J. Song (2013). "Cross-entropy-based adaptive importance sampling using Gaussian mixture". In: *Structural Safety* 42, pp. 35–44.

Lagnoux, A. (2006). "Rare event simulation". In: *Probability in the Engineering and Informational Sciences* 20, pp. 45–66.

Lamboni, M., B. Iooss, A.-L. Popelin, and F. Gamboa (2013). "Derivative-based global sensitivity measures: General links with Sobol' indices and numerical tests". In: *Mathematics and Computers in Simulation* 87, pp. 45–54.

Le Gratiet, L., S. Marelli, and B. Sudret (2017). "Metamodel-Based Sensitivity Analysis: Polynomial Chaos Expansions and Gaussian Processes". In: *Handbook of Uncertainty Quantification*. Ed. by R. Ghanem, D. Higdon, and H. Owhadi. Springer International Publishing. Chap. 38, pp. 1289–1325.

Lebrun, R. (2013). "Contributions à la modélisation de la dépendance stochastique". (in English). PhD thesis. Université Paris-Diderot – Paris VII.

Lebrun, R. and A. Dutfoy (2009a). "A generalization of the Nataf transformation to distributions with elliptical copula". In: *Probabilistic Engineering Mechanics* 24, pp. 172–178.

— (2009b). "Do Rosenblatt and Nataf isoprobabilistic transformations really differ?" In: *Probabilistic Engineering Mechanics* 24, pp. 577–584.

Lee, I., K. K. Choi, Y. Noh, L. Zhao, and D. Gorsich (2011). "Sampling-based stochastic sensitivity analysis using score functions for RBDO problems with correlated random variables". In: *Journal of Mechanical Design* 133.2, pp. 1–10.

Lemaire, M., A. Chateauneuf, and J.-C. Mitteau (2009). *Structural Reliability*. ISTE Ltd & John Wiley & Sons, Inc.

Lemaître, P. (2014). "Analyse de sensibilité en fiabilité des structures". (in English). PhD thesis. Université de Bordeaux.

Lemaître, P., E. Sergienko, A. Arnaud, N. Bousquet, F. Gamboa, and B. Iooss (2015). "Density modification-based reliability sensitivity analysis". In: *Journal of Statistical Computation and Simulation* 85.6, pp. 1200–1223.

Lemieux, C. (2009). *Monte Carlo and Quasi-Monte Carlo Sampling*. Springer Series in Statistics. Springer-Verlag New York, Inc.

Li, L., Z. Lu, F. Jun, and W. Bintuan (2012). "Moment-independent importance measure of basic variable and its state dependent parameter solution". In: *Structural Safety* 38, pp. 40–47.

Li, L., Z. Lu, and C. Chen (2016). "Moment-independent importance measure of correlated input variable and its state dependent parameter solution". In: *Aerospace Science and Technology* 48, pp. 281–290.

Limbourg, P., E. De Rocquigny, and G. Andrianov (2010). "Accelerated uncertainty propagation in two-level probabilistic studies under monotony". In: *Reliability Engineering and System Safety* 95, pp. 998–1010.

Liu, H., W. Chen, and A. Sudjianto (2004). "Probabilistic Sensitivity Analysis Methods for Design Under Uncertainty". In: *Proc. of the 10th AIAA/ISSMO Multidisciplinary Analysis and Optimization Conference*. Albany, NY, USA.

— (2006a). "Relative entropy based method for probabilistic sensitivity analysis in engineering design". In: *Journal of Mechanical Design* 128, pp. 326–336.
— (2006b). "Relative Entropy Based Method for Probabilistic Sensitivity Analysis in Engineering Design". In: *Journal of Mechanical Design* 128.2, pp. 326–336.
Liu, P-L. and A. Der Kiureghian (1986). "Multivariate distribution models with prescribed marginals and covariances". In: *Probabilistic Engineering Mechanics* 1.2, pp. 105–112.
Lu, Z., S. Song, Z. Yue, and J. Wang (2008). "Reliability sensitivity method by line sampling". In: *Structural Safety* 30.6, pp. 517–532.
Madsen, H. O. (1988). "Omission sensitivity factors". In: *Structural Safety* 5.1, pp. 35–45.
Madsen, H. O., S. Krenk, and N. C. Lind (1986). *Methods of Structural Safety*. Prentice-Hall Inc.
Mai, C. V. and B. Sudret (2015). "Computing derivative-based global sensitivity measures using polynomial chaos expansions". In: *Reliability Engineering and System Safety* 134, pp. 241–250.
Marrel, A., B. Iooss, B. Laurent, and O. Roustant (2009). "Calculations of Sobol indices for the Gaussian process metamodel". In: *Reliability Engineering and System Safety* 94, pp. 742–751.
Martins, J. R. R. A. (2012). *A short course on Multidisciplinary Design Optimization, Class Notes for AEROSP 588*.
Mattrand, C. and J.-M. Bourinet (2014). "The cross-entropy method for reliability assessment of cracked structures subjected to random Markovian loads". In: *Reliability Engineering and System Safety* 123, pp. 171–182.
Maume-Deschamps, V. and I. Niang (2018). "Estimation of quantile oriented sensitivity indices". In: *Statistics and Probability Letters* 134, pp. 122–127.
McDowell, J. C. (2018). "The edge of space: Revisiting the Karman Line". In: *Acta Astronautica* 151, pp. 668–677.
Melchers, R. E. (1989). "Importance sampling in structural systems". In: *Structural Safety* 6, pp. 3–10.
— (1999). *Structural Reliability Analysis and Prediction*. Second ed. Wiley.
Melchers, R. E. and M. Ahammed (2004). "A fast approximate method for parameter sensitivity estimation in Monte Carlo structural reliability". In: *Computers & Structures* 82, pp. 55–61.
Metropolis, N. and S. Ulam (1949). "The Monte Carlo Method". In: *Journal of the American Statistical Association* 44.247, pp. 335–341.
Metropolis, N., A. W. Rosenbluth, M. N. Rosenbluth, and A. H. Teller (1953). "Equation of state calculations by fast computing machines". In: *The Journal of Chemical Physics* 21.6, pp. 1087–1092.
Meyer, M. A. and J. M. Booker (2001). *Eliciting and Analyzing Expert Judgment: A Practical Guide*. ASA-SIAM Series on Statistics and Applied Probability. SIAM.
Meynaoui, A., A. Marrel, and B. Laurent-Bonneau (2018). "Méthodologie basée sur les mesures de dépendance HSIC pour l'analyse de sensibilité de second niveau". In: *Actes des 50ème Journées de Statistique (JDS 2018)*. (in French). Saclay, France.
Millwater, H. and Y. Wieland (2010). "Probabilistic Sensitivity-Based Ranking of Damage Tolerance Analysis Elements". In: *Journal of Aircraft* 47.1, pp. 161–171.
Millwater, H. R. (2009). "Universal properties of kernel functions for probabilistic sensitivity analysis". In: *Probabilistic Engineering Mechanics* 24, pp. 89–99.
Millwater, H. R. and Y. Feng (2011). "Probabilistic sensitivity analysis with respect to bounds of truncated distributions". In: *Journal of Mechanical Design* 133.6, pp. 1–10.
Millwater, H. R., A. Bates, and E. Vazquez (2011). "Probabilistic sensitivity methods for correlated normal variables". In: *International Journal of Reliability and Safety* 5.1, pp. 1–20.
Millwater, H. R., G. Singh, and M. Cortina (2012). "Development of a localized probabilistic sensitivity method to determine random variable regional importance". In: *Reliability Engineering and System Safety* 107, pp. 3–15.
Morio, J. (2010). "Importance sampling: how to approach the optimal density?" In: *European Journal of Physics* 31.2, pp. L41–L48.

Morio, J. (2011a). "Global and local sensitivity analysis methods for a physical system". In: *European Journal of Physics* 32, pp. 1577–1583.
— (2011b). "Influence of input PDF parameters of a model on a failure probability estimation". In: *Simulation Modelling Practice and Theory* 19.10, pp. 2244–2255.
— (2011c). "Non-parametric adaptive importance sampling for the probability estimation of a launcher impact position". In: *Reliability Engineering and System Safety* 96.1, pp. 178–183.
— (2012). "Extreme quantile estimation with nonparametric adaptive importance sampling". In: *Simulation Modelling Practice and Theory* 27, pp. 76–89.
Morio, J. and M. Balesdent (2015). *Estimation of Rare Event Probabilities in Complex Aerospace and Other Systems: A Practical Approach*. Woodhead Publishing, Elsevier.
— (2016). "Estimation of a launch vehicle stage fallout zone with parametric and non-parametric importance sampling algorithms in presence of uncertain input distributions". In: *Aerospace Science and Technology* 52, pp. 95–101.
Morio, J., M. Balesdent, D. Jacquemart, and C. Vergé (2014). "A survey of rare event simulation methods for static input-output models". In: *Simulation Modelling Practice and Theory* 49, pp. 297–304.
Morris, M. D. (1991). "Factorial Sampling Plans for Preliminary Computational Experiments". In: *Technometrics* 33.2, pp. 161–174.
— (2017). *Design of Experiments: An Introduction Based on Linear Models*. Texts in Statistical Science. Chapman and Hall/CRC.
Moutoussamy, V. (2015). "Contributions to structural reliability analysis: accounting for monotonicity constraints in numerical models". PhD thesis. Université Toulouse III – Paul Sabatier.
Munoz Zuniga, M. (2011). "Méthodes stochastiques pour l'estimation contrôlée de faibles probabilités sur des modèles physiques complexes – Application au domaine nucléaire". (in English). PhD thesis. Université Paris-Diderot – Paris VII.
Murangira, A., M. Munoz Zuniga, and T. Perdrizet (2015). "Sensitivity analysis for failure probability estimation of a floating wind turbine under wind and wave loading". Journées de la conception robuste et fiable 2015 – GST Mécanique et Incertain, Paris, France.
Nagel, J. B. (2017). "Bayesian techniques for inverse uncertainty quantification". PhD thesis. ETH Zürich.
Nagel, J. B. and B. Sudret (2016). "A unified framework for multilevel uncertainty quantification in Bayesian inverse problems". In: *Probabilistic Engineering Mechanics* 43, pp. 68–84.
NASA (2009). *Bayesian Inference for NASA Probabilistic Risk and Reliability Analysis (NASA/SP-2009-569)*. Tech. rep. National Aeronautics and Space Administration.
Nataf, A. (1962). "Détermination des distributions dont les marges sont données". In: *Comptes Rendus de l'Académie des Sciences* 225. (in French), pp. 42–43.
Neddermeyer, J. C. (2009). "Computationally Efficient Nonparametric Importance Sampling". In: *Journal of the American Statistical Association* 104.486, pp. 788–802.
— (2010). "Non-parametric partial importance sampling for financial derivative pricing". In: *Quantitative Finance* 11.8, pp. 1193–1206.
Nelsen, R. B. (2006). *An introduction to Copulas*. Second ed. Springer Series in Statistics. Springer-Verlag New York.
Nikolaidis, E., D. M. Ghiocel, and S. Singhal (2004). *Engineering Design Reliability Handbook*. CRC Press.
Oberkampf, W. L. and C. J. Roy (2010). *Verification and Validation in Scientific Computing*. Cambridge University Press.
O'Hagan, A., C. E. Buck, A. Daneshkhah, J. R. Eiser, P. H. Garthwaite, D. J. Jenkinson, J. E. Oakley, and T. Rakow (2006). *Uncertain Judgements: Eliciting Experts' Probabilities*. Statistics in Practice. Wiley.
Owen, A. B. (2014). "Sobol' indices and Shapley value". In: *SIAM/ASA Journal of Uncertainty Quantification* 2, pp. 245–251.

Owen, A. B. and C. Prieur (2017). "On Shapley value for measuring importance of dependent inputs". In: *SIAM/ASA Journal of Uncertainty Quantification* 5, pp. 986–1002.

Paloheimo, E. and M. Hannus (1974). "Structural design based on weighted fractiles". In: *Journal of the Structural Division* 100.7, pp. 1367–1378.

Papadimitriou, C., J. L. Beck, and L. S. Katafygiotis (2001). "Updating robust reliability using structural test data". In: *Probabilistic Engineering Mechanics* 16.2, pp. 103–113.

Papaioannou, I., W. Betz, K. Zwirglmaier, and D. Straub (2015). "MCMC algorithms for Subset Simulation". In: *Probabilistic Engineering Mechanics* 41, pp. 89–103.

Park, C. K. and K.-I. Ahn (1994). "A new approach for measuring uncertainty importance and distributional sensitivity in probabilistic safety assessment". In: *Reliability Engineering and System Safety* 46, pp. 253–261.

Pasanisi, A., E. De Rocquigny, N. Bousquet, and E. Parent (2009). "Some useful features of the Bayesian setting while dealing with uncertainties in industrial practice". In: *Proc. of the 20th European Safety and Reliability Conference (ESREL 2009)*. Prague, Czech Republic.

Pasanisi, A., M. Keller, and E. Parent (2012). "Estimation of a quantity of interest in uncertainty analysis: Some help from Bayesian decision theory". In: *Reliability Engineering and System Safety* 100, pp. 93–101.

Paté-Cornell, M. E. (1996). "Uncertainties in risk analysis: six levels of treatment". In: *Reliability Engineering and System Safety* 54, pp. 95–111.

Patelli, E., H. Pradlwarter, and G. Schuëller (2010). "Global sensitivity of structural variability by random sampling". In: *Computer Physics Communications* 181, pp. 2072–2081.

Pendola, M. (2000). "Fiabilité des structures en contexte d'incertitudes statistiques et d'écarts de modélisation". (in French). PhD thesis. Université Blaise Pascal – Clermont II.

Pendola, M., P. Hornet, A. Mohamed, and M. Lemaire (1999). "Uncertainties arising in the assessment of structural reliability". In: *Proc. of the 13th ASCE Engineering Mechanics Conference*. Baltimore,MD, USA.

Perrin, G. and G. Defaux (2019). "Efficient Evaluation of Reliability-Oriented Sensitivity Indices". In: *Journal of Scientific Computing*. (In Press), pp. 1–23.

Perrin, G., C. Soize, and N. Ouhbi (2018). "Data-driven kernel representations for sampling with an unknown block dependence structure under correlation constraints". In: *Journal of Computational Statistics and Data Analysis* 119, pp. 139–154.

Pianosi, F., K. Beven, J. Freer, J. W. Hall, J. Rougier, D. B. Stephenson, and T. Wagener (2016). "Sensitivity analysis of environmental models: A systematic review with practical workflow". In: *Environmental Modelling & Software* 79, pp. 214–232.

Prieur, C. and S. Tarantola (2017). "Variance-based sensitivity analysis: theory and estimation algorithms". In: *Handbook of Uncertainty Quantification*. Ed. by R. Ghanem, D. Higdon, and H. Owhadi. Springer International Publishing. Chap. 35, pp. 1217–1239.

Proppe, C. (2008). "Estimation of failure probabilities by local approximation of the limit state function". In: *Structural Safety* 30, pp. 277–290.

— (2017). "Markov chain methods for reliability estimation". In: *Proc. of the 12th International Conference on Structural Safety and Reliability (ICOSSAR'17)*. Vienna, Austria.

Qiu, Z., D. Yang, and I. Elishakoff (2008). "Probabilistic interval reliability of structural systems". In: *International Journal of Solids and Structures* 45, pp. 2850–2860.

Rachdi, N. (2011). "Apprentissage Statistique et Computer Experiments – Approche quantitative du risque et des incertitudes en modélisation". PhD thesis. Université Toulouse III – Paul Sabatier.

Rackwitz, R. and B. Fiessler (1978). "Structural reliability under combined random load sequences". In: *Computers & Structures* 9.5, pp. 489–494.

Raguet, H. and A. Marrel (2018). "Target and conditional sensitivity analysis with emphasis on dependence measures". In: *ArXiv e-prints*, pp. 1–48. arXiv: 1801.10047v2 [stat.ME].

Rahman, S. (2009). "Stochastic sensitivity analysis by dimensional decomposition and score functions". In: *Probabilistic Engineering Mechanics* 24, pp. 278–287.

— (2016). "The f-Sensitivity Index". In: *SIAM/ASA Journal of Uncertainty Quantification* 4, pp. 130–162.

Reid, S. G. (2002). "Specification of design criteria based on probabilistic measures of design performance". In: *Structural Safety* 24, pp. 333–345.

Rhode, C. A. (2014). *Introductory Statistical Inference with the Likelihood Function*. Springer International Publishing.

Ridolfi, G. and E. Mooij (2016). "Space Engineering: Modeling and Optimization with Case Studies". In: ed. by G. Fasano and J. D. (Eds.) Pintér. Springer International Publishing. Chap. Regression-Based Sensitivity Analysis and Robust Design, pp. 303–336.

Robert, C. P. (2007). *The Bayesian Choice*. Second ed. Springer Texts in Statistics. Springer-Verlag New York.

Robert, C. P. and G. Casella (2004). *Monte Carlo Statistical Methods*. Second ed. Springer Texts in Statistics. Springer Science+Business Media.

Robinson, E. I., J. Marzat, and T. Raïssi (2018). "Filtering and Uncertainty Propagation Methods for Model-Based Prognosis of Fatigue Crack Growth in Unidirectional Fiber-Reinforced Composites". In: *ASCE-ASME Journal of Risk and Uncertainty in Engineering Systems, Part A: Civil Engineering* 4.4, pp. 1–13.

Ronse, A. and E. Mooij (2014). "Statistical impact prediction of decaying objects". In: *Journal of Spacecraft and Rockets* 51.6, pp. 1797–1810.

Rosenblatt, M. (1952). "Remarks on a Multivariate Transformation". In: *Annals of Mathematical Statistics* 23.3, pp. 470–472.

Roustant, O., J. Fruth, B. Iooss, and S. Kuhnt (2014). "Crossed-derivative based sensitivity measures for interaction screening". In: *Mathematics and Computers in Simulation* 105, pp. 105–118.

Roustant, O., F. Barthe, and B. Iooss (2017). "Poincaté inequalities on intervals – application to sensitivity analysis". In: *Electronic Journal of Statistics* 11, pp. 3081–3119.

Ruan, W. and Z. Lu (2014). "Estimation of Moment-Independent Importance Measure on Failure Probability and Its Application in Reliability Analysis". In: *Journal of Structural Engineering ASCE* 141.8, pp. 1–8.

Rubino, G. and B. Tuffin (2009). *Rare Event Simulation using Monte Carlo Methods*. Wiley Publishing.

Rubinstein, R. Y. (1986). "The score function approach for sensitivity analysis of computer simulation models". In: *Mathematics and Computers in Simulation* 28, pp. 351–379.

— (1997). "Optimization of computer simulation models with rare events". In: *European Journal of Operational Research* 99, pp. 89–112.

— (1999). "The Cross-Entropy Method for Combinatorial and Continuous Optimization". In: *Methodology and Computing in Applied Probability* 1, pp. 127–190.

Rubinstein, R. Y. and D. P. Kroese (2004). *The Cross-Entropy Method. A unified approach to combinatorial optimization, Monte-Carlo simulation and machine learning*. Information Science and Statistics. Springer-Verlag New York.

— (2008). *Simulation and the Monte Carlo Method*. Second ed. Wiley.

Saltelli, A. (2002). "Making best use of model evaluations to compute sensitivity indices". In: *Computer Physics Communications* 145, pp. 280–297.

Saltelli, A., T. H. Andres, and T. Homma (1993). "Sensitivity analysis of model output: An investigation of new techniques". In: *Computational Statistics and Data Analysis* 15, pp. 211–238.

Saltelli, A., S. Tarantola, F. Campolongo, and M. Ratto (2004). *Sensitivity Analysis in Practice: A Guide to Assessing Scientific Models*. Wiley.

Saltelli, A., M. Ratto, T. Andres, F. Campolongo, J. Cariboni, D. Gatelli, M. Saisana, and S. Tarantola (2008). *Global Sensitivity Analysis. The Primer*. Wiley.

Sankararaman, S. (2012). "Uncertainty Quantification and Integration in Engineering Systems". PhD thesis. Vanderbilt University.

Sankararaman, S. and S. Mahadevan (2013a). "Distribution type uncertainty due to sparse and imprecise data". In: *Mechanical Systems and Signal Processing* 37, pp. 182–198.

— (2013b). "Separating the contributions of variability and parameter uncertainty in probability distributions". In: *Reliability Engineering and System Safety* 112, pp. 187–199.

Saporta, G. (2006). *Probabilités, analyse des données et statistique*. Third ed. (in French). Editions Technip.

Schöbi, R. (2017). "Surrogate models for uncertainty quantification in the context of imprecise probability modelling". PhD thesis. ETH Zürich.

Schöbi, R. and B. Sudret (2015). "Propagation of Uncertainties Modelled by Parametric P-boxes Using Sparse Polynomial Chaos Expansion". In: *Proc. of the 12th International Conference on Applications of Statistics and Probability in Civil Engineering (ICASP12)*. Vancouver, Canada.

— (2017). "Global sensitivity analysis in the context of imprecise probabilities (p-boxes) using sparse polynomial chaos expansions". In: *ArXiv e-prints*, pp. 1–26. arXiv: 1705.10061 [stat.CO].

Schöbi, R., B. Sudret, and S. Marelli (2017). "Rare Event Estimation Using Polynomial-Chaos Kriging". In: *ASCE-ASME Journal of Risk and Uncertainty in Engineering Systems, Part A: Civil Engineering* 3.2, pp. 1–12.

Schuëller, G. I. and R. Stix (1987). "A critical appraisal of methods to determine failure probabilities". In: *Structural Safety* 4, pp. 293–309.

Scott, D. W. (2015). *Multivariate Density Estimation: Theory, Practice, and Visualization*. Second ed. Wiley series in Probability and Statistics. Wiley.

Shapley, L. S. (1953). "A value for n-person games". In: *Contributions to the Theory of Games, Volume II*. Ed. by H. Kuhn and A. W. Tucker. Annals of Mathematics Studies. Princeton, NJ: Princeton University Press. Chap. 17, pp. 307–317.

Shekhar, S., H. Xiong, and X. Zhou, eds. (2017). *Encyclopedia of GIS*. Springer International Publishing.

Shinozuka, M. (1983). "Basic Analysis of Structural Safety". In: *Journal of Structural Engineering* 109.3, pp. 721–740.

Silverman, B. W. (1986). *Density Estimation for Statistics and Data Analysis*. Chapman and Hall.

Sobol, I. M. (1993). "Sensitivity estimates for nonlinear mathematical models". In: *Mathematical Modelling and Computational Experiments* 1, pp. 407–414.

— (2001). "Global sensitivity indices for nonlinear mathematical models and their Monte Carlo estimates". In: *Mathematics and Computers in Simulation* 55, pp. 271–280.

Sobol, I. M. and A. Gershman (1995). "On an alternative global sensitivity estimators". In: *Proc. of the Sensitivity Analysis on Model Output (SAMO) Conference 1995*. Belgirate, Italy.

Sobol, I. M. and S. Kucherenko (2009). "Derivative based global sensitivity measures and their link with global sensitivity indices". In: *Mathematics and Computers in Simulation* 79, pp. 3009–3017.

Soize, C. (2017). *Uncertainty Quantification: An Accelerated Course with Advanced Applications in Computational Engineering*. Interdisciplinary Applied Mathematics. Springer International Publishing.

Soize, C. and R. Ghanem (2016). "Data-driven probability concentration and sampling on manifold". In: *Journal of Computational Physics* 321, pp. 242–258.

— (2017). "Probabilistic learning on manifold for optimization under uncertainties". In: *Proc. of the 2nd ECCOMAS Thematic Conference on Uncertainty Quantification in Computational Sciences and Engineering (UNCECOMP 2017)*. Rhodes Island, Greece.

Song, E., B. L. Nelson, and J. Staum (2016). "Shapley effects for global sensitivity analysis: theory and computation". In: *SIAM/ASA Journal of Uncertainty Quantification* 4, pp. 1060–1083.

Song, S., Z. Lu, W. Zhang, and Z. Ye (2009a). "Reliability and sensitivity analysis of transonic flutter using Improved Line Sampling technique". In: *Chinese Journal of Aeronautics* 22, pp. 513–519.

Song, S., Z. Lu, and H. Qiao (2009b). "Subset simulation for structural reliability sensitivity analysis". In: *Reliability Engineering and System Safety* 94.2, pp. 658–665.

— (2010). "Reliability sensitivity by method of moments". In: *Applied Mathematical Modelling* 34.10, pp. 2860–2871.

Song, S., Z. Lu, and Z. Song (2011). "Reliability sensitivity analysis involving correlated random variables by Directional Sampling". In: *Proc. of the 2011 International Conference on Quality, Reliability, Risk, Maintenance, and Safety Engineering*. Xi'an, China.

Spear, R. C. and G. M. Hornberger (1980). "Eutrophication in Peel Inlet. II. Identification of critical uncertainties via generalized sensitivity analysis". In: *Water Research* 14, pp. 43–49.

Straub, D. (2011). "Reliability updating with equality information". In: *Probabilistic Engineering Mechanics* 26, pp. 254–258.

Straub, D. and I. Papaioannou (2015). "Bayesian Updating with Structural Reliability Methods". In: *Journal of Engineering Mechanics ASCE* 314, pp. 538–556.

Straub, D., I. Papaioannou, and W. Betz (2016). "Bayesian analysis of rare events". In: *Journal of Computational Physics* 314, pp. 538–556.

Sudret, B. (2007). "Uncertainty propagation and sensitivity analysis in mechanical models – Contributions to structural reliability and stochastic spectral methods". 230 pages. HDR (French Accreditation to Supervise Research). Université Blaise Pascal – Clermont II.

— (2008). "Global sensitivity analysis using polynomial chaos expansions". In: *Reliability Engineering and System Safety* 93, pp. 964–979.

Sues, R. H. and M. A. Cesare (2005). "System reliability and sensitivity factors via the MPPSS method". In: *Probabilistic Engineering Mechanics* 20, pp. 148–157.

Sueur, R., B. Iooss, and T. Delage (2017). "Sensitivity analysis using perturbed-law based indices for quantiles and application to an industrial case". In: *Proc. of the 10th International Conference on Mathematical Methods in Reliability (MMR 2017)*. Grenoble, France.

Sullivan, T. J. (2015). *Introduction to Uncertainty Quantification*. Vol. 63. Texts in Applied Mathematics. Springer International Publishing Switzerland.

Swiler, L. P. and N. J. West (2010). "Importance Sampling: Promises and Limitations". In: *Proc. of the 51st AIAA/ASME/ASCE/AHS/ASC Structures, Structural Dynamics and Materials Conference*. Orlando, FL, USA.

Taflanidis, A. A. and J. L. Beck (2009). "Stochastic Subset Optimization for reliability optimization and sensitivity analysis in system design". In: *Computers & Structures* 87, pp. 318–331.

Tang, X.-S.., D.-Q. Li, G. Rong, K.-K. Phoon, and C.-B. Zhou (2013). "Impact of copula selection on geotechnical reliability under incomplete probability information". In: *Computers and Geotechnics* 49, pp. 264–278.

Tang, X.-S.., D.-Q. Li, C.-B. Zhou, and K.-K. Phoon (2015). "Copula-based approaches for evaluating slope reliability under incomplete probability information". In: *Structural Safety* 52, pp. 90–99.

Thunissen, D. P. (2005). "Propagating and Mitigating Uncertainty in the Design of Complex Multidisciplinary Systems". PhD thesis. California Institute of Technology.

Tokdar, S. T. and R. E. Kass (2009). "Importance sampling: a review". In: *Wiley Interdisciplinary Reviews: Computational Statistics* 2.1, pp. 54–60.

Tsybakov, A. B. (2009). *Introduction to Nonparametric Estimation*. Springer Series in Statistics. Springer-Verlag New York.

Valdebenito, M. A., H. J. Pradlwarter, and G. I. Schuëller (2010). "The role of the design point for calculating failure probabilities in view of dimensionality and structural nonlinearities". In: *Structural Safety* 32, pp. 101–111.

Valdebenito, M. A., H. A. Jensen, H. B. Hernández, and L. Mehrez (2018). "Sensitivity estimation of failure probability applying line sampling". In: *Reliability Engineering and System Safety* 171, pp. 99–111.

Van Der Waart, A. W. (1998). *Asymptotic statistics*. Cambridge series in statistical and probabilistic mathematics. Cambridge University Press.

Vazquez, E. and J. Bect (2009). "A sequential Bayesian algorithm to estimate a probability of failure". In: *Proc. of the 15th IFAC Symposium on System Identification*. Saint-Malo, France.

Vergé, C., J. Morio, and P. Del Moral (2016). "An island particle algorithm for rare event analysis". In: *Reliability Engineering and System Safety* 149, pp. 63–75.

Walter, C. (2015). "Moving particles: A parallel optimal multilevel splitting method with application in quantiles estimation and meta-model based algorithms". In: *Structural Safety* 55, pp. 10–25.

— (2016). "Using Poisson processes for rare event simulation". PhD thesis. Université Paris Diderot – Paris VII.

Walter, E. (2014). *Numerical Methods and Optimization: A Consumer Guide*. Springer International Publishing.

Walz, G. and H. Riesch-Oppermann (2006). "Probabilistic fracture mechanics assessment of flaws in turbine disks including quality assurance procedures". In: *Structural Safety* 28, pp. 273–288.

Wand, M. P. and M. C. Jones (1995). *Kernel Smoothing*. Chapman and Hall/CRC.

Wang, P., Z. Lu, and Z. Tang (2013a). "A derivative based sensitivity measure of failure probability in the presence of epistemic and aleatory uncertainties". In: *Computers and Mathematics with Applications* 65, pp. 89–101.

— (2013b). "An application of the Kriging method in global sensitivity analysis with parameter uncertainty". In: *Applied Mathematical Modelling* 37, pp. 6543–6555.

— (2013c). "Importance measure analysis with epistemic uncertainty and its moving least squares solution". In: *Computers and Mathematics with Applications* 66, pp. 460–471.

Wang, Y., N. Binaud, C. Gogu, C. Bes, and J. Fu (2016). "Determination of Paris' law constants and crack length evolution via Extended and Unscented Kalman filter: An application to aircraft fuselage panels". In: *Mechanical Systems and Signal Processing* 80, pp. 262–281.

Wang, Y., S. Xiao, and Z. Lu (2018). "A new efficient simulation method based on Bayes' theorem and importance sampling Markov chain simulation to estimate the failure-probability-based global sensitivity measure". In: *Aerospace Science and Technology* 79, pp. 364–372.

Wang, Z. and J. Song (2016). "Cross-entropy-based adaptive importance sampling using von Mises-Fisher mixture for high dimensional reliability analysis". In: *Structural Safety* 59, pp. 42–52.

Wasserman, L. (2004). *All of Statistics: A Concise Course in Statistical Inference*. Springer Texts in Statistics. Springer Science+Business Media.

— (2006). *All of Nonparametric Statistics*. Springer Texts in Statistics. Springer Science+Business Media.

Wei, P., Z. Lu, W. Hao, J. Feng, and B. Wang (2012). "Efficient sampling methods for global reliability sensitivity analysis". In: *Computer Physics Communications* 183, pp. 1728–1743.

Wei, P., Z. Lu, and X. Yuan (2013). "Monte Carlo simulation for moment-independent sensitivity analysis". In: *Reliability Engineering and System Safety* 110, pp. 60–67.

Wei, P., Z. Lu, and J. Song (2015a). "Regional and parametric sensitivity analysis of Sobol' indices". In: *Reliability Engineering and System Safety* 137, pp. 87–100.

Wei, P., Z. Lu, and S. Song (2015b). "Variable importance analysis: a comprehensive review". In: *Reliability Engineering and System Safety* 142, pp. 399–432.

Wei, P., J. Song, and Z. Lu (2016). "Global reliability sensitivity analysis of motion mechanisms". In: *Proceedings of the Institution of Mechanical Engineers, Part O: Journal of Risk and Reliability* 230.3, pp. 265–277.

Wen, Y. K. and H.-C. Chen (1987). "On fast integration for time-variant structural reliability". In: *Probabilistic Engineering Mechanics* 2.3, pp. 156–162.

Wu, Y.-T. (1994a). "Adapative Importance Sampling (AIS)-Based System Reliability Sensitivity Analysis Method". In: *Probabilistic Structural Mechanics: Advances in Structural Reliability Methods*. Ed. by P. D. Spanos and Y.-T. Wu. Berlin Heidelberg: Springer-Verlag, pp. 550–564.

— (1994b). "Computational Methods for Efficient Structural Reliability and Reliability Sensitivity Analysis". In: *AIAA Journal* 32.8, pp. 1717–1723.

Xiao, S., Z. Lu, and L. Xu (2016). "A new effective screening design for structural sensitivity analysis of failure probability with the epistemic uncertainty". In: *Reliability Engineering and System Safety* 156, pp. 1–14.

Yoo, D., I. Lee, and H. Cho (2014). "Probabilistic sensitivity analysis for novel second-order reliability method (SORM) using generalized chi-squared distribution". In: *Structural and Multidisciplinary Optimization* 50, pp. 787–797.

Yun, W., Z. Lu, X. Jiang, and S. Liu (2016). "An efficient method for estimating global sensitivity indices". In: *International Journal for Numerical Methods in Engineering* 108, pp. 1275–1289.

Yun, W., Z. Lu, and X. Jiang (2018). "A modified importance sampling method for structural reliability and its global reliability sensitivity analysis". In: *Structural and Multidisciplinary Optimization* 57, pp. 1625–1641.

Žanić, V. and K. Žiha (1998). "Sensitivity to correlation in multivariate models". In: *Computer Assisted Mechanics and Engineering Sciences* 5.1, pp. 75–84.

— (2001). "Sensitivity to correlations in structural problems". In: *Transactions of FAMENA* 25.2, pp. 1–26.

Zhang, P. (1996). "Nonparametric Importance Sampling". In: *Journal of the American Statistical Association* 91.425, pp. 1245–1253.

Zhang, X. and M. D. Pandey (2013). "Structural reliability analysis based on the concepts of entropy, fractional moment and dimensional reduction method". In: *Structural Safety* 43, pp. 28–40.

Zhang, Y. and A. Der Kiureghian (1994). "Two improved algorithms for reliability analysis". In: *Reliability and Optimization of Structural Systems: Proceedings of the 6th IFIP WG 7.5 Conference*. Ed. by R. Rackwitz, G. Augusti, and A. Borri. Springer US, pp. 297–304.

Zhang, Y., Y. Liu, and X. Yang (2015). "Parametric sensitivity analysis for importance measure on failure probability and its efficient Kriging solution". In: *Mathematical Problems in Engineering* 2015, pp. 1–13.

Zhao, Y.-G., P.-P. Li, and Z.-H. Lu (2018). "Efficient evaluation of structural reliability under imperfect knowledge about probability distributions". In: *Reliability Engineering and System Safety* 175, pp. 160–170.

Zio, E. (2013). *The Monte Carlo simulation method for system reliability and risk analysis*. Springer Series in Reliability Engineering. Springer Science+Business Media.

Zio, E. and N. Pedroni (2012). "Monte Carlo simulation-based sensitivity analysis of the model of a thermal-hydraulic passive system". In: *Reliability Engineering and System Safety* 107, pp. 90–106.

— (2013). *Literature review of methods for representing uncertainty, Cahiers de la Sécurité Industrielle, Report No. 2013-03*. Tech. rep. Foundation for an Industrial Safety Culture, Toulouse, France.

Zuev, K. M. and L. S. Katafygiotis (2011). "Modified Metropolis-Hastings algorithm with delayed rejection". In: *Probabilistic Engineering Mechanics* 26, pp. 405–412.

APPENDIX A

Copulas

Basically, *copulas* correspond to the general and rigorous mathematical tools to model the stochastic dependence between random variables from a theoretical point of view. The general definition of a copula is given by the theorem below (Nelsen, 2006).

Theorem 2 (Sklar's Theorem)**.** *Let $F_{\mathbf{X}}$ be a d-dimensional joint CDF with given marginal CDF F_{X_i}, for $i = 1, \ldots, d$. Then there exists a d-dimensional copula C such that:*

$$F_{\mathbf{X}}(\mathbf{x}) = F_{\mathbf{X}}(x_1, \ldots, x_d) = C\left(F_{X_1}(x_1), \ldots, F_{X_d}(x_d)\right). \tag{A.1}$$

In addition, if the marginal CDFs are continous, then C is unique.

This theorem states that a copula represents the complementary information required to fully specify a joint distribution of a random vector $\mathbf{X}$ regarding the marginal distributions $\{F_{X_i}, i = 1, \ldots, d\}$. A corollary of this Sklar's Theorem (Nelsen, 2006) is given below.

Corollary 1. *Let $F_{\mathbf{X}}$, $\{F_{X_i}, i = 1, \ldots, d\}$ and C be as in Theorem 2, and let $\{F_{X_i}^{-1}, i = 1, \ldots, d\}$ be the inverse CDFs of the corresponding marginals. Then, for any $\mathbf{u} = (u_1, \ldots, u_d)^\top \in [0,1]^d$:*

$$C(u_1, \ldots, u_d) = F_{\mathbf{X}}\left(F_{X_1}^{-1}(u_1), \ldots, F_{X_d}^{-1}(u_d)\right). \tag{A.2}$$

This corollary states that, from a practical point of view, a copula is a joint CDF on the unit hypercube $[0,1]^d$ with uniformly distributed marginals on $[0,1]$. This provides a method to practically construct copulas from a known joint probability distribution.
From the previous Sklar's Theorem, one can make the link between CDFs and PDFs through the following derivations:

$$\begin{aligned} f_{\mathbf{X}}(\mathbf{x}) = \frac{\partial^d F_{\mathbf{X}}(x_1, \ldots, x_d)}{\partial x_1 \ldots \partial x_d} &= \frac{\partial^d C(u_1, \ldots, u_d)}{\partial u_1 \ldots \partial u_d} \prod_{i=1}^{d} \frac{\partial F_{X_i}(x_i)}{\partial x_i} \\ &= c\left(F_{X_1}(x_1), \ldots, F_{X_d}(x_d)\right) \prod_{i=1}^{d} f_{X_i}(x_i) \end{aligned} \tag{A.3}$$

where $c(u_1, \ldots, u_d)$ is the density of copula C. A large variety of copulas is available to model dependence (e.g., normal, Student, Frank, Clayton, among others). For more information about it, one can refer to Lebrun (2013). In this thesis, one will just recall two definitions, respectively those for the independent and normal copulas.

Definition 2 (Independent copula)**.** *The d-dimensional independent copula, for* $\mathbf{u} \in [0,1]^d$*, is given by (respectively for the CDF and PDF):*

$$C_{ind}(u_1, \ldots, u_d) = \prod_{i=1}^{d} u_i \tag{A.4}$$

$$c_{ind}(u_1, \ldots, u_d) = 1. \tag{A.5}$$

Definition 3 (Normal copula)**.** *Let* $\mathbf{u} \in [0,1]^d$ *and* $\Phi_d(\cdot; \mathbf{R}_0)$ *be the d-dimensional standard normal CDF with linear correlation matrix* $\mathbf{R}_0$*. Then, the d-dimensional normal copula (a.k.a. Gaussian copula) parameterized by* $\mathbf{R}_0$ *is given by (respectively for the CDF and PDF):*

$$C_{\mathcal{N}_d}(u_1, \ldots, u_d; \mathbf{R}_0) = \Phi_d\left(\Phi^{-1}(u_1), \ldots, \Phi^{-1}(u_d); \mathbf{R}_0\right) \tag{A.6}$$

$$c_{\mathcal{N}_d}(u_1, \ldots, u_d; \mathbf{R}_0) = \frac{\varphi_d\left(\Phi^{-1}(u_1), \ldots, \Phi^{-1}(u_d); \mathbf{R}_0\right)}{\prod_{i=1}^{d} \varphi\left(\Phi^{-1}(u_i)\right)}. \tag{A.7}$$

For the interested reader, one could refer jointly to a reference monograph on this subject such as the one from Nelsen (2006) and to the general work of Lebrun (2013) about copulas in structural reliability. Finally, for a practical view of dependence modeling using copulas in the context of reliability assessment, one should refer to Dutfoy and Lebrun (2009).

APPENDIX B

Constructing input distributions

In the following, let $\mathcal{X} = \{x^{(1)}, \dots, x^{(N)}\}$ denote a set of N i.i.d. *data points* or *observations*. The basic idea is to characterize the *parent probability distribution* f_X [1] (a.k.a. the *parent law*) of the random variable X based on this set of observations. This characterization can be achieved by various tools, and depends whether this parent distribution is assumed to belong to a parametric family or not, i.e., whether one assumes or not that $f_X \in \mathcal{P}$ with $\mathcal{P}$ such that:

$$\mathcal{P} = \left\{ f_X(\cdot; \boldsymbol{\theta}) \mid \boldsymbol{\theta} \in \mathcal{D}_{\boldsymbol{\theta}} \subseteq \mathbb{R}^k \right\}. \tag{B.1}$$

Section B.1 aims at presenting a few basic parametric statistical methods. Note that, in this section, it is assumed that data points are realizations of a single random variable. However, one could extend the review to methods adapted to a set of i.i.d. observations of a random vector $\mathbf{X}$. However, in engineering practice, a common situation is that only experimental data lead to assess, successively, a statistical inference about the marginal distributions, and then, if possible, the dependence structure (most of the time, only linear correlations are inferred).

Concerning the choice of the parametric family $\mathcal{P}$, it can be achieved in practice by using some *goodness-of-fit* tests to get an objective measure of the best distribution type that would fit the given data (Saporta, 2006). Finally, another common approach to find an input distribution w.r.t. the available information in input is to use the *Maximum Entropy Principle* (Soize, 2017).

Sometimes, it may happen that no conventional parametric density is suitable for modeling the distribution of available data points. In order to circumvent this problem, nonparametric methods are dedicated to this problem. Section B.2 provides a brief review of some basic nonparametric statistical methods. In this section, the multidimensional case for $\mathbf{X}$ is presented since nonparametric methods may be powerful tool for estimating joint distributions and/or copulas.

For more information about the following methods, the interested reader can refer to Wasserman (2004, Chap. 9) for parametric inference and Wasserman (2006) or Tsybakov (2009) for the nonparametric one.

B.1 A few parametric statistical methods

Method of moments. A first approach assumes that the data gathered in $\mathcal{X}$ are realizations of a random variable X whose unknown probability distribution belongs to a parametric family of distributions, denoted $f_X(\cdot; \boldsymbol{\theta})$ where $\boldsymbol{\theta}$ is the vector of unknown distribution parameters. The idea of the method is to match the first two *sample moments* (i.e., sample mean $\widehat{\mu}_{\mathcal{X}}$ and sample

[1] Note that this sentence is a strong abuse of notation. One should write that the parent law should be P_X on $\mathbb{R}$, assuming that P_X is continuous w.r.t. the Lebesgue measure, and whose density is f_X.

variance $\widehat{\sigma}^2_{\mathcal{X}}$) with the moments of the underlying distribution, denoted by $\mu(\boldsymbol{\theta})$ and $\sigma^2(\boldsymbol{\theta})$. The sample moments thus reads:

$$\widehat{\mu}_{\mathcal{X}} = \frac{1}{N}\sum_{j=1}^{N} x^{(j)}, \quad \widehat{\sigma}^2_{\mathcal{X}} = \frac{1}{N-1}\sum_{j=1}^{N}\left(x^{(j)} - \widehat{\mu}_{\mathcal{X}}\right)^2. \tag{B.2}$$

Finally, the distribution parameters $\boldsymbol{\theta}$ are computed by solving: $\mu(\boldsymbol{\theta}) = \widehat{\mu}_{\mathcal{X}}$ and $\sigma^2(\boldsymbol{\theta}) = \widehat{\sigma}^2_{\mathcal{X}}$. This method is rather intuitive and provides a smooth CDF curve.

Maximum likelihood method. In the same manner, the maximum likelihood (ML) method relies on the assumption that the data are drawn from an unknown probability distribution $f_X(\cdot;\boldsymbol{\theta})$ where the vector of distribution parameters $\boldsymbol{\theta}$ is unknown. The *likelihood* function thus reads:

$$\mathcal{L}(\boldsymbol{\theta}|\mathcal{X}) = \prod_{j=1}^{N} f_X(x^{(j)};\boldsymbol{\theta}) \tag{B.3}$$

where $f_X(x^{(j)};\boldsymbol{\theta})$ is the marginal PDF conditioned by $\boldsymbol{\theta}$. Finally, the principle of maximum likelihood (Rhode, 2014) states that the optimal vector of distribution parameters $\widehat{\boldsymbol{\theta}}^{\,\mathrm{ML}}$ is the one that maximizes $\mathcal{L}(\boldsymbol{\theta}|\mathcal{X})$. In practice, the problem can be set in another way, i.e., by looking for $\widehat{\boldsymbol{\theta}}^{\,\mathrm{ML}}$ which minimizes the opposite of the *log-likelihood* function:

$$\widehat{\boldsymbol{\theta}}^{\,\mathrm{ML}} = \underset{\boldsymbol{\theta}\in\mathcal{D}_{\boldsymbol{\theta}}}{\arg\min} \left(-\sum_{j=1}^{N} \log f_X(x^{(j)};\boldsymbol{\theta})\right). \tag{B.4}$$

Asymptotic properties of this estimator can be found, for instance, in Van Der Waart (1998) and Saporta (2006).

B.2 A few nonparametric statistical methods

Empirical CDF. A first nonparametric method consists in estimating the empirical CDF of the set of data $\mathcal{X}$. Then, one can estimate an empirical CDF using:

$$\widehat{F}_X(x) = \frac{1}{N}\sum_{j=1}^{N} \mathbb{1}_{\{x\geq x^{(j)}\}}(x) \tag{B.5}$$

where $\mathbb{1}_{\{x\geq x^{(j)}\}}(\cdot)$ is the indicator function which is equal to unity if the subscript event $\{x \geq x^{(j)}\}$ is verified, and zero otherwise. This estimator provides a stair-shaped curve due to the limited number of samples N. Thus, the empirical CDF $\widehat{F}_X(\cdot)$ is a rather simple and coarse estimate of the underlying CDF $F_X(\cdot)$. Small-sample and asymptotic properties of this estimator can be found, for instance, in Wasserman (2006) or Tsybakov (2009).

Histogram. For density estimation, an *histogram* appear to be one of the most simple density estimator. It is a widely used statistical tool in daily engineering practice. The histogram estimator is rough and mainly depends on a the number of disjoint categories known as *bins*. Thus, the *binwidth* parameter is not easy to tune and may affect the graphical coherence of the visualized distribution.

Kernel density estimation. In a more general setting, if one desires to construct an estimate of the PDF of a random variable, or more generally, of a random vector, with only a set of

realizations as the prior information, the way for solving such a problem relies on using a non-parametric density estimate obtained by *kernel uni-* or *multivariate smoothing*, a.k.a. *kernel density estimation* (KDE) (see, e.g., Silverman, 1986; Wand and Jones, 1995; Scott, 2015).

Let us consider the previous dataset $\mathcal{X} = \{x^{(1)}, \dots, x^{(N)}\}$. $\mathcal{X}$ denotes a univariate set of N i.i.d. observations drawn from an unknown parent density denoted by f_X. Then, its *kernel density estimator* is given by:

$$\widehat{f}_X(x) = \frac{1}{N\eta} \sum_{j=1}^{N} K\left(\frac{x - x^{(j)}}{\eta}\right) \tag{B.6}$$

where $K(\cdot)$ is a univariate *kernel* [2], and $\eta \in \mathbb{R}_{+*}$ is a smoothing parameter known as the *bandwidth*. Two widely used univariate kernels are the *Gaussian* and the *Epanechnikov* ones. They are defined such that:

$$K(x) = \frac{1}{\sqrt{2\pi}} \exp\left[-\frac{x^2}{2}\right] \qquad \text{(Gaussian kernel)} \tag{B.7}$$

$$K(x) = \frac{3}{4}(1 - x^2)\mathbb{1}_{\{|x| \leq 1\}}(x) \qquad \text{(Epanechnikov kernel).} \tag{B.8}$$

If the choice of the kernel $K(\cdot)$ may influence the performance of the estimation in some specific cases, it remains that the most influent parameter is the bandwidth η. This parameter has to be tuned so to find an admissible trade-off between global smoothing and capturing the peaks of the density. It can be optimized following some optimality criteria, such that the *mean square integrated error* (MISE):

$$\text{MISE}(\eta) = \mathbb{E}\left[\int_{\mathbb{R}} \left(\widehat{f}_X(x) - f_X(x)\right)^2 \mathrm{d}x\right]. \tag{B.9}$$

Other estimators can be used such that the *asymptotic mean square integrated error* (AMISE) (Jones et al., 1996), *plug-in* estimators (Botev et al., 2010) or finally *cross-validation*-based estimators (Jones et al., 1996). For more information about these aspects, the reader should refer to the books by Wand and Jones (1995) and Scott (2015).

In the multivariate setting, one can assume that a set $\mathcal{X} = \{\mathbf{x}^{(1)}, \dots, \mathbf{x}^{(N)}\}$ of N i.i.d. observations of a d-dimensional random vector, drawn from an unknown parent density denoted by $f_{\mathbf{X}}$. Thus, its kernel density estimator is given by:

$$\widehat{f}_{\mathbf{X}}(\mathbf{x}) = \frac{\det(\mathbf{H})^{-1/2}}{N} \sum_{j=1}^{N} K_d\left(\mathbf{H}^{-1/2}(\mathbf{x} - \mathbf{x}^{(j)})\right) \tag{B.10}$$

where $\det(\cdot)$ is the determinant operator, $K_d(\cdot)$ is a multivariate (d-dimensional) kernel and $\mathbf{H}$ is a $(d \times d)$-dimensional positive definite symmetric matrix, often named the "*bandwidth matrix*". In a similar fashion than in the univariate case, two widely used kernels are the Gaussian one and the Epanechnikov one, defined such that:

$$K_d(\mathbf{x}) = \frac{1}{(2\pi)^{d/2}} \exp\left[-\frac{1}{2}\mathbf{x}^\top \mathbf{x}\right] \qquad \text{(Gaussian kernel)} \tag{B.11}$$

$$K_d(\mathbf{x}) = \frac{d+2}{2v_d}(1 - \mathbf{x}^\top \mathbf{x})\mathbb{1}_{\{\mathbf{x}^\top \mathbf{x} \leq 1\}}(\mathbf{x}) \qquad \text{(Epanechnikov kernel)} \tag{B.12}$$

where v_d is the volume of the unit sphere in $\mathbb{R}^d$, i.e., $v_d = \int_{\mathbb{R}^d} \mathbb{1}_{\{\mathbf{x}^\top \mathbf{x} \leq 1\}}(\mathbf{x})\mathrm{d}\mathbf{x}$. As for the bandwidth matrix $\mathbf{H}$, it can be optimized using a similar MISE criterion as the one given in Eq. (B.9),

[2] The word "kernel" refers to any non-negative symmetric function that integrates to one.

which reads:

$$\mathrm{MISE}(\mathbf{H}) = \mathbb{E}\left[\int_{\mathbb{R}^d} \left(\widehat{f}_{\mathbf{X}}(\mathbf{x}) - f_{\mathbf{X}}(\mathbf{x})\right)^2 \mathrm{d}\mathbf{x}\right]. \tag{B.13}$$

In common engineering practice (and when d increases), the Gaussian assumption on $f_{\mathbf{X}}$ is often considered. Thus, a widely used approximation for $\mathbf{H}$ is derived from the so-called "*Silverman's rule of thumb*" (Silverman, 1986) which assumes that $\mathbf{H}$ takes the following form:

$$\mathbf{H} = \eta_{\mathrm{Silv}}^2 \begin{bmatrix} \widehat{\sigma}_1^2 & 0 & \dots & 0 \\ 0 & \widehat{\sigma}_2^2 & \ddots & \vdots \\ \vdots & \ddots & \ddots & 0 \\ 0 & \dots & 0 & \widehat{\sigma}_d^2 \end{bmatrix} \tag{B.14}$$

where $\widehat{\sigma}_i^2$ for $i = 1, \dots, d$ is the empirical estimation of the variance of X_i and η_{Silv} is given by:

$$\eta_{\mathrm{Silv}} = \left(\frac{1}{N}\frac{4}{(d+2)}\right)^{\frac{1}{d+4}}. \tag{B.15}$$

APPENDIX C

Transformations

This appendix aims at recalling basic properties of the most common transformations from the *physical space* (a.k.a. the **x**-space) to the *standard normal space* (a.k.a. the **u**-space) used in reliability analysis.

Case of normally distributed and correlated variables. In this case, $\mathbf{X} \sim \mathcal{N}_d(\mathbf{m}_\mathbf{X}, \mathbf{\Sigma}_\mathbf{X})$ where $\mathbf{m}_\mathbf{X}$ and $\mathbf{\Sigma}_\mathbf{X}$ are defined as in Eqs. (2.2) and (2.3). By construction, the covariance matrix reads $\mathbf{\Sigma}_\mathbf{X} = \mathbf{DRD}$, where $\mathbf{R} = [\rho_{ij}]_{d\times d}$ is the linear correlation matrix and $\mathbf{D} = \mathrm{diag}(\sigma_1, \ldots, \sigma_d)$ is the diagonal matrix of standard deviations. Thus, the transformation (and its inverse) directly reads:

$$\mathbf{u} = \mathbf{L}^{-1}\mathbf{D}^{-1}(\mathbf{x} - \mathbf{m}_\mathbf{X}) \tag{C.1}$$

$$\mathbf{x} = \mathbf{DL}(\mathbf{u} - \mathbf{m}_\mathbf{X}) \tag{C.2}$$

where $\mathbf{L}$ is the lower triangular matrix obtained by the Cholesky decomposition of $\mathbf{R} = \mathbf{L}\mathbf{L}^\top$.

The Nataf transformation. This transformation is due to Nataf (1962) and has been popularized in the reliability community by Liu and Der Kiureghian (1986). In this case, $\mathbf{X} = (X_1, \ldots, X_d)^\top$ is described by d marginal distributions (i.e., PDFs f_{X_i} or CDFs F_{X_i}, for $i = 1, \ldots, d$) and a linear correlation matrix $\mathbf{R} = [\rho_{ij}]_{d\times d}$ (i.e., referred to as the normal copula case in Appendix A). The transformation is therefore defined as the following composed application:

$$T = T_{zu} \circ T_{vz} \circ T_{xv} : \left| \begin{array}{ccccccc} \mathcal{D}_\mathbf{X} & \longrightarrow & [0,1]^d & \longrightarrow & \mathbb{R}^d & \longrightarrow & \mathbb{R}^d \\ \mathbf{x} & \longmapsto & \mathbf{v} = T_{xv}(\mathbf{x}) & \longmapsto & \mathbf{z} = T_{vz}(\mathbf{v}) & \longmapsto & \mathbf{u} = T_{zu}(\mathbf{z}) \end{array} \right. \tag{C.3}$$

where $\mathbf{x}$, $\mathbf{v}$, $\mathbf{z}$ and $\mathbf{u}$ are d-dimensional vectors of realizations such that, for $i = 1, \ldots, d$, $v_i = F_{X_i}(x_i)$ and $z_i = \Phi^{-1}(v_i)$. As for the $T_{zu}(\cdot)$ transformation, supplementary technical calculations are required. They are not displayed in this manuscript for the sake of conciseness, but the interested reader should refer to Bourinet (2018). Note that the Nataf transformation presented here can be generalized to encompass more general dependence structures as shown by Lebrun and Dutfoy (2009a).

The Rosenblatt transformation. This transformation is due to Rosenblatt (1952) and has been popularized in the reliability community by Hohenbichler and Rackwitz (1981). In this case, $\mathbf{X}$ is described by its joint distribution (i.e., joint PDF $f_\mathbf{X}$ or joint CDF $F_\mathbf{X}$). The transformation is

therefore defined as the following composed application:

$$T = T_{vu} \circ T_{xv} : \left| \begin{array}{ccccc} \mathcal{D}_{\mathbf{X}} & \longrightarrow & [0,1]^d & \longrightarrow & \mathbb{R}^d \\ \mathbf{x} & \longmapsto & \mathbf{v} = T_{xv}(\mathbf{x}) & \longmapsto & \mathbf{u} = T_{vu}(\mathbf{v}) \end{array} \right. \tag{C.4}$$

where $\mathbf{x}$, $\mathbf{v}$ and $\mathbf{u}$ are d-dimensional vectors of realizations such that, for $i = 1, \ldots, d$, the $T_{vu}(\cdot)$ transformation reads $u_i = \Phi^{-1}(v_i)$. As for the $T_{xv}(\cdot)$ transformation, it is given by the following recursive formula:

$$\begin{aligned} v_1 &= F_{X_1}(x_1) \\ v_2 &= F_{X_2|X_1}(x_2|x_1) \\ v_3 &= F_{X_3|X_1,X_2}(x_3|x_1,x_2) \\ &\ldots \\ v_d &= F_{X_d|X_1,\ldots,X_{d-1}}(x_d|x_1,\ldots,x_{d-1}) \end{aligned} \tag{C.5}$$

where $F_{X_i|X_1,\ldots,X_{i-1}}(\cdot|x_1,\ldots,x_{i-1})$ is the conditional CDF of the variable X_i. Expressions of conditional CDFs can be derived knowing the marginal distributions and the copula (see Bourinet, 2018). However, the definition of the inverse $T^{-1}(\cdot)$ of the Rosenblatt transformation (which may be of interest in practical numerical implementation) may require substantial efforts. As a final remark, one can recall that, in the Rosenblatt transformation, as shown in Eq. (C.5), $d!$ conditioning orders can be chosen, resulting sometimes in differences affecting numerical results associated to specific quantities (e.g., importance factors may be affected by the order, see Chapter 3). However, the core reliability measures (i.e., the failure probability or the reliability index, see Chapter 3) are not impacted by the ordering (Lebrun and Dutfoy, 2009b).

APPENDIX D

Generic algorithms for rare event probability estimation

This appendix aims at providing generic algorithms of a few rare event estimation techniques described in Chapter 3.

D.1 Crude Monte Carlo (CMC)

The CMC sampling technique can be implemented either in the **x**-space or in the **u**-space. Algorithm 7 provides a generic CMC algorithm for failure probability estimation.

Algorithm 7 – Generic CMC algorithm.

1: **Input**:
   ▷ $f_{\mathbf{X}}$, joint PDF of the inputs
   ▷ $g(\cdot)$, LSF
   ▷ N, total number of samples
2: **Algorithm**:
3: Sample: $\{\mathbf{X}^{(j)}\}_{j=1}^{N} \overset{\text{i.i.d.}}{\sim} f_{\mathbf{X}}$
4: Evaluate: $\mathcal{G}_{\mathbf{x}} = \{g(\mathbf{X}^{(1)}), \ldots, g(\mathbf{X}^{(N)})\}$
5: Compute: $\widehat{p}_{\mathrm{f}}^{\mathrm{CMC}} = \frac{1}{N}\sum_{j=1}^{N} \mathbb{1}_{\mathcal{F}_{\mathbf{x}}}(\mathbf{X}^{(j)})$
6: **Output**:
   ▷ $\widehat{p}_{\mathrm{f}}^{\mathrm{CMC}}$, CMC estimate of p_{f}

D.2 Adaptive importance sampling using cross-entropy (AIS-CE)

The AIS-CE sampling technique can be implemented either in the **x**-space or in the **u**-space. Algorithm 8 provides a generic AIS-CE algorithm for failure probability estimation. Further details about the tuning of parameters can be found in Morio and Balesdent (2015) and Bourinet (2018).

Algorithm 8 – Generic AIS-CE algorithm.

Input:
▷ $f_{\mathbf{X}}$, joint PDF of the inputs
▷ $g(\cdot)$, LSF
▷ $h_{\mathbf{X}}(\cdot;\boldsymbol{\lambda})$ with $\boldsymbol{\lambda} \in \mathcal{D}_{\boldsymbol{\lambda}} \subseteq \mathbb{R}^k$, parametric family of auxiliary PDFs
▷ $\boldsymbol{\lambda}_{[0]} \in \mathcal{D}_{\boldsymbol{\lambda}}$, initial values of parameters
▷ N, number of samples per step
▷ $\alpha_{\text{CE}} \in]0,1[$, empirical quantile order (rarity parameter)
Algorithm:
Set: $k = 1$
Sample: $\{\mathbf{X}_{[1]}^{(j)}\}_{j=1}^{N} \overset{\text{i.i.d.}}{\sim} h_{\mathbf{X}}(\cdot;\boldsymbol{\lambda}_{[0]})$
Evaluate: $\mathcal{G}_{\mathbf{x},[1]} = \{g(\mathbf{X}_{[1]}^{(1)}), \ldots, g(\mathbf{X}_{[1]}^{(N)})\}$
Estimate: the empirical α_{CE}-quantile $y_{[1]}$ of the set $\mathcal{G}_{\mathbf{x},[1]}$
While $y_{[k]} > 0$ **do**
    Evaluate: $\mathcal{E}_{\mathbf{x},[k]} = \{\mathbf{X}_{[k]}^{(j)} \mid g(\mathbf{X}_{[k]}^{(j)}) \leq y_{[k]}\}$
    Optimize the parameters of the auxiliary PDF:
    $\boldsymbol{\lambda}_{[k]} = \underset{\boldsymbol{\lambda} \in \mathcal{D}_{\boldsymbol{\lambda}}}{\arg\max} \ \frac{1}{N} \sum_{\mathbf{X}_{[k]}^{(j)} \in \mathcal{E}_{\mathbf{x},[k]}} \frac{f_{\mathbf{X}}(\mathbf{X}_{[k]}^{(j)})}{h_{\mathbf{X}}(\mathbf{X}_{[k]}^{(j)};\boldsymbol{\lambda}_{[k-1]})} \ \ln(h_{\mathbf{X}}(\mathbf{X}_{[k]}^{(j)};\boldsymbol{\lambda}))$
    Set: $k \leftarrow k + 1$
    Sample: $\{\mathbf{X}_{[k]}^{(j)}\}_{j=1}^{N} \overset{\text{i.i.d.}}{\sim} h_{\mathbf{X}}(\cdot;\boldsymbol{\lambda}_{[k-1]})$
    Evaluate: $\mathcal{G}_{\mathbf{x},[k]} = \{g(\mathbf{X}_{[k]}^{(1)}), \ldots, g(\mathbf{X}_{[k]}^{(N)})\}$
    Estimate the empirical α_{CE}-quantile $y_{[k]}$ of the set $\mathcal{G}_{\mathbf{x},[k]}$
End While
Get the total number of levels $k_\#$ such that $y_{[k_\#]} \leq 0$
Set: $y_{[k_\#]} = 0$
Estimate: $\widehat{p}_{\text{f}}^{\text{AIS-CE}} = \frac{1}{N} \sum_{\mathbf{X}^{(j)} \in \mathcal{E}_{\mathbf{x},[k_\#]}} \frac{f_{\mathbf{X}}(\mathbf{X}_{[k_\#]}^{(j)})}{h_{\mathbf{X}}(\mathbf{X}_{[k_\#]}^{(j)};\boldsymbol{\lambda}_{[k_\#-1]})}$
Output:
▷ $\widehat{p}_{\text{f}}^{\text{AIS-CE}}$, AIS-CE estimate of p_{f}

D.3 Nonparametric adaptive importance sampling (NAIS)

The NAIS sampling technique can be implemented either in the **x**-space or in the **u**-space. Algorithm 9 provides a generic NAIS algorithm for failure probability estimation. Further details about the tuning of parameters can be found in Morio (2011c) and Morio and Balesdent (2015).

Algorithm 9 – Generic NAIS algorithm.

Input:
▷ $f_{\mathbf{X}}$, joint PDF of the inputs
▷ $g(\cdot)$, LSF
▷ $K_d(\cdot)$, d-dimensional kernel
▷ N, number of samples per step
▷ $\alpha_{\text{NAIS}} \in]0,1[$, empirical quantile order (rarity parameter)

Algorithm:
Set: $k = 1$ and $h_{[0]} = f_{\mathbf{X}}$
Sample: $\{\mathbf{X}_{[1]}^{(j)}\}_{j=1}^{N} \overset{\text{i.i.d.}}{\sim} h_{[0]}$
Evaluate: $\mathcal{G}_{\mathbf{x},[1]} = \{g(\mathbf{X}_{[1]}^{(1)}), \ldots, g(\mathbf{X}_{[1]}^{(N)})\}$
Estimate: the empirical α_{NAIS}-quantile $y_{[1]}$ of the set $\mathcal{G}_{\mathbf{x},[1]}$
While $y_{[k]} > 0$ **do**
    Estimate: $\widehat{I}_{[k]} = \frac{1}{k\,N} \sum_{[i]=1}^{[k]} \sum_{j=1}^{N} w_{[i]}(\mathbf{X}_{[i]}^{(j)})$
    with: $w_{[i]}(\mathbf{X}_{[i]}^{(j)}) = \mathbb{1}_{\{g(\mathbf{X}_{[i]}^{(j)}) \leq y_{[k]}\}}(\mathbf{X}_{[i]}^{(j)}) \frac{f_{\mathbf{X}}(\mathbf{X}_{[i]}^{(j)})}{\widehat{h}_{[i-1]}(\mathbf{X}_{[i]}^{(j)})}$
    Update the KDE-based PDF:
    $\widehat{h}_{[k+1]}(\mathbf{x}) = \frac{\det(\mathbf{H}_{[k]})^{-1/2}}{k\,N\,\widehat{I}_{[k]}} \sum_{[i]=1}^{[k]} \sum_{j=1}^{N} w_{[i]}(\mathbf{X}_{[i]}^{(j)})\, K_d\left(\mathbf{H}_{[k]}^{-1/2}(\mathbf{x} - \mathbf{X}_{[i]}^{(j)})\right)$
    Set: $k \leftarrow k + 1$
    Sample: $\{\mathbf{X}_{[k]}^{(j)}\}_{j=1}^{N} \overset{\text{i.i.d.}}{\sim} \widehat{h}_{[k]}$
    Evaluate: $\mathcal{G}_{\mathbf{x},[k]} = \{g(\mathbf{X}_{[k]}^{(1)}), \ldots, g(\mathbf{X}_{[k]}^{(N)})\}$
    Estimate the empirical α_{NAIS}-quantile $y_{[k]}$ of the set $\mathcal{G}_{\mathbf{x},[k]}$
End While
Get the total number of levels $k_\#$ such that $y_{[k_\#]} \leq 0$
Set: $y_{[k_\#]} = 0$
Estimate: $\widehat{p}_{\text{f}}^{\text{NAIS}} = \frac{1}{N} \sum_{j=1}^{N} \mathbb{1}_{\{g(\mathbf{X}_{[k_\#]}^{(j)}) \leq y_{[k_\#]}\}}(\mathbf{X}_{[k_\#]}^{(j)}) \frac{f_{\mathbf{X}}(\mathbf{X}_{[k_\#]}^{(j)})}{\widehat{h}_{[k_\#]}(\mathbf{X}_{[k_\#]}^{(j)})}$

Output:
▷ $\widehat{p}_{\text{f}}^{\text{NAIS}}$, NAIS estimate of p_{f}

D.4 Subset sampling (SS)

The SS technique can be implemented either in the **u**-space (see the version by Au and Beck (2001)) or in the **x**-space (see the version by Cérou et al. (2012)). The differences between these two spaces imply a different tuning of the algorithm parameters and different MCMC sampling strategies (as explained in Section D.5). However, Algorithm 10 aims at providing a generic SS algorithm for failure probability estimation. Further details about the tuning of parameters (e.g., practical estimation of the α_{SS}-quantile) can be found in Dubourg (2011), Morio and Balesdent (2015), and Bourinet (2018).

Algorithm 10 – Generic SS algorithm.

Input:
▷ $f_{\mathbf{X}}$ / φ_d, joint PDF of the inputs (after transformation)
▷ $g(\cdot)$ / $\mathring{g}(\cdot)$, LSF (after transformation)
▷ N, number of samples per step
▷ $\alpha_{\text{SS}} \in]0,1]$, empirical quantile order (rarity parameter)
Algorithm:
Set: $k = 0$ and $f_{[0]} = \varphi_d$
Sample: $\{\mathbf{U}_{[0]}^{(j)}\}_{j=1}^{N} \overset{\text{i.i.d.}}{\sim} f_{[0]}$
Evaluate: $\mathcal{G}_{\mathbf{u},[0]} = \{\mathring{g}(\mathbf{U}_{[0]}^{(1)}), \ldots, \mathring{g}(\mathbf{U}_{[0]}^{(N)})\}$
Estimate: the empirical α_{SS}-quantile $y_{[0]}$ of the set $\mathcal{G}_{\mathbf{u},[0]}$
While $y_{[k]} > 0$ **do**
    Determine the subset $\mathcal{F}_{\mathbf{u},[k+1]} = \{\mathbf{U}_{[k]} \in \mathbb{R}^d \mid \mathring{g}(\mathbf{U}_{[k]}) \leq y_{[k]}\}$
    and the conditional PDF $f_{[k+1]} = \varphi_d(\cdot|\mathcal{F}_{\mathbf{u},[k]})$
    Sample: $\{\mathbf{U}_{[k]}^{(j)}\}_{j=1}^{N} \overset{\text{i.i.d.}}{\sim} f_{[k]}$
    Evaluate: $\mathcal{G}_{\mathbf{u},[k]} = \{\mathring{g}(\mathbf{U}_{[k]}^{(1)}), \ldots, \mathring{g}(\mathbf{U}_{[k]}^{(N)})\}$
    Estimate the empirical α_{SS}-quantile $y_{[k]}$ of the set $\mathcal{G}_{\mathbf{u},[k]}$
End While
Get the total number of levels $k_\#$ such that $y_{[k_\#]} \leq 0$
Set: $y_{[k_\#]} = 0$
Estimate: $\widehat{p}_{\text{f}}^{\text{SS}} = (1-\alpha_{\text{SS}})^k \times \frac{1}{N}\sum_{j=1}^{N} \mathbb{1}_{\{\mathring{g}(\mathbf{U}_{[k_\#]}^{(j)}) \leq y_{[k_\#]}\}}(\mathbf{U}_{[k_\#]}^{(j)})$
Output:
▷ $\widehat{p}_{\text{f}}^{\text{SS}}$, SS estimate of p_{f}

D.5 Markov chain Monte Carlo sampling technique for Subset sampling

The aim of *Markov chain Monte Carlo* (MCMC) techniques is to enable an approximate sampling of any arbitrary distribution, denoted as the *target distribution*, which may be not directly available (e.g., typically $\varphi_d(\cdot|E_s)$ in the context of SS as presented in Section 3.5).

Before detailing the usual MCMC algorithms encountered in the context of SS, one recalls some basic principles of *Markov chain* theory. Note that the derivations are achieved in the $\mathbf{u}$-space, for the sake of coherence with the presentation of SS in Section 3.5.

In the following, only a few basic principles about current MCMC samplers used in SS are presented. For the interested reader, more comprehensive reviews (containing numerous references and much more details about derivations and numerical implementation) about MCMC for SS can be found, e.g., in Dubourg (2011, App. B), Papaioannou et al. (2015), and Bourinet (2018, Chap. 1).

A few principles of Markov chain theory. If $\{\mathbf{U}^k, k \in \mathbb{N}\}$ is a time-homogeneous, discrete-time, first-order *Markov chain*, defined in the continuous state-space $\mathbb{R}^d$. Then, one can assure that this Markov chain follows the *Markov property* if it verifies:

Definition 4 (Markov property)**.** *For any event $A \in \mathcal{B}$, with $\mathcal{B}$ the Borel σ-field of $\mathbb{R}^d$, one has:*

$$\mathbb{P}(\mathbf{U}^{k+1} \in A \mid \cap_{m=0}^{k} \{\mathbf{U}^m = \mathbf{u}^m\}) = \mathbb{P}(\mathbf{U}^{k+1} \in A \mid \{\mathbf{U}^k = \mathbf{u}^k\}). \tag{D.1}$$

In other words, the previous definition states that the conditional distribution of $\mathbf{U}^{k+1}$, given $\mathbf{U}^1, \mathbf{U}^2, \ldots, \mathbf{U}^k$, only depends on the previous step $\mathbf{U}^k$. Thus, the random process $\{\mathbf{U}^k, k \in \mathbb{N}\}$ is called a *stationary Markov chain* (i.e., it does not depend on time t). Then, the *transition* PDF $\tau(\mathbf{v}|\mathbf{u})$ which defines the transition between two subsequent states $\mathbf{U}^k$ and $\mathbf{U}^{k+1}$ should be stationary too.

Finally, the joint PDF of a stationary Markov chain is given by a marginal distribution $\varphi_d(\mathbf{u}|E_s)$ and a stationary transition distribution $\tau(\mathbf{v}|\mathbf{u})$ such that:

$$\varphi_d(\mathbf{v}|E_s) = \int_{\mathbf{u}\in\mathbb{R}^d} \tau(\mathbf{v}|\mathbf{u})\varphi_d(\mathbf{u}|E_s)\mathrm{d}\mathbf{u}. \tag{D.2}$$

Eq. (D.2) ensures that if $\mathbf{U}^k \sim \varphi_d(\cdot|E_s)$, then $\mathbf{U}^{k+1} \sim \varphi_d(\cdot|E_s)$ and all the subsequent elements of the chain will be distributed according to $\varphi_d(\cdot|E_s)$. Thus, $\varphi_d(\cdot|E_s)$ is called the *invariant* (a.k.a. stationay) joint PDF of the chain. A sufficient condition for Eq. (D.2) to be fulfilled is the so-called *reversibility condition* given by:

$$\tau(\mathbf{v}|\mathbf{u})\varphi_d(\mathbf{u}|E_s) = \tau(\mathbf{u}|\mathbf{v})\varphi_d(\mathbf{v}|E_s). \tag{D.3}$$

In practice, MCMC aims at producing samples that follow the target distribution by simulating states of a stationary Markov chain whose marginal distribution is the target one. Furthermore, if one starts from a state that is not distributed according to the target distribution, the Markov chain will asymptotically converge to the target stationary distribution, provided that this chain is *aperiodic* and *irreducible*. Briefly, one can sum up these two properties by (Papaioannou et al., 2015):

- *aperiodicity*: $\tau(\mathbf{v}|\mathbf{u})$ should be chosen such that it assigns a non-zero probability for not moving from the current state;

- *irreducibility*: $\tau(\mathbf{v}|\mathbf{u})$ should be chosen such that it assigns a non-zero probability for entering any set in the state-space in a finite number of steps.

As a last characteristic, one can mention the *burn-in period* which is the transient period required for the Markov chain to approximately reaches its stationary state.

Specific context of Subset sampling. In the context of the SS algorithm, MCMC sampling is used to get samples at the step $s+1$ from the conditional PDF $\varphi_d(\cdot|E_s)$. To do so, one uses the samples that fell into the failure domain $\mathcal{F}_{\mathbf{u},s}$ at step s. These specific failure samples form the following elite set:

$$\mathcal{E}_s = \{\mathbf{u}_s^{(j)}, 1 \leq j \leq N \mid \mathbb{1}_{\mathcal{F}_{\mathbf{u},s}}(\mathbf{u}_s^{(j)}) = 1\} \tag{D.4}$$

and are called *seeds* of the Markov chain. They play the role of starting points for the chain and are distributed according to $\varphi_d(\cdot|E_s)$. Consequently, for these samples, the chains have already attained their stationary states from the beginning. Thus, no burn-in period is required for them and all the following states will be distributed according to $\varphi_d(\cdot|E_s)$ (Papaioannou et al., 2015).

Metropolis-Hastings sampler. A first algorithm used for SS (especially in its "multilevel splitting" version, defined in the $\mathbf{x}$-space) is the *Metropolis-Hastings* (MH) sampler as originally proposed by Metropolis et al. (1953) and Hastings (1970).

In this algorithm, the transition PDF is given by:

$$\tau(\mathbf{v}|\mathbf{u}) = a(\mathbf{u},\mathbf{v})q(\mathbf{v}|\mathbf{u}) + (1 - r(\mathbf{u}))\delta_{\mathbf{u}}(\mathbf{v}) \tag{D.5}$$

where $q(\mathbf{v}|\mathbf{u})$ is called the *proposal* PDF, $\delta_{\mathbf{u}}(\mathbf{v})$ is the Dirac mass at $\mathbf{u}$ and $a(\mathbf{u},\mathbf{v})$ is given by:

$$a(\mathbf{u},\mathbf{v}) = \min\left\{1, \frac{\varphi_d(\mathbf{v}|E_s)q(\mathbf{u}|\mathbf{v})}{\varphi_d(\mathbf{u}|E_s)q(\mathbf{v}|\mathbf{u})}\right\} \tag{D.6}$$

and finally, $r(\mathbf{u}) = \int_{\mathbf{v}\in\mathbb{R}^d} a(\mathbf{u},\mathbf{v})q(\mathbf{v}|\mathbf{u})\mathrm{d}\mathbf{v}$. Eq. (D.5) simply states that, to generate a sample of the new state $\mathbf{U}^{k+1}$ conditional to the current state $\mathbf{U}^k = \mathbf{u}$, one considers a *candidate state* $\mathbf{v}$ generated by the proposal PDF $q(\cdot|\mathbf{u})$. This candidate is accepted with probability $a(\mathbf{u},\mathbf{v})$, and thus the chain goes to the state $\mathbf{U}^{k+1} = \mathbf{v}$, or rejected with probability $(1 - r(\mathbf{u}))$ which makes the chain stay at $\mathbf{U}^{k+1} = \mathbf{u}$.

Finally, by combining Eq. (3.57) and Eq. (D.6), one can show (see, e.g., Papaioannou et al., 2015; Bourinet, 2018) that the *acceptance* probability (a.k.a. *move* probability) $a(\mathbf{u},\mathbf{v})$ can take the following form:

$$a(\mathbf{u},\mathbf{v}) = \tilde{a}(\mathbf{u},\mathbf{v})\mathbb{1}_{\mathcal{F}_{\mathbf{u},s}}(\mathbf{v}) \tag{D.7}$$

where $\tilde{a}(\mathbf{u},\mathbf{v}) = \min\left\{1, \frac{\varphi_d(\mathbf{v})q(\mathbf{u}|\mathbf{v})}{\varphi_d(\mathbf{u})q(\mathbf{v}|\mathbf{u})}\right\}$, which means that, the MH sampler can be implemented in two distinct steps:

1. Firstly, draw a candidate sample $\mathbf{v} \sim q(\cdot|\mathbf{u})$ with acceptance probability $\tilde{a}(\mathbf{u},\mathbf{v})$;
2. Secondly, finally decide on the move from $\mathbf{u}$ to $\mathbf{v}$ by checking if $\mathbb{1}_{\mathcal{F}_{\mathbf{u},s}}(\mathbf{v}) = 1$.

More details about numerical implementation can be found in Papaioannou et al. (2015). As a final remark, one can mention a few key points about this MH sampler:

- the previous presentation of the MH sampler is achieved in the $\mathbf{u}$-space due to the fact that, in the reliability context, such an algorithm is easier to tune in this space, mainly due to its scaling and componentwise independence properties. However, it has been originally defined within the $\mathbf{x}$-space (see, e.g., Robert and Casella, 2004, Chap. 7);

- in the **u**-space, the proposal PDF $q(\cdot|\mathbf{u})$ can be chosen among various PDFs. Usually, one may often encounter the d-dimensional standard normal PDF centered at the current state **u** or a d-dimensional uniform PDF, centered on **u** with a symmetric side length;
- when the input dimension d gets larger, this algorithm fails to converge due to the strong correlation appearing between the successive states of the Markov chain (see, e.g., Katafygiotis and Zuev, 2008; Zuev and Katafygiotis, 2011), which consequently deteriorates the acceptance rate as illustrated in Papaioannou et al. (2015).

Modified Metropolis-Hastings algorithm. All the key points mentioned hereabove have led Au and Beck (2001) to modify their MCMC sampler so as to avoid these pitfalls. To do so, they proposed a *modified Metropolis-Hastings* (m-MH) sampler, characterized by a *componentwise* two-step strategy for sampling the candidate state. These steps can be summed up as:

1. Firstly, draw a candidate sample $\mathbf{v} = (v_1, \ldots, v_d)^\top \sim q(\cdot|\mathbf{u}) = \prod_{i=1}^{d} q_i(\cdot|u_i)$ such that, for each $v_i \in \mathbf{v}$ $(i = 1, \ldots, d)$, the componentwise acceptance probability is $\tilde{a}_i(u_i, v_i) = \min\left\{1, \frac{\varphi(v_i)q_i(u_i|v_i)}{\varphi(u_i)q_i(v_i|u_i)}\right\}$;
2. Secondly, finally decide on the move from **u** to **v** by checking if $\mathbb{1}_{\mathcal{F}_{\mathbf{u},s}}(\mathbf{v}) = 1$.

Again, implentation details may be found in Papaioannou et al. (2015) and Bourinet (2018).

Finally, Au and Beck (2001) claim that the choice of the type of proposal distribution should not drastically influence the performance of the algorithm but the spread should play a role. Thus, they advocate the use of a uniform PDF centered at u_i with a width of 2. However, as mentioned by Proppe (2008), for some cases, it may happen that the type of the proposal PDF may also have an influence so that bell-shaped PDFs could lead to a stronger robustness of the algorithm.

As a conclusion, this brief overview just aims at presenting the basic principles of the two main MCMC samplers used in SS. However, this section cannot replace a deeper and more detailed presentation of these notions. The interested reader may find further information in the references mentioned throughout this section.

APPENDIX E

Résumé étendu de la thèse

Contexte

Les systèmes aérospatiaux sont généralement considérés comme étant des « *systèmes complexes* », principalement à cause de leur nature multi-disciplinaire (due au grand nombre de composants hétérogènes qu'ils rassemblent), leur caractère unitaire (i.e., faible nombre d'unités produites) et les conditions d'opérations extrêmes auxquelles ils peuvent être confrontés durant leur vie opérationnelle. La combinaison de ces facteurs fait que les systèmes aérospatiaux sont caractérisés, du point de vue de leur conception, comme des systèmes :

- « *critiques* » ce qui implique que les conséquences associées à une défaillance peuvent être désastreuses, tant d'un point vue économique, environnemental qu'humain ;
- « *hautement-fiables* » ce qui implique que le nombre de défaillances complètes (contrairement à des défaillances partielles, potentiellement mineures) observées de ces systèmes est (doit être) très faible.

La conception et l'analyse de tels systèmes reposent sur l'utilisation à la fois de moyens expérimentaux puissants et d'une grande précision mais qui peuvent être très coûteux à mettre en œuvre, et l'utilisation de modèles mathématiques et physiques, qui, pour être résolus et exploités, passent bien souvent par des étapes de modélisation, simulation et/ou résolution numériques. Ces modèles ont l'avantage de pouvoir se substituer aux essais expérimentaux trop coûteux qui peuvent devenir inaccessibles sous certaines conditions extrêmes voire jamais observées (e.g., simulation d'une collision satellite-débris ou collision météorite-Terre). Ce caractère exploratoire des modèles numériques a aussi un coût non négligeable dès lors que les modèles impliquent un grand nombre de variables d'entrée et font appel à des techniques de résolution coûteuses (e.g., résolution de systèmes d'équations aux dérivées partielles).

Dans un contexte d'analyse de fiabilité des systèmes aérospatiaux, l'enjeu principal concerne la prise en compte des incertitudes, dès le cycle de conception, qui pourraient éventuellement affecter le comportement ou les performances du système dans ses véritables conditions d'opération futures et mener à la défaillance redoutée. En effet, les incertitudes proviennent de multiples sources qui doivent être identifiées, caractérisées et traitées en vue d'assurer la fiabilité du système étudié. Pour ce faire, une méthodologie générale de *quantification des incertitudes* est disponible et adoptée de façon quasi unanime dans de nombreuses branches de l'ingénierie confrontées à des problématiques similaires. Cette méthodologie (qui peut se décliner de plusieurs manières suivant les domaines et le but recherché, voir De Rocquigny (2006a), De Rocquigny (2006b), Sudret (2007), and Iooss (2009)) se compose généralement de quatre grandes étapes détaillées ci-dessous (voir Figure 1.1 présentée en Chapitre 1) :

- **Étape A → Spécification du problème** : la première étape consiste à spécifier le périmètre de l'étude, c'est-à-dire de définir le plus formellement possible le système étudié. Cette étape implique de définir l'ensemble des variables d'entrée et de sortie. Enfin, on doit, lors de cette étape, définir le type d'analyse que l'on souhaite mener par la suite (e.g., analyse d'incertitudes, de fiabilité ou de risque) ce qui implique directement de choisir une *quantité d'intérêt* (e.g., la distribution de la sortie du code, une probabilité de défaillance ou un quantile sur la sortie) ;

- **Étape B → Modélisation des incertitudes** : la deuxième étape consiste à identifier les différentes sources d'incertitudes et/ou d'erreurs. Une fois les sources d'incertitudes identifiées, une phase de modélisation/caractérisation des différents types d'incertitudes recensées doit être réalisée. Mathématiquement, la modélisation des incertitudes peut être réalisée à l'aide de plusieurs formalismes, dont le *cadre probabiliste* est peut-être le plus connu (Apostolakis, 1990; Paté-Cornell, 1996). Toutefois, d'autres formalismes tels que les *probabilités imprécises* ou des cadres *extra-probabilistes* (e.g., intervalles) peuvent être envisagés car mieux adaptés aux spécificités du problème (Beer et al., 2013; Zio and Pedroni, 2013). Le choix du formalisme dépend généralement du type et de la qualité de l'information disponible pour modéliser les incertitudes. Enfin, d'un point de vue décisionnel, on considèrera que l'analyste peut être amené à *caractériser* les incertitudes identifiées selon leur nature supposée, à savoir : d'un côté, les incertitudes dites *aléatoires* considérées comme irréductibles, et de l'autre les incertitudes dites *épistémiques*, c'est-à-dire réductibles par ajout de connaissance ou d'information (e.g., des données) ;

- **Étape C → Propagation des incertitudes** : la troisième étape consiste à propager les incertitudes modélisées en entrée à travers le code numérique. Les quantités de sortie du code sont, de fait, elles aussi impactées par la propagation des incertitudes et deviennent elles-mêmes incertaines. Les méthodes numériques utilisées pour la propagation des incertitudes peuvent varier en fonction de l'objectif affiché en entrée (e.g., caractérisation globale de la distribution de sortie vs. estimation d'une probabilité d'événement rare associée à une queue de distribution) ;

- **Étape D → Analyse inverse** : la quatrième étape intègre généralement deux types d'analyses. La première composante de cette étape, qui n'entre pas dans le cadre de l'étude présentée dans ce manuscrit, concerne le *calage* de code de calcul (Damblin, 2015). La deuxième composante concerne l'*analyse de sensibilité* qui vise à étudier comment la variabilité de certaines quantités en sortie de code peut être attribuée aux incertitudes en entrée (Saltelli et al., 2004).

Hypothèses générales de travail et formulation du problème

Cette thèse traite, de façon générale, du problème de l'analyse de fiabilité (Étape C) et de l'analyse de sensibilité (Étape D) de codes numériques simulant les performances de systèmes aérospatiaux considérés comme complexes, critiques et hautement-fiables. Dès lors, de multiples difficultés sont à prendre en compte et amènent à considérer certaines hypothèses de travail :

- le modèle numérique a été préalablement vérifié, validé et calibré, ce qui implique que, le modèle obtenu est, a priori, la meilleure représentation numérique disponible du comportement du système étudié ;

- le modèle numérique (code de simulation) est considéré comme une « *boîte-noire* », c'est-à-dire que l'ensemble des étapes énoncées précédemment sont considérées comme non-intrusives vis-à-vis du code numérique de simulation. Dès lors, ce code pourrait être possiblement coûteux à évaluer, non-linéaire et en assez grande dimension. Toutefois, dans cette thèse, les cas étudiés sont à la fois représentatifs de certaines des difficultés rencontrées dans les codes industriels (codes non-linéaires, zones de défaillances multiples, probabilités rares) tout en restant abordables du point de vue du coût de calcul (e.g., plusieurs milliers d'appels au code sont envisageables et la dimension du vecteur d'entrée est de l'ordre de la dizaine) ;

- l'analyse de fiabilité consiste à estimer une probabilité de défaillance. Dans le contexte de systèmes hautement-fiables, cette probabilité est supposée associée à un événement rare et est donc supposée très faible. Dès lors, elle devient très coûteuse à estimer par simulations de Monte-Carlo.

- la modélisation des incertitudes en entrée est réalisée dans un cadre probabiliste. Ainsi, les variables de base et leur structure de dépendance sont considérées à travers l'utilisation de variables aléatoires et d'une copule formant un vecteur aléatoire de loi jointe supposée connue, à l'exception de certains paramètres de distribution de certaines lois marginales qui sont peu connus (e.g., à cause d'un manque de données) ou dont la connaissance est uniquement liée à un choix d'expert. Dès lors, l'ensemble de la démarche de quantification des incertitudes est conditionnelle à la connaissance de ces paramètres de distribution.

Dans ce contexte, et compte tenu des hypothèses générales énoncées ci-dessus, cette thèse traite du problème de l'*analyse de fiabilité* et de l'*analyse de sensibilité* de modèles numériques *boîtes-noires* simulant des systèmes caractérisés par des défaillances de type *événements rares*. Les entrées sont des variables incertaines modélisées dans un cadre probabiliste et certains paramètres de distribution sont supposés méconnus ou incertains. Dès lors, le problème principal de la thèse concerne la prise en compte d'un *double niveau* d'incertitudes lors des deux analyses mentionnées précédemment. Ce double niveau est formé par :

- les incertitudes *phénoménologiques*, caractérisant la variabilité naturelle de certaines entrées, modélisées à l'aide de variables aléatoires ;

- les incertitudes portant sur le *modèle probabiliste* lui-même, qui caractérisent le manque de connaissance que l'analyste peut avoir dans le choix de certains paramètres de distribution.

Ce problème est d'un intérêt majeur dans le domaine de la quantification des incertitudes dans les codes numériques. Si de nombreux travaux pionniers, tels ceux de Ditlevsen (Ditlevsen, 1979a; Ditlevsen, 1979b) ou de Der Kiureghian (Der Kiureghian and Liu, 1986; Der Kiureghian, 1988), ont déjà soulevé l'importance cruciale de tenir compte de ce double niveau d'incertitudes dans l'analyse de fiabilité, il apparaît que ce problème est toujours d'actualité, et ce pour plusieurs raisons. Tout d'abord, de nouveaux algorithmes d'estimation de probabilités d'événements rares ont été développés au cours des dernières décennies (e.g., les techniques de type "adaptive importance sampling" ou celles de "subset sampling"). De plus, la complexité des codes de calculs s'est accrue (e.g., chaînage de codes et approches multi-disciplinaires) parallèlement à l'émergence des techniques de métamodélisation. Enfin, de nombreux cadres mathématiques complémentaires du cadre probabiliste ont vu le jour (e.g., techniques bayésiennes, probabilités imprécises) afin de tenir compte de multiples sources d'incertitudes et de pouvoir proposer un traitement numérique adapté (see, e.g., Nagel, 2017; Schöbi, 2017).

Dans cette thèse, le focus est mis sur la prise en compte du double niveau d'incertitudes à travers l'ensemble de la méthodologie de quantification des incertitudes (i.e., les étapes A-B-C-D mentionnées plus haut), dans un contexte d'estimation de probabilité d'événement rare pour

des systèmes aérospatiaux complexes. Par conséquent, la problématique centrale de la thèse peut être résumée comme suit :

Comment tenir compte de ce double niveau d'incertitudes à travers l'ensemble des étapes de quantification des incertitudes ?

On peut décomposer ce problème en trois questions qui relèvent elles-mêmes des étapes mentionnées précédemment :

Q1 – Comment modéliser le deuxième niveau d'incertitudes sur les paramètres de distribution ? ($\hookrightarrow$ **Étape B**)

Q2 – Comment ce deuxième niveau impacte-t-il la mesure de fiabilité ? ($\hookrightarrow$ **Étape C**)

Q3 – Comment relier la variabilité de la mesure de fiabilité à ce double niveau d'incertitudes en entrée ? ($\hookrightarrow$ **Étape D**)

Ainsi, dans cette thèse, on se propose de développer, pour chaque phase depuis l'étape B jusqu'à l'étape D, plusieurs outils et méthodes afin de gérer ce double niveau d'incertitudes. Pour ce faire, plusieurs objectifs scientifiques sont définis dans la section suivante.

Verrous scientifiques et objectifs de la thèse

Partant de la formulation du problème telle que décrite dans la section précédente, cette thèse a pour but de développer une stratégie cohérente en vue de satisfaire les objectifs suivants :

O1 Dresser une revue de l'état de l'art sur les techniques disponibles pour la modélisation et la propagation des incertitudes, ainsi que sur les méthodes d'analyse de sensibilité qui pourraient être adaptées à la problématique de la thèse ;

O2 Développer une stratégie efficace qui vise à prendre en compte et combiner la modélisation des incertitudes sur le modèle probabiliste des entrées et l'estimation de probabilités d'événements rares ;

O3 Proposer de nouveaux outils pour réaliser une analyse de sensibilité fiabiliste en présence d'incertitudes sur le modèle probabiliste des entrées ;

O4 Démontrer la cohérence et l'applicabilité des méthodes proposées à travers leur application sur un cas de simulation représentatif de système aérospatial.

Dans les sections suivantes, des résumés des chapitres de la thèse sont proposés, suivant les trois grandes parties suivantes :

- tout d'abord, les chapitres qui présentent des notions relatives à l'état de l'art ;
- ensuite, les chapitres qui contiennent les apports méthodologiques propres à la thèse et les applications aérospatiales ;
- enfin, les conclusions et perspectives de la thèse, ainsi que la valorisation scientifique des travaux de thèse.

État de l'art

Chapitre 2 – Modélisation des incertitudes pour les modèles numériques de type entrée-sortie

Ce chapitre a pour but d'introduire, de façon concise, les principaux concepts mathématiques fondamentaux utiles en quantification des incertitudes, avec un focus spécifique sur le cadre probabiliste. Les notions de sources et de types d'incertitudes y sont décrites. La classe et les caractéristiques des modèles étudiés (e.g., codes numériques de type boîte-noire) y sont introduites. Enfin, un inventaire des quantités d'intérêt pouvant être étudiées en sortie de code (e.g., variable scalaire de sortie, moments de cette variable, probabilité de dépassement de seuil ou quantile) est proposé au regard des différents types d'analyses pouvant être menées (e.g., analyse d'incertitudes, de fiabilité ou de risque).

Chapitre 3 – Estimation de probabilité d'événement rare

Ce chapitre a pour but de passer en revue un panel de techniques numériques adaptées à l'estimation de probabilité d'événement rare. Pour chaque classe d'algorithme, une brève présentation historique et générale est donnée dans un premier temps. Dans un deuxième temps, une formulation mathématique est proposée afin de montrer à la fois les liens et les différences entre les différentes classes d'algorithmes. Dans un troisième et dernier temps, les principaux avantages et inconvénients sont explicités et quelques pistes d'approfondissement sont données en fin de chaque section. Pour finir, ce chapitre se conclut par une synthèse regroupant quelques recommandations fondamentales à propos de l'utilisation pratique d'algorithmes d'estimation de probabilités d'événements rares.

Chapitre 4 – Analyse de sensibilité d'une sortie de modèle et d'une mesure de fiabilité

Ce chapitre a pour but de proposer une revue de la litérature concernant les méthodes d'analyse de sensibilité fiabiliste. Dans un premier temps, les principales méthodes relatives à l'*analyse de sensibilité basée sur la sortie de modèle* (SAMO) sont présentées. Dans un deuxième temps, les notions et concepts relatifs à l'*analyse de sensibilité fiabiliste* (ROSA) sont introduits et les différentes classes de méthodes identifiées dans la litérature sont présentées de façon à exhiber à la fois les liens profonds entre les méthodes ainsi que de faire ressortir leurs différences. Cette deuxième partie vise à proposer une revue de litérature de façon à identifier les grandes tendances et enjeux liés à la réalisation d'analyses de type ROSA.

Apports méthodologiques et applications

Chapitre 5 – Analyse de fiabilité en présence d'incertitudes sur les paramètres de distribution

Ce chapitre traite du problème de l'estimation de probabilités d'événements rares en présence d'incertitudes sur les paramètres de distribution. Pour ce faire, les incertitudes associées au modèle probabiliste des entrées sont traitées à travers un cadre bayésien, c'est-à-dire en considérant une loi a priori sur les paramètres de distribution incertains. Dès lors, la mesure de fiabilité considérée n'est plus la probabilité de défaillance traditionnelle scalaire. Celle-ci devient conditionelle à l'état de connaissance sur les paramètres. Ainsi, une mesure de défaillance pouvant être considérée est la *probabilité de défaillance prédictive* qui incorpore les effets des deux niveaux d'incertitudes. Dans ce chapitre, deux approches numériques adaptées pour l'estimation de cette quantité sont présentées. Ces approches sont dénommées *approche imbriquée*

(ou *nested reliability approach*, NRA) et *approche augmentée* (ou *augmented reliability approach*, ARA). Une comparaison numérique du couplage de ces deux approches avec plusieurs algorithmes d'estimation de probabilités d'événements rares (e.g., *subset sampling*) est menée et validée à travers l'utilisation de plusieurs cas-tests. In fine, l'approche présentant les meilleurs performances vis-à-vis de plusieurs critères définis dans ce chapitre (ici, l'approche ARA est la plus performante) est conservée comme étant conforme au regard des objectifs de la thèse.

Chapitre 6 – Analyse de sensibilité fiabiliste locale en présence d'incertitudes sur les paramètres de distribution

Ce chapitre vise à étendre les résultats obtenus dans le chapitre précédent au cadre de l'analyse de sensibilité fiabiliste. En effet, partant d'une stratégie d'estimation de la probabilité de défaillance prédictive dans le cadre de l'approche ARA, de nouveaux estimateurs de sensibilités fiabilistes locales sont proposés afin d'évaluer la robustesse de l'estimation de la probabilité vis-à-vis du double niveau d'incertitudes. Plus spécifiquement, on suppose que, de par la structure bayésienne hiérarchique du modèle probabiliste des entrées, on souhaite tester la robustesse de la mesure de fiabilité estimée par rapport aux choix des hyper-paramètres de la densité a priori charactérisant l'incertitude épistémique sur le paramètre incertain. De par la nature du problème, des indices de sensibilités locaux à base de *score functions* (Rubinstein, 1986; Rubinstein and Kroese, 2008; Millwater, 2009; Song et al., 2009b) sont proposés. De plus, une technique d'échantillonnage à base de tirages préférentiels adaptatifs, est proposée dans le cadre ARA afin d'estimer conjointement la probabilité de défaillance prédictive et les sensibilités de façon simultanée, sans appel supplémentaire au code numérique. Enfin, l'ensemble de la méthodologie est appliquée à deux cas-tests en vue de démontrer son efficacité, d'autant plus que l'occurrence de l'événement redouté de défaillance devient rare.

Chapitre 7 – Analyse de sensibilité fiabiliste globale en présence d'incertitudes sur les paramètres de distribution

Ce chapitre vise à compléter l'approche locale proposée dans le chapitre précédent par une approche globale. En effet, l'idée principale est d'étudier comment adapter une certaine classe d'indices de sensibilités fiabilistes globaux, appelés dans ce manuscrit « *indices de Sobol sur la fonction indicatrice* » (Li et al., 2012; Lemaître, 2014), au contexte du double niveau d'incertitudes. La formulation de ces indices et leur extension au double niveau est proposée dans un premier temps. Cette extension s'appuie sur une vision « *désagrégée* »du vecteur des variables d'entrée affectées par une incertitude épistémique sur leurs paramètres de distribution (Schöbi and Sudret, 2017). Par la suite, une méthodologie est proposée afin d'estimer ces indices dans un contexte de calcul de probabilité de défaillance associée à un événement rare. Cette méthodologie s'appuie sur la combinaison entre, d'une part, l'adaptation d'estimateurs existants (Perrin and Defaux, 2019) de ces indices au double niveau, et d'autre part, de l'utilisation d'une nouvelle approche d'estimation par noyaux disponible dans la littérature (Perrin et al., 2018). Si ces contributions sont relativement récentes, l'originalité des travaux présentés dans ce chapitre résulte dans leur couplage et leur adaptation à la contrainte du double niveau d'incertitudes ce qui en accroit les difficultés intrinsèques d'utilisation (e.g., dimension, complexité des densités à estimer). Pour finir, cette méthodologie est appliquée à deux cas-tests afin de démontrer son efficacité, et plus particulièrement quand l'occurence de l'événement redouté devient rare. De plus, les applications numériques viennent surligner les gains en termes d'interprétations que peuvent apporter ce genre d'analyses dans un contexte de double niveau d'incertitudes.

Chapitre 8 – Application à un cas de retombée d'un étage de lanceur

Ce chapitre constitue une mise en perspective des apports méthodologiques de la thèse à travers leurs applications successives à un code numérique représentatif du domaine aérospatial. Le modèle considéré vise à simuler la retombée d'un étage de lanceur spatial au travers du calcul de sa trajectoire en phase balistique. Dans ce chapitre, les outils méthodologiques dévéloppés et présentés dans les trois chapitres précédents sont testés sur ce cas à des fins de validation. Les performances, avantages et limites de chaque outil sont donnés.

Conclusions

Ces travaux de thèse sont constitués, outre d'une analyse de l'état-de-l'art sur plusieurs domaines de la gestion des incertitudes, d'un certain nombre de contributions qui ont été valorisées (ou sont en cours de valorisation) au travers de publications scientifiques. Ainsi, une liste mentionnant les principales contributions et les publications associées est proposée ci-dessous.

1. Approche imbriquée vs. approche augmentée (*NRA* vs. *ARA*)
   - ▷ Chabridon V., M. Balesdent, J.-M. Bourinet, J. Morio and N. Gayton (2017). "Evaluation of failure probability under parameter epistemic uncertainty: application to aerospace system reliability assessment". In: *Aerospace Science and Technology* 69, pp. 526–537.
   - ▷ Chabridon V., N. Gayton, J.-M. Bourinet, M. Balesdent and J. Morio (2017). "Some Bayesian insights for statistical tolerance analysis". In: *Actes du 23ème Congrès Français de Mécanique (CFM 2017)*, Lille, France.
2. Analyse de sensibilité fiabiliste locale (*local ROSA*)
   - ▷ Chabridon V., M. Balesdent, J.-M. Bourinet, J. Morio and N. Gayton (2018). "Reliability-based sensitivity estimators of rare event probability in the presence of distribution parameter uncertainty". In: *Reliability Engineering and System Safety* 178, pp. 164–178.
   - ▷ Chabridon V., M. Balesdent, J.-M. Bourinet, J. Morio and N. Gayton (2017). "Reliability-based sensitivity analysis of aerospace systems under distribution parameter uncertainty using an augmented approach". In: *Proc. of the 12th International Conference on Structural Safety & Reliability (ICOSSAR 2017)*, Vienna, Austria.
3. Analyse de sensibilité fiabiliste globale (*global ROSA*)
   - ▷ Rédaction d'un chapitre d'ouvrage scientifique en cours
4. Application de ces méthodologies à un cas aérospatial réaliste
   - ▷ Derennes P., V. Chabridon, J. Morio, M. Balesdent, F. Simatos, J.-M. Bourinet and N. Gayton (2018). "Nonparametric importance sampling techniques for sensitivity analysis and reliability assessment of a launcher stage fallout". In: *Optimization in Space Engineering*. Ed. by G. Fasano and J. Pintér. Springer International Publishing. (To Appear).
   - ▷ Chabridon V., M. Balesdent, J.-M. Bourinet, J. Morio and N. Gayton (2018). "Nonparametric adaptive importance sampling strategy for reliability assessment and sensitivity analysis under distribution parameter uncertainty – Application to launch vehicle fallback zone estimation". In: *Actes des 10èmes Journées Fiabilité des Matériaux et des Structures (JFMS 2018)*, Bordeaux, France.

Les perspectives liées à ces travaux de thèse sont de plusieurs natures. Elles peuvent, dans un premier temps, consister en des améliorations directes, à court terme, de certaines des contributions présentées dans cette thèse. Elles peuvent, dans un deuxième temps, concerner des aspects plus méthodologiques, voire contenir certaines questions ouvertes. Enfin, elles peuvent aussi concerner les applications, soit des apports méthodologiques de ces travaux à d'autres domaines, soit une généralisation à d'autres systèmes et/ou analyses issus du monde aérospatial. Les perspectives évoquées ici sont abondament discutées et documentées dans le Chapitre 9. Le lecteur est donc invité à s'y référer pour plus d'informations.

Résumé

Les systèmes aérospatiaux sont des systèmes complexes dont la fiabilité doit être garantie dès la phase de conception au regard des coûts liés aux dégâts gravissimes qu'engendrerait la moindre défaillance. En outre, la prise en compte des incertitudes influant sur le comportement (incertitudes dites « aléatoires » car liées à la variabilité naturelle de certains phénomènes) et la modélisation de ces systèmes (incertitudes dites « épistémiques » car liées au manque de connaissance et aux choix de modélisation) permet d'estimer la fiabilité de tels systèmes et demeure un enjeu crucial en ingénierie. Ainsi, la *quantification des incertitudes* et sa méthodologie associée consiste, dans un premier temps, à modéliser puis propager ces incertitudes à travers le modèle numérique considéré comme une « boîte-noire ». Dès lors, le but est d'estimer une quantité d'intérêt fiabiliste telle qu'une probabilité de défaillance. Pour les systèmes hautement fiables, la probabilité de défaillance recherchée est très faible, et peut être très coûteuse à estimer. D'autre part, une analyse de sensibilité de la quantité d'intérêt vis-à-vis des incertitudes en entrée peut être réalisée afin de mieux identifier et hiérarchiser l'influence des différentes sources d'incertitudes. Ainsi, la modélisation probabiliste des variables d'entrée (incertitude épistémique) peut jouer un rôle prépondérant dans la valeur de la probabilité obtenue. Une analyse plus profonde de l'impact de ce type d'incertitude doit être menée afin de donner une plus grande confiance dans la fiabilité estimée. Cette thèse traite de la prise en compte de la *méconnaissance du modèle probabiliste des entrées* stochastiques du modèle. Dans un cadre probabiliste, un « *double niveau* » d'incertitudes (aléatoires/épistémiques) doit être modélisé puis propagé à travers l'ensemble des étapes de la méthodologie de quantification des incertitudes. Dans cette thèse, le traitement des incertitudes est effectué dans un cadre bayésien où la méconnaissance sur les paramètres de distribution des variables d'entrée est caractérisée par une densité a priori. Dans un premier temps, après propagation du double niveau d'incertitudes, la *probabilité de défaillance prédictive* est utilisée comme mesure de substitution à la probabilité de défaillance classique. Dans un deuxième temps, une analyse de sensibilité locale à base de *score functions* de cette probabilité de défaillance prédictive vis-à-vis des hyper-paramètres de loi de probabilité des variables d'entrée est proposée. Enfin, une analyse de sensibilité globale à base d'indices de Sobol appliqués à la variable binaire qu'est l'indicatrice de défaillance est réalisée. L'ensemble des méthodes proposées dans cette thèse est appliqué à un cas industriel de retombée d'un étage de lanceur.

Mots-clés : analyse de fiabilité • probabilité d'événement rare • approches bayésiennes • échantillonnage préférentiel • statistiques non-paramétriques • analyse de sensibilité • systèmes aérospatiaux

Abstract

Aerospace systems are complex engineering systems for which reliability has to be guaranteed at an early design phase, especially regarding the potential tremendous damage and costs that could be induced by any failure. Moreover, the management of various sources of uncertainties, either impacting the behavior of systems ("aleatory" uncertainty due to natural variability of physical phenomena) and/or their modeling and simulation ("epistemic" uncertainty due to lack of knowledge and modeling choices) is a cornerstone for reliability assessment of those systems. Thus, *uncertainty quantification* and its underlying methodology consists in several phases. Firstly, one needs to model and propagate uncertainties through the computer model which is considered as a "black-box". Secondly, a relevant quantity of interest regarding the goal of the study, e.g., a failure probability here, has to be estimated. For highly-safe systems, the failure probability which is sought is very low and may be costly-to-estimate. Thirdly, a sensitivity analysis of the quantity of interest can be set up in order to better identify and rank the influential sources of uncertainties in input. Therefore, the probabilistic modeling of input variables (epistemic uncertainty) might strongly influence the value of the failure probability estimate obtained during the reliability analysis. A deeper investigation about the robustness of the probability estimate regarding such a type of uncertainty has to be conducted. This thesis addresses the problem of taking *probabilistic modeling uncertainty* of the stochastic inputs into account. Within the probabilistic framework, a "*bi-level*" input uncertainty has to be modeled and propagated all along the different steps of the uncertainty quantification methodology. In this thesis, the uncertainties are modeled within a Bayesian framework in which the lack of knowledge about the distribution parameters is characterized by the choice of a prior probability density function. During a first phase, after the propagation of the bi-level input uncertainty, the *predictive failure probability* is estimated and used as the current reliability measure instead of the standard failure probability. Then, during a second phase, a local reliability-oriented sensitivity analysis based on the use of *score functions* is achieved to study the impact of hyper-parameterization of the prior on the predictive failure probability estimate. Finally, in a last step, a global reliability-oriented sensitivity analysis based on Sobol indices on the indicator function adapted to the bi-level input uncertainty is proposed. All the proposed methodologies are tested and challenged on a representative industrial aerospace test-case simulating the fallout of an expendable space launcher.

Keywords: reliability analysis • rare event probability estimation • Bayesian approaches • importance sampling • nonparametric statistics • sensitivity analysis • aerospace systems